INVESTIGATION OF THE EFFECT OF AXIAL LOADS ON THE SHEAR STRENGTH OF REINFORCED CONCRETE BEAMS

by

HEM CHANDRA BARA, B. Tech., M.Sc., DIC

A thesis submitted for the Degree of Doctor of Philosophy in the Faculty of Engineering of the University of London.

Imperial College of Science and Technology, London.

March, 1971

ABSTRACT

The research work reported in this thesis is devoted primarily to the investigation of the effect of axial loading on the shear strength of rectangular reinforced concrete beams with web reinforcement.

The behaviour of concrete members subjected to shear and bending stresses is described at different stages of loading; and their resistances against shear failure predicted by some of the existing theories are checked with test results. Most of these empirical theories based on limited test evidence are found to be unsatisfactory.

The experimental part of beam tests consisted of testing of 31 beams with and without axial forces. The magnitude of axial forces was varied systematically during this investigation, while other parameters are not varied.

The different failure modes are treated separately. The first theory is concerned with shear cracking/diagonal tension failure of rectangular beams, which is based on principal tensile stress criterion of failure.

The second theory deals with shear failure of beams following shear cracking, the failure mode of which is shearing. The ultimate resistance against shear failure is given by the summation of shear carried by the concrete compressive zone and the web reinforcement.

The third theory predicts strengths of beams failing in shear compression. It is based on the "arch" theory; and the compatibility conditions are employed to evaluate the depth of neutral axis at failure.

A few tests were carried out to study shear transfer across a preformed crack due to interlock.

A separate theory is put forward to predict strengths of beams failing in bond.

On the whole, the proposed equations are found to predict results in good agreement with the test values and a full comparison is given in Chapter 7.

ACKNOWLEDGEMENTS

The author is grateful to Professor A.L.L. Baker, D.Sc., F.I.C.E., F.I.Struct.E., under whose supervision the research work of the thesis was carried out.

The author would also like to extend his grateful thanks to Dr. P.E. Regan for his valuable suggestions and guidance throughout the work.

A further debt of gratitude is extended to Dr. C.W. Yu, Ph.D., D.I.C., M.I.C.E., M.A.S.C.E., for providing the laboratory facilities. Thanks are also due to the laboratory staff of the Concrete Structures and Technology Section, Imperial College, for their help in the experimental part of this investigation.

The Construction Industry, Research and Information Association (CIRIA) also deserves gratitude for the assistance afforded by their contract with the Imperial College.

The author acknowledges with gratitude the financial grant given by the Government of Assam, India, and also by the Sir Ernest Cassel Education Trust, which made the research work possible.

Thanks are also due to Miss E. Bridgman and Mrs. J. McGregor for typing the manuscript.

Finally the author would like to express his deep gratitude to his parents for their encouragement to him all the work through.

CONTENTS

		Page
Abstract		2
Acknowledgements		4
Contents		5
List of Figures		12
List of Tables		19
Nomenclature		23
CHAPTER 1: INTRODUCTION.		26
CHAPTER 2: STUDY OF THE BEHAVIOUR AND MODE OF SHEAR FAILURE		30
2.1	Introduction.	30
2.2	Types of shear failure.	30
2.3	Behaviour of rectangular beams without web reinforcement.	31
2.3.1	Beams with long shear span to effective depth ratios.	31
2.3.2	Behaviour of beams with short shear span to effective depth ratios.	32
2.4	Behaviour of rectangular beams with web reinforcement.	35
2.4.1	Beams with long shear span to effective depth ratios.	35
2.4.2	Beams with short shear spans.	36
2.4.3	Beams with very short shear spans.	37
2.5.	Description and inclination of failure plane.	37
2.6	Parameters affecting the shear capacity of reinforced concrete beams.	38

Page

2.6.1 Influence of shear span to effective depth ratios. 38

2.6.2 Influence of concrete strength. 40

2.6.3 Effect of ratio of tensile steel. 40

2.6.4 Influence of web reinforcement. 40

2.6.5 Effect of compression reinforcement. 43

2.6.6 Influence of manner of loading. 44

2.6.7 Effect of axial forces. 44

2.6.8 Conclusions. 46

CHAPTER 3: STUDY OF PREVIOUS WORKS ON SHEAR AND REVIEW OF THE EXISTING THEORIES. 48

3.1 Shear cracking theories - 49

3.1.1 Empirical shear cracking equations: 49

a) Classical theory.

b) shear cracking equation of ACI-ASCE Committee (326).

c) CEB equation.

d) Empirical equation of Mattock.

e) Empirical equation of Petersson.

3.1.2 Analytical shear cracking equations. 61

a) Kani's shear cracking equation.

b) Regan's shear cracking theory.

3.2 Theories predicting ultimate strength of a section in shear. 66

3.2.1 Empirical equations. 66

a) Mörsch Truss Analogy.

b) Pin-jointed truss (Baker and Ahmad).

c) ACI-ASCE Committee (326) equation.

d CEB equation.

e) Mattock's equation.

		Page
3.2.2	Shearing failure theory.	77
3.2.3	Plane of minimum strength method.	79
	a) Russian Code Method.	
	b) Hillerborg's equation.	
3.2.4	Shear-compression Theories.	86
	a) Empirical shear compression equations of Laupa, Kani, Lownds (Modified Smith's equation).	
	b) Analytical shear-compression equations of Bjuggren, Regan, Walther.	
CHAPTER 4:	EXPERIMENTAL INVESTIGATION: BEAM TESTS.	98
4.1	Introduction	98
4.2	Test specimens.	99
4.2.1	Features common to all beams.	99
4.2.2	Description of specimens.	100
4.3.	Materials and fabrication.	101
4.3.1	Concrete.	101
4.3.2	Reinforcement.	105
4.3.3	Casting and curing.	105
4.4	Testing Arrangements.	108
4.4.1	Test rig.	108
4.4.2	Support conditions.	110
4.4.3	Loading arrangements.	110
4.5	Instrumentation.	121
4.6	Testing procedure.	122
4.7	Behaviour of test beams.	122
4.7.1	Restrained beams with axial tension.	122
4.7.2	Restrained beams with no axial load.	124
4.7.3	Restrained beams with axial compression.	124

		Page
4.7.4	Simply supported beams with axial tension.	125
4.7.5	Simply supported beams with no axial load.	126
4.7.6	Simply supported beams with axial compression.	126
4.8	Test results.	126
4.9	Examination of test results.	126
CHAPTER 5:	INVESTIGATION AND STUDY OF PAST WORK ON AGGREGATE INTERLOCK, DOWEL ACTION AND BOND FAILURE:	160
5.1	Aggregate Interlock.	160
5.1.1	Mechanism of shear transfer by Aggregate interlock.	160
5.1.2	Factors influencing aggregate interlocking.	160
5.1.3	Past work on aggregate interlock, Mattock, Taylor, Fenwick and Paulay.	161
5.1.4	Experimental Investigation.	168
5.1.5	Estimate of shear carried by aggregate interlock.	175
5.2	Study of dowel theories. R. Jones, Krefeld and Thurston, Regan, Baumann, Arroyo.	183
5.3	Bond failure.	193
CHAPTER 6:	THEORETICAL INVESTIGATION:	203
6.1	Introduction.	203
6.2	Development of shear cracking theory.	203
6.2.1	Failure criterion.	203
6.2.2	Assumptions.	203
6.2.3	Derivation.	205
6.3	Equilibrium conditions of the shear span after shear cracking.	212

		Page
6.4	Development of shearing equation.	213
6.4.1	Evaluation of concrete contribution in carrying shear.	214
6.4.2	Evaluation of contribution of web reinforcement.	221
6.5	Development of shear-compression equation.	222
6.5.1	Introduction.	222
6.5.2	Assumptions for the development of shear-compression equation.	224
6.5.3	Solution for ultimate neutral axis depth.	228
6.6	Shear carried by dowel action of tensile steel.	239
6.7	Transition from diagonal tension or shearing failure to shear compression failure.	243
6.8	Proposed theory on bond failure.	246
6.9	Treatment of a section at the point of contraflexure when subject to axial force.	251
CHAPTER 7:	COMPARISON AND DISCUSSION OF TEST RESULTS WITH DIFFERENT THEORIES:	
7.1	Shear cracking of simply supported, point-loaded rectangular beams with $a/d_1 > 2.5$.	254
7.2	Shear cracking of restrained and Knee frame point-loaded rectangular beams with $\frac{M}{Qd_1} > 2.5$.	264
7.3	Shear cracking of knee frame members with $M/Qd_1 < 2.5$.	269
7.4	Shear failure of Knee frame members without web reinforcement, $M/Qd_1 < 2.5$. (Shear-compression failure).	272
7.5	Shear failure of restrained and simply supported rectangular beams with vertical stirrups, $M/Qd_1 > 2.5$ (Shearing failure)	283

Page

7.6 Shear failure of simply supported and restrained rectangular beams with web reinforcement and axial force. $a/d_1 < 2.5$. (Shear compression failure). 288

7.7 Shear failure of point-loaded, simply supported and Restrained T-beams with web reinforcement. 292

7.8 Discussion of Comparisons. 295

7.8.1 Scale and shape effects. 295

7.8.2 Comparison of test results of rectangular beams with shear cracking equations. 295

7.8.3 Comparison of test results of rectangular beams without web reinforcement and $M/Qd_1 < 2.5$. Shear compression failure. 298

7.8.4 Comparison of test results of rectangular beams with web reinforcement and $M/Qd_1 > 2.5$. Shearing failure. 298

7.8.5 Comparison of test results of rectangular beams with web reinforcement. (Shear compression failure). 298

7.9 Comparison of test results of beams failing in bond. (Secondary failure mode). 299

CHAPTER 8:

Conclusions and proposals for future research: 301

8.1 General conclusions. 301

8.2 Influence of the parameters affecting the shear strength of a beam. 303

8.2.1 Influence of axial force. 303

8.2.2 Influence of shear span to effective depth ratio (M/Qd_1 or a/d_1). 304

8.2.3 Influence of concrete strength. 305

Page

8.2.4 Influence of ratio of tensile steel ($rst = \frac{Ast}{bd_1}$) 305

8.2.5 Effect of Aggregate interlock. 305

8.2.6 Effect of web reinforcement ratio ($^{Aq}/_{bs}$). 306

8.3 Proposals for future research. 306

References 308

LIST OF FIGURES

		Page
1.	Beam showing diagonal tension failure.	33
2.	Beam showing shearing failure.	33
3.	Beam showing shear compression failure.	33
4.	Beam showing pure shear failure.	33
5.	Effect of a/d_1 ratio on the shear strength of beams without web reinforcement.	39
6.	Influence of concrete strength on the shear strength.	41
7.	Influence of percentage of vertical stirrups on shear strength of rectangular beams.	42
8.	Effect of axial force on Vc/bd_1 for different a/d_1 ratios of reinforced concrete beams.	45
9.	Peeling off of teeth in beams without web reinforcement.	62
10.	Internal forces in a beam cracked in flexure.	62
11.	Dowel action of tensile steel.	62
12.	Mörsch Truss Analogy.	67
13.	Figure showing number of stirrups crossed by a shear crack.	67
14.	Arch Analogy. Stirrups provide hanging supports to secondary arches.	70
15.	Modified Truss Analogy.	70
16.	Free body diagram of shear span.	70
17.	Test. frame.	109
18.	Loading Arrangements of beams.	111
19.	Details of holes and reinforcement in Nib.	112
20.	Details of reinforcement of Test beams.	113
21.	Reinforcement details of Test beams.	114
22.	Details of reinforcement of Test beams.	115

Page

23. Details of reinforcement of Test beams. 116

24. Details of reinforcement of Test beams. 117

25. Stress-strain curves of concrete. 118

26. Stress-strain curves for steel. 119

27. Stress-strain curves for Mild steel. 120

28. Figure shows strain in top steel of beam B_{12}. 130

29. Figure shows strain in bottom steel of beam B_{12}. 131

30. Figure shows strain in stirrups of beam B_{12}. 132

31. Plot of $^{Qtest}/_{bd_1}$ vs $^{N}/_{bd_1}$ for different $^{M}/_{Qd_1}$ ratios. 133

32. Plot of vertical force against displacement. 134

33. Plot of vertical force against displacement. 135

34. Influence of shear span/Effective depth ratio on inclination of diagonal crack. 136

35. Plot of $^{Qult}/_{bd_1}$ vs Tan θ. 137

36. Figure shows strain in top steel of beam B_{24}. 138

37. Figure shows strain in bottom steel of beam B_{24}. 139

38. Figure shows strain in top steel of beam B_{24}. 140

39. Figure shows strain in stirrups of beam B_{24}. 141

40. Figure shows strain in top steel of beam B_{25}. 142

41. Figure shows strain in bottom steel of beam B_{25}. 143

42. Figure shows strain in stirrups of beam B_{25}. 144

43. Figure shows strain in top steel of beam B_{26}. 145

44. Figure shows strain in bottom steel of beam B_{26}. 146

45. Plot of strain in steel against span at different loads (2 x shear) of beam B_{26}. 147

46. Typical strain diagrams of beam B_{27}. 148

47. Crack patterns of test beams B_2, B_7 and B_{12}. 152

48. Crack patterns of test beams B_1, B_4, B_5 and B_3. 153

49. Crack patterns of test beams B_{20}, B_{30}, B_{17} and B_{18}. 154

50. Crack patterns of test beams B_{23}, B_{28}, B_{15} and B_{22}. 155

51. Crack patterns of test beams B_{24}, B_{25}, B_{27} and B_{29}. 156

52. Crack patterns of test beams B_{6}, B_{8}, B_{10} and B_{13}. 157

53. Crack patterns of test beams B_{14}, B_{9}, B_{11} and B_{19}. 158

54. Crack patterns of test beams B_{31}, B_{16}, B_{21} and B_{26}. 159

55. Details of push-off specimens for interlock Tests. (Mattock). 162

56. Details of specimen with test rig for interlock Tests. (Taylor). 162

57. Details of specimen with test rig for interlock Tests. (Fenwick). 165

58. Aggregate interlock action. 165

59. Displacements across flexural crack in beams. (Taylor). 165

60. Shear stress vs shear displacement curves. (Fenwick). 167

61. Shear stress vs shear displacement curves. (Fenwick). 167

62. Details of beam FA_4. (Fenwick). 167

63. Specimen for Aggregate interlock test. Group 1. 170

64. Specimen for Aggregate interlock test. Group 2. 170

65. Plot of shear stress against crack width. (Group 2). 177

66. Plot of vertical force vs crack width. (Group 1). 178

67. Plot of vertical force vs slip. (Group 1). 179

68. Plot of shear force vs crack width. (Group 2). 180

69. Plot of shear force vs slip. (Group 2). 181

70. Plot of shear force vs slip. (Group 2). 182

71. Equilibrium conditions used by Jones. 185

72. Specimen for dowel test (Jones). 185

73. Dowel action of tensile steel. (Regan). 185

74. Details of specimens for dowel tests. (Krefeld and Thurston).

a) Dowel specimen.

b) beam specimen. 188

75. Details of specimens for dowel test. (Baumann). 188

76. Details of beam specimens for tests on bond failures. (Mathey and Watstein). 195

77. Details of pull-out specimens. (Mathey and Watstein). 195

78. Details of beam specimens for tests on bond failures. (Ferguson and Thompson). 197

79. Effect of bar cover on bond stress. (Ferguson and Thompson). 198

80. Effect of stirrups on bond resistance. (Ferguson and Thompson). 198

81. Specimen for tests on bond failures. (Östlund). 200

82. Effect of web reinforcement on steel stress. (Östlund). 200

Page

83. Plot of steel stress vs lap length. (Losberg). 201

84. Plot of steel stress vs Concrete strength. (Losberg). 201

85. Plot of steel stress vs bottom cover/bar diameter. (Losberg). 202

86. Effect of stirrups on steel stress. (Losberg). 202

87. Plot of steel stress vs side cover/bar diameter. (Losberg). 202

88. Plot of steel stress vs lap length. (Losberg). 202

89. Section subjected to axial force. 207

90. Equilibrium of shear span after shear cracking. 207

91. Shear stress distribution in compression zone. 207

92. Relation between uniaxial Tensile and compressive strengths of concrete. 211

93. Failure criteria expressed as failure envelopes. (Walther and Guralnick). 218

94. Failure criteria expressed as limiting shear stresses. ($^{Ut}/_{Ucyl} = 0.1$). 218

95. Stresses above flexural cracks due to bond force. 218

96. Free body diagram of internal forces after shear cracking. 219

97. Strain diagram for flexural neutral axis depth. 219

98. Stirrups crossed by shear crack. 219

99. No **arching** in beams with long shear spans. ($^{a}/_{d_1} > 2.5$). 225

Page

100. Transverse force carried by inclined compression after shear cracking. ($a/d_1 < 2.5$). 225

101. Concrete stress blocks.

a) CEB stress block.

b) Assumed stress block. 225

102. Ultimate moments of over-reinforced beams failing in flexure. 227

103. Statically determinate model beam. 230

104. Particular solution diagrams. 230

105. Flexibility coefficient diagrams. 231

106. Stress-strain curve used for estimation of Ec value at ultimate stage. 231

107. Stress in concrete due to dowel shear at the level of tensile steel. (Baumann). 241

108. Dowel action in short beams. 241

109. Internal forces of a beam with stirrups after cracked in flexure and shear. 241

110. Transition of the failure modes for varying M/Qd_1 ratios. 245

111. Plot of $Qcalc/Qtest$ vs M/Qd_1 ratios. Shear cracking of rectangular beams. 275

112. Plot of $Qcalc/Qtest$ vs M/Qd_1 ratios. Shear cracking of rectangular beams. 276

113. Plot of $Qcalc/Qtest$ vs Ucyl. Shear cracking of rectangular beams. 277

114. Plot of $Qcalc/Qtest$ vs Ucyl. Shear cracking of rectangular beams. 278

115. Plot of $Qcalc/Qtest$ vs rst% Shear cracking of rectangular beams. 279

Page

116. Plot of $^{Qcalc}/_{Qtest}$ vs rst%.

Shear cracking of rectangular beams. 280

117. Plot of $^{Qcalc}/_{Qtest}$ vs $^{N}/_{bd_1}$.

Shear cracking of rectangular beams. 281

118. Plot of $^{Qcalc}/_{Qtest}$ vs $^{N}/_{bd_1}$.

Shear cracking of rectangular beams. 282

LIST OF TABLES

Page

1. Mix proportion by weight. 102
2. Details of test beams.
   Group A. Restrained beams. 103
3. Details of test beams.
   Group B. Simply supported beams. 104
4. Concrete strengths. 106
5. Properties of reinforcement. 107
6. Test results of beams. 127
7. Test results.
   Group A. Restrained beams. 128
8. Test results.
   Group B. Simply supported beams. 129
9. Test results of interlock specimens.
   Group 1. 174
10. Test results of interlock specimens.
    Group 2. 174
11. Effect of cover on steel stress. (Östlund). 200
12. Statistical comparison of $^{Qcalc}/_{Qtest}$ values of Simply supported beams without web reinforcement. 258
13. Shear cracking/diagonal tension failure of simply supported single-point loaded rectangular beams with $^{a}/_{d_1} > 2.5$. (Mattock). 259
14. Comparison of $^{Qcalc}/_{Qtest}$ values of simply supported single point loaded rectangular beams with $^{a}/_{d_1} > 2.5$. (Mattock). 260
15. Shear cracking/diagonal tension failure of simply supported two-point loaded rectangular beams with $^{a}/_{d_1} > 2.5$. (Mukhapadhyay). 261

Page

16. Comparison of $^{Qcalc}/_{Qtest}$ values of simply supported two-point loaded rectangular beams with $^{a}/_{d_1} > 2.5$. (Mukhapadhyay). 262

17. Shear cracking/diagonal tension failure of simply supported single point loaded rectangular (stub) beams with $^{a}/_{d_1} > 2.5$. (De Cossio and Siess). 263

18. Comparison of $^{Qcalc}/_{Qtest}$ values of simply supported (stub) beams subjected to single point load. (De Cossio and Siess). 263

19. Statistical comparison of $^{Qcalc}/_{Qtest}$ values of Knee frame and restrained beams. 264

20. Shear cracking/diagonal tension failure of restrained (Knee frame) point loaded rectangular beams with $^{M}/_{Qd_1} > 2.5$. (Morrow and Viest). 265

21. Comparison of $^{Qcalc}/_{Qtest}$ values for Knee frame rectangular members . $^{M}/_{Qd_1} > 2.5$. 266

22. Shear cracking/diagonal tension failure of rectangular restrained beams. $^{M}/_{Qd_1} > 2.5$. (Sayani). 267

23. Comparison of $^{Qcalc}/_{Qtest}$ values of rectangular restrained beams. $^{M}/_{Qd_1} > 2.5$. (Sayani). 268

24. Statistical comparison of $^{Qcalc}/_{Qtest}$ (shear cracking) values of Knee frame members. $^{M}/_{Qd_1} < 2.5$. 269

25. Shear failure of Knee frame members with no web reinforcement. $^{M}/_{Qd_1} < 2.5$. (Morrow and Viest). 270

Page

26. Shear failure of Knee frame members with no web reinforcement. $M/Qd_1 < 2.5$. Baldwin and Viest. 270

27. Comparison of Q_{calc}/Q_{test} (cracking) values of Knee frame members with no web reinforcement. $M/Qd_1 < 2.5$. (Morrow and Viest). 271

28. Comparison of Q_{calc}/Q_{test} (cracking) values of Knee frame members with no web reinforcement. $M/Qd_1 < 2.5$. (Baldwin and Viest). 271

29. Statistical comparison of Q_{calc}/Q_{test} (ultimate) values of Knee frame members with no web reinforcement. $M/Qd_1 < 2.5$. 273

30. Comparison of Q_{calc}/Q_{test} (ultimate) values of Knee frame members without web reinforcement. $M/Qd_1 < 2.5$. 274

31. Statistical comparison of Q_{calc}/Q_{test} values of rectangular beams with web reinforcement. (shearing failure). 285

32. Shear failure of restrained and simply supported rectangular beams with vertical stirrups. (shearing failure). 286

33. Comparison of Q_{calc}/Q_{test} values of shear failure of restrained and simply supported rectangular beams with vertical web reinforcement. (shearing failure). 287

34. Statistical comparison of Q_{calc}/Q_{test} values of simply supported and restrained beams with vertical web reinforcement. (shear compression failure). 289

Page

35. Shear failure of rectangular simply supported and restrained beams with vertical web reinforcement. (shear compression failure). 290

36. Comparison of Q_{calc}/Q_{test} values of rectangular simply supported and restrained beams with vertical web reinforcement. (shear compression failure). 291

37. Shear failure of simply supported and restrained point-loaded T-beams with web reinforcement. (shear-compression failure). 293

38. Statistical data from comparison of shear cracking theories of rectangular beams. 296

39. Comparison of Q_{calc}/Q_{test} values of beams failing in bond calculated by the proposed equation. 299

NOMENCLATURE

The following is the summary of the symbols used repeatedly in the thesis. Any other symbols used than those below are defined in any part of the thesis where they appear.

A	Total area of cross-section of a member.
Aq	Area of one member of shear reinforcement.
As	Total area of longitudinal steel across a section = (Asc + Ast).
Asc	Area of compression reinforcement.
Ast	Area of tension reinforcement.
a	shear span.
b	breadth of rectangular beam.
c	Length of horizontal projection of shear (inclined) crack.
d	Overall depth of cross-section of a member.
d_1	Effective depth of cross-section of a member.
Ec	Modulus of elasticity of concrete.
Es	Modulus of elasticity of steel.
e_{cc}	Concrete compressive strain.
e_{st}	Tensile strain in steel.
Fcc	Longitudinal compressive force in concrete.
Fst	Longitudinal force in tensile steel.
fs	Steel stress.
fx	Stress in concrete.
fy	Yield or proof stress of steel.
fyq	Yield or proof stress of shear reinforcement.
j	Elastic lever arm factor ($^7/_8$).
L	Anchorage or bond length.

l	Span of member.
la	Internal lever arm.
M	External bending moment.
m	Modular ratio $(\frac{Es}{Ec})$.
N	Axial force.
n_o	Flexural neutral axis depth factor.
n	Elastic neutral axis depth factor.
$\bar{n}$	Ultimate neutral axis depth factor.
$\bar{n}_o$	Ultimate neutral axis depth factor. without axial load.
Q	External shear force.
Qc	Shear force supported by concrete.
Qcr	Shear force causing shear cracking.
Qd	Shear force carried by dowel action of tensile steel.
Qsc	Shear force in shear compression failure minus the dowel shear.
Qult	Shear force at failure.
Qw	Shear force supported by shear reinforcement.
q	Shear stress.
r_s	Ratio of longitudinal steel $(^{As}/_{bd})$.
r_{sc}	Ratio of compression steel $(^{Asc}/_{bd_1})$.
r_{st}	Ratio of tension steel $(^{Ast}/_{bd_1})$.
r_q	Ratio of shear reinforcement $(^{Aq}/_{bs})$.
s	Spacing of shear reinforcement measured along the axis of tension steel.
Ucyl	Standard (6" x 12") cylinder crushing strength of concrete.
Ut	Uni-axial tensile strength of concrete.
Uw	Standard (6") cube crushing strength of concrete.
α	Inclination of shear reinforcement to the axis of the tension reinforcement.

Δ_{cc} Deformation of concrete.

Δ_{st} Tensile steel deformation.

θ Angle of inclination of shear (critical) cracks to the axis of tensile steel.

ϕ Diameter of reinforcement.

CHAPTER - 1

INTRODUCTION

Although the primary concern in the design of reinforced concrete is one of flexure, the effects of shear cannot be disregarded as is demonstrated by the significant proportion of structural failures that can be attributed to shear .

Flexural stresses can be evaluated relatively accurately by classical methods - elastic theory before cracking and cracked section theory thereafter. However similarly rational approaches are not available for calculations for members failing in shear , partly because of the large number of parameters influencing such failures.

Shear failure is preceded by the formation of an inclined crack (or cracks). The formation of the inclined cracks necessitates radical changes in structural behaviour. If a beam is not capable of supporting the redistributed forces collapse occurs immediately.

In beams, with shear cracking resistances higher than their flexural failure loads, there is no problem of shear failure, but web reinforcement has to be provided in most beams with shear cracking loads lower than their flexural capacities if shear failure is to be prevented. Some short beams do not fail at their shear cracking loads even if web reinforcement is not provided but such reinforcement is none the less generally necessary if full flexural strengths are to be attained.

Though the field of research in shear is fertile and a large number of investigators has been attracted to it in the last twenty years, relatively little work was done in the preceding thirty to forty years.

Before 1900 two schools of thought existed regarding the mechanism of shear failure. The first believed that shear failures

were caused by horizontal shear stresses. The second, which was proved to be reasonable and is generally accepted today, believed the cause of failure to be diagonal tension, which view was first advanced by Ritter as early as 1899. From this understanding there grew the realisation that the function of web reinforcement is to replace concrete in tension, rather than to act as a series of "shear keys".

It was Mörsch in Germany who clarified the problem of diagonal tension failure, with the argument that, if a plane is subjected to pure shear, then another plane at 45° to it is subject to pure tensile stresses of the same magnitude as the shear stresses, and since concrete is much weaker in tension than in shear it is on the latter plane that failure will occur. He developed an equation for diagonal tension cracking, which is still present in many Codes of Practice, and also developed the now classical truss analogy, which is even more widely used though often in a modified form.

A new approach to shear design was introduced in the Soviet Union during the second world war and this method, which is reviewed in chapter 3, was the first ultimate load analysis, but had little influence outside Russia. However a number of investigators, notably Clark whose work was published in America in 1950, was realising the considerable defects of the Mörsch methods, particularly their failure to take account of the influence of span/depth ratio on shear strength.

Since 1950 a great deal of work has been done on shear and many different theories and equations have been proposed, but very little of this effort has been concerned with members subjected to axial loads other than prestress.

It appears that no work at all had been done on members subjected to axial tension before the occurrence of a shear failure in a warehouse at Wilkins Airforce depot, Ohio. The cause of the warehouse

failure was investigated in 1956 by Elstner and Hognestad[13] who concluded that it was due to the combined action of stresses arising from external loads, shrinkage and temperature effects.

Although this failure gave new impetus to research on shear very little of the ensuing work was concerned with the effects of axial loading. Nevertheless the recommendations of a joint ACI-ASCE Committee, which served as the basis of the shear clauses of the 1963 ACI code, included an equation for members subject to axial forces (tension or compression). The current Soviet code also has recommendations for such members, based on apparently rather limited experimental work in Russia, and the 1970 CEB code contains separate equations for tensioned and compressed members, the derivation of which is not explained.

The published experimental data on axially loaded members is very limited and only three authors (Lownds, Mattock and Sayani) appear to have done work on tensioned members, in spite of a general belief that tension should reduce resistance and is frequently present due to temperature and shrinkage effects. Less frequently in for example Vierendeel girders tension due to external loading can be a dominant effect. Somewhat more work has been done with compression presumably out of interest in portal legs and multistorey buildings in earthquake regions.

Theoretical work on axially loaded members is restricted to modifications of code equations for members free from axial loads (noteably by Mattock) and a modification of a shear-compression equation made by Lownds.

The object of the research reported in this thesis was the development of an analytical approach to shear including the effects of axial forces and the provision of experimental data, for beams with web reinforcement, to accompany it. Different failure modes

are treated separately and three different equations are developed to predict failures.

Chapter 2 offers a general discussion of shear failure including the modes of failure and the parameters influencing them. Chapter 3 is a review of existing theories on shear and, although biased towards methods taking account of axial load effects, includes theories in which no reference is made to axial loading. Chapter 4 is devoted to the main experimental part of this research, and the results of tests on beams with axial tension and compression are presented.

Chapter 5 reports experimental work on aggregate interlock across cracks, and a study of works on interlock effects, dowel action by tensile steel and secondary failures of anchorages.

In chapter 6 three separate equations are developed to predict failure loads in shear. The first is a shear cracking equation based on a principal tensile stress criterion of failure. The second is a "shearing" equation developed along the same lines as one proposed by Placas, but making allowance for the effects of axial loads. The third and final one is a shear-compression equation developed from considerations of strength and deformation compatibility for a model of a beam containing flexual and shear cracks. The effects of axial forces are considered, and dowel action by the main steel is taken into account in short spans.

A separate equation is also presented in this chapter to evaluate the strength of a beam against bond and anchorage failure.

Chapter 7 presents comparisons between test results and the predictions of the author's and other theories. The test results are those from chapter 4 and those of other investigators.

In the final chapter 8, conclusions are drawn regarding shear failure, particularly in the presence of axial loading. Part of this chapter is devoted to a few proposals for further research.

STUDY OF THE BEHAVIOUR AND MODES OF SHEAR FAILURES IN REINFORCED CONCRETE BEAMS PARTICULARLY RECTANGULAR BEAMS WITH AND WITHOUT AXIAL LOADING:

2.1 Introduction:

This chapter is entirely devoted to the study of the different modes of shear failure and the behaviour of reinforced concrete beams at different load stages. Other modes, such as flexure and secondary bond failure are not discussed.

Shear failure is different from flexural failure in that it occurs after or at the breakdown of beam action. Shear stresses are believed to be partly responsible for the premature failure, even though it is difficult to say exactly what stress combinations caused failure.

The modes of shear failure of beams are dependent on a number of variables. By varying the parameters, it is possible to achieve different failure modes in beams. The purpose of this chapter is to study the problem of shear in general and to depict failure modes of beams in shear.

2.2 Types of shear failure:

a) Diagonal tension failure:

Shear affects the behaviour of a beam without web reinforcement by the formation of a diagonal crack. This diagonal crack is believed to form along a plane where a critical stress condition exists arising out of shear and longitudinal stresses. So long as the diagonal crack is not formed, the effect of shear on the behaviour of the beam is of little significance. Collapse of beam is obtained generally immediately after the formation of the diagonal crack.

This type of failure is generally observed in beams without web reinforcement and with relatively long shear spans ($^{a}/_{d_1} > 2.5$).

b) Shearing failure:

With the inclusion of web reinforcement, the equilibrium conditions of the shear span are modified, and a redistribution of the internal forces takes place. The beam does not collapse at the shear (diagonal) cracking load, but fails only when shearing of the compression zone above the inclined crack takes place.

This failure mode is frequently observed in beams with long shear spans ($^{a}/_{d_1} > 2.5$) and with web reinforcement.

c) Shear compression failure:

In relatively short beams, the above mentioned modes are not observed. A diagonal crack may be formed, but the formation of this crack is not sufficient to cause failure of the beam. The propagation of the diagonal crack is slower, but it grows towards the load point with each increment of vertical load. Even when the crack is of considerable width the beam can sustain more load. The crack penetrates into the compression zone. Finally, failure can occur due to crushing of the concrete compression zone. This type of failure is referred to as "shear compression" failure.

This mode of failure is predominent in beams with short shear spans ($^{a}/_{d_1} < 2.5$) with and without web reinforcement.

2.3 Behaviour of rectangular beams without web reinforcement:

2.3.1 Beams with long shear span to effective depth ratios:

Until the formation of the flexural cracks, all beams behave almost identically and the stresses at different load stages can be predicted sufficiently accurately by elastic theory. But this analysis is of no use as soon as the cracks appear. Due to bending upon application of transverse load, tensile stresses are produced in the tensile zone of the beam and once these stresses reach the

tensile strength of concrete, flexural cracks are produced. These flexural cracks first appear near the position of maximum moment and as the transverse loading is increased, the vertical flexural cracks propagate upwards. Upon further loading more similar cracks appear away from the position of maximum moment.

This process continues until the shear cracking load is attained. At this load stage, an inclined (shear) crack starts appearing either as an extension of an existing flexural crack or independently, and travels in the direction of increasing moment. The appearance of the shear crack (cracks) marks the end of the beam action.

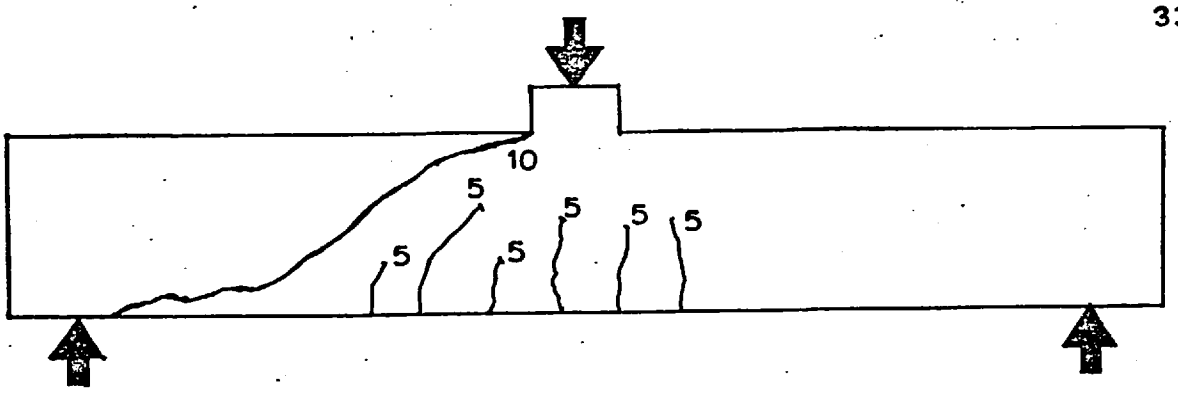
The inclined cracks which form generally near the middle or the neutral axis position, propagate more rapidly towards the tensile zone than the compressive zone. The inclination of the crack in the tensile zone is more or less constant and is nearly 45°. But the inclination varies as the crack penetrates into the compressive zone.

If any further load can be sustained, the shear crack progresses more inside the compression zone and the width of the crack is increased. As a result the concrete loses its capacity to carry shear either as its intrinsic capacity or by aggregate interlocking. Thus the unbalanced vertical component of shear subjects the tensile reinforcement to a downward pull which in turn compresses the concrete below it and starts to tear away the concrete cover upto the support. The compressive zone, at this stage, being incapable of carrying all the portion of unaccounted vertical shear gives way.

This mode of failure is designated as "Diagonal tension failure" and is illustrated in fig. 1. In this case, the increase of load after the formation of shear cracks is very small or even non-existent.

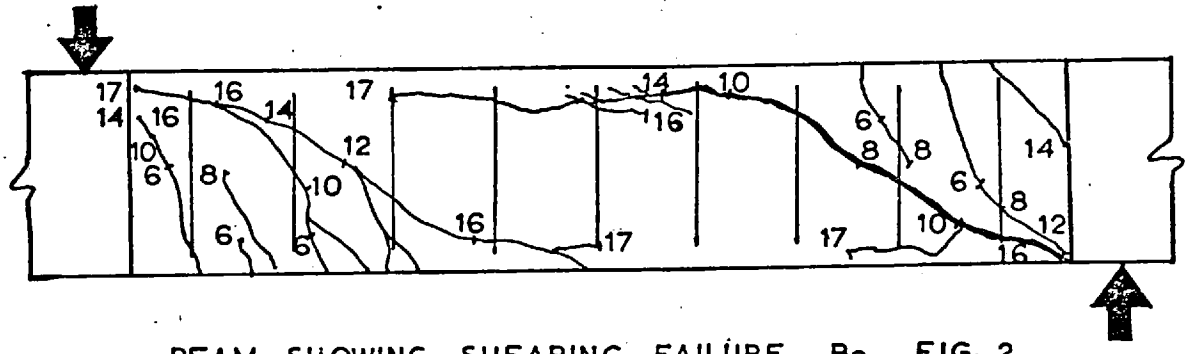
2.3.2 Behaviour of beams with short shear span to effective depth ratios:

In short beams it is possible for the first shear cracks to form

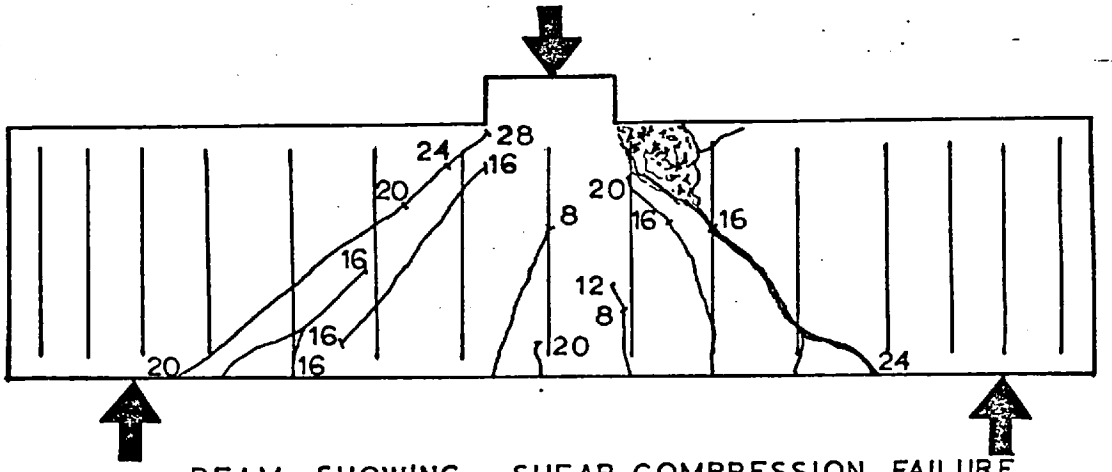


BEAM SHOWING DIAGONAL TENSION FAILURE J_1 (DIB)

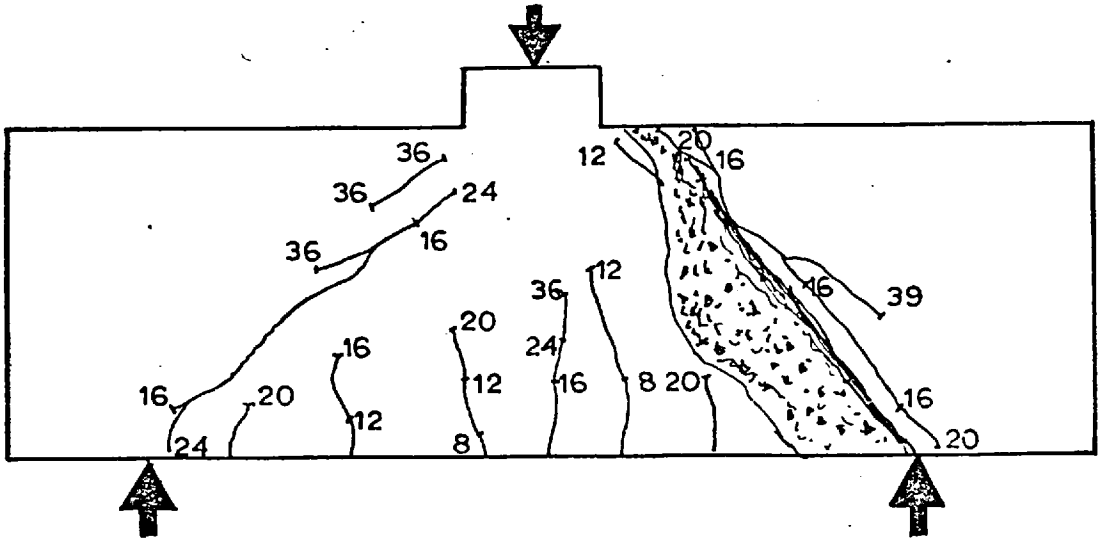
FIG. 1.



BEAM SHOWING SHEARING FAILURE B_3. FIG. 2.



BEAM SHOWING SHEAR COMPRESSION FAILURE J_{17} (DIB) FIG. 3.



BEAM SHOWING PURE SHEAR FAILURE J_{12} (DIB)

FIG. 4.

independently of flexural cracks. After shear cracking the failure is never achieved so quickly as is the case in long beams. Even after the widening of the shear crack, the compression zone is capable of sustaining further load. The beam action is destroyed at this stage and due to redistribution of stresses, truss or tied arch action is developed inside the beam. But the development of arch action is restricted by the manner of application of vertical loading.

After shear-cracking, the above-mentioned action develops invariably in a short beam provided it is loaded directly on the compressive zone and supported on the opposite face.

From the physical behaviour of directly loaded beams and the appearance of failure in them, it is apparent that the failure is different from the one already described, and is also different from flexure. Firstly, it is different from flexural failure in that the beam no longer behaves like a true beam. It can be described as a tied arch, the tensile reinforcement acting as tie. Secondly, the depth of the compression zone at the tip of the inclined crack can not be equated to the flexural neutral axis depth. Strain readings in concrete and tensile steel indicate that flexural theory cannot be applied to the analysis of this type of structure. The load is directly transferred to the support through an inclined thrust. Measurements of strains along the assumed line of thrust show the existence of inclined compression and thereby support the arching theory.

The arch action is responsible for the residual strength of the beam. It is predominant in short span beams, because while the inclined crack penetrates into the compression zone, its growth is restricted to the face of the vertical load point (in case of a point load).

Finally, failure in such cases is attributable to the failure of the compression zone (crown of the arch) in compression and is referred to as "shear compression failure" (see fig. 3).

This above mentioned failure mode may not be present if the manner of loading is changed from direct to indirect, with the help of cross-beams. Failure may occur immediately after the formation of the shear crack (cracks) as the inclined crack is no longer restricted in its growth inside the compressive zone (due to the vertical compressive stresses resulting from the direct vertical loading). Secondly, if the supports and load points are away from the surface of the beam, the development of arch action is improbable. So in such cases, even in short beams, without web reinforcement, the failure mode is diagonal tension and not shear compression. However the manner of loading is of little significance so far as shear cracking load is concerned.

A different failure mode can also be achieved by applying axial loads to a beam. If axial tension is applied to a beam which would otherwise fail in shear compression, it may fail in diagonal tension. (ref. 48). Similarly, upon application of axial compression, the failure mode can be changed from diagonal tension to shear compression in beams without web reinforcement.

2.4 Behaviour of rectangular beams with web reinforcement:

2.4.1 Beams with long shear span to effective depth ratios:

In the presence of web reinforcement, the equilibrium equations of the shear span are modified, though web reinforcement does not appear to influence the flexural and shear cracking loads appreciably.

From strain readings on stirrups, it appears that they are practically unstressed until they are crossed by an inclined crack. (see chapter - 4). The primary function of the web reinforcement is to bind together the two pieces of concrete already crossed by a crack, and as a result, when the crack width increases the stirrups are stressed in tension. As expressed in Kani's theory[21], they

provide supports by which the concrete below a crack is hung on to the compression zone. The progress of the inclined crack is considerably arrested and the tearing action at the level of tensile steel is reduced which helps the tensile steel to transfer shear across the crack by dowel action.

When the diagonal crack is fully formed, redistribution of internal forces takes place. To achieve this redistribution web reinforcement helps considerably. If sufficient web reinforcement is provided flexural failure may be obtained instead of shear failure.

The possibility of shear transfer across a shear crack by aggregate interlock was thought of no significance in the past. But experiments (chapter - 5) on aggregate interlock show that a considerable portion of shear in a beam can be transferred across a crack by aggregate interlock, provided, of course, the crack width is small. Taylor [54,55] Fenwick[14, 15,43] and Hofbeck, Ibrahim and Mattock[19] also found similar results based on their experimental work. The web reinforcement which holds the two faces of the shear crack together thus increases the possibility of shear transfer due to friction.

The principal shear cracking actions which develop in a beam with web reinforcement are described above. When vertical loading of the beam is continued, the web reinforcement yields. At this stage, the compression zone, which is unable to sustain the extra unbalanced load, gives way. In this case, failure of the compression zone is due to shearing.

The above-mentioned failure mode is observed in beams of long shear spans ($a/d_1 > 2.5$) with web reinforcement. (fig. 2).

2.4.2 Beams with short shear spans:

The shear carrying mechanism in this type of beams is the same as described in the previous section. But the final failure is different in that collapse is caused by crushing of the compressive

zone instead of shearing near the load point (see fig. 3).

2.4.3 Beams with very short shear spans:

Failure is believed to be caused by pure shear in beams with very short shear spans. The vertical load is directly transferred to the supports by inclined thrusts, so that other than arching, the above mentioned shear carrying actions may not be present in this case. Even web reinforcement may not be of much use to increase strength. (fig. 4).

2.5 Description and inclination of failure plane:

Shear failure does not occur along a vertical plane as in case of flexural failure. It occurs always along an inclined plane, having in general an irregular shape. The initiation of the diagonal crack starts near the middle of the beam section and approximately at a distance of d_1 from the position of maximum moment. Then it propagates both ways until the critical condition is reached.

Since in the shortest beams the inclination of the crack is not uniform in the tensile and compressive zones, the failure surface is not plane. The inclination inside the tensile zone is nearer to 45°. But when it penetrates into the compressive zone its inclination is reduced. This is reasonable, because the compressive stresses vary across the depth from a maximum value at top to zero at the position of neutral axis. A reasonable overall value for the average slope seems to be 1 : 2 ($\frac{c}{d_1} = 2$) (see chapter - 4).

Although the inclination inside the compressive zone is never uniform and is always smaller than 45°, the inclination of the failure plane at the neutral axis and below is in substantial accord with the truss analogy. Ohja[41] assumes that the failure plane has two inclinations and on this assumption develops equations to predict average inclination of the failure plane.

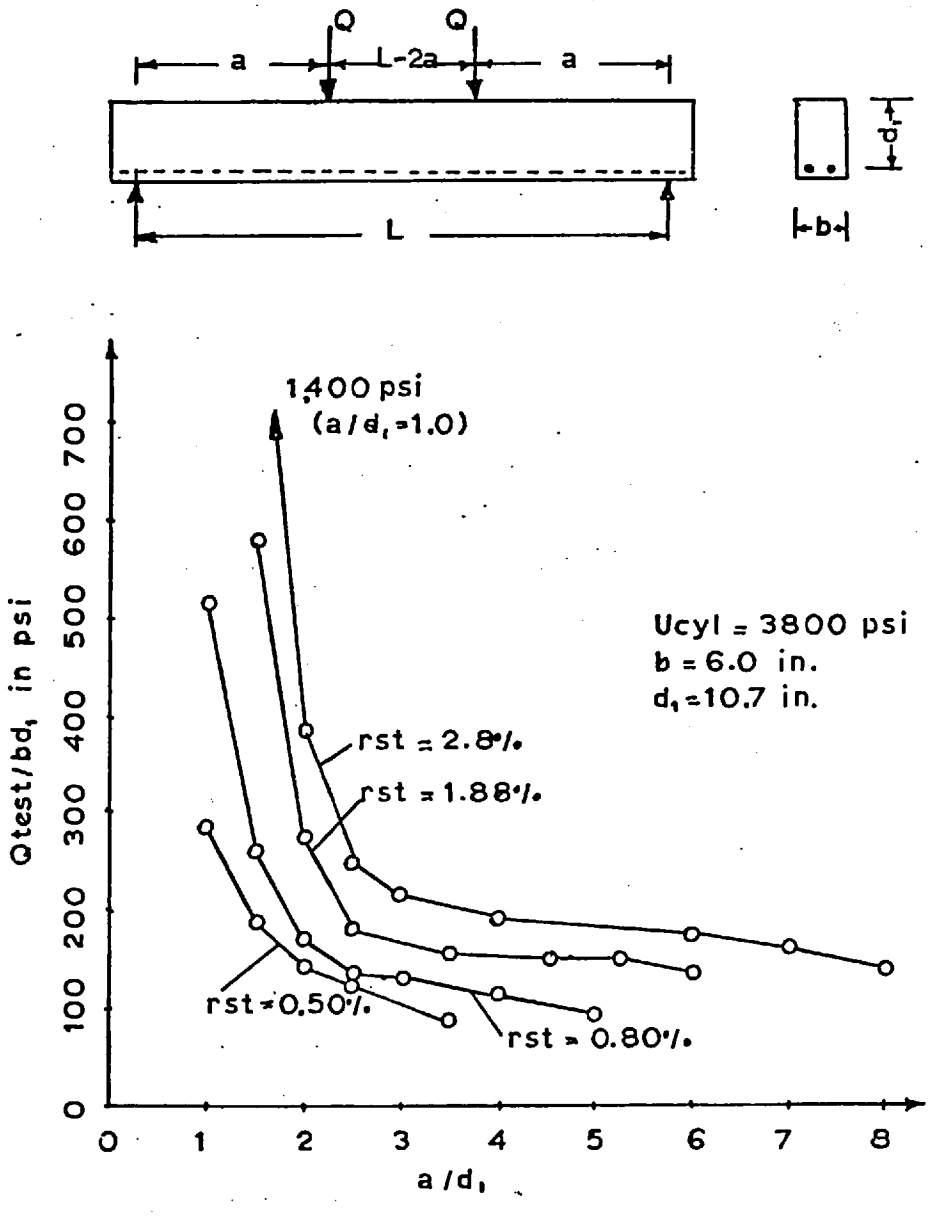
2.6 Parameters affecting the shear capacity of reinforced concrete beams:

There are quite a number of variables which are believed to influence the shear strength of a concrete beam subject to bending and shear stresses. During the last decade, much work has been done throughout the world to determine both qualitatively and quantitatively the influence of each of them on the shear capacity of a beam. But the problem of shear as such has remained unsolved. The influence of some of the parameters known so far is discussed below.

2.6.1 Influence of shear span to effective depth ratio:

Shear span is the distance measured along the axis of the beam from the section of maximum moment to the nearest section of zero moment. This amounts to the distance between the load point and the support of a simply supported beam loaded with two symmetrical loads or one point load. Similarly, in case of a uniformly loaded beam, shear span is one half of the distance between the two supports.

In the past, it was thought that shear span to effective depth ratio had only a minor influence on the shear strength of beams. But the research works reported so far from many parts of the world suggest that shear span to effective depth ratio has considerable effect on the shear strength of a concrete member. It is such an important parameter that it nearly controls the behaviour and mode of failure of beams. Fig. 5 shows the influence of shear span to effective depth ratio on the shear capacity of rectangular beams with two symmetrical point loads reported by Kani[23]. It seems probable as Kani suggested that a transition ratio of a/d_1 exists which could be considered to be about 2.5 for beams with practical tensile reinforcement. If the a/d_1 ratio is smaller than 2.5, beams fail in shear compression while with greater ratios than that they fail by other modes. However this transition ratio is not strictly a constant, but is dependent on a number of parameters (see fig. 5).



EFFECT OF a/d, RATIO ON THE SHEAR STRENGTH OF BEAMS WITHOUT WEB REINFORCEMENT (KANI)

FIG. 5.

2.6.2 Influence of concrete strength:

Concrete strength influences appreciably the ultimate load of beams failing in shear compression. The shear strength of a beam is increased with the increasing concrete strength, but the rate of increase is reduced with increasing concrete strength. Fig. 6 shows the influence of concrete strength on the ultimate load carrying capacity of beams. The beams were loaded directly with two symmetrical point loads. For comparison, other parameters were not varied.

2.6.3 Effect of ratio of tensile steel:

With increasing ratios of tensile steel, the shear strength of beams is increased. Tensile reinforcement has various roles to play. After the formation of flexural cracks, it controls their growth as well as widths. Secondly, after the formation of the inclined crack, when a beam is transformed to an arch, the tensile reinforcement acts as a tie.

Another possibly important function of tensile reinforcement is that it transfers shear across a crack acting as dowel.

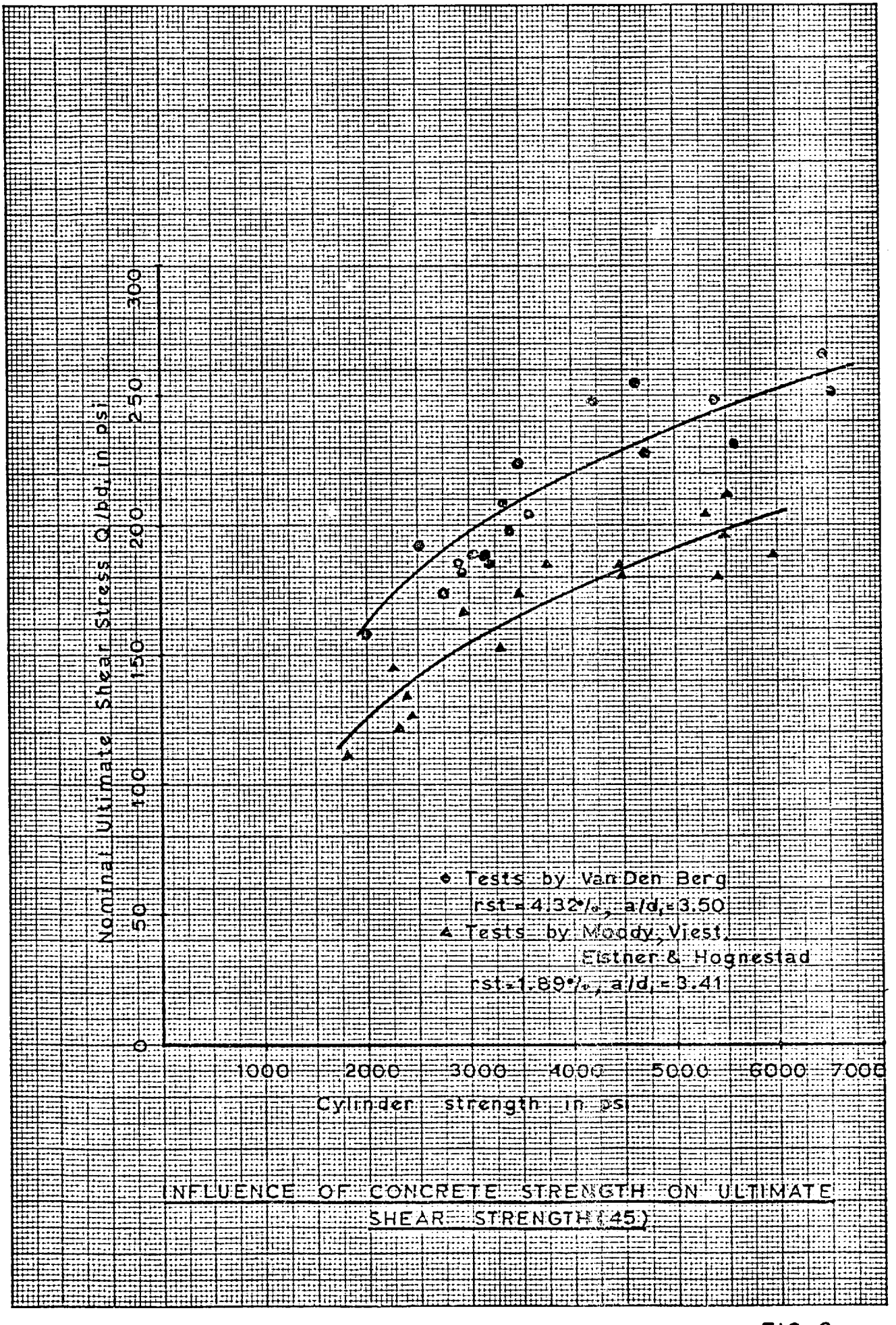
The ultimate load is not affected by the yield stress of the reinforcement so long as the failure is not caused by yielding of the reinforcement.

The influence of main steel ratio is much more prominant than concrete strength which is illustrated in fig. 5.

2.6.4 Influence of web reinforcement:

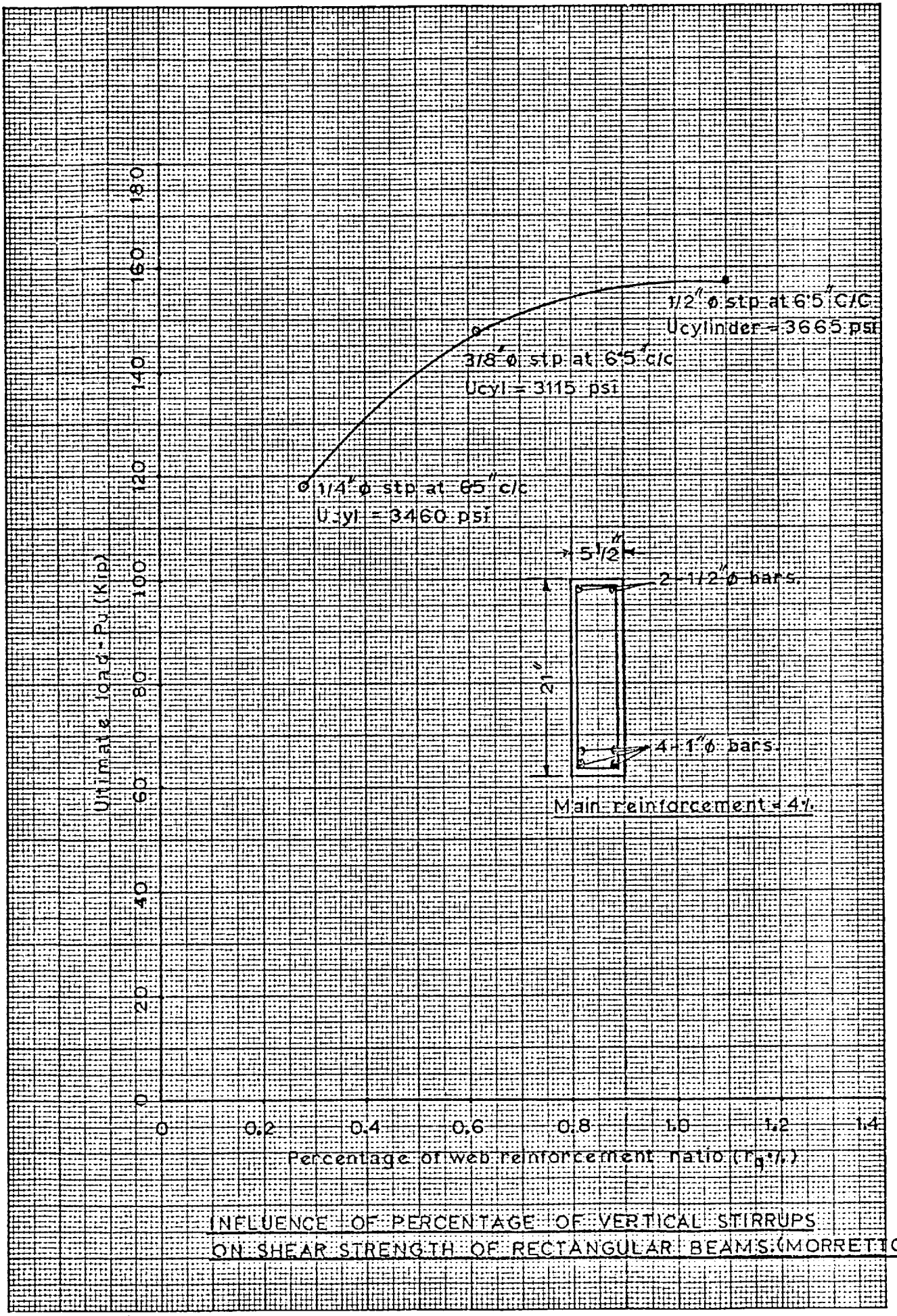
From the comparison of shear forces carried by reinforced concrete beams with and without web reinforcement, the influence of web reinforcement on the ultimate load is found to be considerable. The shear reinforcement not only influences the load carrying capacity of the beam but also changes the failure mode. Web reinforcement further restricts the growth and widths of cracks.

The shear strength of a beam is increased with increasing ratios of web reinforcement, but below a certain amount of web reinforcement,



INFLUENCE OF CONCRETE STRENGTH ON ULTIMATE SHEAR STRENGTH (45)

FIG. 6.



INFLUENCE OF PERCENTAGE OF VERTICAL STIRRUPS ON SHEAR STRENGTH OF RECTANGULAR BEAMS. (MORRETTO)[53]

FIG. 7.

its effect is negligible and as a result the beam does not gain in strength as expected. Similarly, web reinforcement cannot possibly go on increasing the shear strength of a beam indefinitely. The ultimate strength of a beam is at the same time dependent on other parameters. Fig. 7 shows the effect of web reinforcement on the ultimate shear strengths of beams.

It is evident from the graph that the rate of increase in shear strength with increasing web reinforcement is greater at low values of ratio of web reinforcement ($rqfyq = \frac{Aq}{bs} fyq$) than at high ones.

2.6.5 Effect of compression reinforcement:

The effect of compression reinforcement on shear is still obscure. Some investigators (Wilby)[39], found that with increasing ratios of compression steel, the shear strength is decreased. He argued that it was due to the high horizontal shearing stress in the concrete at the level of compression reinforcement, with rapid consequent horizontal splitting of concrete at that level and release of bond. His conclusion was that the influence of compression reinforcement is either non-existent or harmful to the shear strength of a beam. Similar findings were reported by other researchers.

Since compression reinforcement affects the depth of neutral axis and strength of the compressive zone, if the failure is dependent on the strength of the compressive zone, then compression steel should have some bearing on the shear strength. This may be the reason why another school of thought exists and the investigators do take into account a beneficial effect of compression reinforcement. In some cases, it may be possible for compression reinforcement to account for the loss of concrete area, offsetting the harmful effect already memtioned, and provide a slightly higher compressive resistance.

Compression reinforcement resists failure of a secondary nature when a beam is subjected to axial tension. With a lesser amount of compression (or rather top) steel, the ultimate strength of a beam

subjected to axial tension is reduced.

2.6.6 Influence of manner of loading:

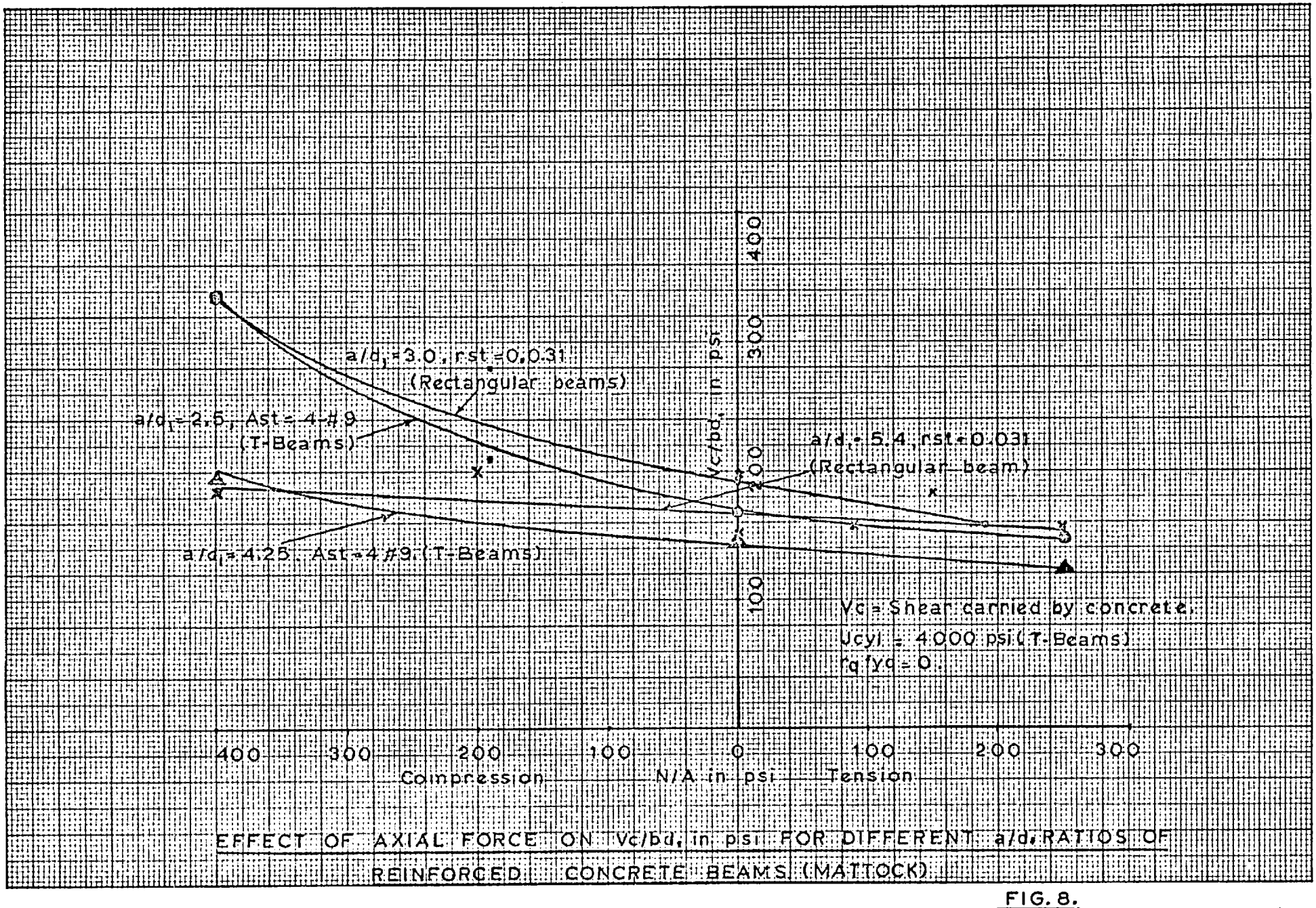
Generally, in the laboratory, testing is done by directly applying the load on the top surface of a beam. In practice, such ideal conditions hardly exist. Loading is commonly through secondary members or in other words the beams are loaded indirectly. Test results obtained with indirect types of loading suggest that manner of loading has some bearing on shear strength of a beam. If beams are loaded through cross-members the increase of shear strength with decrease of shear span to effective depth ratio is found to be less than in case of beams with the dire ' type of loading.

The influence of manner of loading on beams failing in diagonal tension is of little significance. But its influence is remarkable in case of some beams without shear reinforcement failing in shear compression. This indirect type of loading leaves little chance for the beam to develop arch or truss action and as a result in the absence of these two actions the beam fails prematurely in diagonal tension and not in shear compression. This phenomemon is attributable to the fact that a direct load induces vertical stresses below it inside the beam. These stresses restrict the growth of the inclined crack in case of direct loading and extra strength is added to the beam by the uncracked compressive zone left over the crack. Also, it helps in the development of the arch action. In this case, failure is by shear compression and not by diagonal tension.

Similarly, in beams with web reinforcement, the failure mode may be changed from shear compression to shearing if the loading is indirect instead of direct.

2.6.7 Effect of axial forces:

Axial force influences the shear strength of reinforced concrete beams. Sometimes the failure mode is also affected. If axial compression is applied, in addition to bending moments and shear



EFFECT OF AXIAL FORCE ON Vc/bd, in psi FOR DIFFERENT a/d RATIOS OF REINFORCED CONCRETE BEAMS (MATTOCK)

FIG. 8.

forces, the shear strength of beams increases while on the other hand, with the application of axial tension, the shear strength is decreased. The effects of axial forces on shear strength are illustrated in fig. 8 for beams without shear reinforcement. Axial tension does not affect the shear cracking load much, but axial compression affects it considerably.

An axial force affects the compatibility and equilibrium conditions of the shear span of a beam. It does not affect the equation of vertical equilibrium as such. But its effect on the neutral axis depth influences the shear capacity of the beam.

The effect of axial force on the mode of failure of a beam is interesting. Axial compression can change the mode from diagonal tension to shear compression while axial tension can have the reverse effect.

The effect of axial forces on the shear strength of a beam is illustrated in fig. 8 for beams without web reinforcement.

2.6.8 Conclusions:

The shear cracking load is that at which the inclined crack is fully developed. A beam cannot fail in shear before the formation of an inclined shear crack. So for a beam to fail in shear, the pre-requisite is the formation of shear cracks. All beams show signs of distress at the shear cracking load, because this is the stage at which true beam action is destroyed. If a beam is capable of sustaining more load by other actions it continues to do so. Under these circumstances, it is logically necessary to devise some means of predicting the shear cracking load of a beam.

After the formation of shear cracks, the behaviour of a beam is changed, which warrants a separate analysis in order to predict the ultimate load it can sustain. This analysis is valid only when the beam has some residual strength. Otherwise, it fails at the

shear cracking load.

In such an analysis, the effects of all the parameters discussed in the previous sections need to be considered. Any analysis made neglecting the effect of some of them would not be generally valid.

CHAPTER - 3

STUDY OF PREVIOUS WORKS ON SHEAR AND REVIEW OF THE EXISTING THEORIES ON THE SHEAR STRENGTH OF BEAMS SUBJECTED TO BENDING MOMENT, SHEAR FORCE AND AXIAL LOAD.

Shear failure is not a single failure problem and any theory based on a single type of shear failure cannot depict the true failure mechanisms. From the physical behaviour and modes of failure of beams, it is apparent that different theories and analyses are needed to predict the strengths of beams of differing types and load configurations. Many of the theories do not take account of this and consequently predict erronous results.

Reinforced concrete beams failing in shear undergo transformations from one load carrying mechanism to another when loaded to failure. The first and the important change in behaviour of a beam takes place following shear cracking. This change in behaviour is also dependent on shear reinforcement if present, and the failure mode is found to be different with and without the presence of shear reinforcement in beams with long shear spans. Beams with short shear spans do not fail at the shear cracking loads even in the absence of shear reinforcement, and the failure mode is not diagonal tension but shear compression.

A large number of theories exist which can be employed to predict strength of reinforced concrete beams failing in shear.

The theories that are put forward so far by researchers can broadly be classified into two categories :-

1. Theories predicting shear cracking loads or failure loads in case of diagonal tension failure ; and

2. Theories predicting ultimate strengths of members with shear cracks.

3.1 Shear cracking theories:

3.1.1 Empirical shear cracking equations:

a) Classical theory:

This famous theory is due to Mörsch and has until recently been widely accepted as the basis of design in the codes of practice of many countries.

He propounded that shear failure in beams was due to diagonal tension rather than to horizontal shear, and he developed an equation for a nominal shear stress[2]. His argument is based on the fact that if a state of pure shear stress exists, then tensile stresses of the same magnitude must exist on a plane inclined to the shear plane at 45° angle. If in any section, the tensile stress is very small compared to the shear stress, then the nominal shear stress can be regarded as the measurer of diagonal tensile stress. His equation

$$q = \frac{Q}{bla} \qquad 3.1.1$$

is intended to predict the diagonal tensile stress at a section of a beam on the following assumptions -

a) Concrete and steel are homogenous and isotropic.

b) Stresses do not exceed the proportional limits.

c) Beams have constant cross-sections.

d) The distribution of the shearing stresses is uniform across the widths of beams.

e) Concrete carries no flexural tension below the neutral axis but carries a uniform (and maximum) shear throughout the tensile zone.

If the shear stress q is equated to the tensile strength of concrete the method gives very unsafe predictions of shear resistance in many cases.

b) Shear cracking equation of ACI - ASCE Committee (3 2 6)[2].

The collapse of a warehouse roof due to the shear failure of a beam without web reinforcement prompted the research conducted in the field of shear in America during the last decade; and as a result many empirical equations predicting the first shear cracking load were presented to the Committee.

The Committee finally accepted the following equation to predict shear cracking loads -

$$\frac{Qcr}{bd_1} = K_1\sqrt{Ucyl} + K_2 \, rst \, \frac{Qd_1}{M} \qquad 3.1.2$$

Before the acceptance of the above equation by the Committee, I.M. Viest[2] made an attempt to develop an equation for diagonal cracking loads based on the principal tensile stress theory.

The following are the assumptions -

1. Variations in the lever arm factor may be neglected.
2. Diagonal tensile cracking occurs when ft(max) exceeds the tensile strength of concrete.

   where ft(max) = maximum principal tensile stress.
3. The tensile strength of concrete is proportional to the square root of the cylinder strength of concrete.
4. The modulus of elasticity of concrete is constant.
5. The modulus of elasticity of concrete is proportional to the square root of the cylinder strength.

The equation of principal tensile stress gives -

$$ft(max) = \tfrac{1}{2}ft + \sqrt{(\tfrac{1}{2}ft)^2 + q^2} \qquad 3.1.3$$

where ft = magnitude of longitudinal tensile stress and

q = magnitude of shear stress in a section under consideration.

The magnitude of tensile stress in the concrete is difficult to determine once flexural cracks are formed. Hence Viest made a further assumption that the tensile stress in the concrete is proportional to the tensile stress in steel computed by cracked section theory.

This gives -

$$ft = c^1 \times \frac{fs}{m}$$

$$= c \frac{M}{m\ rst\ bd_1^2\ la} \qquad 3.1.4$$

where - c^1 and c are constants

M = External bending moment.

m = modular ratio.

rst = Ratio of tensile steel to area of concrete ($^{Ast}/_{bd_1}$)

la = lever arm.

Neglecting variations in the moment lever arm and changing the constant,

$$ft = F_1 \frac{M}{m\ rst\ bd_1^2} \qquad 3.1.5$$

where F_1 is a new constant.

Similarly, in absence of any direct method to find it, the magnitude of the shear stress was assumed proportional to the average

shear stress in the cross-section.

$$q = F_2 \frac{Q}{bd_1} \qquad 3.1.6$$

where F_2 = constant

Q = shear force

Substituting the values of ft and q in equation 3.1.3, a relationship for the critical external shear force is obtained as:

$$\frac{Q}{bd_1} = \frac{ft(max)}{\frac{1}{2}F_1 \, M/m \; rst \; Qd_1 + \sqrt{(\frac{1}{2}F_1 \, M/m \; rst \; Qd_1)^2 + F_2^2}} \qquad 3.1.7$$

From assumptions (2), it follows that

$$ft(max) = Ut \, ,$$

and with $m = \frac{Es}{Ec}$; the above equation can be rewritten as

$$\frac{Q}{bd_1 Ut} = \frac{1}{C_1 \frac{Ec}{Es \; rst} \times \frac{M}{Qd_1} + \sqrt{(C_1 \frac{Ec}{Es \; rst} \times \frac{M}{Qd_1})^2 + C_2^2}} \qquad 3.1.8$$

where C_1 and C_2 are new constants.

The above equation is dependent on two parameters composed of groups of variables - namely - $Q/bd_1 Ut$ and $(\frac{Ec}{Es \; rst})(\frac{M}{Qd_1})$

The parameters can again be simplified on basis of assumptions 3, 4 and 5. Thus the above two parameters become -

$$Q/bd_1\sqrt{Ucyl} \quad \text{and} \quad \sqrt{\frac{Ucyl}{rBt}} \cdot (\frac{M}{Qd_1})$$

Experimental values of the parameter $Q/bd_1\sqrt{Ucyl}$ and the inverse of the parameter $\sqrt{\frac{Ucyl}{rst}} \cdot (\frac{M}{Qd_1})$ were plotted and the graph was represented

by two straight lines giving the following relationship.

$$\frac{Qcr}{bd_1\sqrt{Ucyl}} = 1.9 + (2500) \times \frac{rst\ Qd_1}{M\sqrt{Ucyl}} \leq 3.5 \qquad 3.1.9$$

in lbf and inch units.

where Qcr = external shear at diagonal tensile cracking load.

Ucyl = Cylinder strength of concrete in psi.

$\sqrt{Ucyl}$ is also in psi unit.

M = External bending moment at the section considered.

The committee further put restrictions on the section to be analysed by the equation. The equation should be applied to any section subject to the following limits -

1. If the shear span 'a' $> 2d_1$, the equation shall not apply within a distance d_1 from either the load point or the support.
2. If $2d_1 \geq a \geq 0.75\ d_1$, the equation shall be applied only at the section located in the middle of the shear span.
3. If $a < 0.75\ d_1$, the equation shall not apply at all.

In all cases, the upper limit to Qcr/bd_1, of $3.5\sqrt{Ucyl}$ must be retained.

Effect of axial force on shear strength:

If, in addition to bending moment and shear, an axial force is applied to a section, the shear strength of the section is affected. The committee took account of the effect of axial load on longitudinal stresses considering only the moment equilibrium equation .

If a section is subject to a bending moment M and an axial force N, then they may be replaced by an eccentric load N acting

at a distance 'e' from the centre of the tensile reinforcement;

where $e = \frac{M}{N} + (d_1 - d/2)$

Using the conventional straight line theory, the equilibrium of moments about the centroid of the internal compressive force in the concrete gives the following expression for steel stress

$$fs = \frac{N(e - la)}{Astla}$$

Also, $N(e - la) = M + N(d_1 - la - d/2)$

$$= M + N\,d_1(1 - \frac{la}{d_1} - \frac{d}{2d_1})$$

And $Astla = la\,rst\,bd_1$

$$\therefore fs = \frac{M + \beta N d_1}{rst\,bd_1\,la}, \qquad \text{where } \beta = (1 - \frac{la}{d_1} - \frac{d}{2d_1})$$

N = +ve for compression.

Thus, the committee believed that if the bending moment at any section were corrected, the previous equation should be applicable to members with axial load.

$$\frac{Qcr}{bd_1} = 1.9\sqrt{Ucyl} + 2500\,\frac{rst\,Qd_1}{M + \beta N d_1} \qquad 3.1.10$$

The upper limit of $\frac{Qcr}{bd_1}$ without axial load is $3.5\sqrt{Ucyl.}$ This implies that the diagonal tensile strength is independent of the longitudinal tensile stress when the bending moment is very small. On this assumption the committee assumed that when M = 0, the effect of axial load would be its effect on the principal tensile stresses.

If a portion of a member is uncracked, then the longitudinal stress = $\pm N/bd_1$ (or more correctly $\frac{N}{bd}$)

From the principal stress equation -

$$f_t(max) = -\tfrac{1}{2}N/bd_1 + \sqrt{(-\tfrac{1}{2}N/bd_1)^2 + (F_2\,Q/bd_1)^2},$$

which gives

$$\frac{Qcr}{bd_1} = \frac{ft(max)}{F_2}\sqrt{1 + \frac{N}{bd_1\, ft(max)}}$$

Assuming that principal tensile stress is equal to $ft(max) = 7.5\sqrt{Ucyl}$, to evaluate F_2, when there is no axial load, and M = 0,

$$\frac{Qcr}{bd_1} = \frac{ft(max)}{F_2} \times 1 = 3.5\sqrt{Ucyl}$$ (the upper limit of $\frac{Qcr}{bd_1}$)

so $$\frac{Qcr}{bd_1} = 3.5\sqrt{Ucyl}\sqrt{1 + \frac{N}{bd_1\, 7.5\sqrt{Ucyl}}}$$

or $$\frac{Qcr}{bd_1\sqrt{Ucyl}} = 3.5\sqrt{1 + \frac{0.133N}{bd_1\sqrt{Ucyl}}} \qquad 3.1.11$$

For the practical range of concrete strengths the term $\frac{0.133}{\sqrt{Ucyl}}$ varies between 0.0015 and 0.003. So the committee replaced the term $\frac{0.133}{\sqrt{Ucyl}}$ by a constant value of 0.002. Accordingly, the upper limit to diagonal tensile strength of members with axial load becomes -

$$\frac{Qcr}{bd_1\sqrt{Ucyl}} = 3.5\sqrt{1 + \frac{0.002N}{bd_1}} \qquad 3.1.12$$

Thus, the Committee's equation to predict shear cracking (diagonal tension failure) load of members subjected to combined bending moment, shear force and axial load is

$$\frac{Qcr}{bd_1\sqrt{Ucyl}} = 1.9 + 2500\,\frac{rst\, Qd_1}{M + \beta Nd_1\sqrt{Ucyl}}$$

$$\leq 3.5\sqrt{1 + \frac{0.002N}{bd_1}} \qquad 3.1.13$$

In general, the ACI equation is fairly safe for beams with normal shear spans and percentages of tensile steel. Only the influence of

high ratios of tensile steel is underestimated in comparison with test results. On the otherhand, beams with higher concrete strengths and low percentages of tensile steel may be unsafe[45].

c) CEB Equation :

The CEB[10] does not recommend in principle, the design of any beam type member, without shear reinforcement and suggests that the limit state should not be reached by failure of the concrete.

The CEB design method is based on the Ritter-Mörsch lattice, and the design tangential (shear) stress is calculated from the equation -

$$\tau_o^* = \frac{Tr^*}{boh} \qquad 3.1.14$$

where τ_o^* = Design value of tangential (shear) stress in the web of a member.

Tr^* = Reduced design shear force.

bo = Width of web

h = Effective height (depth) of the member.

The CEB has not formulated any shear cracking equation as such. For comparison, it is advisable to use the equation for beams with web reinforcement ignoring the contribution of the web reinforcement to ultimate load. (see section 3.2.)

Thus, the CEB shear cracking equation would be

$$\frac{Qcr}{bd_1} = 0.1875\sqrt{Ucyl}\ (0.5 + 33\ \frac{Ast}{bd_1}) \quad \text{without any axial load.} \qquad 3.1.15$$

In the presence of axial compression -

$$\frac{Qcr}{bd_1} = 0.1875\sqrt{Ucyl}\ (1 + 2\ \frac{N/bd_1}{Ucyl})(0.5 + 33\ \frac{Ast}{bd_1}) \qquad 3.1.16$$

and in presence of axial tension -

$$\frac{Qcr}{bd_1} = 0.1875\sqrt{Ucyl}\,(1 - 6\,\frac{N/bd_1}{Ucyl})(0.5 + 33\,\frac{Ast}{bd_1}) \qquad 3.1.17$$

in N and mm units.

where $(0.5 + 33\,\frac{Ast}{bd_1}) \leqslant 1$ for both cases.

In all cases N is positive.

These equations have been transformed from design equations as explained in section 3.2. The equations appear preferable to the ACI equation in that the effect of tensile reinforcement is taken in a better way. So far as long shear spans are concerned, this equation does not predict any change in strength for varying shear spans. If the tensile reinforcement term is neglected, the strength predicted by the above equations is about half that predicted by the ACI equation. Thus it altogether avoids the prediction of any unsafe results arising out of overestimation of the concrete's contribution and underestimation of the tensile reinforcement's contribution. So far as axial loads are concerned, they predict a rapid decrease in strength with axial tension, and a slower increase in strength with axial compression. As a result, though they predict strengths of beams without axial loads in good agreement with test results, yet are found to be conservative in the other two cases. Since the equations are completely empirical, these inherent drawbacks could be rectified by replacing the present constants by more suitable ones.

d) Empirical equation of Mattock:

A recent empirical equation taking the effect of axial force into account is due to A.H. Mattock[36] who tried to develop a method of design which would be applicable to prestressed as well as reinforced beams with or without axial forces. He tested 31 rectangular beams

with varying shear spans, percentages of tensile reinforcement, concrete strengths and axial forces. These beams were without web reinforcement.

He observed that axial loads affected the flexural cracking loads but apparently did not affect the increment of shear between flexural cracking and shear cracking.

So he made an attempt to revise the ACI 318-63 equation for prestressed concrete beams -

$$Qcr = 0.6\ b\ d_1\sqrt{Ucyl} + \frac{Mcr}{\frac{M}{Q} - d_{\frac{1}{2}}} + Qd \qquad 3.1.18$$

where $Mcr = \left(\frac{I}{y}\right)\left(6\sqrt{Ucyl} + fpe - fd\right)$, in F.P.S. units.

Qd = dead load shear

fpe = extreme fibre stress due to prestress, psi

fd = extreme fibre stress due to dead load, psi

$Ucyl$ = cylinder strength of concrete, psi

I = second moment of area of section about its centroid.

y = distance from centroid to extreme fibre in the tensile zone.

so that it could be used for predicting shear strengths of reinforced concrete beams.

His object was to replace the term $0.6\ bd\sqrt{Ucyl}$ by one dependent on the flexural reinforcement as well as the concrete strength.

By examining his test data, he found out that the increment of shear force between flexural cracking and shear cracking was dependent on two parameters -

1. the percentage of flexural reinforcement, and
2. the modular ratio $\left(\frac{Es}{Ec}\right)$

He thought it better to correlate the increment of shear between flexural cracking and shear (diagonal) cracking with the product of the modular ratio and percentage of tensile steel instead of correlating with them separately.

From the plot of his data he arrived at a relationship -

$$\frac{\text{Increment of shear stress}}{\sqrt{Ucyl}} = 1.25 + 5.0\ mr_{st} \qquad 3.1.19$$

where m = modular ratio $= \frac{Es}{Ec}$

$= 29{,}000{,}000/_{w^{1.5}}\ 33\sqrt{Ucyl}$

w = unit weight of concrete. (weight/cu ft)

rst = ratio of tensile steel to concrete area.

$= As/_{b\ d_1}$

$Ucyl$ = cylinder strength of concrete in psi

$\sqrt{Ucyl}$ = also in psi

The equation for diagonal (shear) cracking becomes ?

$$\frac{Qcr}{bd_1} = (1.25 + 5\ m\ rst)\sqrt{Ucyl} + \frac{Mcr}{(\frac{M}{Q} - d_{1/2})\ bd_1} + \frac{Qd}{bd_1} \qquad 3.1.20$$

in foot pounds units

He found that the above equation did not give satisfactory results so far as the rectangular bonded prestressed beams of Sozen, Zwoyer and Siess[49] were concerned. Therefore for these beams he adopted another equation to fit the test results -

$$\frac{\text{shear stress increment}}{\sqrt{Ucyl}} = (1.75 - \frac{0.036}{mrst} + 4.0\ m\ rst) \qquad 3.1.21$$

Thus the equation becomes -

$$\frac{Qcr}{bd_1} = (1.75 - \frac{.036}{mrst} + 4.0\ m\ rst)\sqrt{Ucyl} + \frac{Mcr}{(\frac{M}{Q} - d_{1/2})\ bd_1} + \frac{Qd}{bd_1}$$

3.1.22

The applicability of equation 3.1.20 is dependent on the percentage of tensile steel. He limited its applicability to rst% > 1%, whereas equation 3.1.22 can be used for any amount of flexural reinforcement.

The upper limit of these two equations is

$$\frac{Qcr}{bd_1} = 3.5\sqrt{Ucyl} + 0.3\ {}^{N}/_{A} \qquad 3.1.23$$

If there is prestress, then ${}^{N}/_{A}$ is replaced by fpc, the average stress due to prestress, N = axial force

A = area of concrete (bd)

Equation 3.1.20 as it stands is not strictly reducible if rst = 0. But as is obvious when rst = 0, the increment of shear stress between flexural cracking and shear cracking is zero, which is not the trend of the equation.

Comparisons of test results with Mattock's equation are given in chapter 7.

Since his equation is applicable only for beams without web reinforcement, the shear cracking load is compared. But as Leonhardt[29] observed that test results of beams without web reinforcement are not sufficient as a guide to develop design equation, it was not possible to examine the equation thoroughly in terms of results for beams with web reinforcement without modification.

However, the attempt to develop one equation to predict the shear cracking strengths of prestressed and reinforced beams deserves appreciation.

c) Empirical equation of Petersson:[45]

Petersson proposed an empirical equation of the form -

$$Qc/bd_1 = 1.3\ Uw^{1/3}(rst\%)^{\frac{1}{2}} \qquad 3.1.24$$

where $\frac{Qc}{bd_1}$ and Uw are in Kg/cm^2 unit.
and also $Uw^{1/3}$ in Kg/cm^2 unit.

This is a shear cracking equation and is not applicable for the shear compression type of failure. Petersson considers the limiting value of a/d_1 for the two types of failure is equal to 3.5 for point loaded beams.

In case of T-beams, b is replaced by bw, the web breadth.

This equation predicts the influence of tensile reinforcement on shear nearer to reality than the ACI and CEB equations.

3.1.2 Analytical shear cracking equations:

a) Kani's[22,45] shear cracking equation:

Kani assumes that after the formation of flexural cracks, the block of concrete in between any two cracks behaves like a plain concrete cantilever. The block of concrete is assumed to be rigidly connected to the concrete compression zone and loaded at its end by the bond force (fig. 10). Shear cracking is assumed to be the flexural failure of the concrete cantilevers.

Using simple bending theory the flexural resistance of each tooth

$$= R\, bx^2/6 \qquad 3.1.25$$

where R = modulus of rupture strength of concrete

x = distance between two flexural cracks.

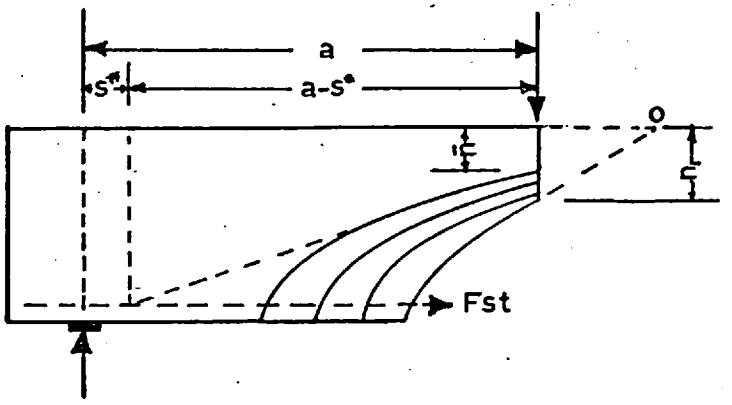
If the tooth is loaded with a bond force F_b, then the moment at the fixed end

$$= F_b\, h \qquad 3.1.26$$

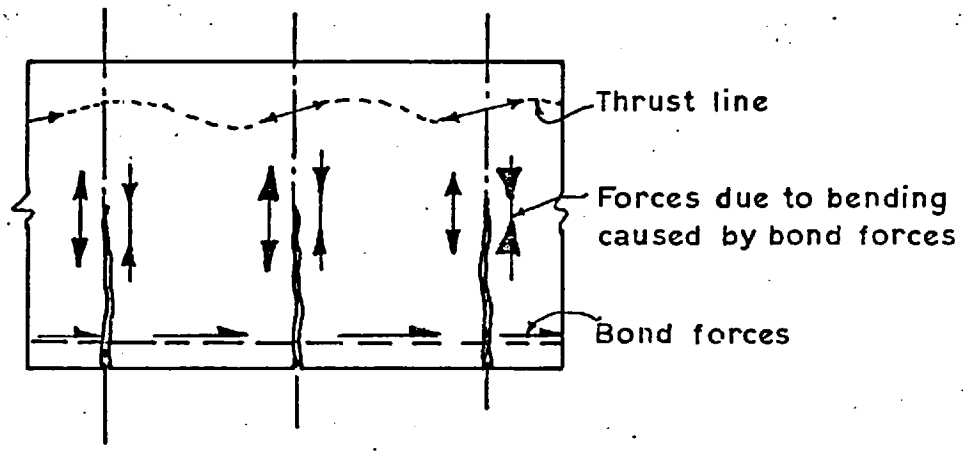
when h = depth of penetration of flexural cracks measured from the centre of tensile steel.

Equating the above two equations for failure of the cantilever -

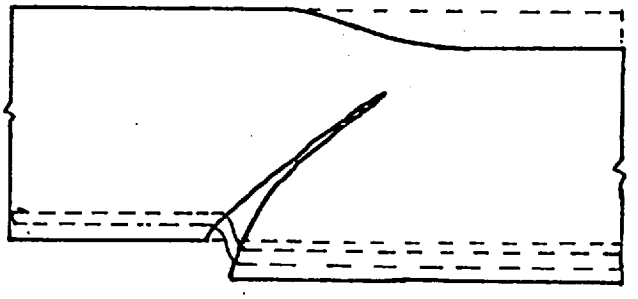
$$F_b = \frac{R\, bx^2}{6h} \qquad 3.1.27$$



PEELING OFF OF TEETH IN BEAMS WITHOUT WEB REINFORCEMENT (KANI) FIG. 9.



INTERNAL FORCES IN A BEAM CRACKED IN FLEXURE (KANI) FIG. 10.



DOWEL ACTION OF TENSILE STEEL FIG. 11.

For a simply supported beam loaded with one central or two symmetrical point loads -

$$F_b = \frac{dM}{dx} \times \frac{x}{la} = \frac{Qx}{la} \qquad 3.1.28$$

From equations 3.1.27 and 3.1.28,

$$\frac{Qx}{la} = \frac{R\, bx^2}{6h}$$

or

$$Q = \frac{R\, b\, la\, x}{6h} \qquad 3.1.29$$

where Q is the shear cracking load.

It is obvious that the value of $\frac{x}{h}$ is not easy to determine. Thus, the equation developed by Kani to predict shear cracking load is not as simple as it appears to be. A crack pattern is to be assumed first. Also to find the minimum strength, the minimum value of $\frac{x}{h}$ is to be found out. Moreover, the flexural cracks are not always parallel, and the physical appearance of a beam at the time of shear cracking does not suggest the failure of the concrete cantilever envisaged by Kani.

In his theory, Kani completely neglected the effect of dowel action of tensile steel and shear transfer by interlock.

Even neglecting the effect of interlock, dowel action of tensile steel alone produces a couple opposite to that produced by the bond force.

The writer believes this may be the reason why his theory does not agree with test results.

b) Regan's shear cracking theory, [45,44]

Regan made an attempt to analyse theoretically a section failing in shear depending on physical behaviour. He developed three different equations for different types of shear cracking conditions -

1. shear cracking of rectangular sections already cracked in flexure.
2. shear cracking of T, L, and I sections cracked in flexure.

Derivation of equation for case a).

He assumes that in the presence of flexural cracks at a section, the shear is carried by the inclination of the thrust $(\frac{Qc}{Foc})$ in the concrete. His assumptions are -

1. At a section containing a flexural crack, the bond between concrete and steel is destroyed.
2. In order to calculate the shear stress distribution above the crack, he uses the condition of horizontal equilibrium of the longitudinal stresses. The strain profile across the section is assumed to be linear and the stress-strain curve to be parabolic.
3. He uses a biaxial failure criterion for Concrete obtained from the Mohr's circles for uniaxial tension and compression with a common tangent.

For shear cracking of a section already cracked in flexure, his simplified equation is

$$Q_{cr} = q_{cr} \text{ no } bd_1 \qquad 3.1.30$$

where q_{cr} = critical average shear stress.

$= Ucyl^{2/3}$, both are in lbf/in^2.

no = neutral axis depth factor for fully developed stress block with extreme fibre strain of $E'_{cc} = .0035$.

The equation for no is given by

$$\frac{no^2}{1 - no} = \frac{E_s \; rst \; E'_{cc}}{^2/_3 U_{cyl}} = \psi$$

$$\text{or} \qquad no = \tfrac{1}{2}\left[-\psi + \sqrt{\psi^2 + 4\psi}\right]$$

Derivation of equation for case b).

In this case he considers Kani type concrete "teeth" of the web between flexural cracks. It is assumed that flexural failure of the teeth is avoided due to redistribution of bond and also due to couples caused probably by aggregate interlocking forces across the cracks. The failure of the teeth is assumed to be in shear or combined bending and shear.

His equation is

$$Qcr = 0.6 \; q_{cr} \; b_r \; d_1 \qquad 3.1.31$$

Derivation of equation for case c).

The equation is obtained from principal tensile stress analysis and then as a numerical approximation

$$Qcr = \left(1 - 0.5 \; \frac{M}{Qd_1}\right) q_{cr} \; bd_1 \qquad 3.1.32$$

where $\frac{M}{Qd_1}$ is to be considered at a distance d_1 from the load point.

This equation is also applicable to flanged beams by substituting br (web breadth) for b when the value of Qcr given by this equation is greater than those given by equations 3.1.30 and 3.1.31.

c) Attempts have been made by a number of other researchers to produce theoretical work in this field. Among them are Lorentsen, Krefeld and Thurston and Jones. A full account of their work is given in reference 45.

The Regan theory of shear cracking is based on study of physical

behaviour of beams and would be more realistic than other theories, except for its complete neglect of interlock. (see chapter - 5). His approach of connecting equilibrium equations with compatibility conditions is new in this field. The empirical validity of this theory is supported by more than 1000 test results [45,44]. His proposed equations can be used to predict the shear cracking load of a beam subject to axial loads provided the effect of axial load is taken account of in calculation of neutral axis depth (no d_1). But his equations go wrong when applied to a section at the point of contraflexure of a continuous beam, subject to axial tension in which case no and thence Qcr become zero which is far from correct.

3.2. Theories predicting ultimate strength of a section in shear

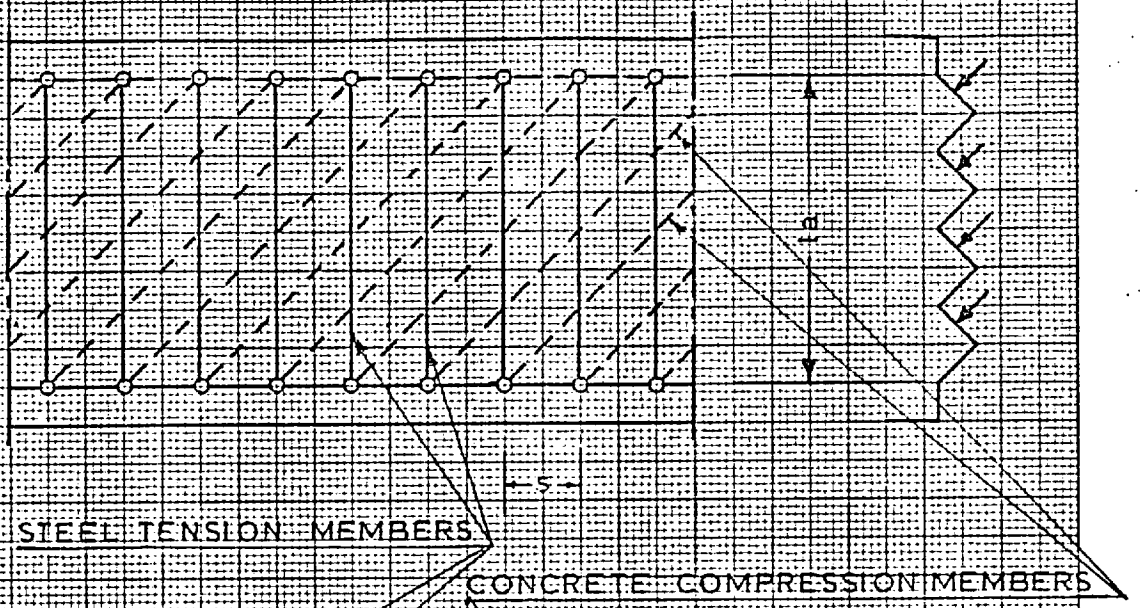
3.2.1. Empirical equations:

a) Mörsch Truss Analogy:

The behaviour of a reinforced concrete beam with web reinforcement may be assumed to be similar to a truss[2]. The compressive zone of the beam acts as the top chord and the tensile steel as the bottom chord of the model truss (fig - 12). The web reinforcement and the concrete in the tensile zone are the web members. The basic assumptions are -

1) The tensile reinforcement carries only horizontal flexural tensile stresses.
2) The concrete compressive zone above the neutral axis carries only horizontal flexural compressive stresses.
3) All inclined and vertical tensile stresses are taken care of by the stirrups and bent-up bars.

In order to develop a general expression for the stresses in the stirrups, the stirrups are assumed to be inclined to the axis of the beam at an angle α and the inclination of the crack to be θ.



MÖRSCH TRUSS ANALOGY. FIG. 12.

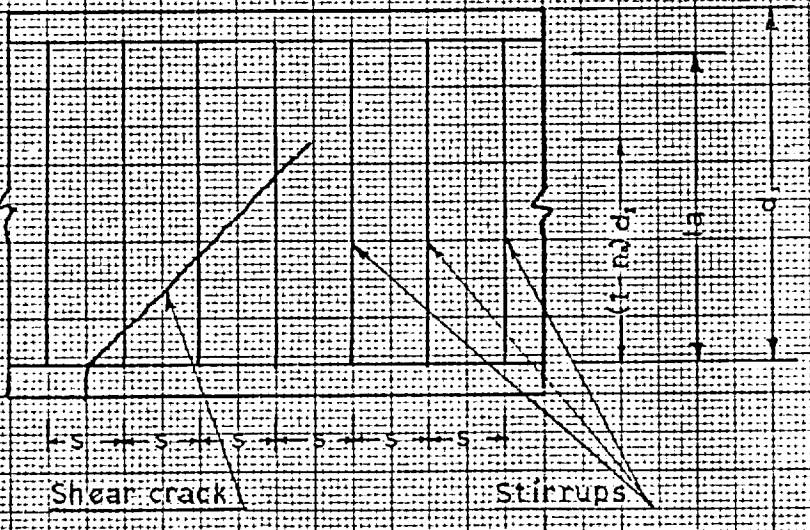


FIGURE SHOWS NUMBER OF STIRRUPS CROSSED BY A SHEAR CRACK. FIG. 13.

$$s = Z\cot\theta + Z\cot\alpha$$

$$= Z\,\frac{\sin\alpha\cot\theta + \cos\alpha}{\sin\alpha}$$

$$e = s\sin\alpha = Z(\sin\alpha\cot\theta + \cos\alpha)$$

where e = spacing of stirrups in direction perpendicular to the stirrups.

α = angle of inclination of stirrups with respect to the axis of the beam.

θ = inclination of diagonal crack.

la = lever arm.

$Aq\ fyq$ = Area times the (yield) stress of one stirrup.

The total vertical force carried by stirrups (only those crossed by the diagonal crack).

$$= Aq \times fyq \sin\alpha\, n \qquad 3.2.1$$

Number of stirrups crossed by the diagonal crack

$$n = \frac{la}{Z} = \frac{la(\sin\alpha\cot\theta + \cos\alpha)}{e}$$

External shear force carried by stirrups

$$= Aq\ fyq\ \sin\alpha\ \times\ \frac{la(\sin\alpha\cot\theta + \cos\alpha)}{e}$$

$$= Q$$

$$\text{or } Aq\ fyq = \frac{Qe}{\sin\alpha\,(\sin\alpha\cot\theta + \cos\alpha)\,la} \qquad 3.2.2$$

If the stirrups are vertical, $\alpha = 90^{\circ}$ and in addition, if the inclination of the diagonal crack $\theta = 45^{\circ}$, then the equation 3.2.2 becomes -

$$Aq\ fyq = \frac{Qs}{la} \qquad (e = s)$$

Again if area of web reinforcement is expressed as $Aq = r_q\, bs$, then,

$$r_q\, bs\ fyq = \frac{Qs}{la}$$

$$\text{or} \quad r_q \, fyq = \frac{Q}{bla} \qquad 3.2.3$$

For inclined stirrups,

$$(\sin \alpha \cot \theta + \cos \alpha) \sin \alpha = K$$

$$= \text{Efficiency factor}$$

and

$$\frac{Q}{bla} = K \, rq \, fyq \qquad 3.2.4$$

K has a maximum value of 1.2 for $\alpha = 67.5^{\circ}$, when $\theta = 45^{\circ}$

The nominal form of the classical theory assumes that the inclination of diagonal cracks is 45°, which is not supported by test observations.

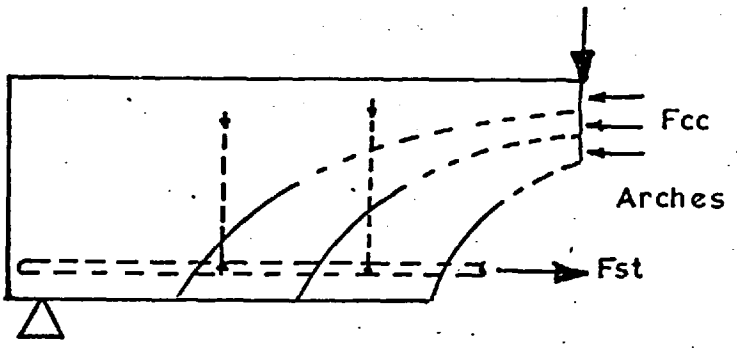
So long as the crack angle does not change, axial load, tension or compression, will not affect the shear strength but in reality, the effect of axial loads in shear strength is observed.

Finally, the reduction of stiffness of the compression chord due to the penetration of the diagonal crack is ignored as is all shear carried by the compressive zone.

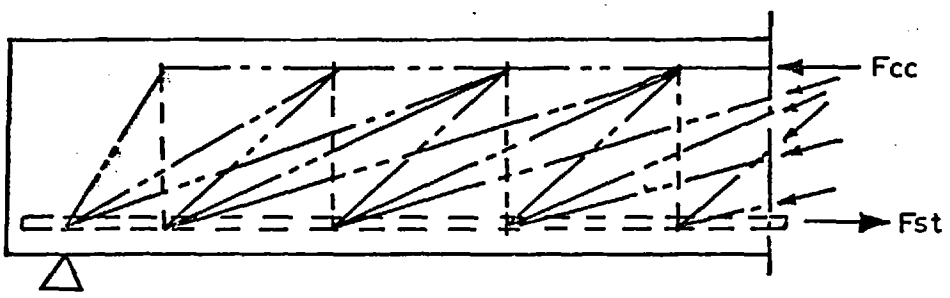
In comparison with test data the classical truss is extremely inaccurate.

b) Pin-jointed truss (Baker and Ahmad)[6]

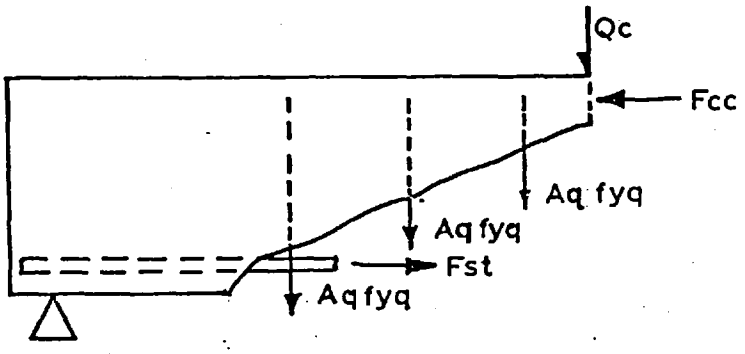
The original analogous truss used for the design of web reinforcement in many countries has been elaborated by several researchers. An important contribution to this end was made by Baker and Ahmad. The statically indeterminate truss proposed by them is shown in fig. 15. If the proper stiffnesses for the different members of the truss can be ascertained with due regard to the crack pattern and if suitable limits to their strengths can be predicted, a useful model can be constructed. But the problem of finding the proper stiffnesses and the limiting strengths under different loading conditions remains unsolved.



ARCH ANALOGY (KANI)
STIRRUPS PROVIDE HANGING SUPPORTS TO SECONDARY ARCHES. FIG. 14.



MODIFIED TRUSS ANALOGY
(BAKER & AHMAD). FIG. 15.



FREE BODY DIAGRAM OF SHEAR SPAN
(BORISHANSKY). FIG. 16.

HYPOTHESES FOR SHEAR CARRING MECHANISM OF BEAMS WITH WEB REINFORCEMENT

c) ACI - ASCE Committee (326) equation[2]

The Committee's equation for the shear strength of beams with web reinforcement but free from axial load is

$$\frac{Qult}{bd_1} = 1.9\sqrt{Ucyl} + (2500 \text{ psi})\, rst\, \frac{Qd_1}{M} + K\, r_q\, fyq \qquad 3.2.5$$

in lbf. in units

where Qult = Ultimate shear force.

r_q = ratio of shear reinforcement (Aq/bs) sin α

fyq = yield or proof stress of shear reinforcement.

s = spacing of web reinforcement along the axis of main reinforcement.

K = Efficiency factor of web reinforcement.

= (sin α cot θ + cos α) sin α.

α = angle between shear and tensile reinforcement.

θ = angle of the inclined (critical) crack with the axis of main reinforcement.

The contribution of web reinforcement to the ultimate shear strength is thus a term additive to the shear cracking load.

Analysis carried out on the basis of this equation is subject to the following limitations -

1. α shall not be less than 30°.

2. For rectangular or I-sections with vertical web reinforcement only, $Qult/bd_1$, shall not exceed $8\sqrt{Ucyl}$.

3. For T-sections, for rectangular sections or I-sections in which the angle α is less than 70° or for rectangular sections or I-sections having combined vertical stirrups and bent-up bars, $Qult/bd_1$ shall not exceed $10\sqrt{Ucyl}$.

4. K r_q fyq shall not be less than 0.41 N/mm^2 (60 psi).

5. fyq shall not exceed 414 N/mm^2 (60,000 psi) for the calculation of K r_q fyq.

Two more points regarding detailing of the beams may be mentioned here.

1. Longitudinal reinforcement shall be extended a distance equal to the effective depth of the member and a further distance equal to the nominal anchorage length (12 ϕ) of the bar beyond the section where it is no longer needed to resist flexural stresses.

2. Web reinforcment shall be continued a distance equal to the effective depth of the member beyond the length over which it is theoretically required.

The upper limits of $Qult/bd_1$ and fyq are intended in order to avoid any premature failure prior to the yielding of the web reinforcement.

In presence of axial load, the committee's ultimate equation becomes -

$$\frac{Qult}{bd_1} = 1.9\sqrt{Ucyl} + (2500 \text{ psi}) \frac{rst\ Qd_1}{M + \beta N d_1} + K\, r_q\, fyq \quad 3.2.6$$

Although Viest made a theoretical approach based on principal stress theory for the prediction of shear cracking strength, in the author's opinion, the final equation is a semi-empirical one. It may rightly visualise the variables involved in the shear strength of a beam, but it is hard to see the validity of the assumption that after the formation of flexural cracks, the normal tensile stress in the concrete is proportional to the flexural tensile stress in steel.

The contribution of the concrete compression zone is only marginally dependent on tensile steel and on the M/Qd_1 ratio, which means even if rst is zero, the beam is predicted to be able to carry load, thus under-estimating the effect of tensile reinforcement in resisting shear. No mention is made of compression steel in the Committee's equation.

Comparison of test strengths with those calculated by the ACI-ASCE Committee equation shows that it is always fairly conservative and more so when axial compression is present. Also with high axial tension, the contribution of the concrete compressive zone being totally ignored, it gives a very high factor of safety. (See chapter 7).

With the addition of the contribution of shear reinforcement, the equation is transformed into one predicting ultimate strength. In fact, this equation predicts a strength which is the summation of the concrete strength (shear cracking strength) and the additional contribution of web reinforcement. In other words, it can be said that the Committee believes the contribution of the concrete compression zone is constant at any stage of loading, which in the author's opinion is a doubtful conclusion.

Lastly, the effect of M/Qd_1 ratio is grossly underestimated which can be seen from the test results of short beams. (See chapter 7).

The analysis of stirrup forces in this equation is based on the Mörsch truss analogy already commented upon in the previous section.

d) CEB equation:

The CEB[10] recommends a minimum percentage of web reinforcement for any member but this minimum percentage of web steel is not necessary for certain members such as wide beams, lintels and slabs. The maximum inclination of web reinforcement to the tensile steel is 90° and the minimum is 45°. The relative volume of stirrups should not be less than 0.25% for mild steel and 0.14% for high quality deformed steel.

Other limitations so far as the ultimate strengths are concerned are -

1. With vertical stirrups, bent-up and orthogonal bars used as web reinforcement, the maximum ultimate strength governed by the

concrete is the lesser of the following two but may be increased by 10% in favourable circumstances -

$$5\ ^{N}/_{mm^2} \quad \text{or} \quad 0.20\ R_b'^*,$$

where $R_b'^*$ = design compressive strength of concrete.

2. With 45^o inclined stirrups the ultimate value can be increased to $6\ ^{N}/_{mm^2}$ or $0.25\ R_b'^*$ and may be increased by 15% for favourable conditions.

The following are the equations proposed in the CEB recommendation for the shear strength of reinforced concrete beams with web reinforcement.

1) without axial load

$$\eta_1 = 1 - 1.25 \sqrt{\frac{R'bk}{\tau_o^*}}\ \psi = \eta_o \qquad 3.2.7$$

in $^{N}/_{cm^2}$ units

2) with axial compression -

$$\eta_1 = 1 - 1.25 \sqrt{\frac{R'bk}{\tau_o^*}}\ (1 + 2\ \frac{\sigma'^*_o}{R_b'^*})\psi \qquad 3.2.8$$

in $^{N}/_{cm^2}$

and

3) with axial tension -

$$\eta_1 = 1 - 1.25 \sqrt{\frac{R'bk}{\tau_o^*}}\ (1 - 6\ \frac{\sigma'^*_o}{R_b'^*})\psi \qquad 3.2.9$$

in $^{N}/_{cm^2}$

where Rbk' = characteristic strength of concrete

τ_o^* = design value of nominal shear stress.

$= {}^{Q^*}/_{bd_1}$

σ_o^* = design value of $^{N}/_{bd_1}$

= axial force (compression or tension)

$R_b'^*$ = design strength of concrete

$= \frac{Ucyl}{1.5}$

$\psi = (0.5 + 33\ \frac{Ast}{bd_1}) \leqslant 1$

and $\eta_1 = \dfrac{\text{amount of shear reinforcement to be used}}{\text{amount of shear reinforcement by Mörsch}}$

$$= \frac{r_q}{1.15\ \tau_o^*}\ (fyq^*)\ (\sin\alpha + \cos\alpha)\ \sin\alpha$$

or $$\eta_1 = \frac{r_q\ fyq^*}{1.15\ \tau_o^*} \qquad 3.2.10$$

when $\alpha = 90^o$

$\therefore$ from 3.2.8 and 3.2.10,

$$\frac{r_q\ fyq^*}{1.15\ \tau_o^*} = 1 - 1.25\sqrt{\frac{R_{bk}'}{\tau_o^*}}\ \left(1 + 2\ \frac{\sigma_o'^*}{R_b'^*}\right)\psi$$

or $$\tau_o^* = \frac{r_q\ fyq}{1.15} + 1.25\sqrt{R_{bk}'}\ \left(1 + 2\ \frac{\sigma_o'^*}{R_b'^*}\right)\psi \qquad 3.2.11$$

Assuming R_{bk}' represents a tensile resistance of concrete and a partial safety factor of 1.5 is intended to be applied to the tensile strength.

Equation 3.2.11 becomes in ultimate load conditions -

$$Qult/bd_1 = \frac{r_q\ fyq}{1.15} + 1.25 \times 1.5\sqrt{Ucyl}\ \left(1 + 2\ \frac{N/bd_1}{Ucyl}\right)\left(0.5 + 33\ \frac{Ast}{bd_1}\right)$$

or $$Qult/bd_1 = 0.87\ r_q\ fyq + 1.875\sqrt{Ucyl}\ \left(1 + 2\ \frac{N/bd_1}{Ucyl}\right)\left(0.5 + 33\ \frac{Ast}{bd_1}\right)$$

in N and cm units 3.2.12

Similarly the other equations 3.2.7 and 3.2.9 become -

$$Qult/bd_1 = 0.87\ r_q\ fyq + 1.875\sqrt{Ucyl}\ \left(0.5 + 33\ \frac{Ast}{bd_1}\right) \qquad 3.2.13$$

and $$Qult/bd_1 = 0.87\ r_q\ fyq + 1.875\sqrt{Ucyl}\ \left(1 - 6\ \frac{N/bd_1}{Ucyl}\right)\left(0.5 + 33\ \frac{Ast}{bd_1}\right)$$

in N and cm units 3.2.14

for conditions with no axial load and with axial tension respectively.

If $a/d < 2$, $Qult/bd_1$ is to be multiplied by $a/2d$ in all cases, to take account of the effect of a/d_1 ratio, apparent in beams with short shear spans when the failure mode is shear compression and large shear forces can be sustained. It seems quite reasonable with respect to the concrete term but not so for the shear reinforcement term.

In the case of uniformly distributed loads, the shear force for calculation may be taken at a distance of $d/2$ from the support.

The CEB equation as already explained is preferable to ACI equation with test results of beams with and without axial forces (see chapter 7), than ACI equation. Moreover it accounts for the increase in strengths of beams with short shear spans, although the analysis has no theoretical basis like the ACI's.

e) Mattock's equation [36,18]:

Mattock studied the effectiveness of web reinforcement in the presence of axial loads[18]. His work mainly comprised of T-sections, though some of his test beams were restrained T-beams, with their flanges in tension in parts of the span. He did not observe any reduction or gain in strength from shear reinforcement for axial tension or compression with the same amount of web reinforcement.

Based on his test results and working on the ACI 318-63 equation, he proposed two equations to take account of the effect of web reinforcement in predicting ultimate strength of a beam.

$$Qult/bd_1 = Qc/bd_1(ACI) + 1.75\ rq\ fyq \qquad 3.2.14$$

in psi

$$\text{for } rq\ fyq\ (\min) \leqslant r_q\ fyq \leqslant 0.06\ Ucyl\sqrt{\frac{b}{b_r}}\sqrt{\frac{Qd_4}{M}}$$

where b = width of the flexural compression zone

b_r = width of web

$$\text{and} \qquad Qult/bd_1 = \frac{Qc}{bd_1}\ (ACI) + 0.5\ r_q\ fyq + 0.075\ Ucyl\sqrt{\frac{b}{br}}\sqrt{\frac{Qd_1}{M}} \qquad \text{in psi} \qquad 3.2.15$$

$$\text{for}\ \ r_q\ fyq > 0.06\ Ucyl\sqrt{\frac{b}{br}}\sqrt{\frac{Qd_1}{M}}$$

The above two equations were intended to apply to T-beams, but if the ratio $\frac{b}{br}$ is set equal to unity, they can be applied to rectangular beams.

As already discussed in section 3.1., Mattock proposed a shear cracking equation for rectangular beams with and without axial forces. Thus to compare the ultimate loads, his shear cracking equation will be used instead of the ACI - 318 - 63 equation. The equations, then, can be written as

$$Qult/bd_1 = \frac{Qc}{bd_1}\ (Mattock) + 1.75\ r_q\ fyq \qquad 3.2.16$$

$$\text{for}\ \ r_q\ fyq\ (min) \leqslant r_q\ fyq \leqslant 0.06\ Ucyl\sqrt{\frac{Qd_1}{M}} \qquad \text{in psi}$$

$$\text{and} \quad Qult/bd_1 = \frac{Qc}{bd_1}\ (Mattock) + 0.5\ r_q\ fyq + 0.075\ Ucyl\sqrt{\frac{Qd_1}{M}} \qquad 3.2.17$$

$$\text{for}\ r_q\ fyq > 0.06\ Ucyl\sqrt{\frac{Qd_1}{M}} \qquad \text{in psi}$$

Comparisons with test results and a discussion of these equations are given in chapter 7.

3.2.2 Shearing failure theory:

Beams with web reinforcement do not fail at the shear cracking load. The failure mode is different from that of the diagonal tension and is often not one of shear-compression. During the investigation of rectangular beams with web reinforcement, a mode of failure was observed which is believed to take place by shearing of the compressive

zone above the inclined crack. The same mode of failure was observed by Placas[44] and is referred to as "shearing failure" of the compression zone by Regan and Placas[46]. This is similar to the "plastic" shear failure mode for concrete described by Letchtenberg[31]. Regan and Placas developed an equation using a Coulomb type failure criterion to predict the ultimate load of reinforced concrete beams in shear.

According to this theory, the shearing mode of failure is governed by the equation of vertical equilibrium.

They proposed two equations for the shear force resisted by concrete alone.

a) $\frac{Qc}{bd_1} = 12.5\ (rst\ Ucyl\ \frac{d_1}{a})^{1/3}$ 3.2.18

for rectangular beams in lbs and inch units

and b) $Qc = 25\ Ucyl^{1/3}(br + 6")t$ 3.2.19

in lbs and inch units

for T-beams

The portion of the shear carried by web reinforcement is additive in both cases and is equal to -

$$Qw = b\ r_q\ fyq\ a$$

where a is the horizontal projection of the critical inclined crack.

The full derivation of the shearing equation is available in a departmental report[46] and also in reference 44.

In principle the assumed failure criterion is of a Coulomb type, but as a result of a number of approximations, the equation practically loses the essence of its theoretical value.

On the whole, the idea of shearing failure is quite new and realistic, and therefore Placas and Regan deserve full credit. The idea of drawing a separation line between diagonal tension failure and shearing failure seems more realistic than the ACI, CEB approach of taking the contribution of the concrete to the shear strength of a beam with stirrups as being equal to the diagonal tensile strength of

a plain webbed beam.

3.2.3 Plane of minimum strength Method:

Unlike the ACI-ASCE Committee[2] or CEB[10] methods this method is based on a physical analysis at the limit state and does not predict the strength of concrete and web reinforcement independently. It is reasonable that when the shear crack increases in length, the number of effective stirrups increases, but on the other hand, the depth of concrete compressive zone contributing towards the shear strength of the beam decreases. This fact is completely ignored by the ACI-ASCE or CEB analysis.

In practice, shear cracks are never straight, but for analysis, they are idealised to straight lines. A beam is free to fail in shear along any such plane when loaded to failure. The minimum strength of the beam is obtained by finding the weakest plane and hence this method is called the "Plane of Minimum Strength".

Since this method of predicting strength in shear tends to give overestimates for all but shorter beams failing in shear compression, it can virtually be regarded as a shear compression equation so far as the prediction of shear strength of a beam is concerned.

a) Russion Code Method:[8,2]

The Russian method is due to Borishansky. He approached the problem of shear from the angle of limit analysis. He made use of the equilibrium equations. The contribution of flexural and web reinforcements (bent up beams) in carrying shear as dowels was neglected. The horizontal projection of the inclined (shear) crack was assumed to be variable and the resistance of the concrete along the plane of failure was assumed to be inversely proportional to the horizontal projection of the shear crack 'c'.

Based on the above assumptions, the concrete strength Qc can be written as

$$Qc = 0.15\, p_{cb}\, bd_1^2/c \qquad 3.2.20$$

where p_{cb} = design compressive strength of concrete in bending and the constant 0.15 was determined empirically

The shear carried by web reinforcement is

$$Qw = \sum F_{wi} \sin \alpha + \sum F_w \qquad 3.2.21$$

where F_{wi} = force in one stirrup inclined at angle α to the axis of the beam

F_w = force in one stirrup inclined at right angles to the axis of the beam

Qw is also dependent on the horizontal projection of the shear crack 'c', and Qw can be written as

$$Qw = cq_w \qquad 3.2.22$$

where q_w is the vertical force carried by the web reinforcement per unit length of the member.

In the calculation of q_w, the design stress of web reinforcement is reduced by a factor of 0.8 to avoid the assumption of all stirrups yielding.

$$q_w = m_n\, m_s\, f_s\, Aw\, n/s,$$

where m_n = coefficient to take account of the possibility that web reinforcement does not yield always prior to failure. (0.8)

m_s = coefficient for uniformity of steel

f_s = design stress of web reinforcement

Aw = area of one leg of a vertical stirrup

n = number of legs of stirrups in one section of a member.

s = spacing of stirrups along the axis of the member.

The combined resistance of the member against shear failure is

$$Q = Q_c + Q_w = 0.15\, p_{cb}\, bd_1^2/c + cq_w \qquad 3.2.23$$

A certain plane exists along which the resistance of a member is minimum and the minimum strength is obtained as follows -

1. By differentiating Q with respect to the variable 'c' and then equating the differential to zero for minimum condition, an expression for 'c' is obtained.

2. Substituting the value of 'c' in equation 3.2.23, the minimum strength is obtained and is

$$Q = \sqrt{0.6\, p_{cb}\, bd_1^2\, q_w} \qquad 3.2.24$$

This value of Q is again multiplied by another factor which is in general equal to unity and is of little significance so far as the present analysis is concerned.

Equation 3.2.24 is applicable to beams with web reinforcement. In absence of web reinforcement, and in a beam subject to central point load, Q is equal to the minimum value of Qc.

$$Q = \text{constant} \times p_{cb}\, bd_1 \left(\frac{d_1}{a}\right) \qquad 3.2.25$$

Equation 3.2.20 is based on experimental results and is empirical in nature. But, the method adopted, thereafter, in the calculation of concrete and web reinforcement contributions is interesting, especially as the Russian Code was the first to adopt an ultimate design approach. One main drawback of this analysis is that the influence of the tensile reinforcement is completely unrepresented which is quite contrary to known test results.[23]

The assumption that all the stirrups crossing the inclined plane are active is hard to believe since the stirrups inside the compression zone may not be stressed at all. This may be the reason which led to the adoption of a factor of 0.8.

In the derivation of equation 3.2.24, the stirrup forces are considered to be providing a uniformly distributed force q_w. But if the stirrups are widely spaced, a considerable error might be committed in the estimate of q_w, which can be seen from the following consideration.

If $c = 2s$, then $q_w c = 2 q_w s$

But the crack may cross only one stirrup instead of two if the crack starts just beyond a stirrup.

The above consideration led to modification of equation 3.2.24 to the following form -

$$Q = \sqrt{0.6\, p_{cb}\, b d_1^2\, q_w} - q_w s \qquad 3.2.26$$

If transverse reinforcement is fairly uniform and the longitudinal steel is heavy, the above correction is unnecessary[8].

Equation 3.2.25 suggests a shear compression type of failure and predicts a constant bending moment; and not constant shear at the time of failure. This may be true so far as shear compression failure is concerned. Other shear compression theories also predict constant moments and not shears.

Application of the Russian Method to beams subject to Axial load, bending moment and shear force:

1. Beams subject to axial compression, bending and shear[8].

In this method, the beneficial effect of axial compression on the shear strength of a beam is completely ignored and no extra analysis is made. This conclusion is based on undescribed experimental studies alone and it is stated that the beams can be treated as if they are not axially loaded.

2. Beams subject to axial tension, bending and shear[8]:

The effect of axial tension on the shear strength of beams is taken into account only when the "eccentricity at the head of the inclined crack is less than $1.5d_1$". This conclusion is based on test results of beams without web reinforcement. With the above condition being satisfied, the observed reduction of shear strength was between 20 and 30% due to axial tension. Thus a reduction factor K is introduced in the calculation of Qc, and Qc is given by -

$$Qc = K \cdot \frac{0.15\, p_{cb}\, bd_1^2}{c} \qquad 3.2.27$$

where $K = \frac{eo}{d_1} - 0.5 \leq 1$

and e_o = eccentricity of the resultant tensile force in the section at the head of the inclined crack.

It is evident that when

$$\frac{eo}{d_1} = 0.5 ,$$

K = 0, which means Qc, the concrete's contribution in carrying shear is zero.

Under these circumstances, the whole of the external shear is to be supported by web reinforcement.

Treatment of a section at the point of Contraflexure

As already mentioned, if $\frac{eo}{d_1}$ is less than or equal to 0.5, concrete is not cooperating in carrying shear. The external moment at a section at the point of contraflexure is zero theoretically. In that case eo = 0 and hence no contribution of concrete can be accounted for, as such all the shear is to be carried by stirrups. This leads to further problems in that a vertical section can cross no stirrups at all. But test evidence shows that even under these circumstances, the

stirrups become operative and carry load. This resulted in a further assumption that -

when $\frac{eo}{d_1} \leq 0.5$, the whole of the shear is to be carried by stirrups crossed by a plane inclined at an angle of 60^o to the axis of the member and no other plane needs to be considered.

The available explanation of the Russian Code Method does not present any theoretical analysis nor any argument in considering the effect of axial forces. The equations are apparently entirely empirical. It seems unreasonable to say that the calculated and test values are in good agreement as stated in reference 38 with axial compression. This is far from generally true. So long as $\frac{eo}{d_1}$ is greater than 2, the calculated and test values are in goodagreement,but for values of $\frac{eo}{d_1} \leq 2$, Qtest is higher than Qcal. The maximum value of $\frac{Qtest}{Qcal}$ is 1.30 for $\frac{eo}{d_1} \simeq 1.7$.

Similarly, the equation with axial tension is unsafe for $\frac{eo}{d_1} = 2$ and 1.30, whereas it is conservative for values of $\frac{eo}{d_1} < 1$. Thus, it seems, the effect of axial force considered is not correct and can cause serious errors.

The above mentioned equations are compared, with other theories, with the author's test results and further comments are made in chapter 7.

b) Hillerborg's[45] equation:

This method can be considered a slight improvement on the Russian one in that the effect of tensile reinforcement is taken into account in the analysis.

The shear force carried by concrete across an inclined plane is

$$Qc = 4.2 (U_w)^{1/3} \sqrt{rst\%} \frac{d_1}{c} bd_1 \qquad 3.2.28$$

where all the quantities are in Kg/cm^2 units

and the contribution of web reinforcement

$$Qw = b\, r_q\, fyq\, {}^{c}/_{2} \qquad 3.2.29$$

The total shear force is obtained by addition of Qc and Qw.

$$Qult = Qc + Qw \qquad 3.2.30$$

and the minimum strength is obtained as in the previous method for the critical ratio of ${}^{c}/_{d_1}$, where

$$\frac{c}{d_1} = \sqrt{840\, U_w^{1/3} \sqrt{rst\%}/(r_q\%)(fyq)} \qquad 3.2.31$$

Substituting this value of ${}^{c}/_{d_1}$ in equation 3.2.30,

$$Qult = \sqrt{0.084\, U_w^{1/3} \sqrt{(rst\%)(r_q\%)fyq}}\; bd_1$$

or

$$\frac{Qult}{bd_1} = \sqrt{0.084\, U_w^{1/3} \sqrt{(rst\%)(r_q\%)\; fyq}} \qquad 3.2.32$$

When no minimum value of (Qc + Qw) exists within the shear span or in other words 'c' > 'a', the minimum strength is obtained by substituting 'a' in place of 'c'.

This method is preferable to the Russians' in that it takes into account the effect of longitudinal steel in carrying shear. Secondly, the overestimate in the claculation of the contribution of web reinforcement is avoided by considering just the half of the Russian value. This is reasonable, because the stirrups in the tensile zone only are operative so long as the inclined crack does not progress into the compression zone. But it would have been more reasonable to consider $(1 - n)\, d_1 \cot\theta$ as the crack length, where θ is the inclination of the failure crack to the axis of tensile reinforcement and nd_1 is the depth of uncracked concrete above the failure crack. Hillerborg also stated that his equation should be applied only to the direct type of loading. If a member is loaded through cross-beams, sufficient reinforcement must be provided in order to transfer the load to the assumed load position.

The general criticism applicable to both the Russian's and Hillerborg's methods is that the transverse force equation should not be used in ultimate load analysis if failure is not of the transverse (shearing) type.

Hillerborg did not consider the effect of axial load in his equation and for this reason, his equation could not be checked with test results of beams with axial load.

3.2.4 Shear Compression Theories:

a) Empirical shear compression equations:

1. Laupa's shear compression equation[45]:

The most important empirical shear compression equation is that of Laupa. He expressed his equation in the following form -

$$M_s^1 / bd_1^2 \, Ucyl = \bar{n} (1 - k_2 \bar{n}) k_1 k_3$$

where $\bar{n}$ = ultimate neutral axis depth factor above the critical crack.

Then assuming $\bar{n}$ to be related to the elastic neutral axis depth factor n,

$$M_s^1 / bd_1^2 \, Ucyl = nF(Ucyl) \qquad 3.2.33$$

for beams without compression reinforcement;

and $$M_s^1 / bd_1^2 \, Ucyl = (n + mr_{sc}) F(Ucyl) \qquad 3.2.34$$

for beams with compression reinforcement

where m = modular ratio

$= 5 + \frac{10,000}{Ucyl}$, when Ucyl is in lbsf inch units

Then the function F(Ucyl) is evaluated from test results as

$$F(Ucyl) = 0.57 - 4.5\ Ucyl/_{10}5$$

Thus
$$M_s^1/bd_1^2\ Ucyl = (n + mr_{sc})(0.57 - 4.5\ Ucyl/_{10}5) \quad 3.2.35$$

in lbsf inch units

He observed that the above equation and the equation of the ultimate moment for a member failing in flexure are similar and comparing them, he obtained the relationship

$$\bar{n} = 1.11 - \sqrt{1.23 - 0.926\ n}$$

Laupa's equation gives good agreement with test results of beams of shear span to effect depth ratios between 1.17 and 4.80.

His equation for beams with web reinforcement is

$$\frac{M_s}{M1_s} = 1 + 2\ r_q\ fyq/_{1000} \quad 3.2.36$$

where M_s = ultimate shear compression moment of a beam with web reinforcement.

M_s^1 = ultimate shear compression moment of a beam without web reinforcement.

Laupa's equation is to be applied at the true section of failure for a uniformly loaded beam and not at the section of maximum moment.

A full discussion on his method is available in reference 45.

His equation predicts that the ultimate moment of a beam with web reinforcement does not depend on $\frac{M}{Qd_1}$ ratio and as a result constant web reinforcement is necessary if the $\frac{M}{Qd_1}$ ratio is less than the critical one; but if $\frac{M}{Qd_1}$ ratio is greater than the critical, no web reinforcement is necessary. In other words, there would be abrupt change in the requirement of web reinforcement which is unlikely.

Though empirical in nature, Laupa's equation can be made use of as a design method and is by far the best of all the empirical shear compression equations.

Other empirical shear compression equations are by Zwoyer[45] and Moody, Viest, Elstner and Hognestad[45]. Zwoyer's was the first published shear compression equation. Moody's equation is the second and in general, his approach is similar to Laupa's and comments on his method are available elsewhere[45].

2. Kani's[22,45] shear compression theory:

The most common belief among almost all researchers is that after the breakdown of the beam action, a beam behaves like a tied arch, the tie being the tensile reinforcement of the beam. It is of interest that the behaviour of the beam after the formation of the diagonal crack is completely different from that pertaining previously. The concrete above the crack is subject to a thrust action. The compressive force is transfered from the load point to the support by the arch action. The stirrups (if any) are assumed by Kani to act as hanging supports.[21] He considered the stirrups to transfer the vertical components of the interior arch reactions to the outermost arch (see fig. 14). The number of interior arches is dependent on the number of inclined cracks. Kani assumed that the blocks of concrete in between inclined cracks form interior arches, whereas other researchers recognise only one primary arch above the diagonal cracks and look at the blocks as parts of a lattice system formed with the web reinforcement. Kani's idea of interior arch is a new development in this regard, but this is largely a matter of a new terminology rather than a new theory.

Kani made use of the arching theory in his empirical approach in deriving a shear compression equation for beams without shear reinforcement.

He assumed that all the cracks are formed as shown in fig. 9, and they are directed to a point 'O' on the extreme fibre of the compressed surface. He gave the expression for ultimate neutral axis depth as -

$$\frac{\bar{nd}_1}{nd_1} = d_1/[a - s^* + nd_1] \qquad 3.2.37$$

where $\bar{nd}_1$ = the neutral axis depth at the head of the inclined crack (at the crown of the residual crack).

nd_1 = the neutral axis depth when there is no shear crack.

s^* = the distance between the support and the last crack.

In his expression, he considered nd_1 to be equal to $n_1 d_1$ (flexural neutral axis depth when tensile reinforcement yields).

Then on the assumption that s^* and nd_1 are generally very much smaller than 'a'

$$\frac{\bar{nd}_1}{nd_1} = \frac{d_1}{a}$$

and if $nd_1 = n_1 d_1$

$$M_{sult}/M_{Fult} = \frac{d_1}{a} \qquad 3.2.38$$

where M_{sult} = ultimate bending moment at the time of shear failure.

and M_{Fult} = ultimate flexural moment.

Another factor K is introduced in the above equation to take care of the influence of vertical stresses in the vicinity of a point load applied to the top surface of a beam.

Then

$$\frac{M_{sult}}{M_{Fult}} = \frac{d_1}{Ka} \qquad 3.2.39$$

From the above equation, it is evident that shear compression moment is directly dependent on a/d_1 ratio which is not substantiated

by test results. The use of the yield stress of tensile steel in calculation of nd_1 is proved to be wrong, because shear compression failures are not necessarily preceeded by yielding of tensile steel. His recent idea regarding the function of web reinforcement in carrying shear as described above is available in reference 21. But he did not put forward any equation and hence no real comment can be made on this most recent theory.

3) Lownds' equation[48] (Modified Smith's equation):

Lownds' equation is a modified form of Smith's shear compression equation for beams without axial loads and web reinforcement. Lownds introduced a factor in the above-mentioned equation to take the effect of axial load into account while predicting the shear strength of a beam subject to shear, bending and axial load.

The modified equation is given as

$$\frac{Qcr}{bd_1} = (\sqrt{rst} - 0.17\ rst)\left(\frac{d_1}{a}\right)\left(1 - \frac{N}{2\ f'_t\ bd_1}\right) \qquad 3.2.40$$

where f'_t = tensile strength of concrete (modulus of rupture)

$= 9.5\sqrt{Ucyl}$ in lbsf inch units.

In fact, the modified Smith equation is a shear compression equation and thus agrees well with test results of beams with axial tension so long as the failure mode is shear compression; but when failure is not by shear compression, Lownds' equation is found to be conservative[48]. The equation is completely empirical and not very satisfactory because of its peculiar way of taking the effect of tensile reinforcement into account.

b) Analytical shear compression equations:

All the analytical shear compression theories assume that failure

is caused by crushing of the reduced compressive zone above the head of an inclined crack.

This type of failure is governed by the rotational equilibrium rather than vertical equilibrium.

The general equation used for shear compression mode of failure is

$$M = F_{cc} (1 - k_2 \bar{n}) d_1 + r_q f_{yq} b \frac{c^2}{2} \qquad 3.2.41$$

when M = moment about the level of tensile reinforcement at the section of loading.

1. Bjuggren[45,50]:

Equation 3.2.41 is useful only when $\bar{n}d_1$ can be determined reasonably accurately. Byuggren's approach was to calculate the extreme compressed fibre deformation and the deformation of the tensile steel and then to find out the depth of compression zone.

His assumptions were -

a) Total deformation of the extreme compressed fibre of concrete along the length of the shear crack can be obtained by integrating the top fibre strains calculated for linear distributions of strains in the uncracked concrete and a parabolic stress-strain curve.

b) The deformation is assumed to be independent of the crack length 'c'.

c) The deformation is assumed to be influenced by the shape of the thrust line in the concrete.

d) The deformation of the tensile steel is influenced by the crack length 'c' and the web reinforcement.

The expression for $\bar{n}d_1$ is given by

$$\bar{n}d_1 = \frac{\phi}{2} \left(-1 + \sqrt{1 + \frac{4}{\phi}}\right) d_1 \qquad 3.2.42$$

where ϕ = $2\ rst\ E_s\ \varepsilon'_{cc}/\gamma\mu\ cUw$

γ = coefficient for deformation of concrete

$\Delta cc = \varepsilon'_{cc}/\gamma$, where ε'_{cc} = concrete compressive strain.

$\frac{1}{\gamma}$ = $0.06\ d_1\ \cot\beta$, for a straight thrust line above the crack.

and $\frac{1}{\gamma}$ = $0.02\ d_1\ (2\ \cot\beta + \cot\beta_o)$, for a parabolic thrust line or two straight lines, the point of intersection being at a distance of less than $1.2\ \bar{n}d_1$ from the compressed surface.

where β = angle between the thrust and the compressed surface at the head of the crack.

β_o = corresponding angle at the other end of the shear crack.

Deformation of steel $\Delta st = \mu\ c\ fst/Es$

where $$\mu = \frac{1}{2}\left[1 + \frac{Ast\ la}{Ast^*\ la + \sum Aqn\ Xn}\right]$$

where Ast = Area of main steel at the head of the shear crack.

Ast* = Area of main steel at the head of the other end of the shear crack.

la = lever arm of tensile steel at the section considered.

Aqn = Area of shear reinforcement crossing crack.

Xn = lever arm of the stirrup force about the centre of compressive force.

If the yield stress of web steel is lower than that of tensile steel, the area of web reinforcement is reduced in the ratio of the yield stresses.

After determining the critical section, the depth of ultimate neutral axis '$\bar{n}d_1$' is found by an iterative method.

2. Regan[45,50,51]:

Regan's approach is similar to Bjuggren's, but his simplifications make his theory more useful. He calculated the deformation of the top fibre of compressed concrete

$$\Delta_{cc} = \lambda \varepsilon'_{cc}\, c,$$

where λ = coefficient, dependent on the slope of the thrust line.

and steel deformation -

$$\Delta_{st} = c\, f_{st}/E_s$$

where f_{st} = steel stress at the cracked section.

In his analysis, he neglected the influence of stirrups on the deformation of concrete and steel on the grounds that it increases Δ_{cc} as well as Δ_{st}. The factors causing the change of shape of the thrust line i.e. loads along the crack length are ignored because, most of the deformation of concrete is concentrated at the sections near the head of the crack.

His compatibility condition is independent of the ultimate load and his equation for the ultimate neutral axis depth is

$$\bar{n} = \frac{n_o^2}{n_o + \frac{Qd_1}{M} \cdot \frac{c}{d_1}} \qquad 3.2.43$$

where no is the reference (flexural) neutral axis depth and is given by

$$\frac{n_o^2}{1 - n_o} = \frac{3\, r_{st}\, E_s\, \varepsilon'_{cc}}{2\, U_{cyl}}$$

Q = External shear force

M = External moment at the section under consideration

and $\varepsilon'_{cc} = 0.0035$

Regan believes that the minimum strength crack need be considered only when the shear force acting on the concrete at the head of shorter shear cracks is greater than or equal to the shear resistance of the uncracked concrete calculated from the following equation -

$$Qc = Q_{ult} - r_q \, fyq \, bc \geq q_{cr} \, \bar{n} bd_1 \qquad 3.2.44$$

The sign of inequality is applicable when 'c' cannot increase physically or when the concrete at the head of the crack crushes before 'c' reaches the length given by an equality sign.

After finding the value of $\bar{n}$ from equation 3.2.43 and then by simultaneous solution of equations 3.2.41 and 3.2.44, the solution for ultimate moment is obtained.

If the value of 'c' given by the solution of the simultaneous equations is greater than the length 'c' corresponding to a minimum strength according to the moment equation, then the minimum value is used.

If the calculated value of 'c' exceeds the length available, the solution for the ultimate moment is obtained upon substitution of the available length 'c' and the corresponding '$\bar{n}$' into equation 3.2.41.

He presented his solutions graphically relating $\frac{Qult}{no \; Ucyl \; bd_1}$ to $\frac{Q.d_1}{M}$ for different values of r_q fyq/Ucyl.

3. Walther[45,50,60]:

Walther believes the deformation of the concrete compressive zone is due to rotation about the head of the crack combined with a deformation of the web.

He assumed the total shortening of the top compressed fibre

$\Delta_{cc} = \varepsilon'_{cc} \, d_1 \sqrt{\bar{n}}$,

where ε'_{cc} = the ultimate strain of concrete (when subject to shear and compression).

The ultimate strain is thus assumed to be independent of the crack length.

In calculating the deformation of the steel, he took into account the bond conditions and web distortions which made the analysis more complicated than the other theories.

His equation for ultimate neutral axis depth is given as

$$\bar{n} = \left[\frac{\varepsilon'_{cc} \psi^3 \, rst \, Es}{K_q \, K_b \, U_{pr}} \right]^{2/3} \qquad 3.2.45$$

where $\varepsilon'_{cc} = 0.003$ against Regan's value of $\varepsilon'_{cc} = 0.0035$

$$\psi = \frac{K_1 \, K_3 \, U}{U_{pr}} = \frac{1}{1 + 3.2 \left[\frac{Qd_1}{M} (1 - \eta) \right]^2}$$

η = "degree of shear safeguard"

$$= \frac{\text{shear reinforcement provided}}{\text{shear reinforcement required by Mörsch Truss Analogy}}$$

The amount of shear reinforcement required by Mörsch Truss analogy is

$$r_q \, fyq = \frac{Qult}{b \, la}$$

Kq = Coefficient for deformation of web due to shear for vertical shear reinforcement.

$$= \frac{Qult - Qcr}{Qcr} (1 - 0.75\eta)$$

$Qcr = 0.65\sqrt{Uw}$ in Kgf and cm units.

Kb = bond coefficient.

$$= \left[0.9 + 30 \frac{rst}{U_{pr}} \right] Kr \sqrt{\frac{\phi}{\phi_o}}$$

where U_{pr} is in Kgf and cm units

Kr = surface roughness coefficient for tension reinforcement = 1.0 for deferred bars and = 1.5 for plain bars.

ϕ = diameter of tension reinforcement.

ϕ_o = reference diameter = 26 mm.

Regan and Walther assume the stirrup stress to be either the yield or proof stress whereas Bjuggren considers it to be the same as that in the tensile steel crossed by the crack.

It is quite likely that stirrups very near to the compressive zone may be lightly stressed not reaching yield stress, but the contribution of stirrups towards the ultimate moment is not considerable and so is of little significance.

These theories differ considerably in estimating the horizontal projection of the crack 'c'.

None of these theories is simple enough to be used for design purposes as such. But with the help of design charts for various parameters provided by Regan, his method is the simplest. Bjuggren's method needs a trial and error process for calculation and hence is very time consuming. Walther's analysis is systematic but not simple to use for design purposes because of a number of coefficients involved which needs to be evaluated.

None of these theories considers the effect of axial load on the shear strength of beams failing in shear compression. So their validity could not be checked with test results of beams subject to axial load. Regan's theory is checked and discussed fully in a Ph.D. thesis submitted to the University of London by Placas[44] with test results of beams without axial load.

Under these circumstances, the number of theories that could be checked with author's test results is limited. Only those theories which take into account the effect of axial load on the shear strength of beams are checked and discussed in detail.

The following are the theories used for further checks and discussion -

1. ACI-ASCE Committee's equation (326)

2. CEB draft code equations

3. Mattock's empirical equation, based on ACI-ASCE committee equation for prestressed beams.

4. Method of the Russian code (Borishonsky).

CHAPTER 4

EXPERIMENTAL INVESTIGATION: BEAM TESTS

4.1. Introduction:

This chapter is devoted to the experimental part of the research carried out in order to support the theoretical investigation. Relatively little work has so far been done in this field and with the test results available from it, it is impossible to draw conclusions regarding the influence of axial force on the shear strength of reinforced concrete beams.

A test programme was, therefore, designed and thirtyone rectangular reinforced concrete beams were tested. The investigation was restricted to rectangular beams with web reinforcement, the axial load being external.

The main variables were the axial forces and the ratio of shear span to effect depth. To study the effect, if any, of axial forces on the behaviour of web reinforcement, the web reinforcement was varied in a few beams. (It was thought that with axial tension steeper crack might form and a less number of stirrups would then cross any one crack). Although in the majority of the beams the top and bottom steel were equal, a few beams had less compression than tension steel. One beam was cast with a lower concrete strength than the others.

4.2. Test specimens:

The beams were divided into two groups -

A. Restrained and

B. Simply supported in order to study the effect of axial loading on beams with different support conditions.

Again groups A and B were further subdivided according to the nature of the axial loading to which beams were subjected in addition to bending and shear.

series 1. Beams subjected to axial tension.

series 2. Beams subjected to no axial load.

series 3. Beams subjected to axial Compression.

4.2.1 Features common to all beams:

The overall dimensions of the cross-section were the same for all the test specimens and were 152 x 305 mm (6" x 12"). It was intended as far as possible not to introduce any scale effect and the adopted cross-section was believed to be not too far from a practical size.

All beams had similar types of reinforcement. KS60 steel was used for tensile reinforcement. The percentage of such steel was fixed in such a way that shear failures could be achieved. Most of the beams had $\frac{Ast}{bd_1}$ ratio (rst) of 1.46%, which is also very close to practical conditions. In the majority of the beams the tension and compression reinforcement were identical, while in the remainder the compression reinforcement was nominal and comprised approximately of 0.4% of plain round mild steel.

All the beams were reinforced in shear with mild steel stirrups. The percentage of web reinforcement was varied in only three beams.

4.2.2 Description of Specimens:

GROUP A: Restrained Beams:

The geometry of the beams under this category was the same for all. All the beams were 3.960 m (13'.0") long and were tested with shear span to effective depth ($^{a}/_{d_1}$) ratios of 2.8. The percentage of tensile reinforcement was 1.46 except in beams B_{29} and B_{30}. In these two beams, the percentage of tensile reinforcement was varied to 0.97% and 2.0% respectively. In beams B_5 and B_{23} the compression reinforcement at the top (see fig. 20) was cut at a distance of 0.457 m (1'6") from the point of contraflexure with the intention of studying the effect of curtailment of bars when a beam is subjected to axial loads.

With the existing test set-up, it was not possible to test beams with $^{a}/_{d_1}$ ratios other than 2.8, but it was believed that if a substantial number of tests were done with this shear span to effective depth ratio, a fair idea of the effect of axial forces on the shear strength of beams could be obtained.

All the beams had nibs (see Fig. 19) on both sides of them and the centre to centre distance between the nibs was 1.524 m (5'.0"). The axial loads were applied to the beams through these nibs.

All the beams except B_{25} and B_{26} had equal shear reinforcement. In beams B_{25} and B_{26} the shear reinforcement was varied to study the effect of axial load on shear carrying capacity of web reinforcement.

The main details of the beams in this group are given in table 2.

GROUP B: Simply Supported Beams:

All the beams in this group except B_6 were tested with two symmetrical point loads. Beam B_6 was tested with one central point load. In this group beams of varying shear span to effective depth ratios were tested.

As in the previous group, the tensile reinforcement ratio was 1.46% for all the beams. Compression reinforcement was varied from 1.46% to 0.34%

Shear reinforcement was generally 5.5 mm ($^{7}/_{32}$") diameter stirrups at centres of 152 mm (6"). Only in beam B_{31} was the shear reinforcement different, being of 6 mm ($^{1}/_{4}$") diameter stirrups at 100 mm (4") centres.

The main features of the beams are given in table 3.

4.3. Materials and fabrication:

4.3.1. Concrete:

The concrete mix adopted for this investigation was intended to give a cube strength of 40 N/mm^2 (6000 psi) at 28 days. Only in one beam was the concrete mix varied to give a 28 day strength of about 20 N/mm^2 (3000 psi). The object of switching over to another mix was to study whether the effect of axial load on shear strength of beams is uniform.

The reason for adopting a 40 N/mm^2 mix was that concrete of this strength is widely used these days in construction works.

The concrete was made of Thames Valley river gravel of maximum size 19 mm ($^{3}/_{4}$"), sand and ordinary portland cement. The mix proportins by weight for the different components are given in table 1. The sieve number referred to in the table corresponds to British Standard (Imperial) specifications.

The different components of the concrete mixes were batched dry and the concrete was mixed in a 0.113 m^3 (4 cuft) capacity Eirich counter rotating pan mixer.

Control Specimens:

From every mix of concrete two 152 x 152 mm (6" x 6") cubes for crushing and one 152 x 228 mm (6" x 9") cylinder for splitting were

Table 1. Mix proportions by weight. Maximum size of aggregates 19 mm ($^3/_4$")

Items	Sizes	41.0 N/mm^2(6000 psi) Mix proportions by weight	20.5 N/mm^2 (3,000 psi) Mix proportions by weight.
Coarse Aggregate	9.5-19mm ($^3/_8$- $^3/_4$")	2.21	2.75
Fine Aggregate	5-9.5 mm ($^3/_{16}$-$^3/_8$")	1.14	1.90
Coarse Sand	25-5 mm (25 - $^3/_{16}$")	1.39	2.20
Fine Sand	100-25	0.61	0.95
Ordinary Portland Cement	-	1.00	1.00
Water	-	0.61	0.95

Table 2. Details of test beams.

GROUP A RESTRAINED BEAMS:

SERIES 1 b = 152 mm, d = 305 mm, d_1 = 272 mm.

Beam No.	Reinforcement rst%	Reinforcement rsc%	fsy N/mm²	$\frac{M}{Qd_1}$	dia of web reinforcement	spacing of web reinf.	fyq N/mm²
B_1	1.46	1.46	630	2.8	5.5	152	316
B_2	1.46	1.46	630	2.8	5.5	152	316
B_4	1.46	1.46	630	2.8	5.5	152	316
B_5	1.46	-	630	2.8	5.5	152	316
B_7	1.46	1.46	630	2.8	5.5	152	316
B_{12}	1.46	1.46	630	2.8	5.5	152	316

SERIES 2 b = 152 mm, d = 305 mm, d_1 = 272 mm

Beam No.	Reinforcement rst%	Reinforcement rsc%	fsy N/mm²	$\frac{M}{Qd_1}$	dia of web reinforcement	spacing of web reinf.	fyq N/mm²
B_3	1.46	1.46	630	2.8	5.5	152	316

SERIES 3 b = 152 mm, d = 305 mm, d_1 = 272 mm
d_1 for B_{30} is 264 mm.

Beam	Reinforcement rst%	Reinforcement rsc%	fsy N/mm²	$\frac{M}{Qd_1}$	dia of web reinforcement	spacing of web reinf.	fyq N/mm²
B_{15}	1.46	1.46	630	2.8	5.5	152	316
B_{17}	1.46	1.46	630	2.8	5.5	152	316
B_{18}	1.46	1.46	630	2.8	5.5	152	316
B_{20}	1.46	1.46	630	2.8	5.5	152	316
B_{22}	1.46	1.46	630	2.8	5.5	152	316
B_{23}	1.46	-	630	2.8	5.5	152	316
B_{24}	1.46	1.46	630	2.8	5.5	152	316
B_{25}	1.46	1.46	630	2.8	6.0	100	258
B_{27}	1.46	1.46	630	2.8	6.0	100	258
B_{28}	1.46	1.46	630	2.8	5.5	152	316
B_{29}	0.97	0.97	630	2.8	5.5	152	316
B_{30}	2.0	2.0	630	2.9	5.5	152	316

Note :- Main steel - 16 mm (5/8") dia KS60 steel
Compress " - 16 mm (5/8") " KS60 steel
Stirrup " - 5.5 mm (7/32") " S
6.0 mm (1/4") " MS

Table 3. details of test beams

GROUP B SIMPLY SUPPORTED BEAMS:

SERIES 1 b = 152 mm, d = 305 mm, d_1 = 272 mm

Beam No.	Reinforcement		fsy N/mm^2	$\frac{M}{Qd_1}$	Dia of web reinf. mm	spacing of web reinf. mm	fyq N/mm^2
	rst%	rsc%					
B_6	1.46	1.46	630	3.9	5.5	152	316
B_8	1.46	0.34	630	1.96	5.5	152	316
B_{10}	1.46	1.46	630	1.96	5.5	152	316
B_{13}	1.46	1.46	630	1.5	5.5	152	316
B_{14}	1.46	0.34	630	1.5	5.5	152	316

SERIES 2 b = 152 mm, d = 305 mm, d_1 = 272 mm

Beam No.	Reinforcement		fsy N/mm^2	$\frac{M}{Qd_1}$	Dia of web reinf. mm	spacing of web reinf. mm	fyq N/mm^2
	rst%	rsc%					
B_9	1.46	0.34	630	1.96	5.5	152	316
B_{11}	1.46	1.46	630	1.5	5.5	152	316

SERIES 3 b = 152 mm, d = 305 mm, d_1 = 272 mm

Beam No.	Reinforcement		fsy N/mm^2	$\frac{M}{Qd_1}$	Dia of web reinf. mm	spacing of web reinf. mm	fyq N/mm^2
	rst%	rsc%					
B_{16}	1.46	1.46	630	1.96	5.5	152	316
B_{19}	1.46	1.46	630	1.96	5.5	152	316
B_{21}	1.46	0.34	630	1.96	5.5	152	316
B_{26}	1.46	1.46	630	2.8	5.5	152	316
B_{31}	1.46	1.46	630	3.46	6.0	100	258

Note: Main steel - 16 mm ($5/8$") dia KS 60 steel
compression-steel - 16 mm ($5/8$") dia KS 60 "
9.5 mm ($3/8$") dia webond steel
stirrups - 5.5 mm ($7/32$") dia M.S.
6.0 mm ($1/4$") dia M.S.

cast and cured under identical conditions with the beams. Moreover, 152 x 305 mm (6" x 12") cylinders for crushing were also cast from some mixes.

Cylinder crushing strengths of concrete and split cylinder strengths, all obtained on the day of testing of the beams, are shown in table 4. The cylinder crushing strengths quoted are 0.8 times the cube strength, which ratio was found to be reasonable in the cases where control cylinders were taken.

Fig. 25 shows the stress-strain curves of the 41.5 N/mm^2 (6000 psi) concrete at 36 and 28 days.

4.3.2 Reinforcement:

Particular attention was paid in detailing the beams in order to avoid any premature flexural failure. In view of this, high strength Ks 60 deformed steel was used with a practicable percentage of tensile steel. In most cases, the same steel was also used as compression reinforcement, but in a few cases welbond (420 N/mm^2) deformed steel was used for compression reinforcement.

For other secondary and shear reinforcements mild steel and plain bars were used.

The particulars of reinforcements are given in table 5. Figs 26 and 27 show the stress-strain curves for the different steels.

4.3.3. Casting and curing:

All the beams were cast in steel moulds placed horizontally. When the reinforcing cage was made to the required dimensions, it was placed inside the mould and plastic spacers were attached to give sufficient cover. Generally, three batches of concrete were required for each beam but in the shorter beams two batches were sufficient.

The beams had nibs 1.52 m (5'.0") apart, In those to be tested with axial tension, 38 mm ($1\frac{1}{2}$") diameter vertical holes were made

Table 4 Concrete strengths

GROUP A					GROUP B				
Beam No.	Age in days	Uw N/mm^2	Ucyl N/mm^2	Ut N/mm^2	Beam No.	Age in days	Uw N/mm^2	Ucyl N/mm^2	Ut N/mm^2
B_1	21	41.8	33.5	3.2	B_6	21	41.4	33.1	2.48
B_2	19	41.1	32.9	3.10	B_8	20	39.0	31.2	2.37
B_4	20	43.9	35.10	2.95	B_{10}	20	42.8	34.3	2.75
B_5	20	40.9	32.70	2.62	B_{13}	21	37.7	30.2	2.89
B_7	20	40.2	32.2	2.68	B_{14}	21	36.2	29.0	2.64
B_{12}	21	38.7	31.0	2.91					
B_3	21	45.7	36.6	2.9	B_9	21	39.2	31.4	2.65
					B_{11}	20	39.7	31.7	2.86
B_{15}	22	40.5	32.4	2.58	B_{16}	18	36.9	29.5	2.56
B_{17}	18	36.9	29.5	2.79	B_{19}	25	37.5	30.0	2.56
B_{18}	20	36.6	29.3	2.86	B_{21}	19	37.1	29.7	2.20
B_{20}	20	35.6	28.5	2.16	B_{26}	19	38.0	30.4	2.54
B_{22}	20	34.4	27.5	2.48	B_{31}	21	39.3	31.5	2.97
B_{23}	25	37.9	30.3	2.70					
B_{24}	18	38.5	30.8	2.70					
B_{25}	20	37.8	30.2	2.49					
B_{27}	21	35.8	28.6	2.54					
B_{28}	26	17.4	13.9	1.83					
B_{29}	27	44.2	35.4	2.64					
B_{30}	21	39.1	31.3	2.70					

Table 5. Properties of Reinforcements:

Type	Particulars	Diameter (mm)	Yield Stress N/mm^2	Ultimate Stress (N/mm^2)
Tensile Reinforcement	High Tensile deformed KS60	16	630	910
Compression Reinforcement	High Tensile deformed KS60	16	630	910
	Deformed Welbond	9.5 ($^3/_8$")	414	675
Web Reinforcement	Mild steel	5.5 ($^7/_{32}$")	316	426
	Mild steel	6.0 ($^1/_4$")	258	329
	Mild steel	9.5 ($^3/_8$")	407	477
Reinforcement in Nib	Mild steel	12.5 ($^1/_2$")	335	497

N.B. Yield and ultimate stresses are calculated based on the actual areas. Equivalent stresses are then given in metric units.

in each nib on both sides of the beam and were afterwards used to accommodate the rods for vertical loading. In beams to be tested with axial compression horizontal holes were made for the application of the axial compression through horizontal bars. The details of these holes are shown in fig. 19. To avoid any practical difficulty at the time of stripping, 9.5 mm (3/8") thick polystyrene pieces were stuck to the mould on both sides of the nibs. The same moulds were used throughout and the lengths of the beams were adjusted according to requirements by a wooden end block.

After pouring each mix evenly along the length of the beam, the the concrete was vibrated with a 25 mm (1") diameter internal poker vibrator until full compaction was attained. When the beam was fully cast the top of it was levelled and finished with a trowel.

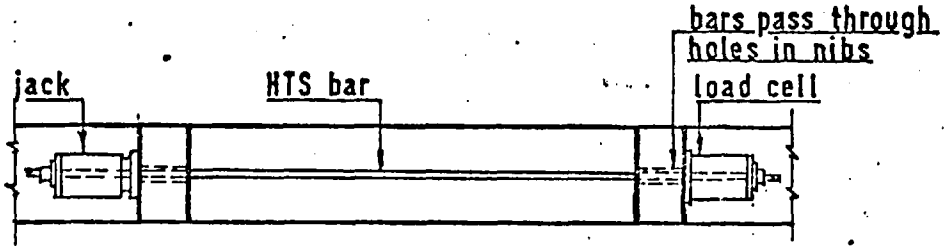
All the beams were cured under the same conditions as far as practicable. 3 to 4 hours after casting, the beams were covered with wet sacks and polethene sheets. After three days, the beams were stripped of the moulds and again cured by covering with wet sacks and polethene sheets for another 3 days. Then the beams were uncovered and left in the laboratory atmosphere until the day of testing. The same procedure was adopted for curing the control specimens.

4.4. Testing Arrangements:

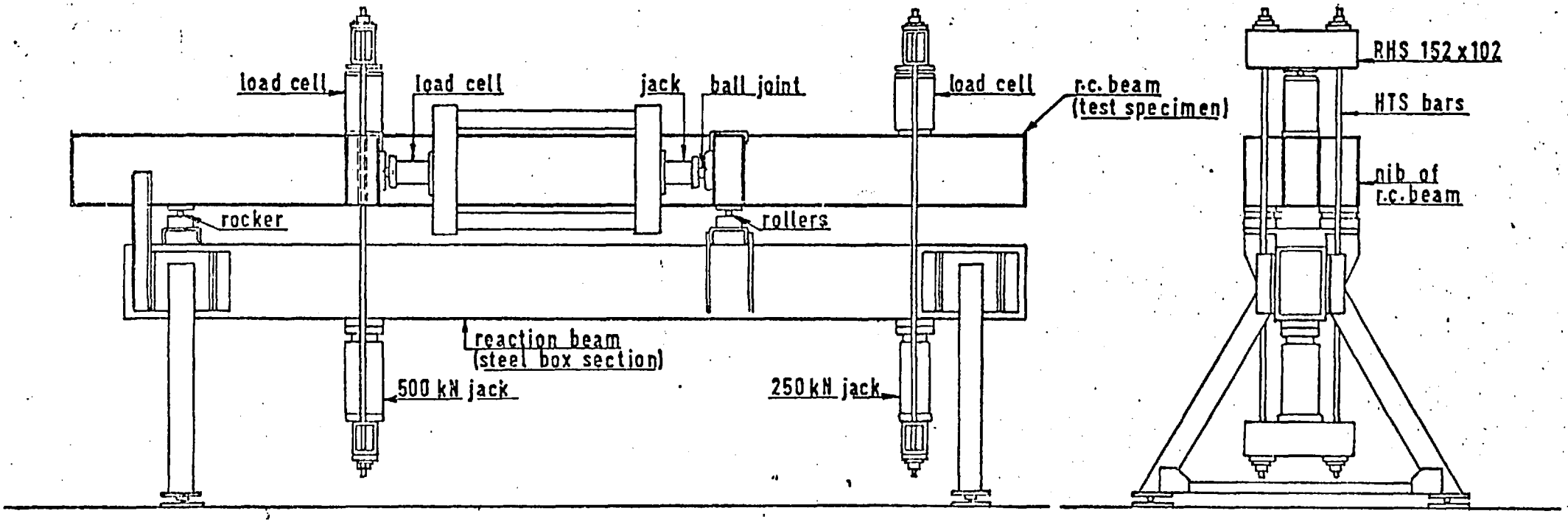
4.4.1 Test rig:

Fig. 18 shows the loading arrangements of the beams. In order to make testing programme simpler, a testing rig was designed (fig. 17) for testing of the beams in group A. Both vertical and horizontal loads were applied to the beams with the help of load cells.

The testing rig was of 3.96 m (13'.0") length, the distance between the two supports positions being 2.29 m (7'6"). On one end there was an over hang of 1.22 m (4'.0").



ARRANGEMENT FOR AXIAL COMPRESSION
REMAINING DETAILS AS BELOW



ARRANGEMENT FOR TESTING WITH AXIAL TENSION

TEST FRAME. FIG. 17.

4.4.2 Support conditions:

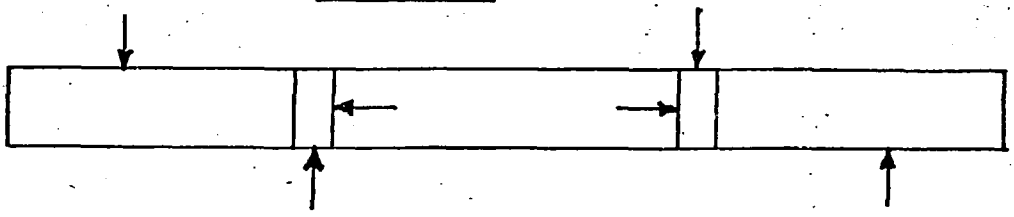
The support systems at the two positions consisted of roller and rocker bearing arrangements, the rocker being at the end and the rollers at the intermediate position. The beams were supported directly on their soffits on 100 x 150 x 25 mm (4" x 6" x 1") mild steel plates. The rocker consisted of two 100 x 150 x 25 mm (4" x 6" x 1") mild steel plates with a central groove to accommodate the 25 mm (1") diameter roller. At the intermediate position, the beam was supported through the cross-members by two roller bearings, consisting of two 100 x 150 x 25 mm (4" x 6" x 1") M.S. plates and 25 mm (1") diameter rollers. In both cases the bottom plates of the bearings were welded to the testing frame. The same type of support arrangements were adopted for the testing of beams in group B. These beams were tested in an all purpose rig with two movable pedestals, as the spans of these beams did not permit their being tested in the original frame.

4.4.3 Loading Arrangements:

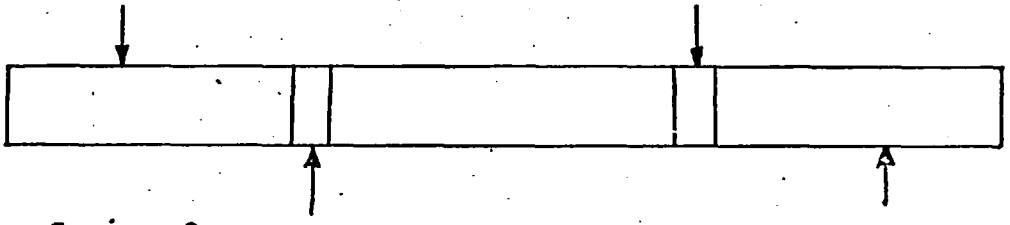
While testing the beams in group A, both vertical and horizontal loads were applied to the beams with the help of jacks and load cells. Three different types of jacks and load cells were used depending on the capacity required. Before testing all the load cells were calibrated. For convenience two hollow cells were used for the testing of the beams in series 3 of both groups. The jacks were manually operated and of 300 KN capacity. In a few cases for loading the beam horizontally on both sides, one pump was used to operate the two horizontal jacks coupling together. On other occasions, two separate pumps were used.

For loading the beams horizontally in series 1 two small frames were used, one on each side of the beam. The frames were put inside

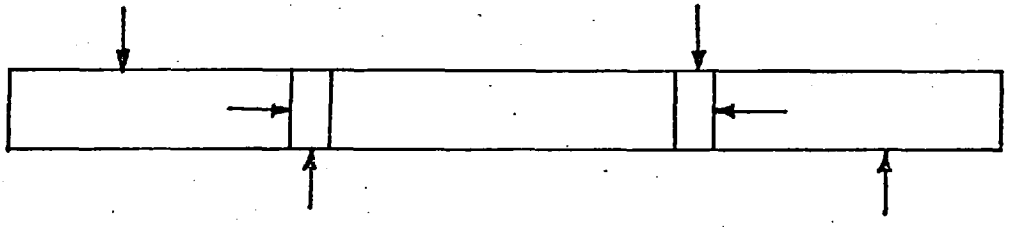
GROUP A



Series 1

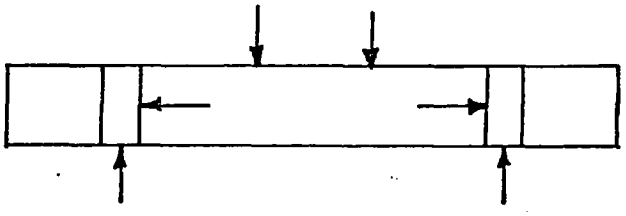


Series 2

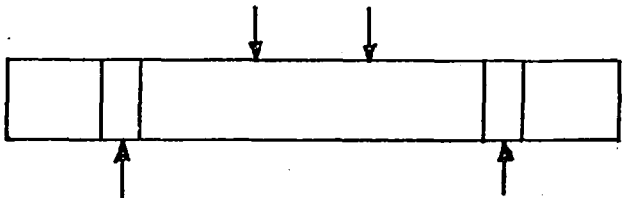


Series 3

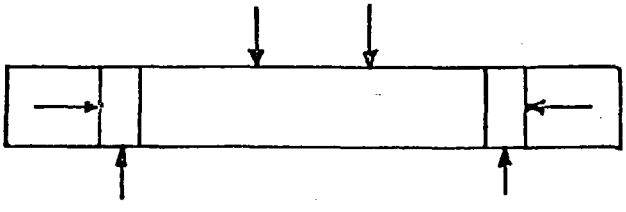
GROUP B



Series 1

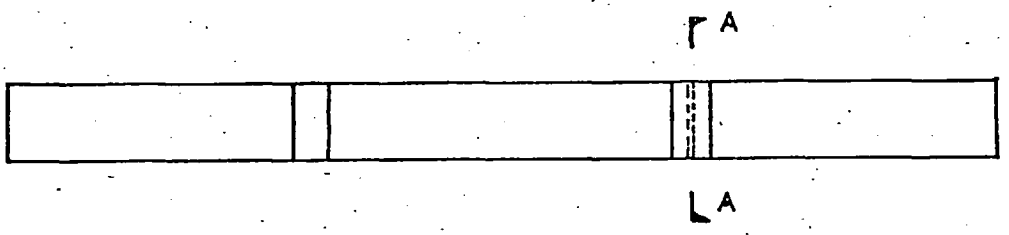


Series 2

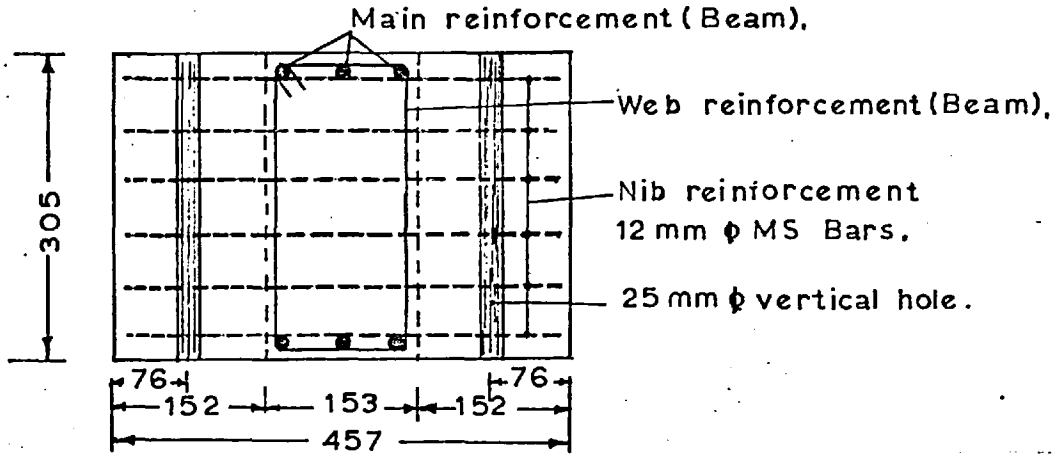


Series 3

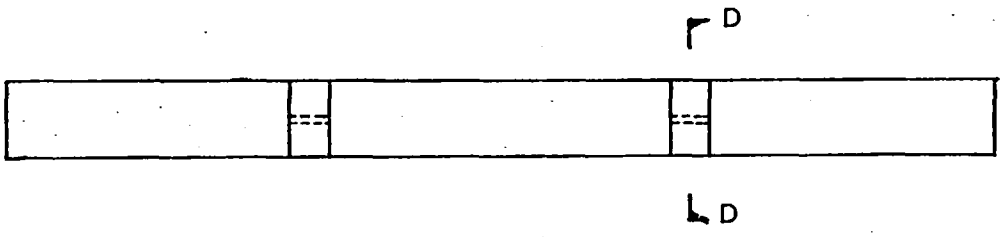
LOADING ARRANGEMENTS OF BEAMS. FIG.18.



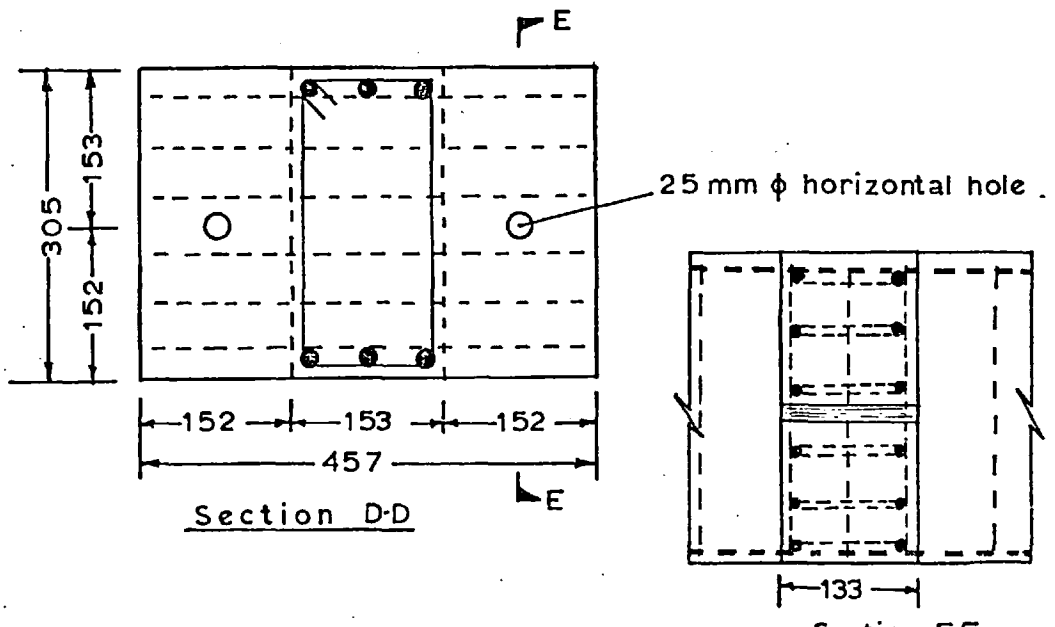
Elevation of Beam showing holes in nib.



Section A-A



Elevation of Beam showing holes in nib.



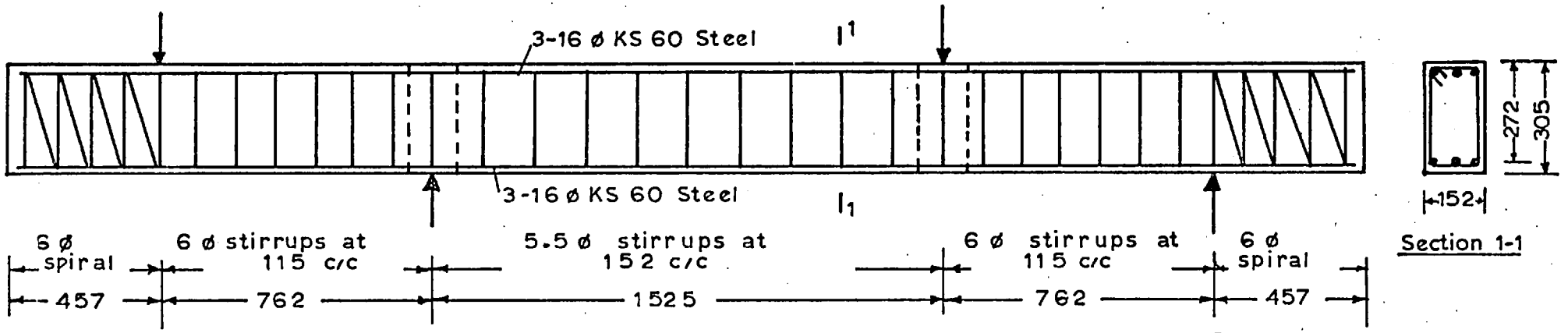
Section D-D

Section E-E

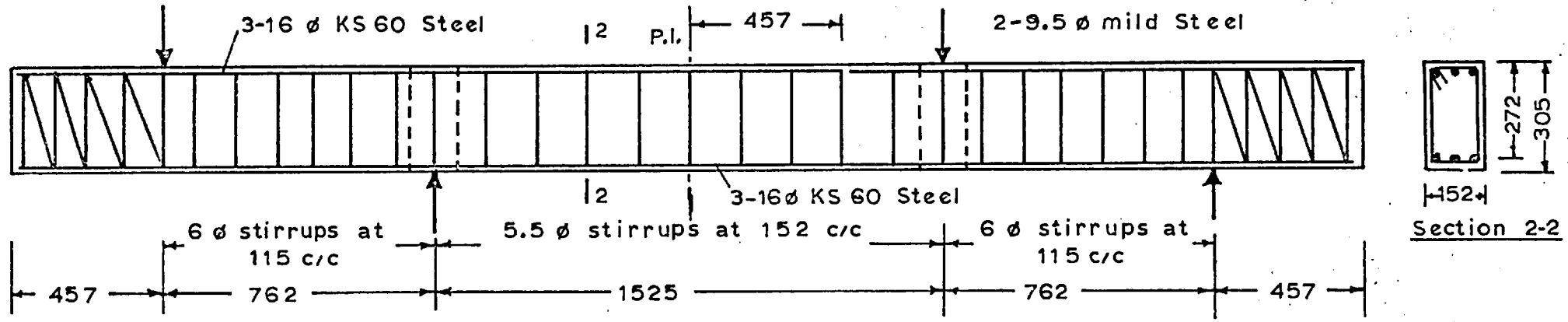
DETAILS OF HOLES & REINFORCEMENT IN NIB

ALL DIMENSIONS ARE IN MM.

FIG. 19.

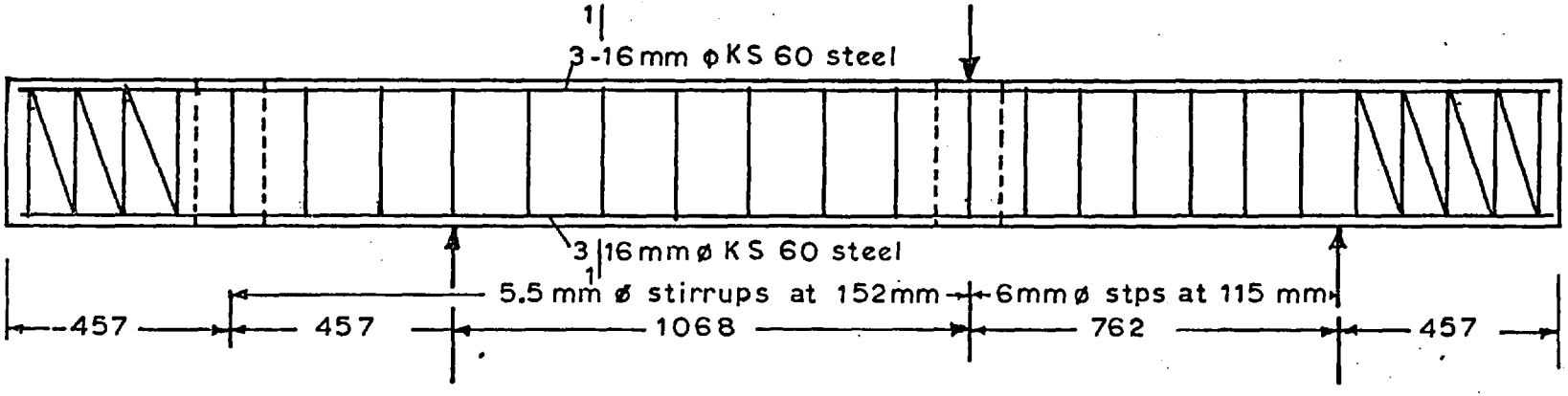


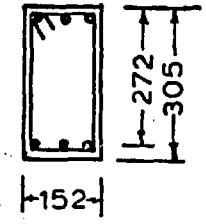
LONGITUDINAL SECTION OF BEAMS $B_1, B_2, B_3, B_4, B_7, B_{12}, B_{15}, B_{17}, B_{18}, B_{20}, B_{22}, B_{24}$ & B_{28}



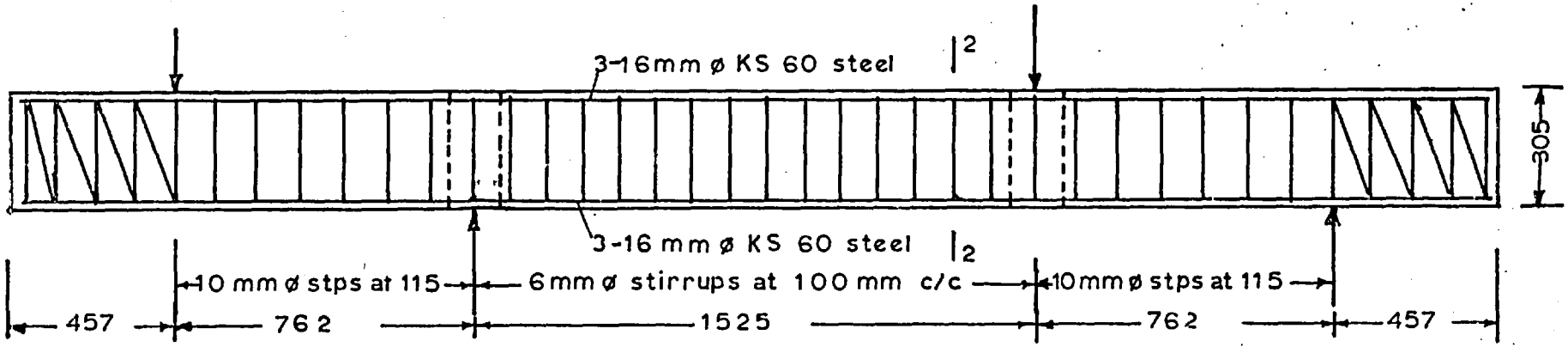
LONGITUDINAL SECTION OF BEAMS B_5 & B_{23}

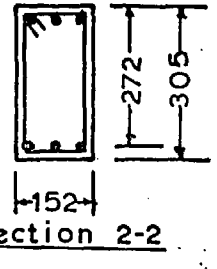
DETAILS OF REINFORCEMENT OF TEST BEAMS. FIG. 20.





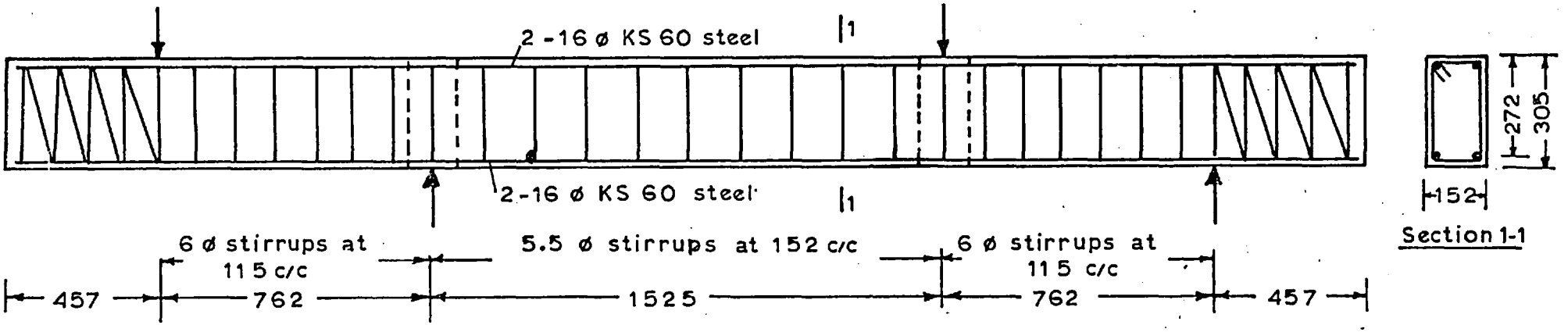
LONGITUDINAL SECTION OF BEAM B_6



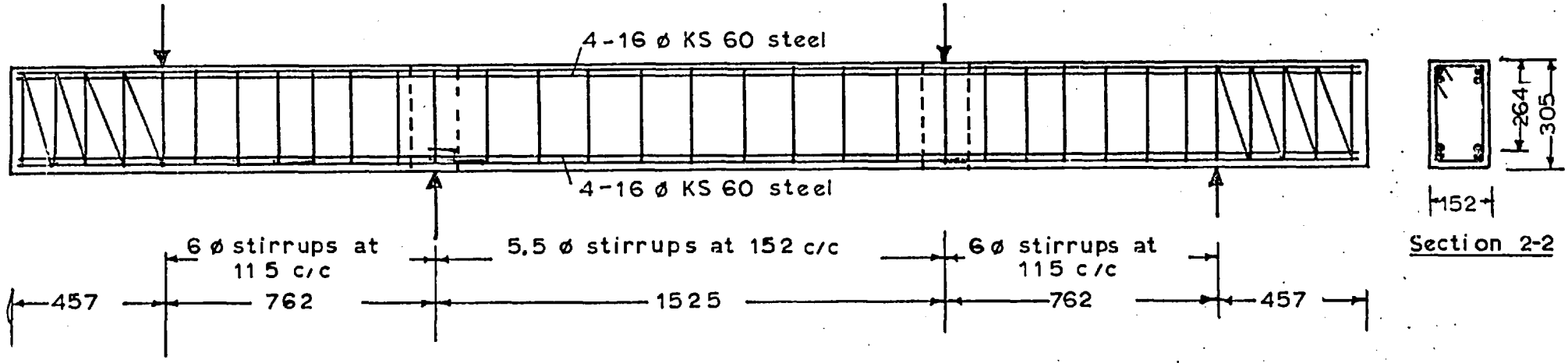


LONGITUDINAL SECTION OF BEAMS B_{25} & B_{27}

REINFORCEMENT DETAILS OF TEST BEAMS. FIG. 21.

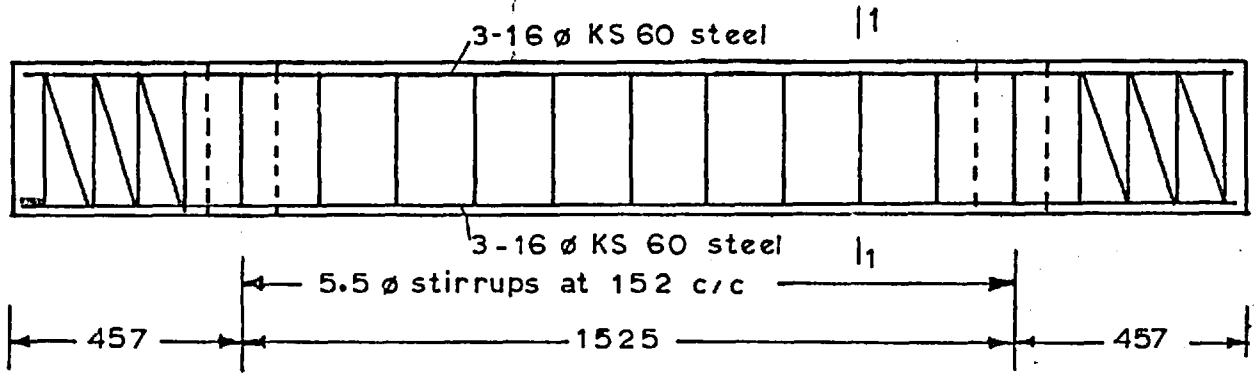


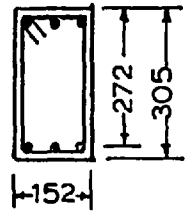
LONGITUDINAL SECTION OF BEAM B_{29}



LONGITUDINAL SECTION OF BEAM B_{30}

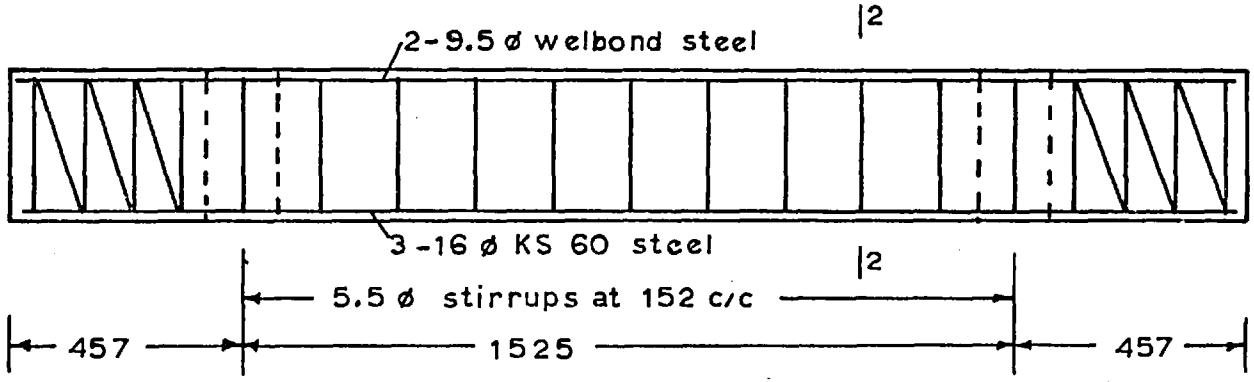
DETAILS OF REINFORCEMENT OF TEST BEAMS. FIG. 22.

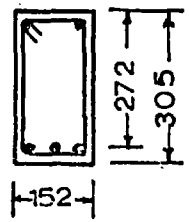




Section 1-1

LONGITUDINAL SECTION OF BEAMS $B_9, B_{10}, B_{11}, B_{13}, B_{16}, B_{19}$ & B_{21}

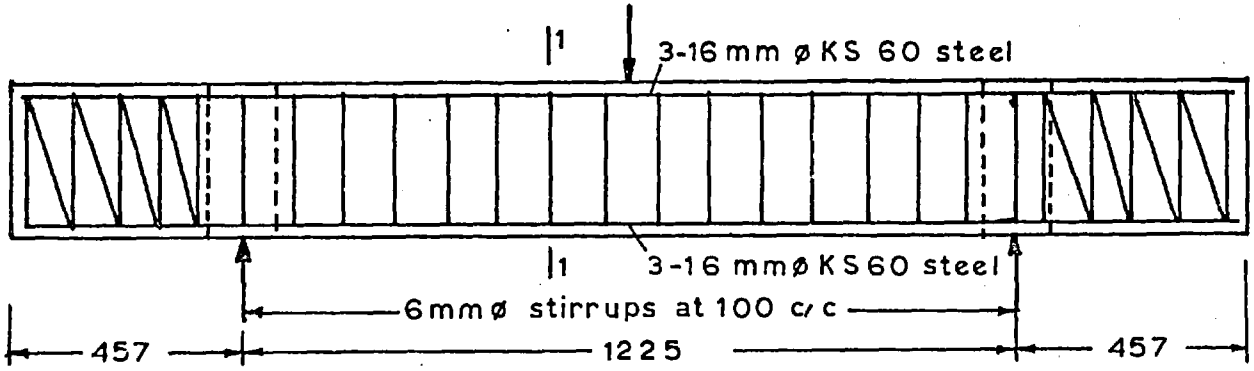




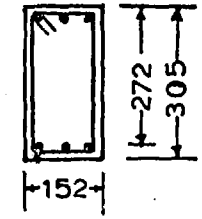
Section 2-2

LONGITUDINAL SECTION OF BEAMS B_8 & B_{14}

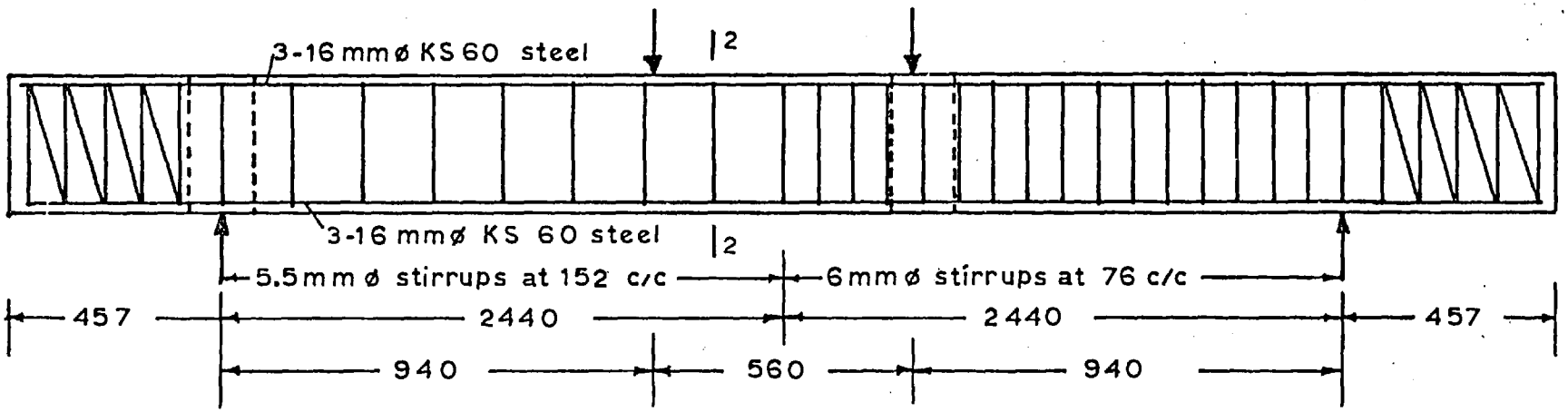
DETAILS OF REINFORCEMENT OF TEST BEAMS. FIG. 23.



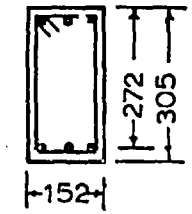
LONGITUDINAL SECTION OF BEAM B_{26}



Section 1-1

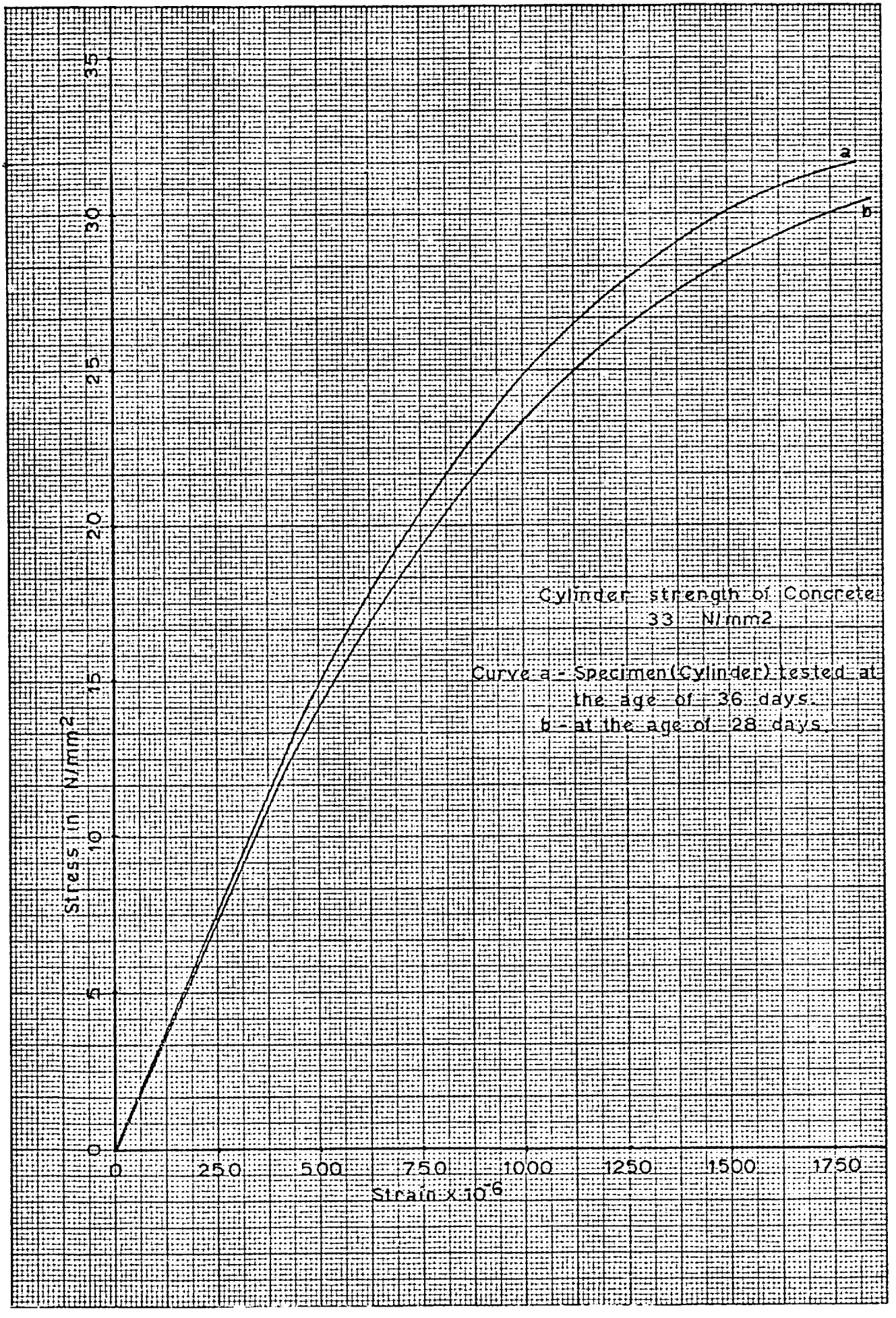


LONGITUDINAL SECTION OF BEAM B_{31}

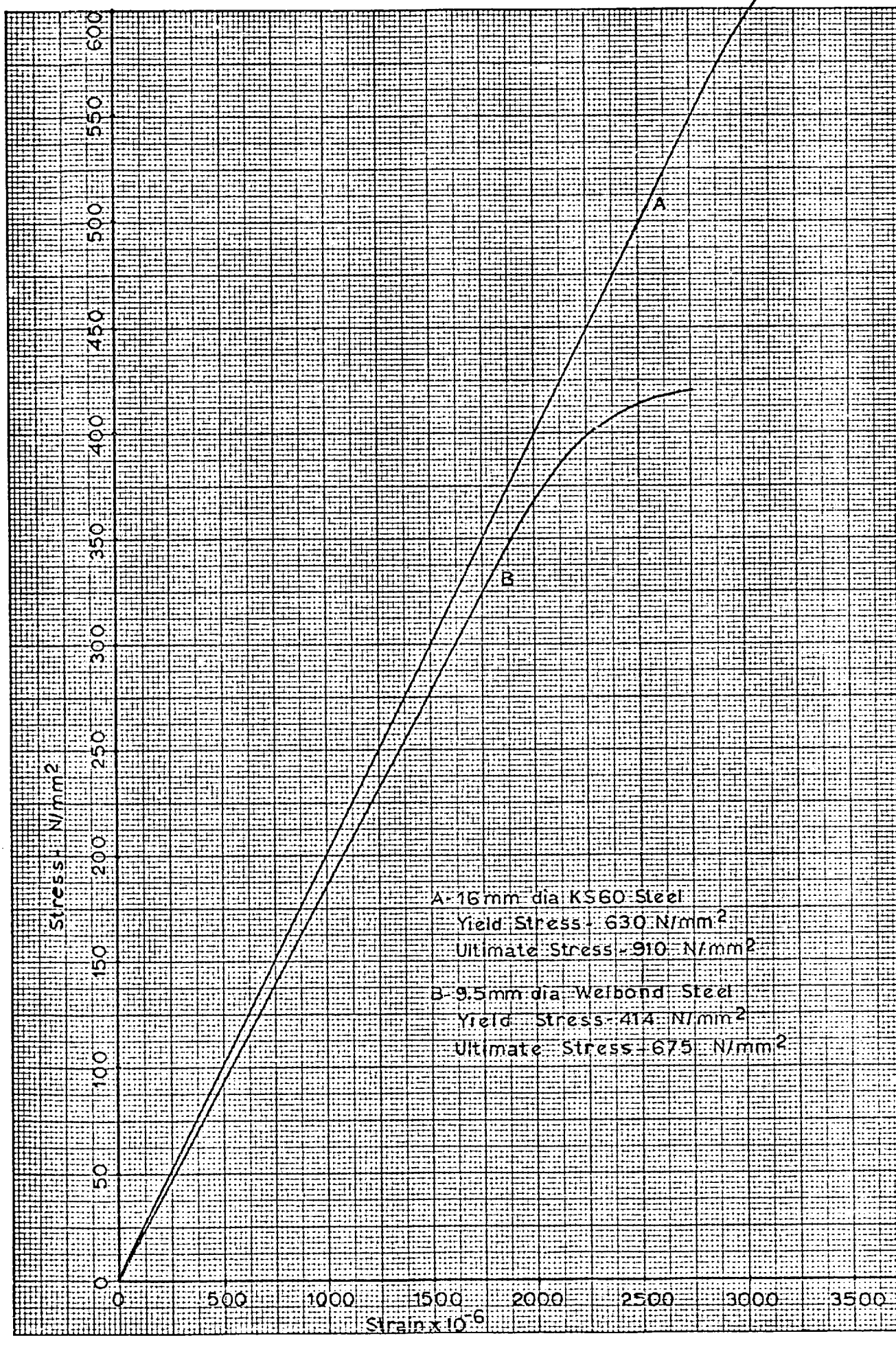


Section 2-2

DETAILS OF REINFORCEMENT OF TEST BEAMS. FIG. 24.

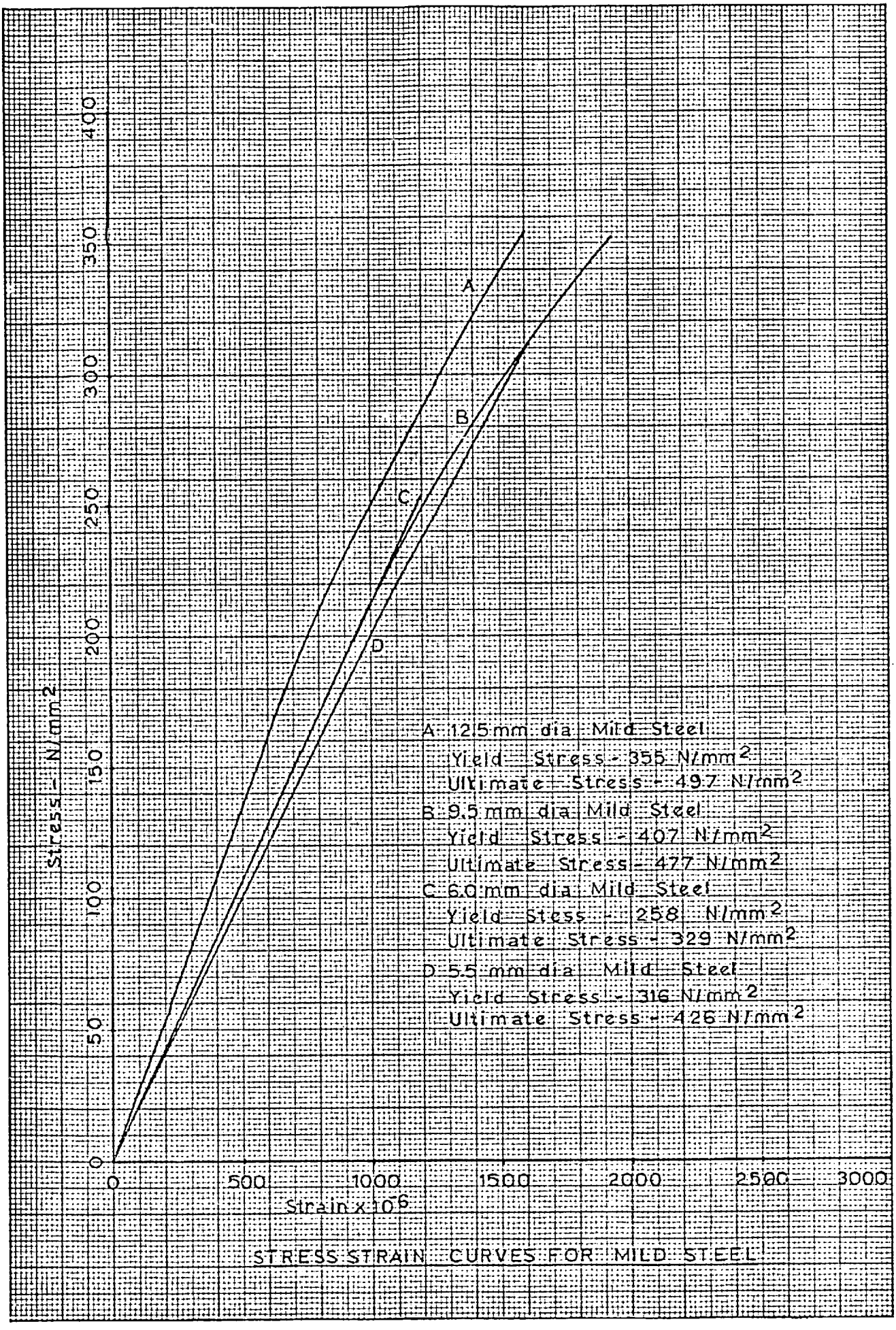


STRESS-STRAIN CURVES OF CONCRETE FIG. 25.



STRESS-STRAIN CURVES FOR STEEL

FIG. 26.



STRESS STRAIN CURVES FOR MILD STEEL

FIG. 27.

the two nibs of the beams. On one side of the frame and nibs, there was a load cell (100 KN) and other side of the frame and nib a jack (100 KN) to apply axial tension to the position of the beam between the two nibs. To keep the loading concentric, ball bearings with two 100 x 100 x 25 mm (4" x 4" x 1") plates were used on the inside faces of the nibs.

Similarly, vertical load was applied with the help of jacks and load cells. Similar types of loading arrangement (two plates and a ball) were adopted for the beams in group A. But for the application of vertical loads in case of beams of group B, a 500 KN jack having ball joints top and bottom was used, mostly as a central point load. For vertical loading in this case, no extra ball bearing was used and the jack bore directly on a 100 x 150 x 25 (4" x 6" x 1") mild steel plate. The arrangement of two symmetrical point loads was achieved using a spreader below the jack, supported at the required loading positions. In all cases, 25 mm (1") thick 100 x 150 mm (4" x 6") M.S. plates were used as bearing plates.

4.5. Instrumentation:

Because of the large number of unknowns involved in the shear failure of beams, attempts were made to measure some of them directly by instrumentation.

To measure the concrete strains on the surface at various load stages, mechanical strain gauges (Demecs) were used. No embeded electrical strain gauge was used, but surface concrete strains were measured in few occasions by electrical resistance gauges.

Steel strains in both longitudinal and transverse (stirrup) steels were measured with electrical resistance gauges. To measure accurately the main steel forces, strain gauges were stuck one on top and one on the bottom of the bar at each instrumented section. The

gauges were protected by three coats of water proofing material.

4.6 Testing Procedure:

The testing procedure in general was the same for all the beams. Loads, both vertical and transverse to the beams in group A were applied with the help of mannually operated jacks and load cells. Except on one occasion, axial loads were applied first in increments of 20 to 50 KN. Strain readings were taken and then the cracks (if any) were marked on the beams after each increment. Only beam B_4 was subjected to axial and vertical loads simultaneously.

In cases when axial load was applied first, it was held constant with its desired magnitude throughout the experiment. Then vertical load was applied. As before strain readings were taken for each increment of vertical load. In all cases the major vertical load (2 x shear force) was initially increased in increments of 40 KN, but near the anticipated failure load this increment was reduced to 20 KN. In the more instrumented beams, near the failure load, the load was increased by 10 KN only so as to record the strain readings more accurately near failure.

4.7. Behaviour of test Beams:

4.7.1 Restrained beams with axial tension:

Six beams (B_1, B_2, B_4, B_5, B_7 and B_{12}) were tested with axial tension and vertical load. The test results are given in table 6. The behaviour of these beams were observed at each load increment. As anticipated, when axial load was applied through nibs to the beams, vertical cracks were formed in the span at intervals of about 150 mm. These cracks first appeared sometimes at the top and sometimes at the middle of the depth. When the axial load was high (170 KN), the cracks were really wide enough to see through. After the formation of the vertical cracks, about $^9/_{10}$ of the axial load was transferred to the

top and bottom steel evenly at sections between cracks. This information was obtained from the steel strain readings of beam B_{12}. (see figs. 28 and 29). Stirrups were practically unstressed.

When vertical load was applied, the crack widths in the compressive zone were reduced while those in the tension zone increased. Sometimes in the compressive zone existing vertical cracks became invisible. The beams did not show any sign of distress at all. Only a few new flexural cracks were formed. Then when the shear cracking load was attained, inclined cracks were formed. The stirrups were practically unstressed until the shear cracking load was attained.

After the formation of an inclined crack, the physical behaviour of a beam was changed, and it started showing signs of increasing distress at each load increment.

From the strain readings (see fig. 30) on the stirrups it was apparent that the stirrups picked up load very rapidly after the formation of the inclined crack. They continued to carry increasing loads until their yield stresses were attained.

The critical inclined crack penetrated further into the compression zone with increasing load, and ultimately failure took place in a mode which was different from both shear-compression and diagonal tension. Though the crack patterns in the beam were very similar to those in beams failing in diagonal tension at the initial cracking stage (see figs. 47 and 48), the addition of web reinforcement affected the ultimate failure mode in these beams. All the beams in this series behaved identically and it is believed that final failure occurred due to shearing of the remaining compression zone at the head of the inclined crack, the failure mode is referred to as "shearing failure".

The inclination and horizontal projection of the critical cracks were observed in each beam of this series. Fig. 34 shows the plot of the inclination against a/d_1 ratios for all the beams tested during this investigation.

In beam B_5, the compression reinforcement was cut at a distance of 0.457 m (1'6") inside the compression zone from the point of contra-flexure. When axial load was applied, a big vertical crack was formed at this section. So in order to avoid local failure, axial load was kept constant as low as 70 KN. Then vertical load was applied. With the application of vertical load, the crack width reduced considerably and before failure it was hard to believe that there was any crack at all. The interesting thing was that the beam did not show any sign of distress until the formation of an inclined crack. The critical crack crossed through the existing vertical crack. This leads to the belief that considerable shear forces can be transferred across a crack if the two surfaces in contact are subjected to compression. In comparison to other beams, this beam carried a little less load.

4.7.2 Restrained beams with no axial load:

Only one beam B_3 was tested without axial load. The behaviour of this beam was very similar to those tested with axial tension. The only difference was the absence of vertical cracks. Even so the behaviour at different load stages and the ultimate failure mode were the same as in the previous series of beams.

4.7.3 Restrained beams with axial compression :

Twelve beams were tested in this series varying the magnitude of axial compression from 100 KN to 200 KN, while most of the other parameters were kept constant. As axial compression was applied first in all cases, the flexural cracking load was increased. Upon further loading, inclined cracks appeared, but the inclination of such cracks was smaller than in the beams of the previous series. Also the number of cracks was very limited as can be seen from the photographs (see figs 49, 50 and 51). Before failure, a considerable depth of compression zone was available which supports the contention that axial compression

should increase the depth of the neutral axis.

The most outstanding effect of axial compression was the increase in failure load and the change in mode of failure of some of the beams (see table 6). From the table it is evident that the failure load was increased in all cases. As a result of the increase in shear capacity, some of the beams showed signs of failing in bond. Splitting occurred at the level of top reinforcement in the tensile zone near the end of the inclined crack and then towards the point of contra-flexure. Because of the problem of bond failure, no beam was tested with an axial compression of more than 200 KN. However, the experimental results leave no doubt about the effect of axial compression on the shear capacity of reinforced concrete beams. The number of flexural cracks, their growth and widths were reduced due to axial compression. The beams were comparatively stiffer.

4.7.4 Simply supported beams with axial tension:

Five beams with varying shear span to effective depth ratios were tested in this series. The behaviour of all the beams was the same as that of the previous group until the formation of a shear crack. Beam B_6 was tested with a central load and a shear span/effective depth ratio of 3.9. Its behaviour and strength were similar to those of the restrained beams with similar axial tensile loads.

The other four beams with shorter shear spans behaved differently as was anticipated. Their shear span to effective depth ratios were 1.96 and 1.5 in beams B_8, B_{10} and B_{13}, B_{14} respectively. These beams were much stronger so far as ultimate load carrying capacity was concerned. In each the inclined crack penetrated into the compressive zone, thereby reducing the ultimate neutral axis depth. But the growth of this crack was halted below the load and ultimate failure was caused by crushing of the reduced compressive zone. The failure mode is believed to be shear compression.

4.7.5 Simply supported beams with no axial load:

Only two beams B_9 and B_{11} were tested in this series and their shear span to effective depth ratios were 1.96 and 1.5 respectively. The behaviour and mode of failure of these two beams were similar to those of the beams in the previous series with axial tension.

4.7.6 Simply supported beams with axial compression:

As expected, the addition of axial compression delayed the flexural cracking and thereby increased the shear cracking loads. All the beams except B_{26} appeared to fail in shear compression. Beam B_{26} failed in bond. Bond cracks appeared well after shear cracking and only just before the last load increment. It was realised that bond failure was not so much of a problem in the case of simply supported beams as in the case of restrained beams, but in order to avoid bond failure the axial compression was restricted to 150 KN except in B_{26}. Beam B_{26} was subjected to 200 KN of axial load and as is evident bond failure resulted.

4.8 Test results:

It is very difficult to say exactly at what load the inclined crack is fully developed. But from observation of the beams during the test programme, it seems that shear cracking load can be recorded fairly accurately by ordinary visual inspection. In the case of beams with web reinforcement, the formation of a visible inclined crack is a bit delayed. Table 6 shows the shear cracking loads and ultimate loads at failure of the beams.

The average inclination and horizontal projection of the inclined cracks causing failure are listed in table 6.

4.9 Examination of test results:

Fig. 31 shows the plots of $^{Qcr}/_{bd_1}$ and $^{Qult}/_{bd_1}$ against $\pm\ ^{N}/_{bd_1}$ (compression +ve). From the trend of the curve, it is evident that

Table 6. Test Results of beams

Beam No.	N/bd_1 N/mm^2	a/d_1	Q_{cr}/bd_1 N/mm^2	Q_{ult}/bd_1 N/mm^2	Inclination $\theta_{averg.}$	Horizontal proj. of crack after failure (c) mm	$\frac{c}{d_1}$	Mode of Failure
B_1	-2.41	2.8	1.20	2.28	23°	560	2.06	S
B_2	-4.09	2.8	1.20	2.08	22°	585	2.15	S
B_4	-2.41	2.8	1.44	2.28	22°	585	2.15	S
B_5	-1.68	2.8	1.44	1.92	24°	560	2.06	S
B_7	-4.09	2.8	1.20	2.28	22°	585	2.15	S
B_{12}	-4.09	2.8	1.20	2.23	22°	535	1.97	S
B_3	0	2.8	1.44	2.05	23°	585	2.15	S
B_{15}	+4.82	2.8	2.41	3.13	17°	610	2.24	B(SC)
B_{17}	+3.61	2.8	1.44	2.29	21°	560	2.06	S
B_{18}	+3.61	2.8	2.41	3.01	21°	535	1.97	B(SC)
B_{20}	+2.41	2.8	1.92	2.41	21°	535	1.97	SC
B_{22}	+4.82	2.8	1.92	3.13	22°	510	1.88	B(SC)
B_{23}	+3.61	2.8	1.92	2.89	20°	585	2.15	B(SC)
B_{24}	+4.82	2.8	1.92	2.89	21°	610	2.24	SC
B_{25}	+4.82	2.8	2.41	3.37	20°	610	2.24	B(SC)
B_{27}	+4.82	2.8	1.92	3.37	22°	585	2.15	SC
B_{28}	+3.61	2.8	1.44	1.93	20°	482	1.77	B(SC)
B_{29}	+4.82	2.8	2.41	2.41	23°	560	2.06	F
B_{30}	+2.41	2.9	1.92	2.73	38°	381	1.44	SC
B_6	-2.88	3.9	1.20	2.10	21°	610	2.24	S
B_8	-2.41	1.96	1.44	2.76	38°	381	1.40	SC
B_{10}	-2.41	1.96	1.44	2.97	35°	381	1.40	SC
B_{13}	-2.41	1.50	1.92	3.71	40°	356	1.31	SC
B_{14}	-2.41	1.50	1.92	3.26	43°	305	1.12	SC
B_9	0	1.96	1.92	3.34	37°	407	1.50	SC
B_{11}	0	1.50	2.41	3.95	40°	330	1.21	SC
B_{16}	+3.61	1.96	2.88	4.10	32°	330	1.21	SC
B_{19}	+2.41	1.96	2.41	3.72	29°	356	1.31	SC
B_{21}	+3.61	1.96	2.88	3.72	27°	381	1.40	SC
B_{26}	+4.82	2.8	2.88	3.37	20°	610	2.24	B(SC)
B_{31}	+2.41	3.46	1.44	2.34	23°	685	2.52	S

S = shearing failure
B = Bond failure
SC = Shear compression failure
F = Flexural failure - Beam B_{29} failed near the cantilever e

Table 7. Test Results:

GROUP A: Restrained beams.

Series 1. Beams with axial tension:

Beam No.	Age in days	Ucyl N/mm^2	Ut N/mm^2	rst%	rsc%	$r_q f_{yq}$ N/mm^2	M/Qd_1	N/bd_1 N/mm^2	$Qult/bd$ N/mm^2
B_1	21	33.5	3.2	1.46	1.46	0.66	2.8	2.41	2.28
B_2	19	32.9	3.10	1.46	1.46	0.66	2.8	4.09	2.08
B_4	20	35.10	2.95	1.46	1.46	0.66	2.8	2.41	2.28
B_5	20	32.70	2.62	1.46	-	0.66	2.8	1.68	1.92
B_7	20	32.2	2.68	1.46	1.46	0.66	2.8	4.09	2.28
B_{12}	21	31.0	2.91	1.46	1.46	0.66	2.8	4.09	2.23

Series 2. Beams with no axial load:

Beam No.	Age in days	Ucyl N/mm^2	Ut N/mm^2	rst%	rsc%	$r_q f_{yq}$ N/mm^2	M/Qd_1	N/bd_1 N/mm^2	$Qult/bd$ N/mm^2
B_3	21	36.6	2.9	1.46	1.46	0.66	2.8	0	2.05

Series 3. Beams with axial compression:

Beam No.	Age in days	Ucyl N/mm^2	Ut N/mm^2	rst%	rsc%	$r_q f_{yq}$ N/mm^2	M/Qd_1	N/bd_1 N/mm^2	$Qult/b$ N/mm^2
B_{15}	22	32.4	2.58	1.46	1.46	0.66	2.8	4.82	3.13
B_{17}	18	29.5	2.79	1.46	1.46	0.66	2.8	3.61	2.29
B_{18}	20	29.3	2.86	1.46	1.46	0.66	2.8	3.61	3.01
B_{20}	20	28.5	2.16	1.46	1.46	0.66	2.8	2.41	2.41
B_{22}	20	27.5	2.48	1.46	1.46	0.66	2.8	4.82	3.13
B_{23}	25	30.3	2.70	1.46	-	0.66	2.8	3.61	2.89
B_{24}	18	30.8	2.70	1.46	1.46	0.66	2.8	4.82	2.89
B_{25}	20	30.2	2.49	1.46	1.46	1.05	2.8	4.82	3.37
B_{27}	21	28.6	2.54	1.46	1.46	1.05	2.8	4.82	3.37
B_{28}	26	13.9	1.83	1.46	1.46	0.66	2.8	3.61	1.93
B_{29}	27	35.4	2.64	0.97	0.97	0.66	2.8	4.82	2.41
B_{30}	21	31.3	2.70	2.00	2.00	0.66	2.9	2.41	2.73

Table 8. Test results:

GROUP B. Simply supported beams.

Series 1. Beams with axial tension:

Beam No.	Age in days	Ucyl N/mm^2	Ut N/mm^2	rst%	rsc%	$r_q f_{yq}$ N/mm^2	M/Qd_1	N/bd_1 N/mm^2	$Qult/bd_1$ N/mm^2
B_6	21	33.1	2.48	1.46	1.46	0.66	3.9	2.88	2.10
B_8	20	31.2	2.37	1.46	0.34	0.66	1.96	2.41	2.76
B_{10}	20	34.3	2.75	1.46	1.46	0.66	1.96	2.41	2.97
B_{13}	21	30.2	2.89	1.46	1.46	0.66	1.5	2.41	3.71
B_{14}	21	29.0	2.64	1.46	0.34	0.66	1.5	2.41	3.26

Series 2. Beams with no axial load:

Beams No.	Age in days	Ucyl N/mm^2	Ut N/mm^2	rst%	rsc%	$r_q f_{yq}$ N/mm^2	M/Qd_1	N/bd_1 N/mm^2	$Qult/bd$ N/mm^2
B_9	21	31.4	2.65	1.46	1.46	0.66	1.96	0	3.34
B_{11}	20	31.7	2.86	1.46	1.46	0.66	1.5	0	3.95

Series 3. Beams with axial compression:

Beam No.	Age in days	Ucyl N/mm^2	Ut N/mm^2	rst%	rsc%	$r_q f_{yq}$ N/mm^2	M/Qd_1	N/bd_1 N/mm^2	$Qult/bd$ N/mm^2
B_{16}	18	29.5	2.56	1.46	1.46	0.66	1.96	3.61	4.10
B_{19}	25	30.0	2.56	1.46	1.46	0.66	1.96	2.41	3.72
B_{21}	19	29.7	2.20	1.46	0.34	0.66	1.96	3.61	3.72
B_{26}	19	30.4	2.54	1.46	1.46	1.05	2.8	4.82	3.37
B_{31}	21	31.5	2.97	1.46	1.46	0.66	3.46	2.41	2.34

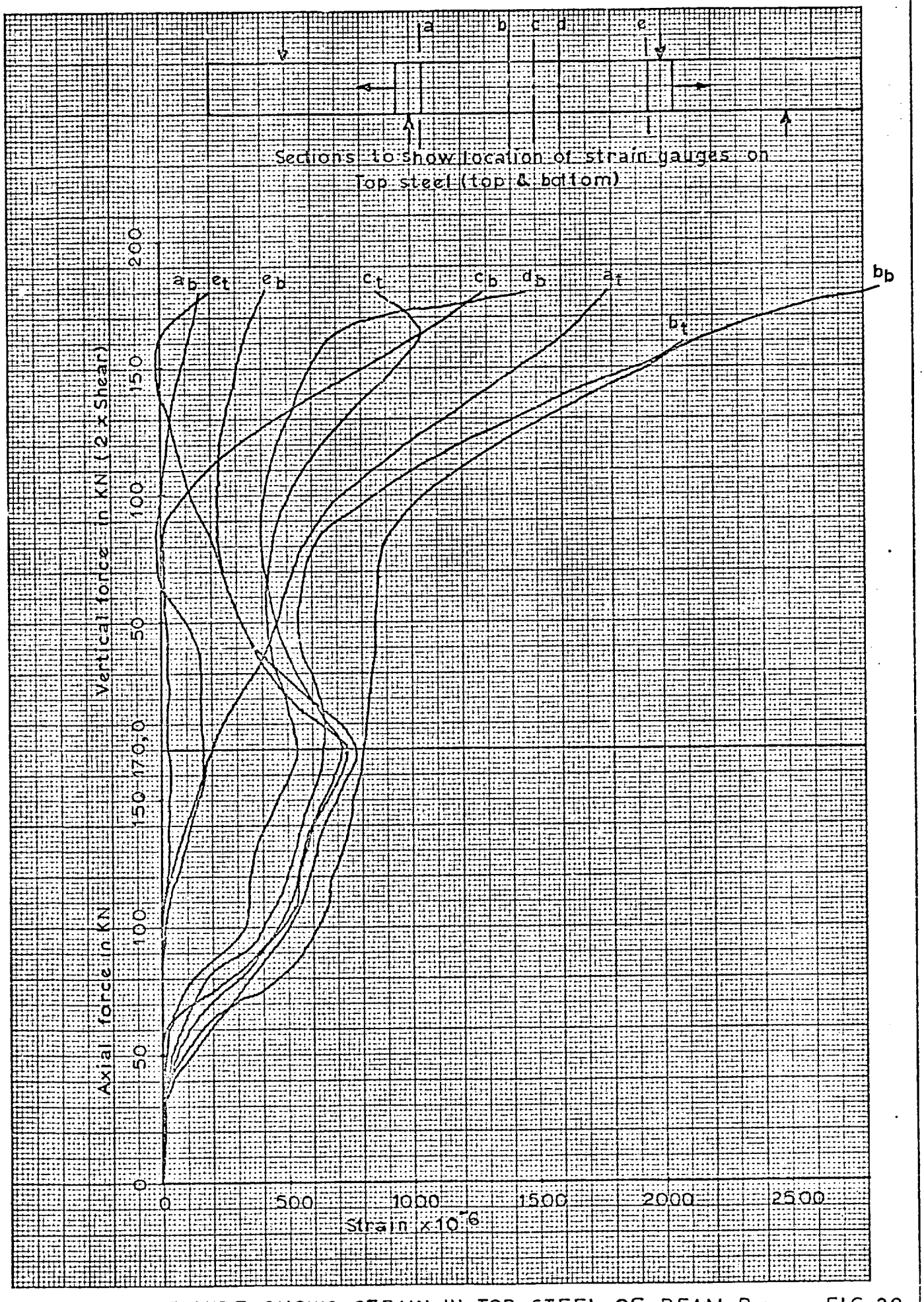


FIGURE SHOWS STRAIN IN TOP STEEL OF BEAM B_{12} FIG. 28.

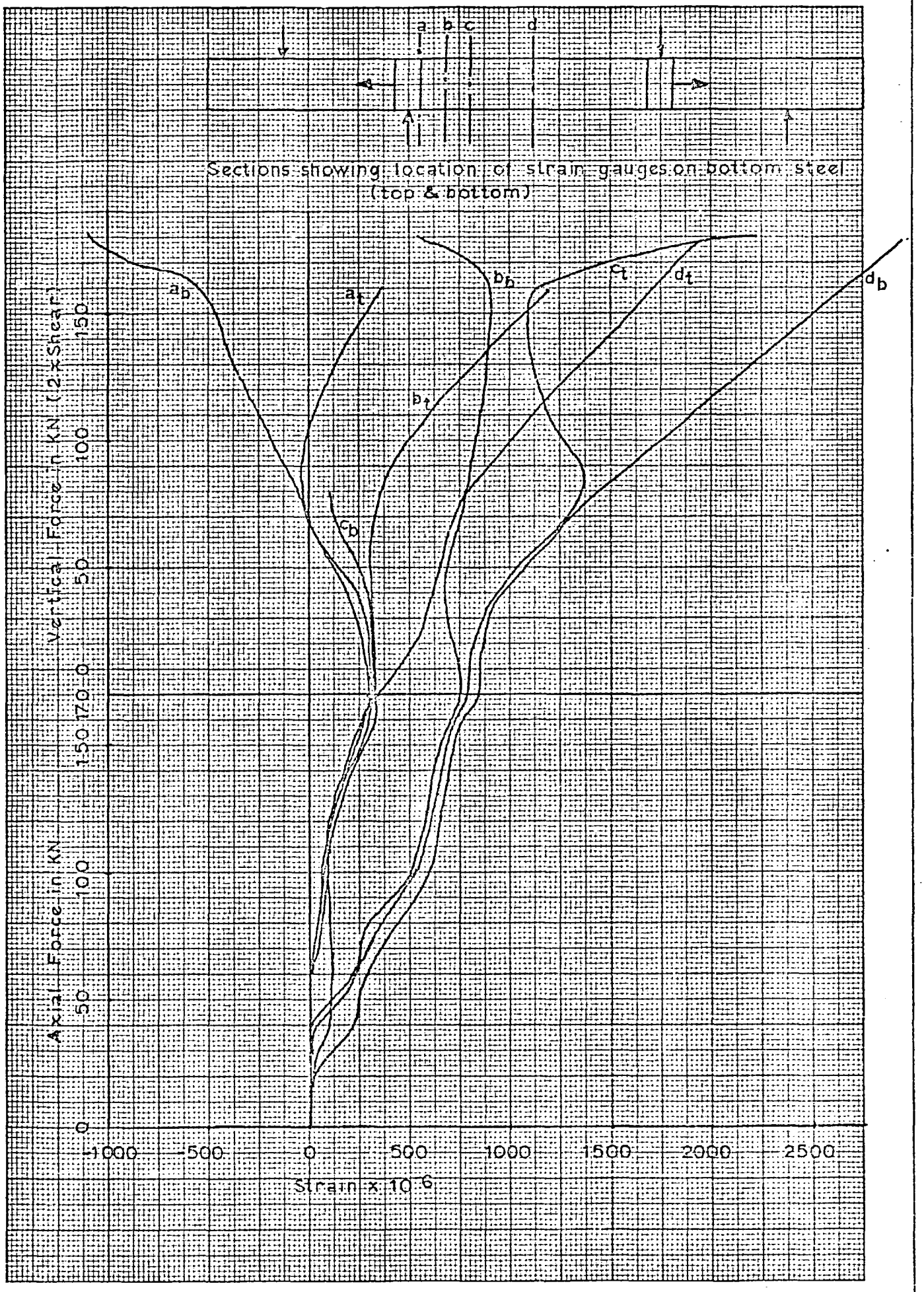


FIGURE SHOWS STRAIN IN BOTTOM STEEL OF BEAM B_{12}. FIG. 29.

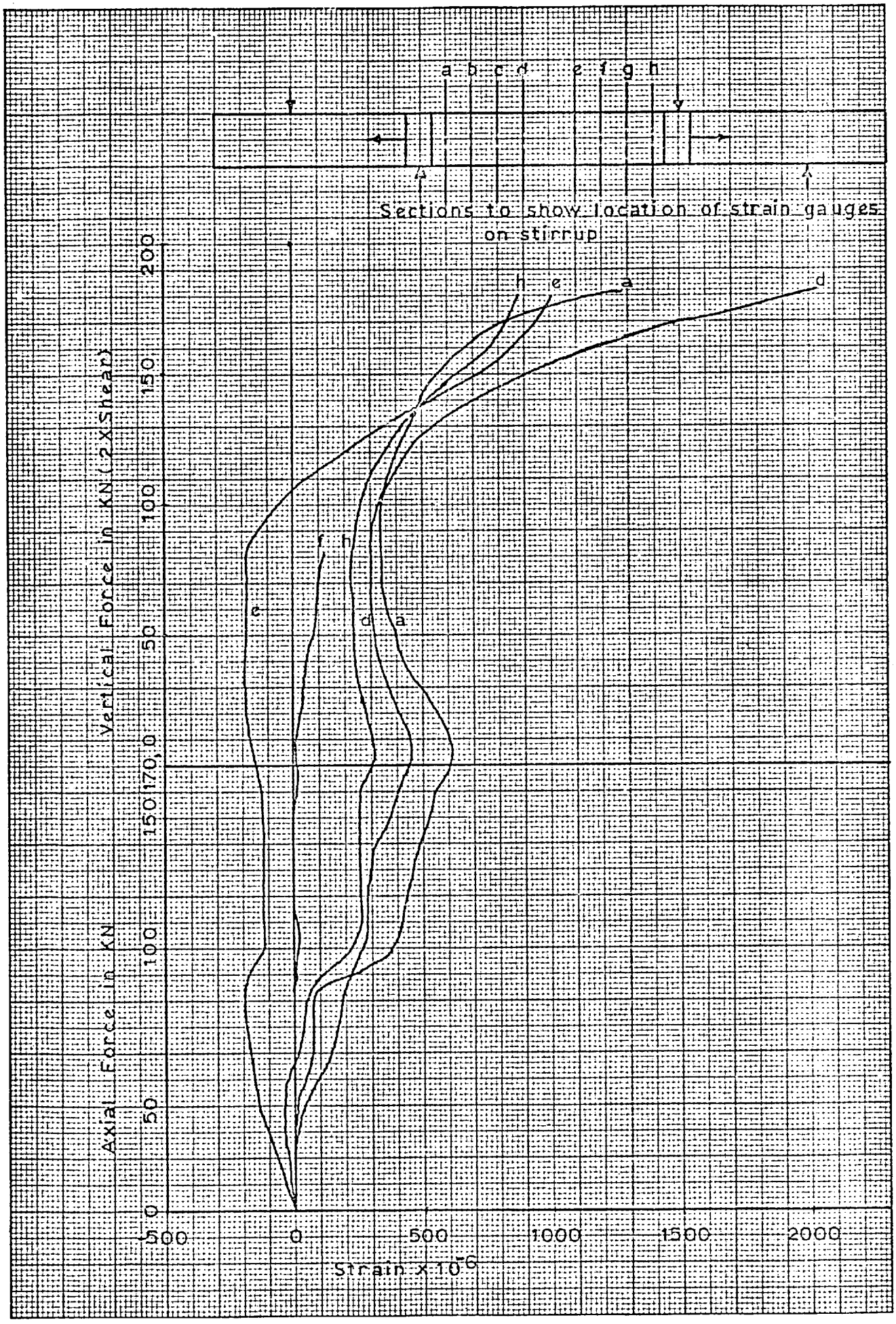
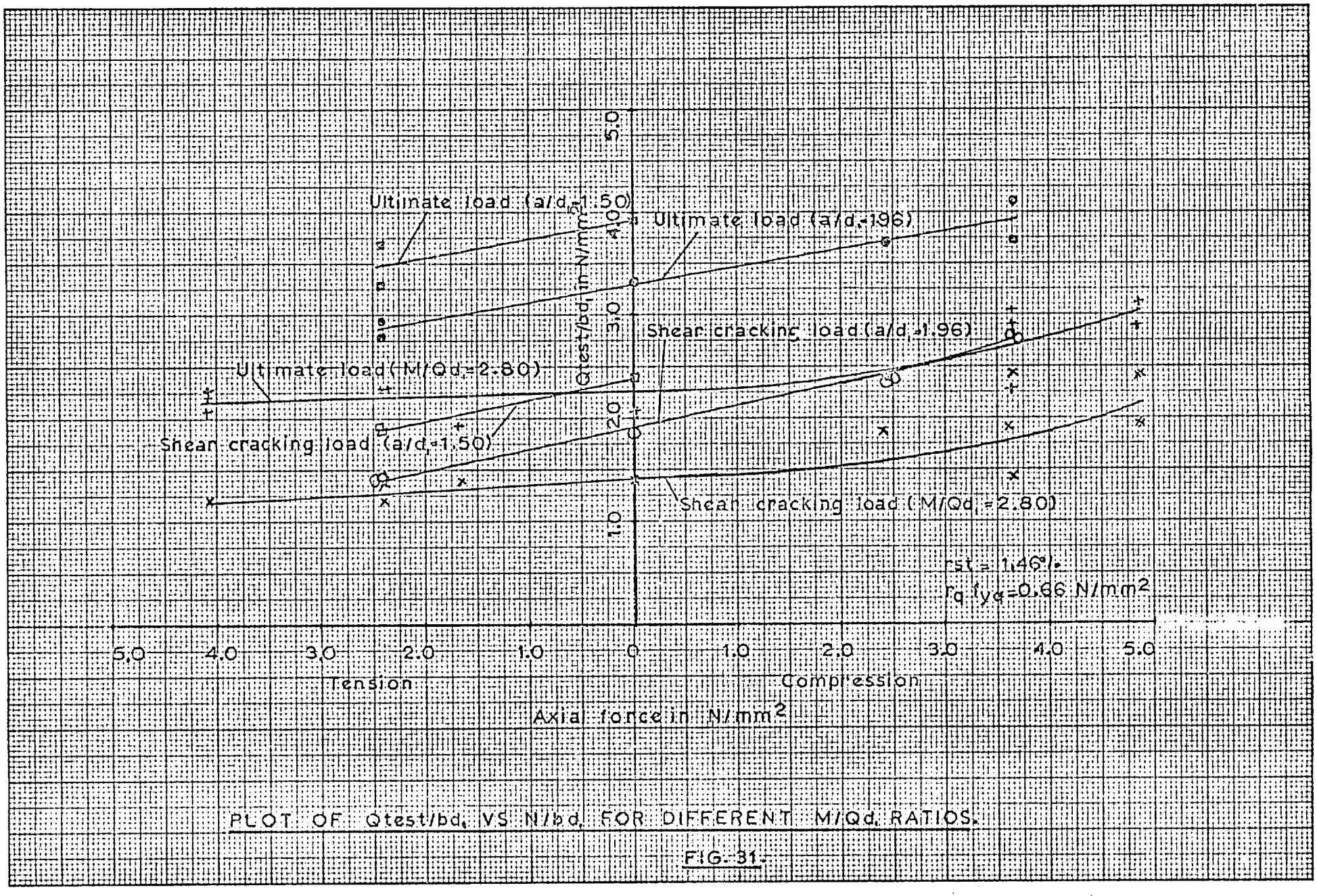
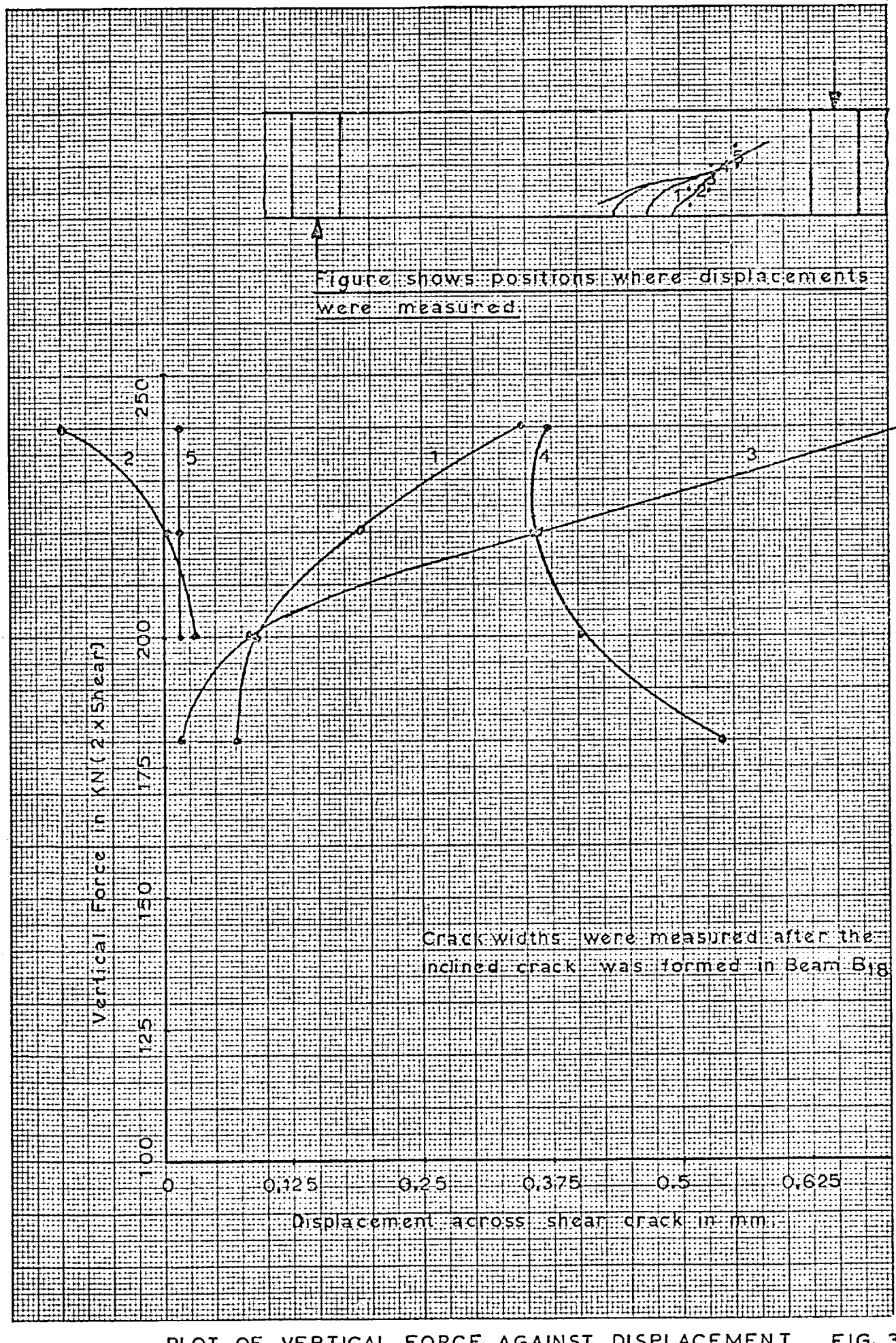


FIGURE SHOWS STRAINS IN STIRRUPS OF BEAM B_{12}. FIG.30.



PLOT OF Qtest/bd, VS N/bd, FOR DIFFERENT M/Qd, RATIOS.

FIG. 31.



PLOT OF VERTICAL FORCE AGAINST DISPLACEMENT FIG. 32.

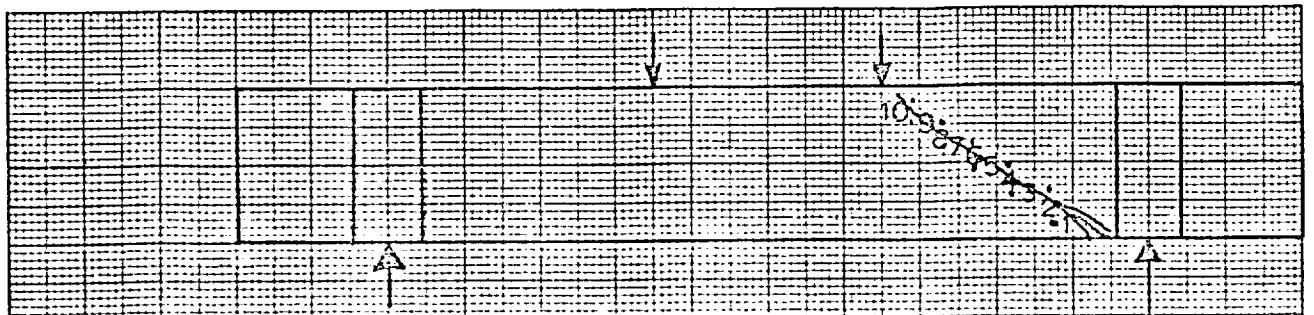


Figure shows positions where displacements were measured.

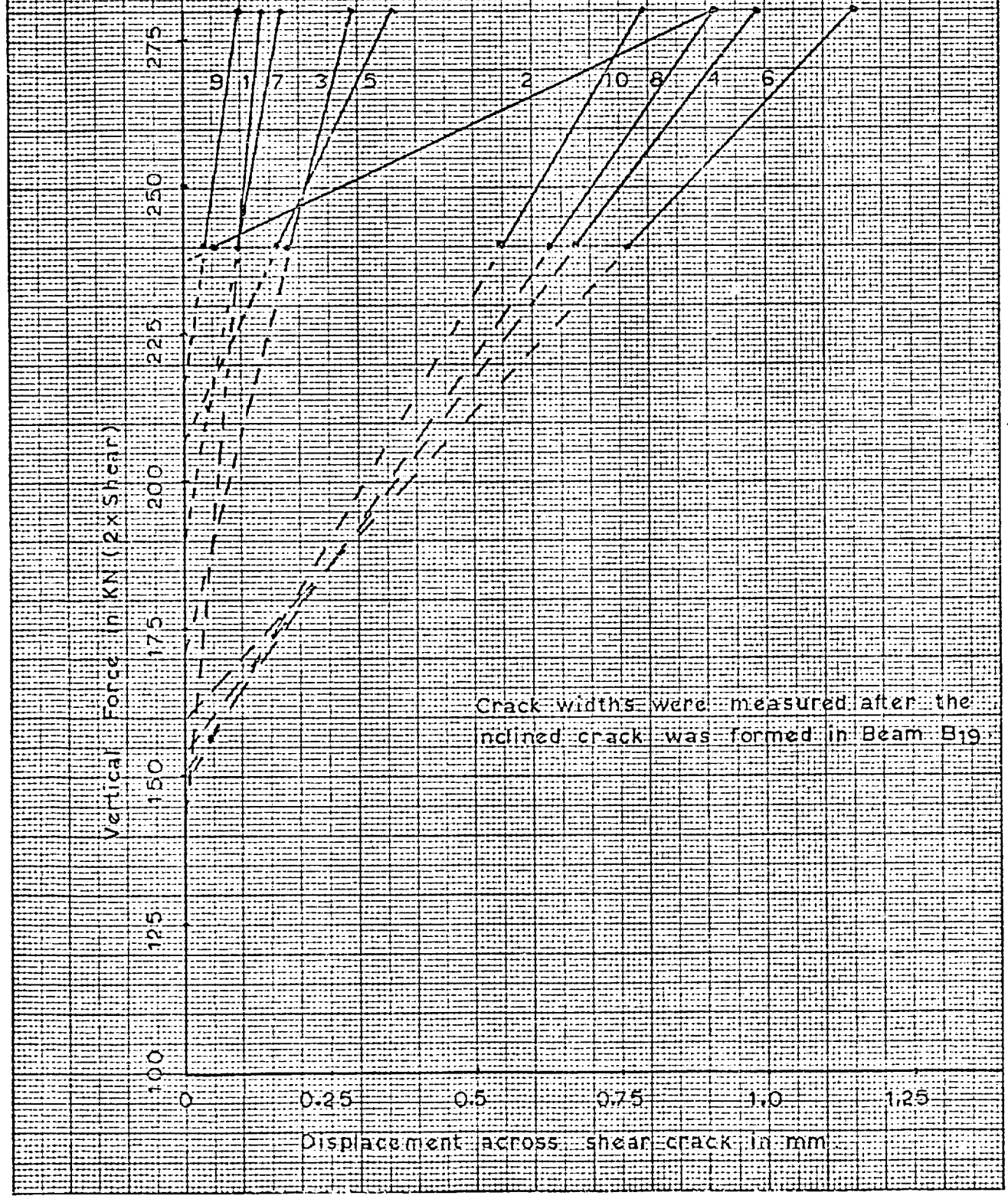
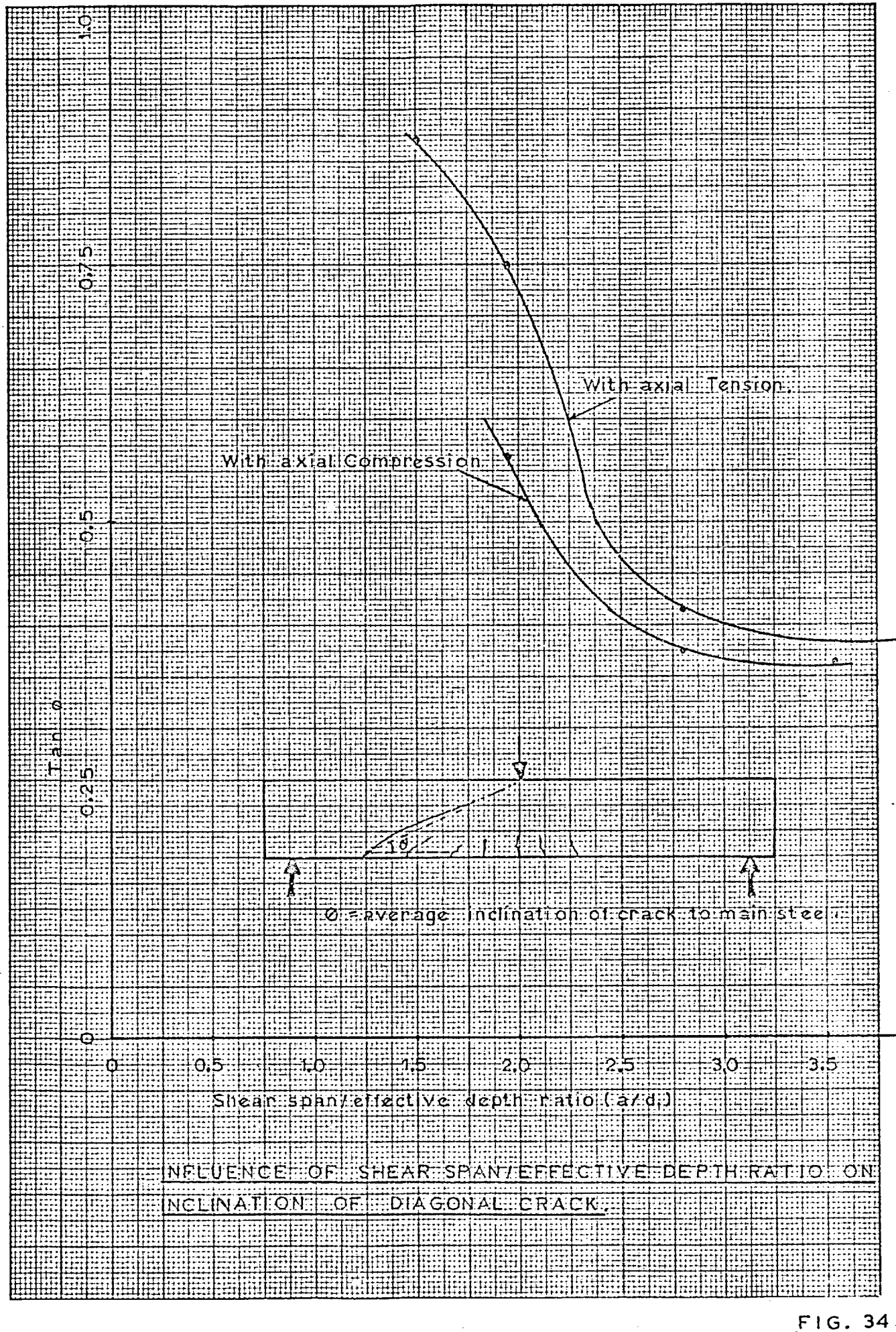


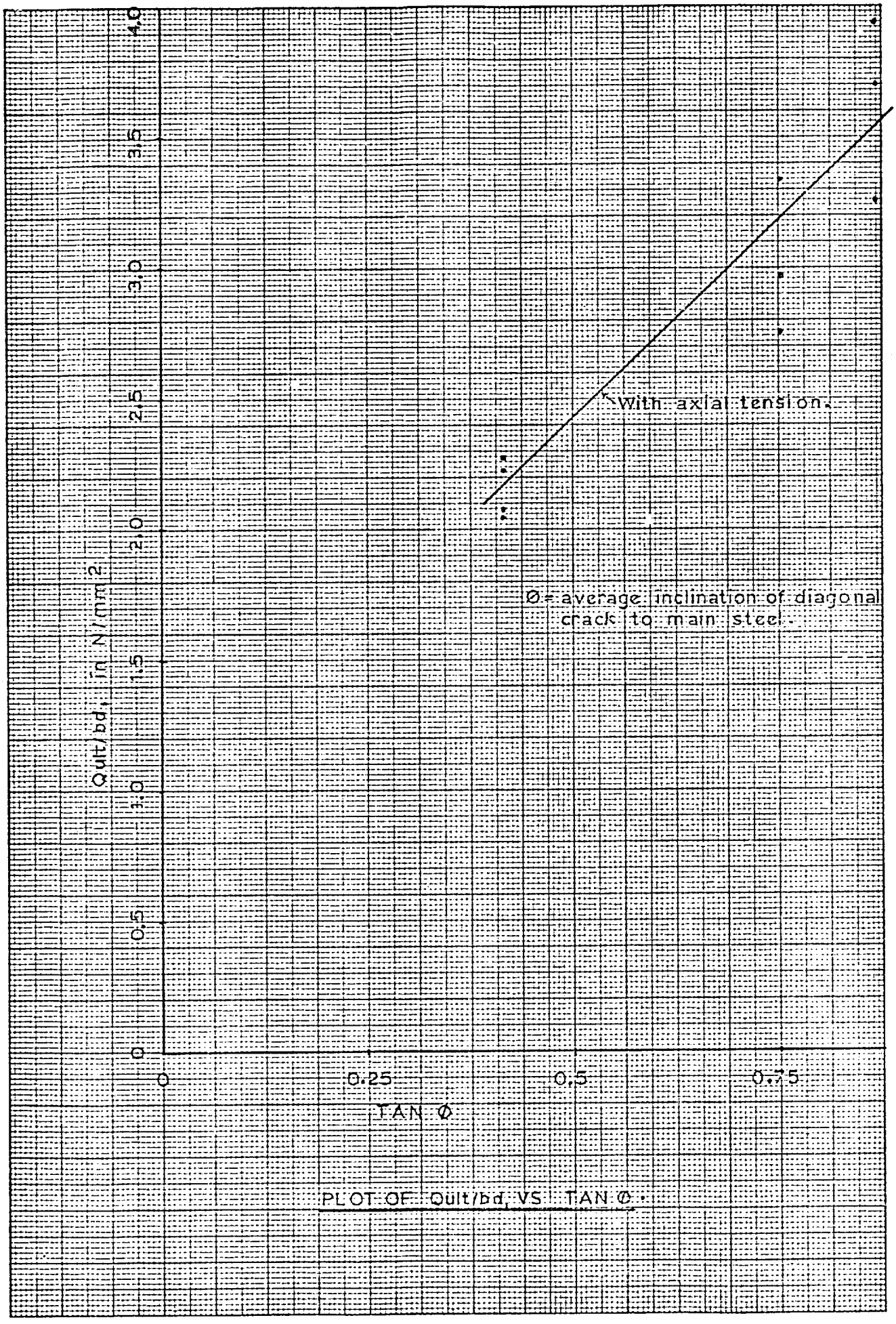
FIG. 33. PLOT OF VERTICAL FORCE AGAINST DISPLACEMENT



θ = average inclination of crack to main steel.

INFLUENCE OF SHEAR SPAN/EFFECTIVE DEPTH RATIO ON INCLINATION OF DIAGONAL CRACK.

FIG. 34.



PLOT OF Qult/bd VS TAN Ø.

FIG. 35.

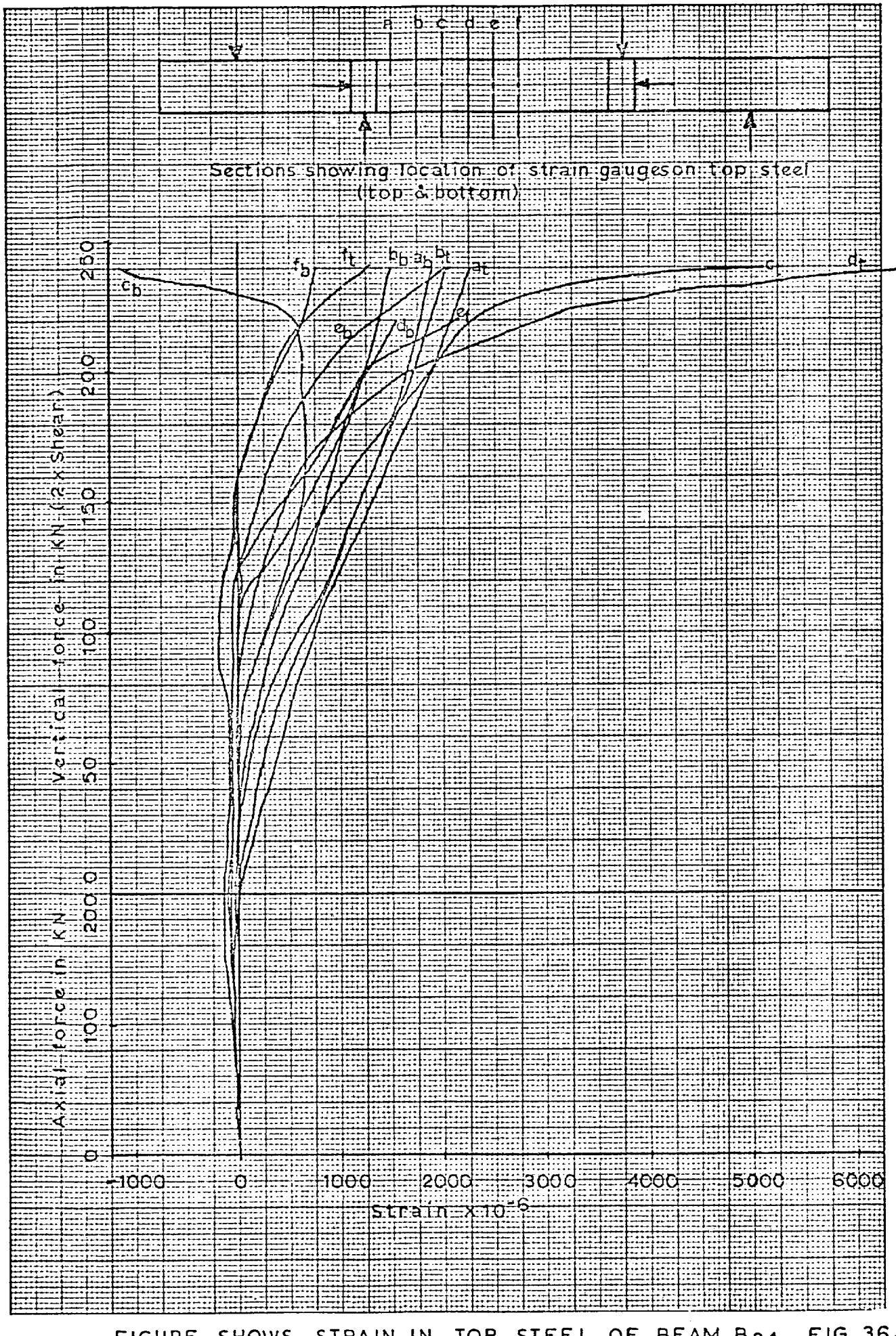


FIGURE SHOWS STRAIN IN TOP STEEL OF BEAM B_{24} FIG. 36.

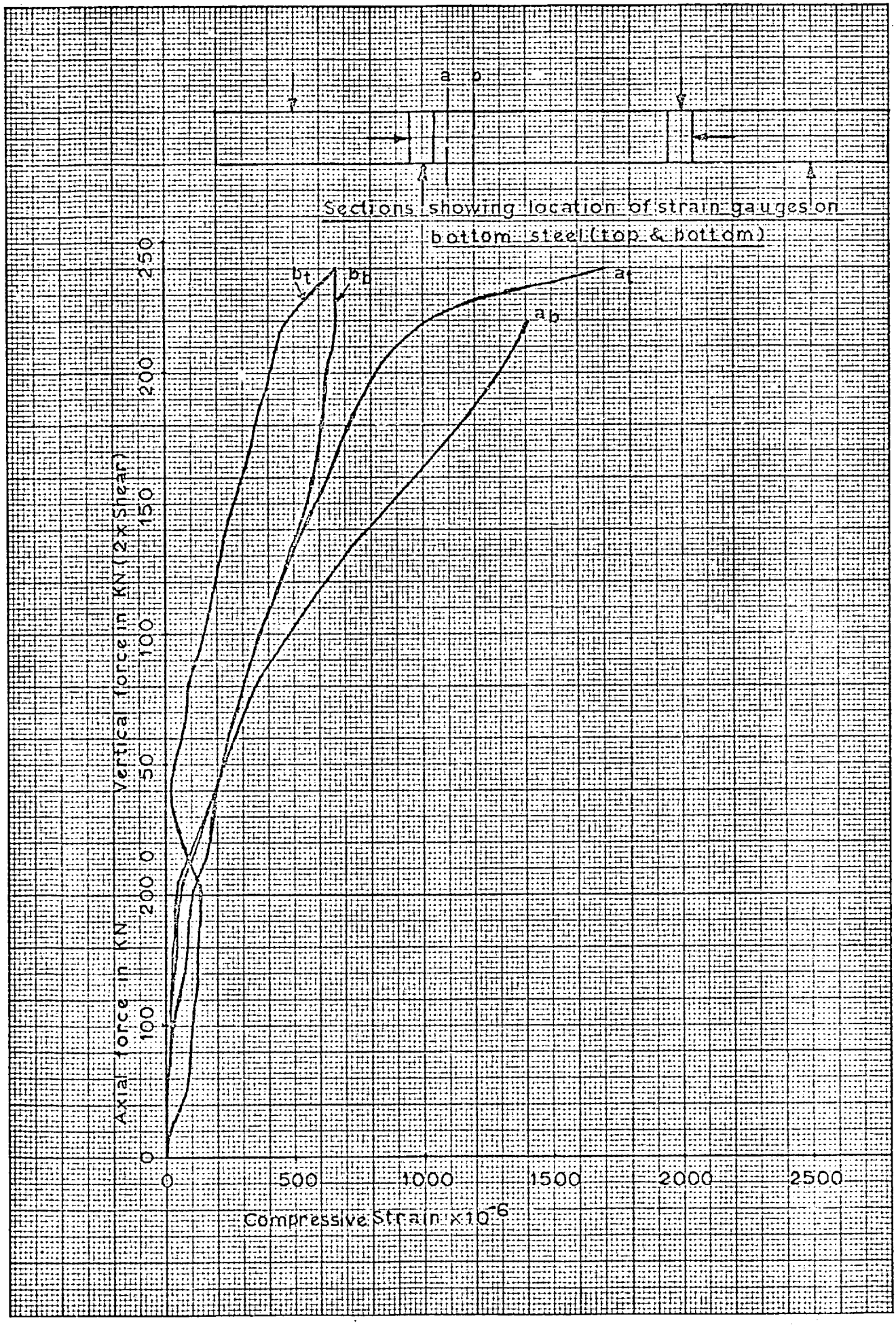


FIGURE SHOWS STRAIN IN BOTTOM STEEL OF BEAM B_{24}. FIG.37.

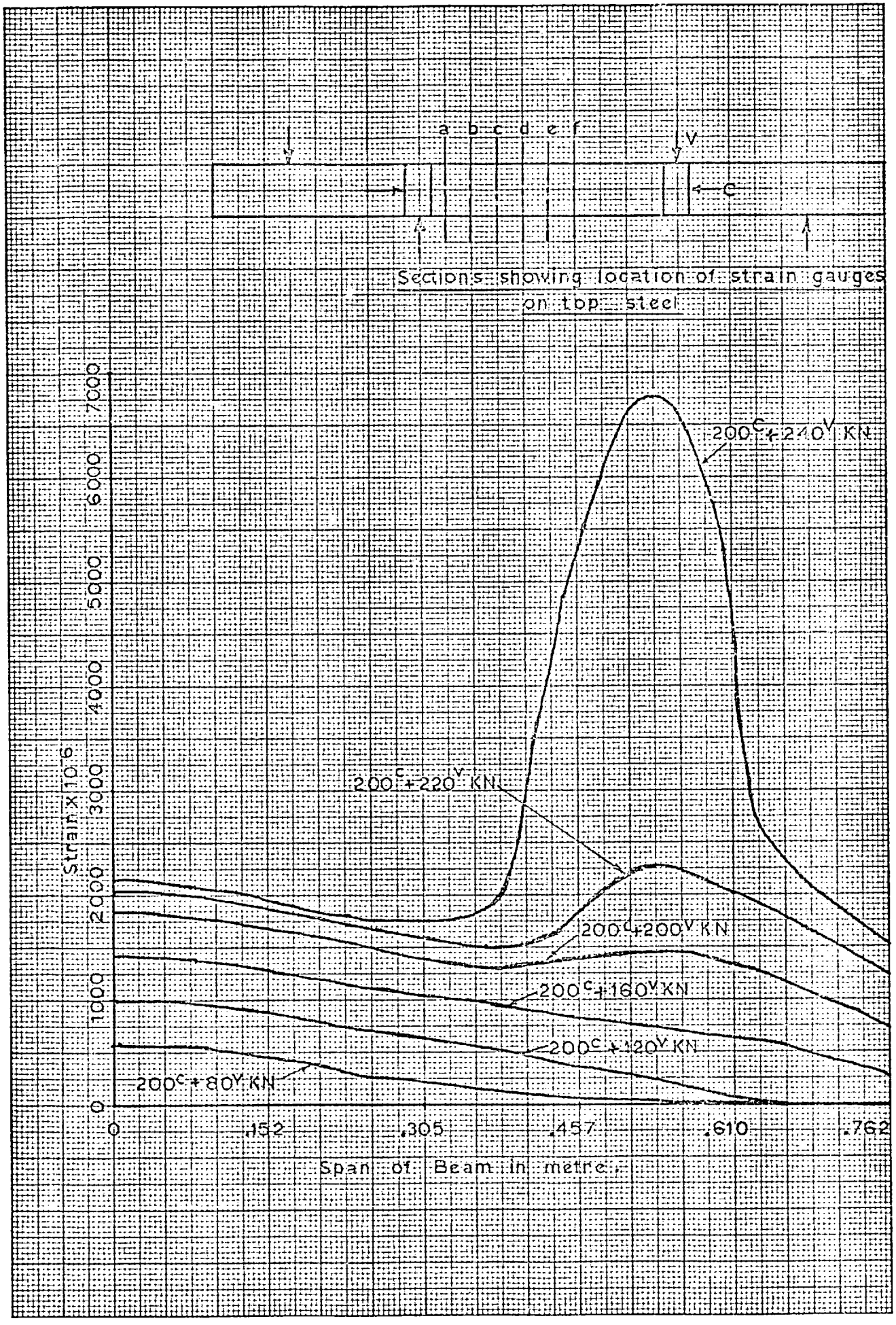


FIGURE SHOWS STRAIN IN TOP STEEL OF BEAM B_{24} FIG. 38.

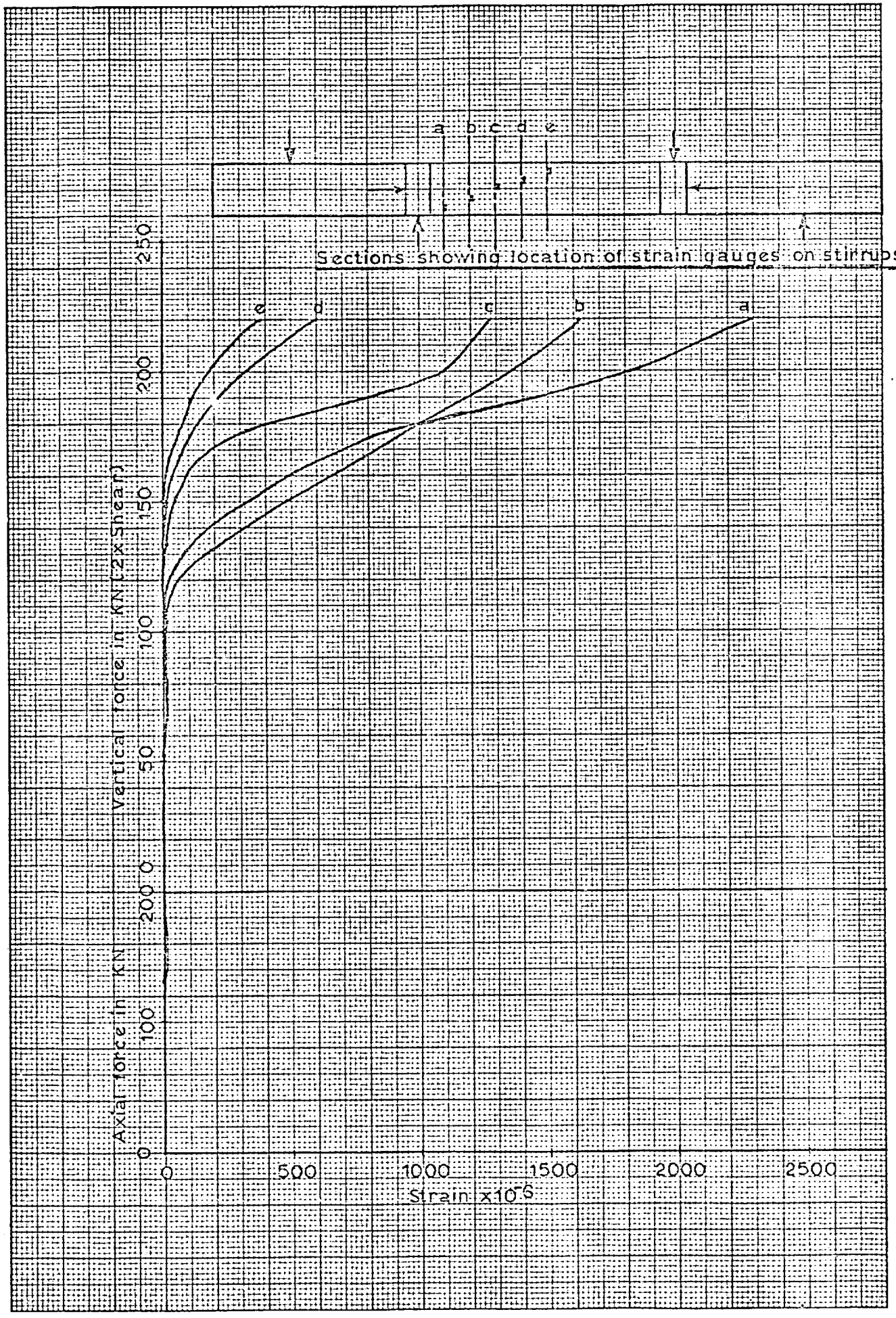


FIGURE SHOWS STRAIN IN STIRRUPS OF BEAM B_{24}. FIG. 39.

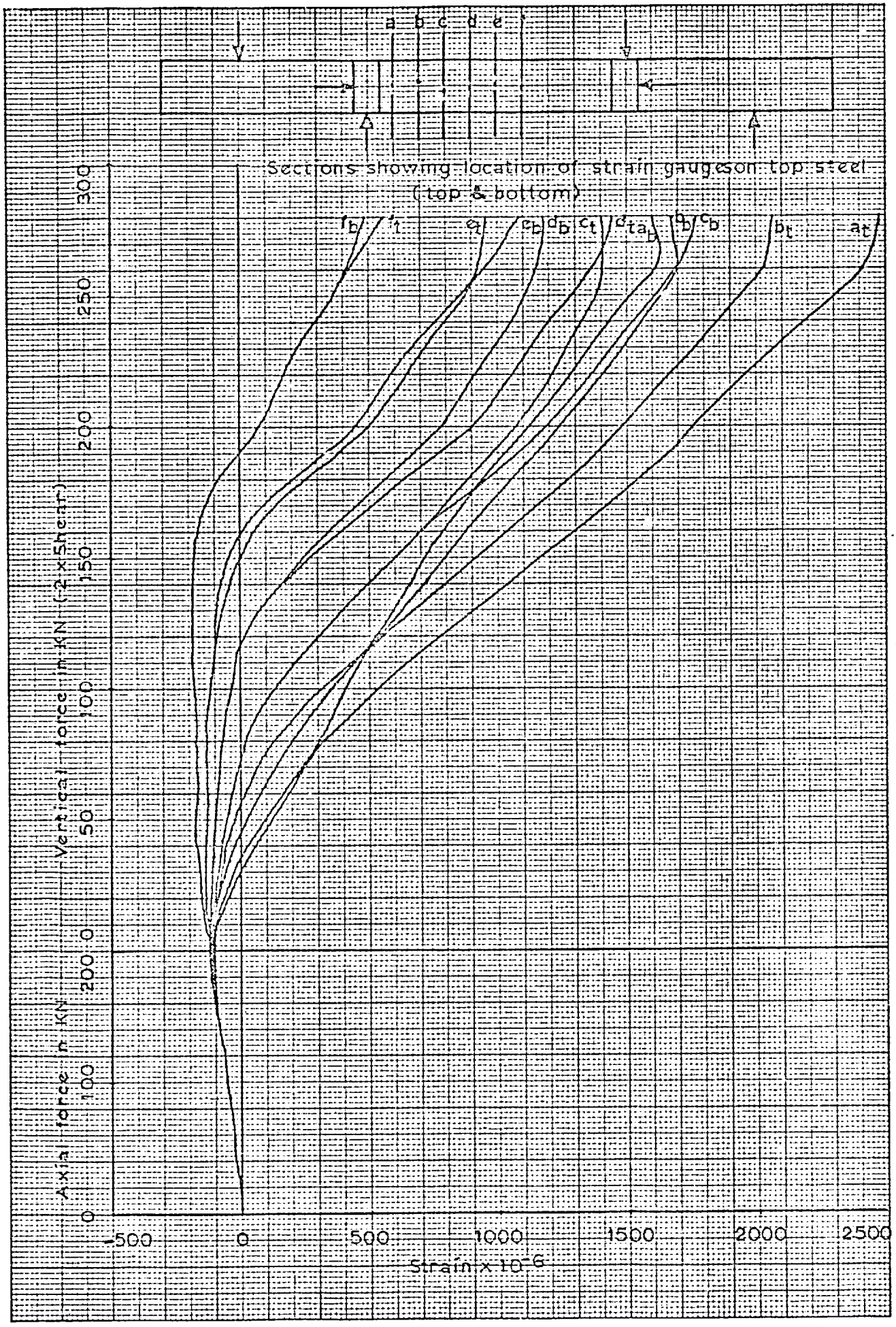


FIGURE SHOWS STRAIN IN TOP STEEL OF BEAM B_{25} FIG. 40.

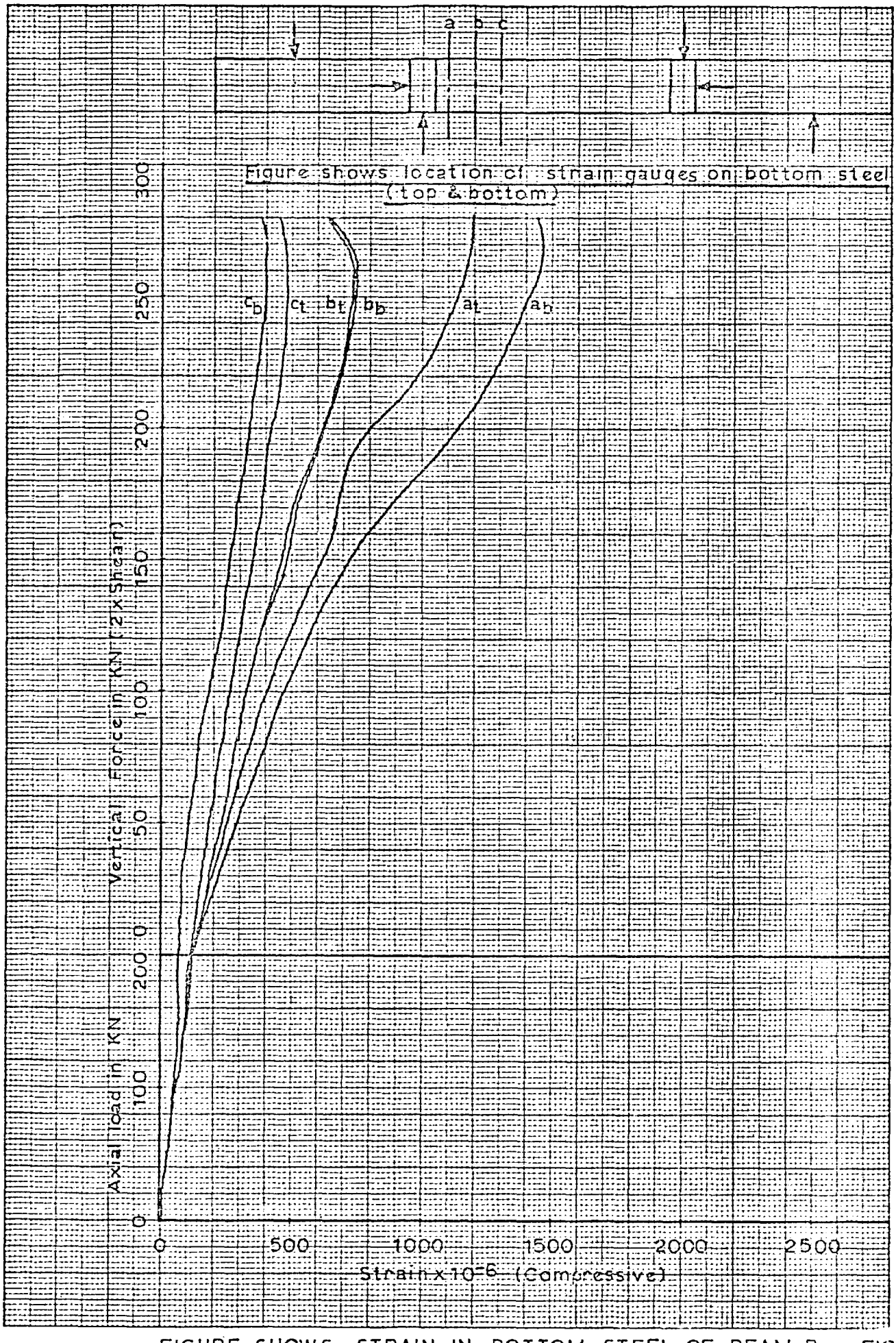


FIGURE SHOWS STRAIN IN BOTTOM STEEL OF BEAM B_{25}. FIG. 41.

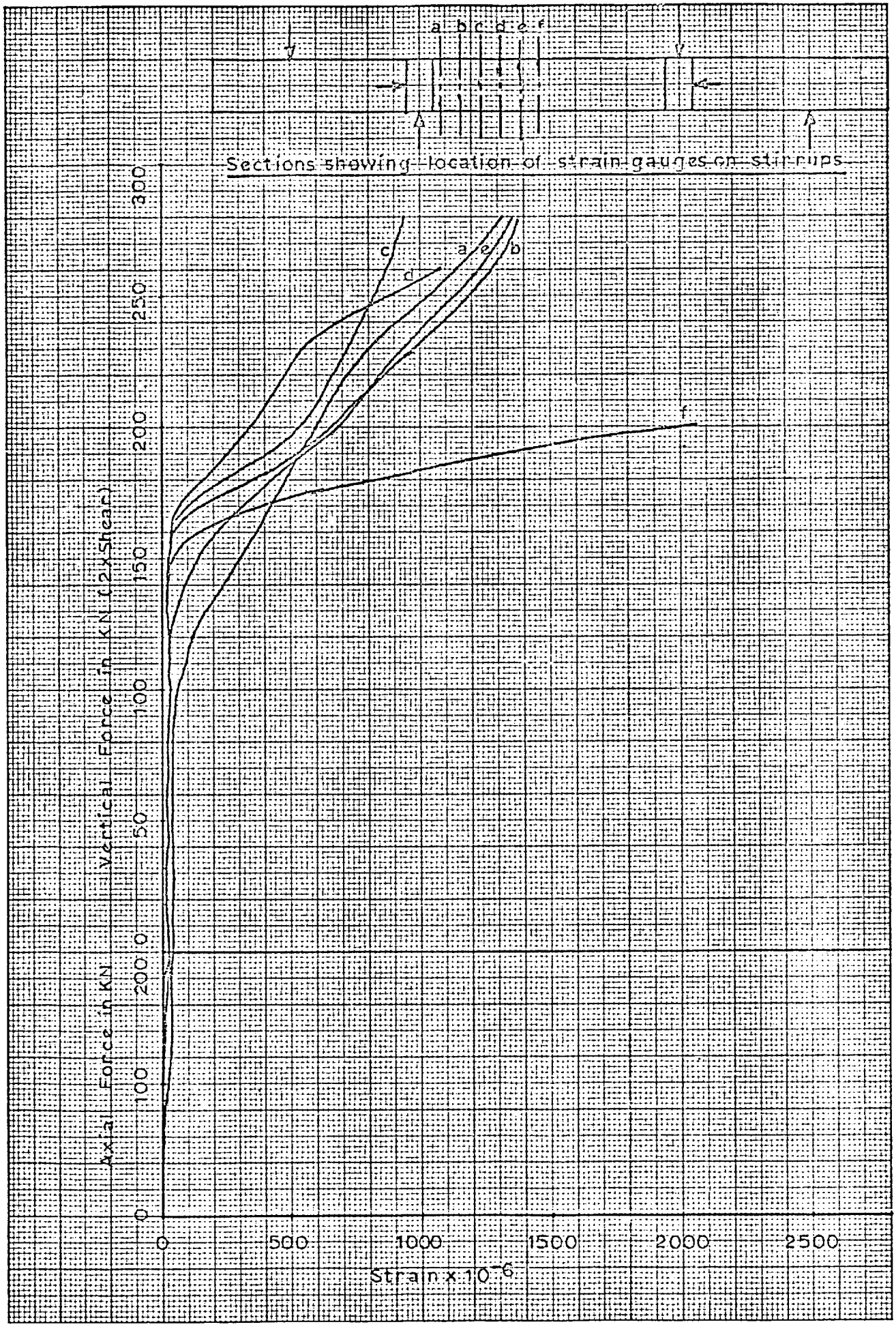


FIGURE SHOWS STRAIN IN STIRRUPS OF BEAM B_{25} FIG. 42.

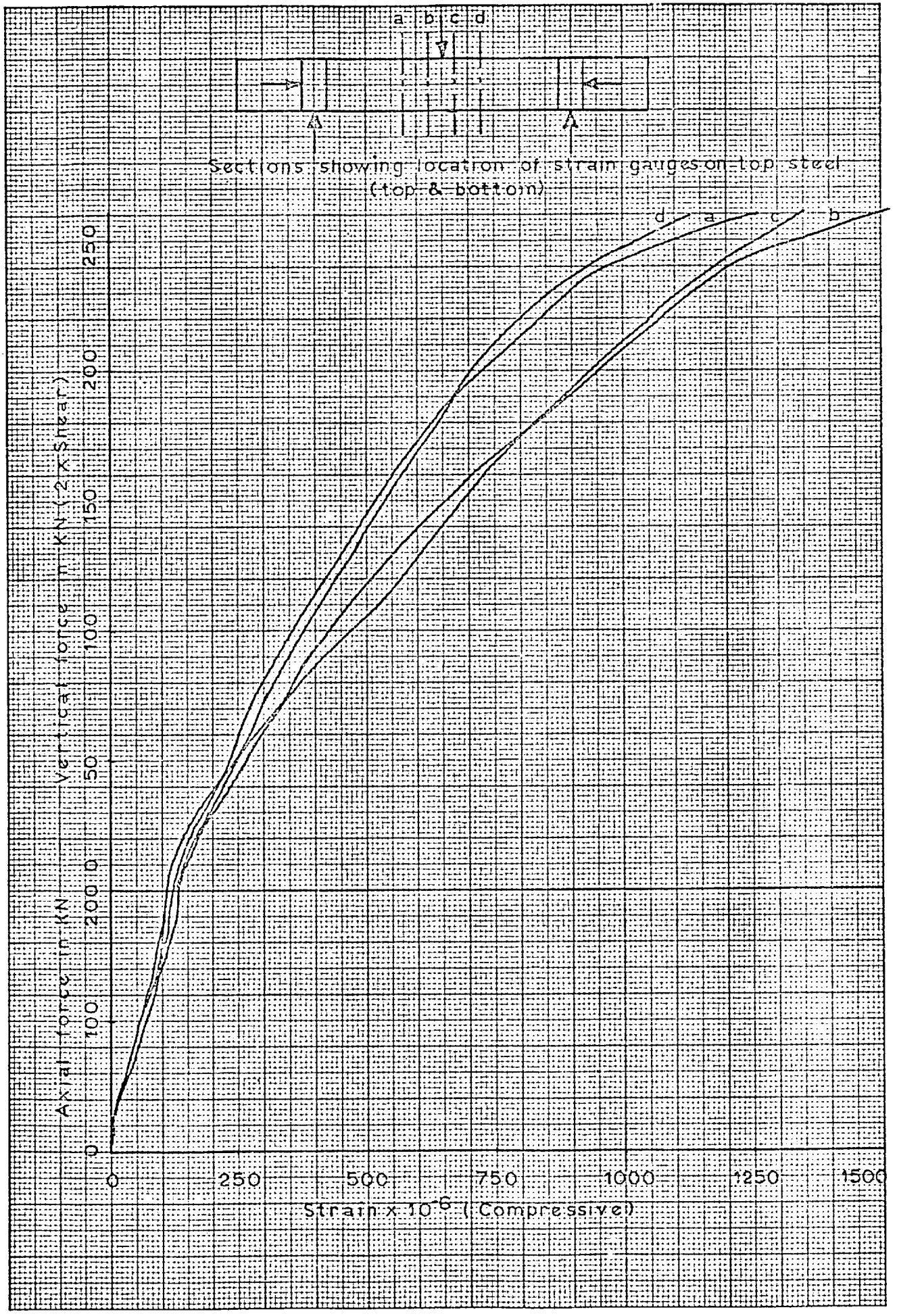


FIGURE SHOWS STRAIN IN TOP STEEL OF BEAM B_{26} FIG. 43.

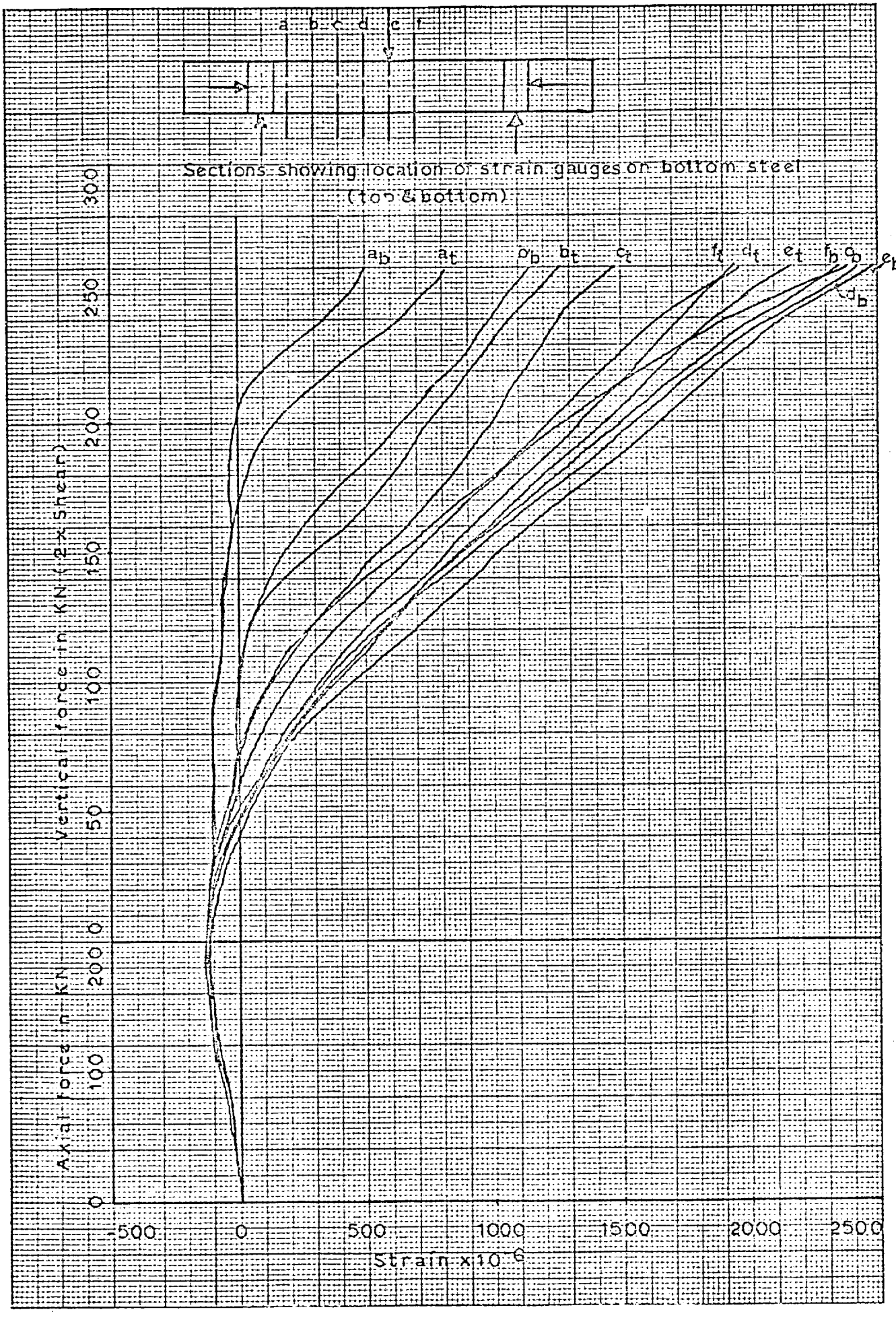


FIGURE SHOWS STRAIN IN BOTTOM STEEL OF BEAM B_{26} FIG. 44.

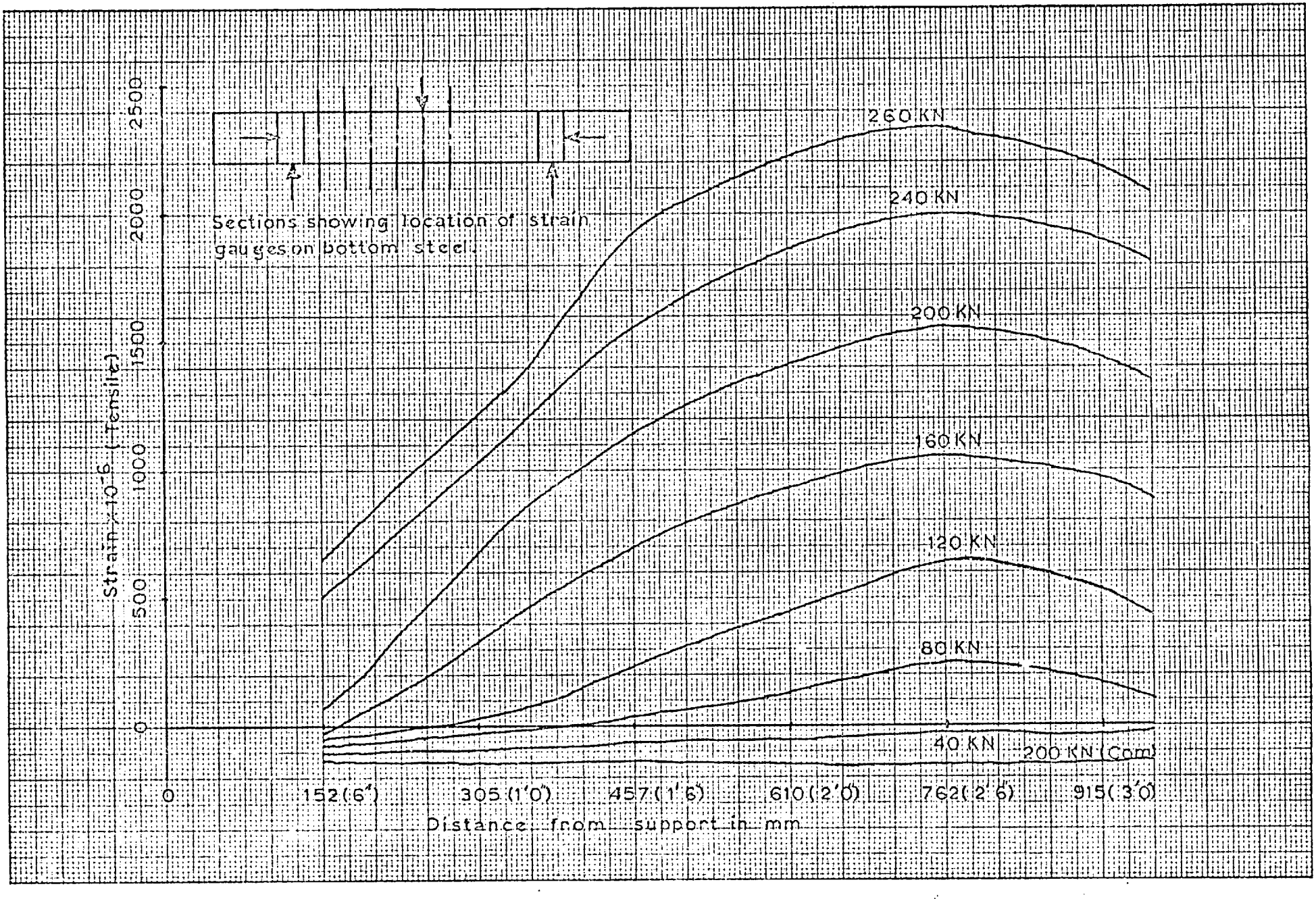
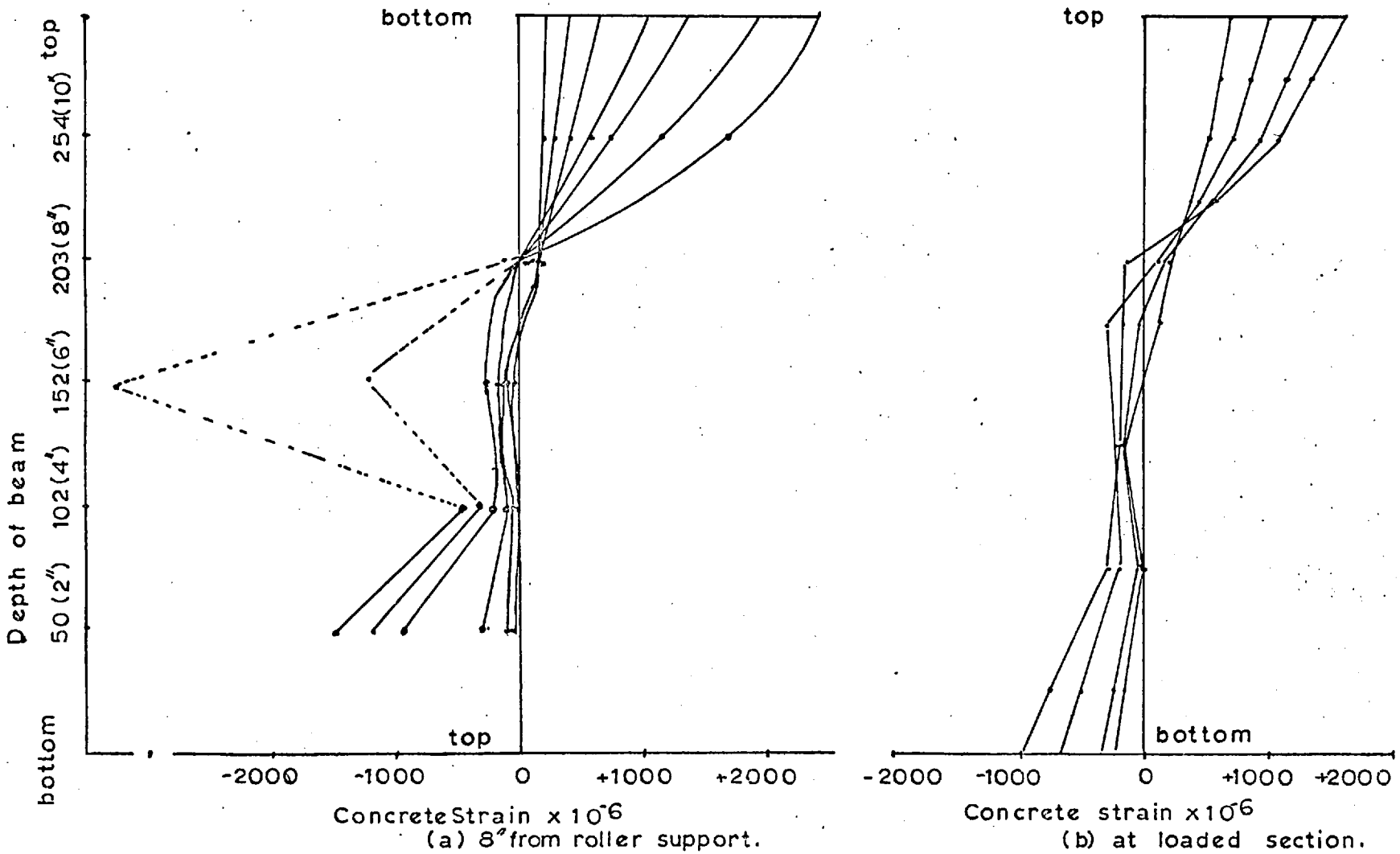


FIG. 45. PLOT OF STRAIN IN STEEL AGAINST SPAN AT DIFFERENT LOADS (2 x SHEAR) OF BEAM B26



TYPICAL STRAIN DIAGRAMS OF BEAM B27.

FIG. 46.

the detrimental effect of axial tension on the shear strength of reinforced concrete beams with web reinforcement is not large, contrary to expectation and also contrary to various existing theories. Axial compression however, does increase the shear capacity of reinforced concrete beams with web reinforcement.

Axial compression affects the mode of failure of rectangular beams. It transforms the mode from that of shearing to shear compression provided the magnitude of axial compression is adequate.

Examination of the test results in table 7 shows that axial compression in all cases increased the shear cracking load and also the ultimate shear capacity of the beams. On the other hand axial tension has less influence on both the shear cracking and ultimate loads depending on the type of failure. Where the failure mode is shear compression, the effect is quite considerable but axial tension has a negligible influence on shear strength of beams if the failure mode is either shearing or diagonal tension.

It is observed that shear strength is considerably increased with decreasing ratios of shear span/effective depth. Increase in shear strength is also achieved with an increase in the ratio of tensile steel (see table 7). The same is of course true for increasing ratios of web reinforcement.

As regards the ultimate behaviour of the two groups of beams (Group A and B), it seems that there is practically no difference in strength though physically the crack patterns were not the same in the restrained and simple spans.

From the test results it is obvious that the influence of axial force is not dependent on other parameters such as concrete strength, tensile steel ratio, web reinforcement ratio and exists although to varying extents at all shear span to effective depth ratios.

Recorded strain readings on both the tensile and compression steel confirm that axial compression is shared both by concrete and steel,

whereas axial tension is carried mostly by compression and tensile steel after the formation of pure tension vertical cracks in the concrete due to axial load. (see beam B_{12}).

Web reinforcement does not carry any load until it is crossed by an inclined shear crack. This fact was observed in several beams, B_{12}, B_{24} and B_{25}. (figs. 30, 39 and 42).

All the stirrups crossing the critical inclined cracks yielded prior to failure. This statement is made on the assumption that the strain at failure can be found by extending the line of the strain/load curve from the least recorded strain.

The force carried by web reinforcement is not influenced by the addition of axial force.

Just before failure, tensile strains were produced in the "compression" steel of beam B_{12} presumably due to the propagation of inclined crack inside the compression zone.

The sections at points of contraflexure did not show any signs of distress in shear when subjected to axial tension and shear. The section was found to be stronger in shear than sections further into the shear span.

The measurements of crack widths across a shear crack show that before failure the vertical displacement is much greater than the horizontal movement(see fig.32 and 33).

The surface strain readings (demec) show that a linear stress-strain relationship exists until flexural cracking. Between flexural cracking and shear cracking, the presence of cracks causes some deviation from linearity, and when the inclined shear cracks are formed, the behaviour of the beam is completely changed.

The strain readings in the tensile steel suggest that the strain in the steel is almost uniform from the load point upto the tail of the inclined crack, which is consistent with the arch action developed

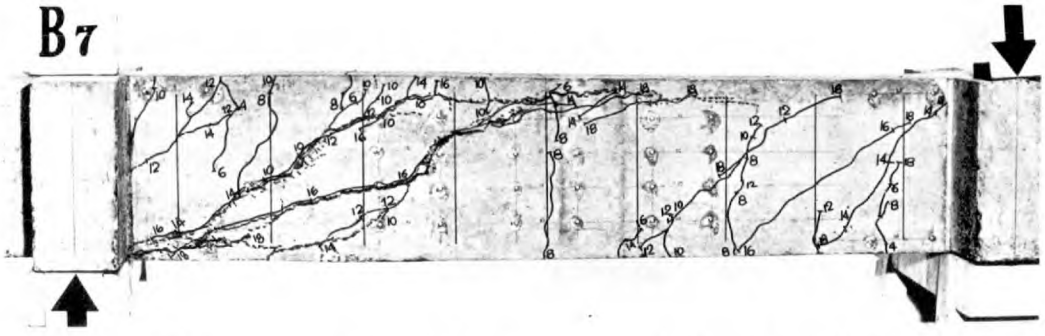
in the beam, (B_{24}, B_{25}, B_{26}).

Further examination of the test results in table 6 shows that the inclination of the failure crack is constant when $a/d_1 > 2.5$ but the inclination increases rapidly when a/d_1 is smaller than 2.5, (see fig. 34). Axial tension seems to increase the inclination of the critical crack while axial compression does the reverse. The plot of inclination vs Q_{ult}/bd_1 (with axial tension only) indicates that a linear relationship may exist between them. (see fig. 35).

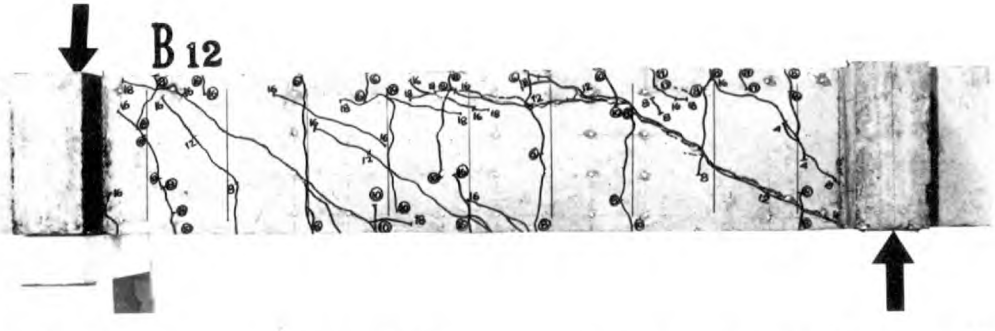
Further detailed observations from these tests are presented in the following chapters in the context of the development of a theory of shear failure in axially loaded beams.



$a/d_1 = 2{\cdot}8$ rst = 1·46 % $N/bd_1 = -4{\cdot}09\ N/mm^2$

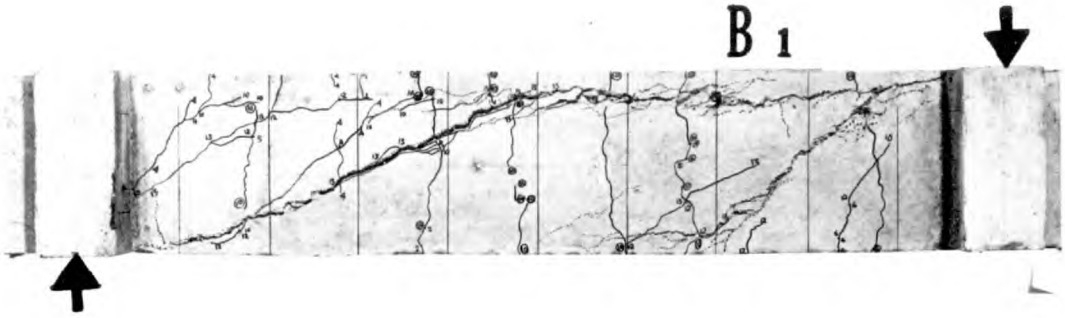


$a/d_1 = 2{\cdot}8$ rst = 1·46 % $N/bd_1 = -4{\cdot}09\ N/mm^2$

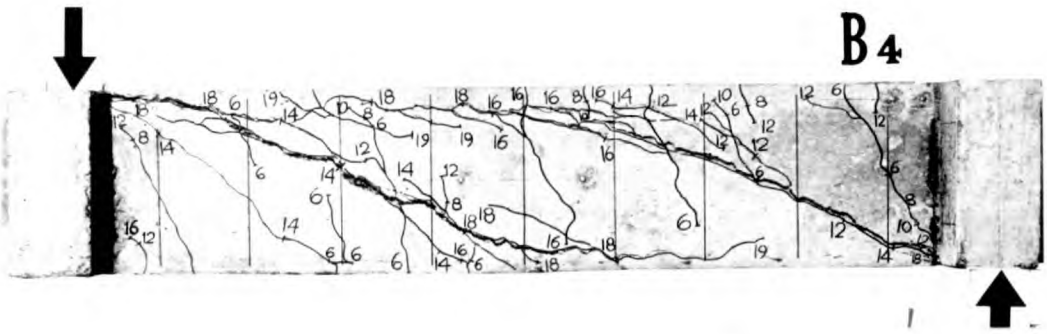


$a/d_1 = 2{\cdot}8$ rst = 1·46 % $N/bd_1 = -4{\cdot}09\ N/mm^2$

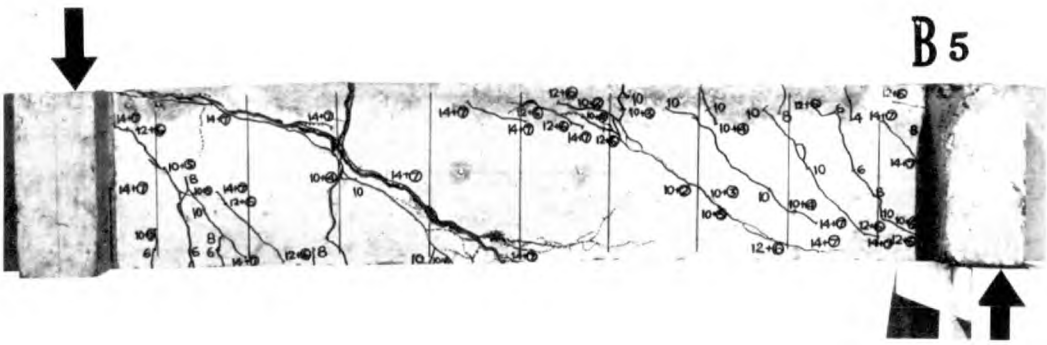
CRACK PATTERNS OF TEST BEAMS. FIG. 47.



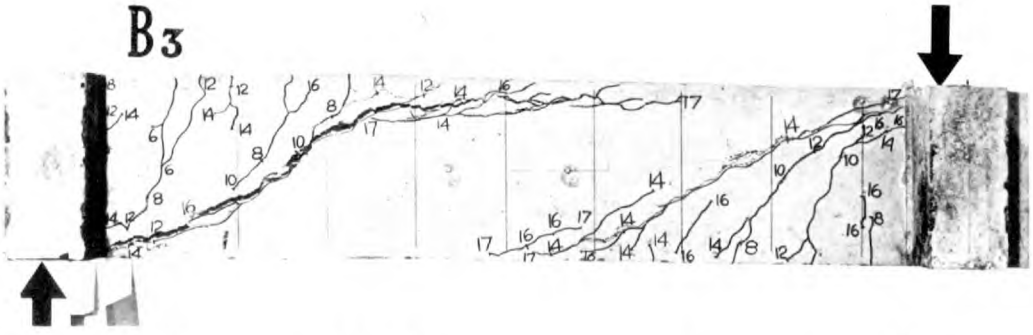
$a/d_1 = 2{\cdot}8$ rst = 1·46% $N/bd_1 = -2{\cdot}41\ N/mm^2$



$a/d_1 = 2{\cdot}8$ rst = 1·46% $N/bd_1 = -2{\cdot}41\ N/mm^2$

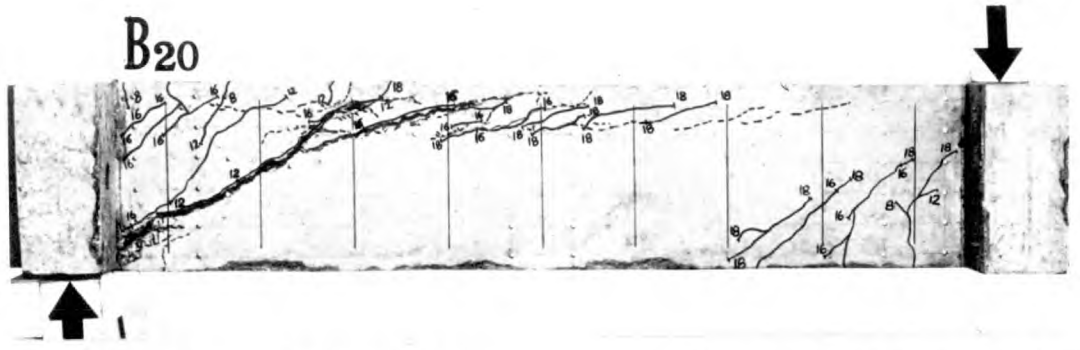


$a/d_1 = 2{\cdot}8$ rst = 1·46% $N/bd_1 = -1{\cdot}68\ N/mm^2$

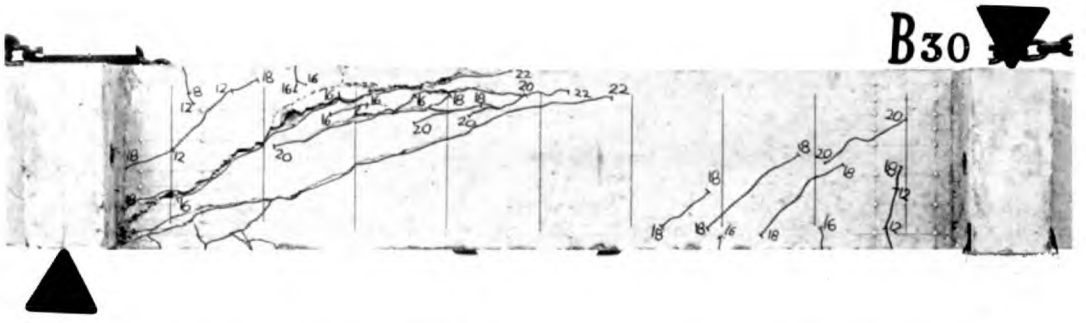


$a/d_1 = 2{\cdot}8$ rst = 1·46% $N/bd_1 = 0\ N/mm^2$

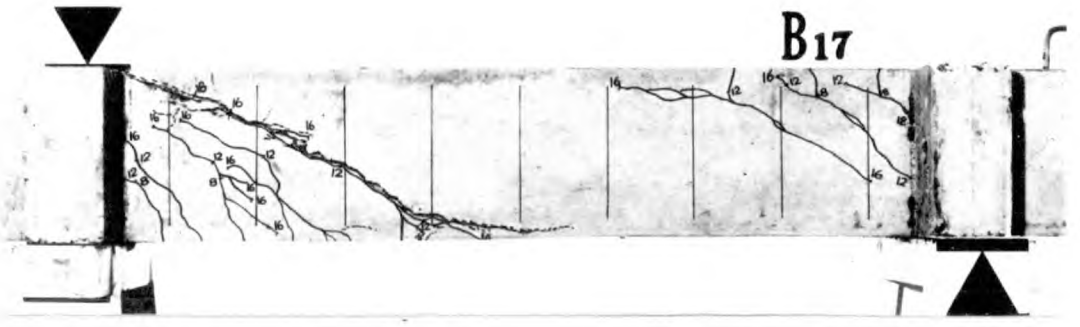
CRACK PATTERNS OF TEST BEAMS. FIG. 48.



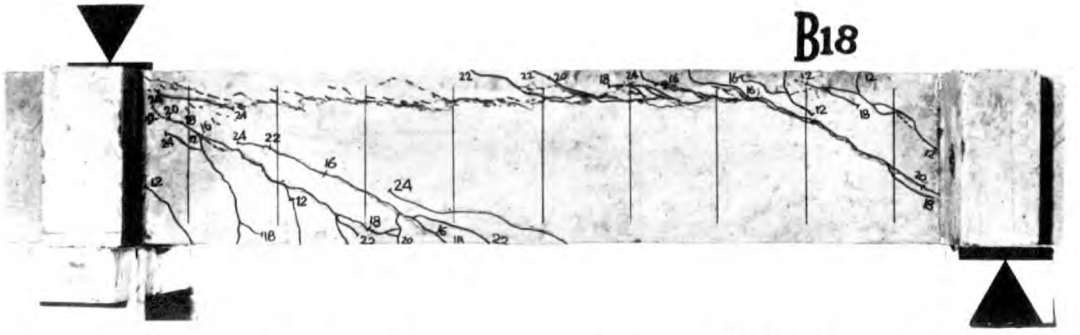
$a/d_1 = 2{\cdot}8$ rst $= 1{\cdot}46\%$ $N/bd_1 = +2{\cdot}41\ N/mm^2$



$a/d_1 = 2{\cdot}9$ rst $= 2{\cdot}0\%$ $N/bd_1 = +2.41\ N/mm^2$

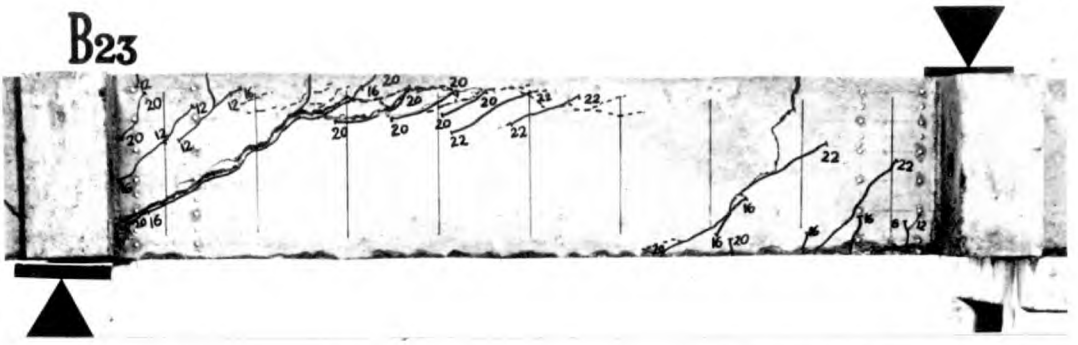


$a/d_1 = 2{\cdot}8$ rst $= 1{\cdot}46\%$ $N/bd_1 = +3{\cdot}61\ N/mm^2$

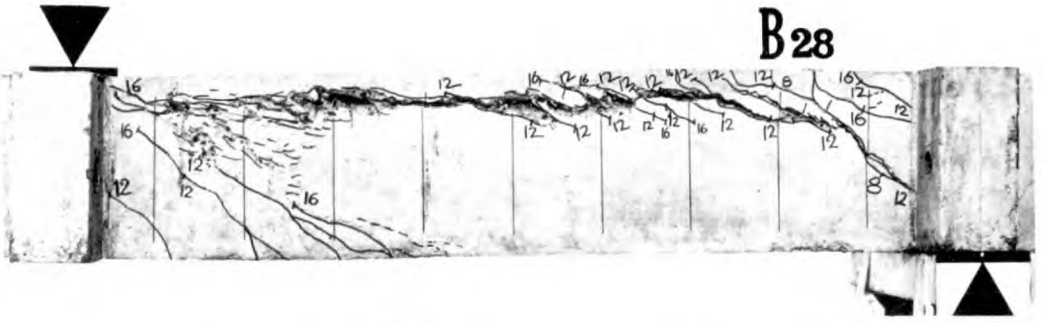


$a/d_1 = 2{\cdot}8$ rst $= 1{\cdot}46\%$ $N/bd_1 = +3{\cdot}61\ N/mm^2$

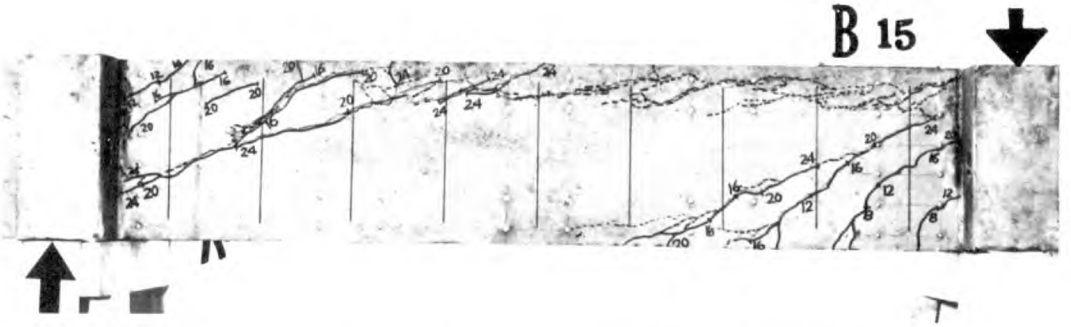
CRACK PATTERN OF TEST BEAMS. FIG. 49.



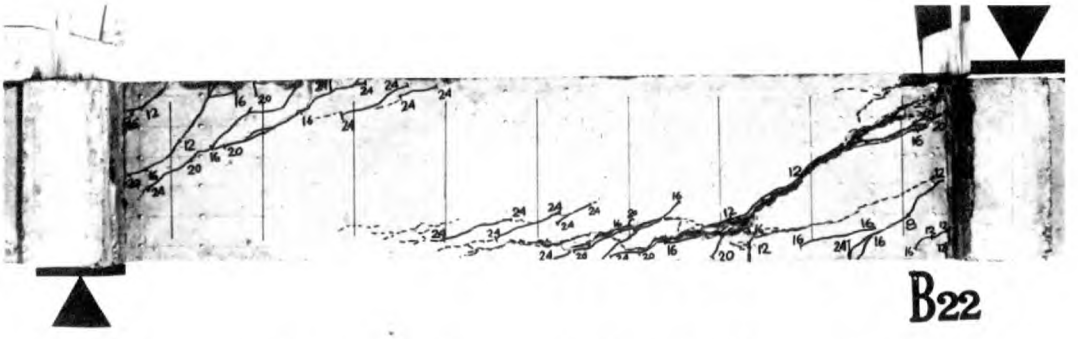
$a/d_1 = 2{\cdot}8$ rst = 1·46% $N/bd_1 = +3{\cdot}61\ N/mm^2$



$a/d_1 = 2{\cdot}8$ rst = 1·46% $N/bd_1 = +3{\cdot}61\ N/mm^2$

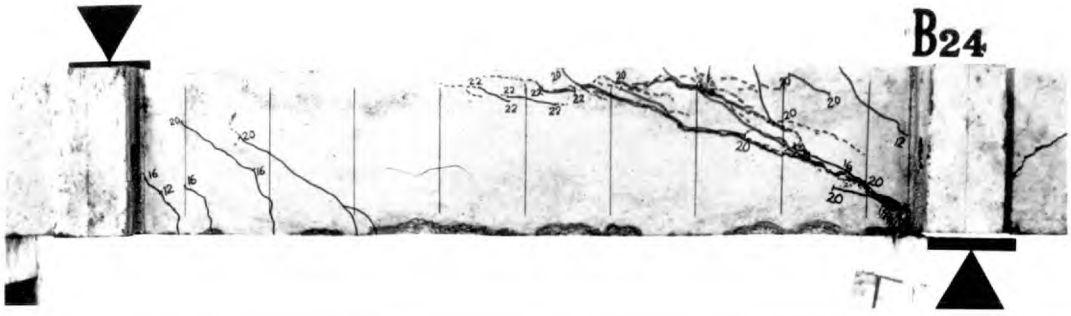


$a/d_1 = 2{\cdot}8$ rst = 1·46% $N/bd_1 = +4{\cdot}82\ N/mm^2$

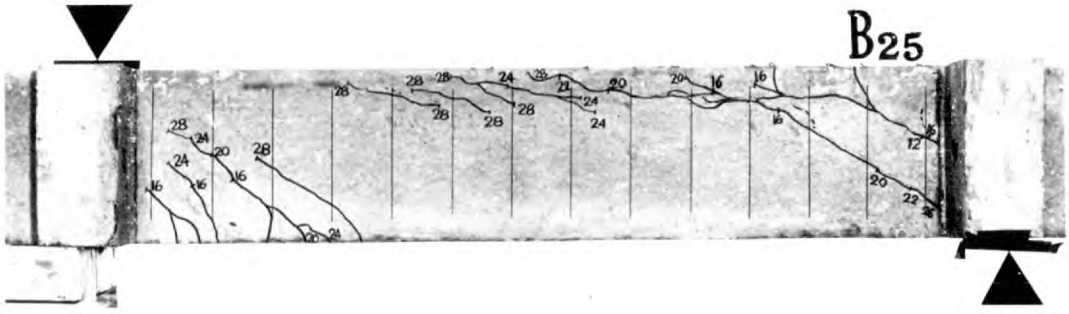


$a/d_1 = 2{\cdot}8$ rst = 1·46% $N/bd_1 = +4{\cdot}82\ N/mm^2$

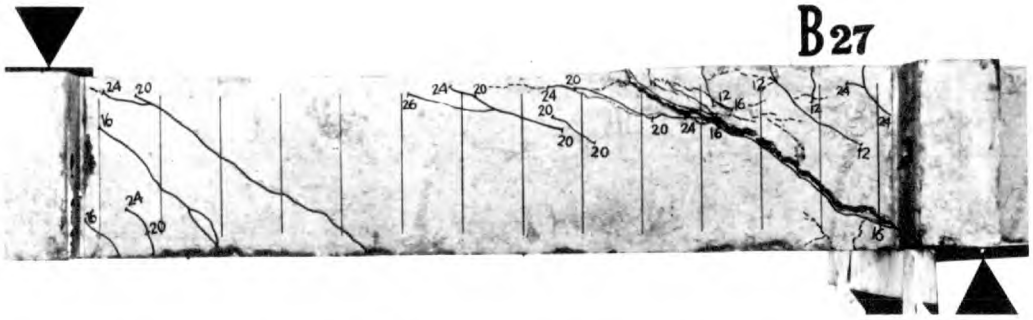
CRACK PATTERNS OF TEST BEAMS. FIG. 50.



$a/d_1 = 2{\cdot}8$ rst = 1·46% $N/bd_1 = +4{\cdot}82\ N/mm^2$



$a/d_1 = 2{\cdot}8$ rst = 1·46% $N/bd_1 = +4{\cdot}82\ N/mm^2$

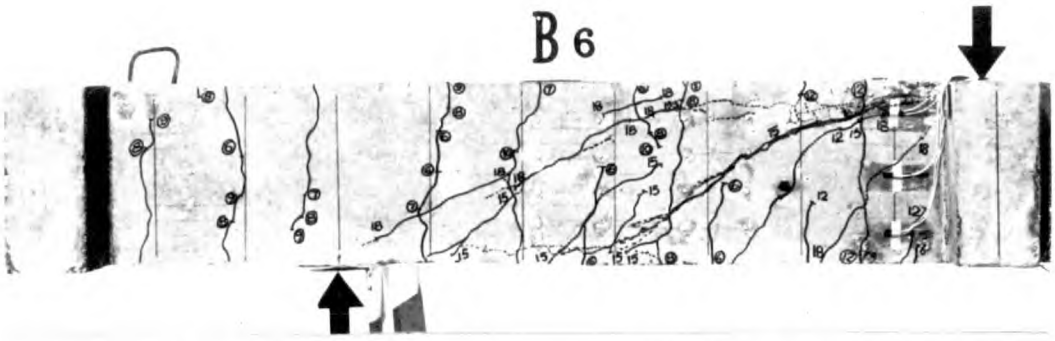


$a/d_1 = 2{\cdot}8$ rst = 1·46% $N/bd_1 = +4{\cdot}82\ N/mm^2$

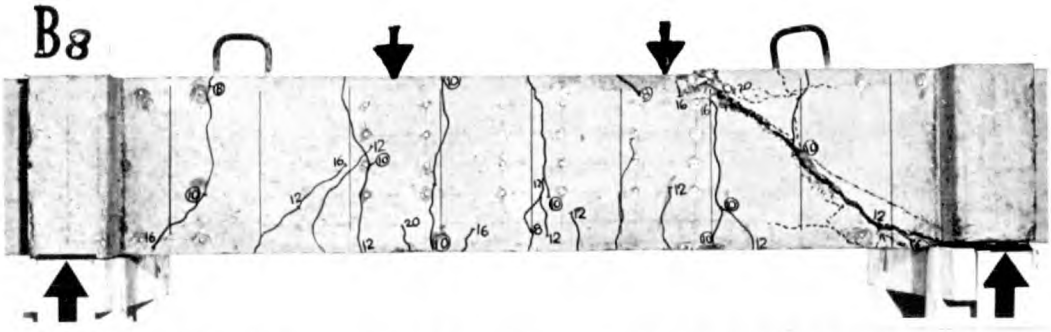


$a/d_1 = 2{\cdot}8$ rst = 0·97% $N/bd_1 = +4{\cdot}82\ N/mm^2$

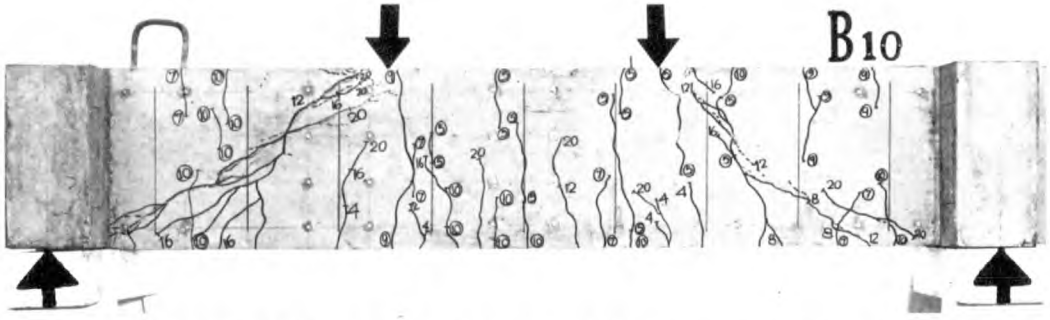
CRACK PATTERNS OF TEST BEAMS. FIG. 51.



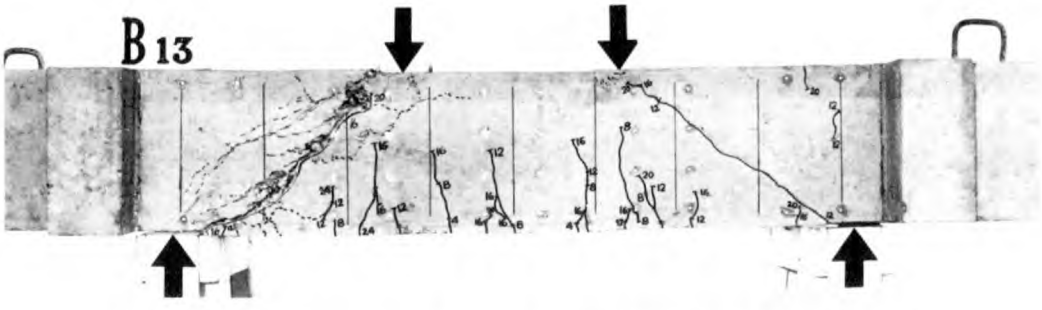
$a/d_1 = 3{\cdot}9$ $\quad rst = 1{\cdot}46\%$ $\quad N/bd_1 = -2{\cdot}88\ N/mm^2$



$a/d_1 = 1{\cdot}96$ $\quad rst = 1{\cdot}46\%$ $\quad N/bd_1 = -2{\cdot}41\ N/mm^2$

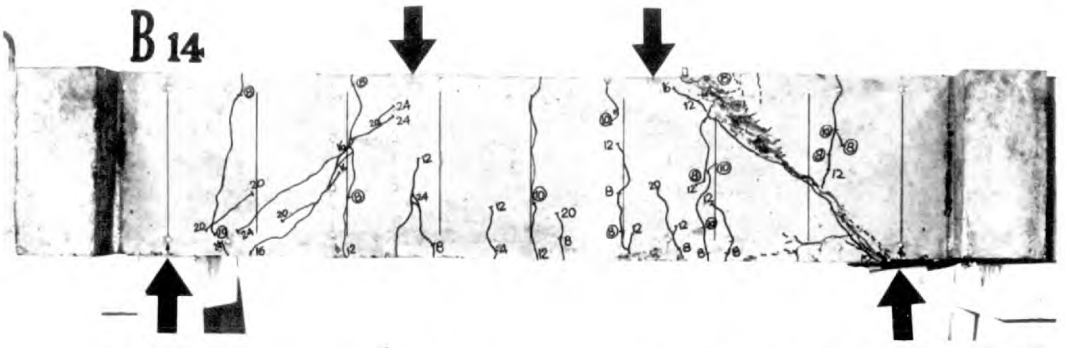


$a/d_1 = 1{\cdot}96$ $\quad rst = 1{\cdot}46\%$ $\quad N/bd_1 = -2{\cdot}41\ N/mm^2$

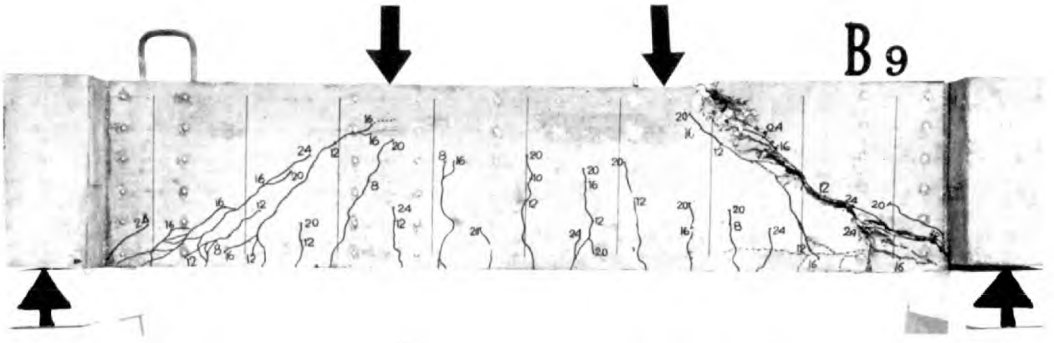


$a/d_1 = 1{\cdot}5$ $\quad rst = 1{\cdot}46\%$ $\quad N/bd_1 = -2{\cdot}41\ N/mm^2$

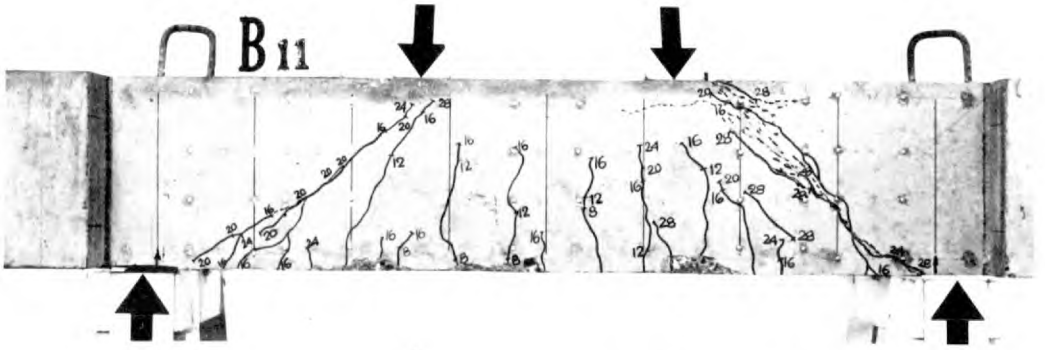
CRACK PATTERNS OF TEST BEAMS. FIG. 52.



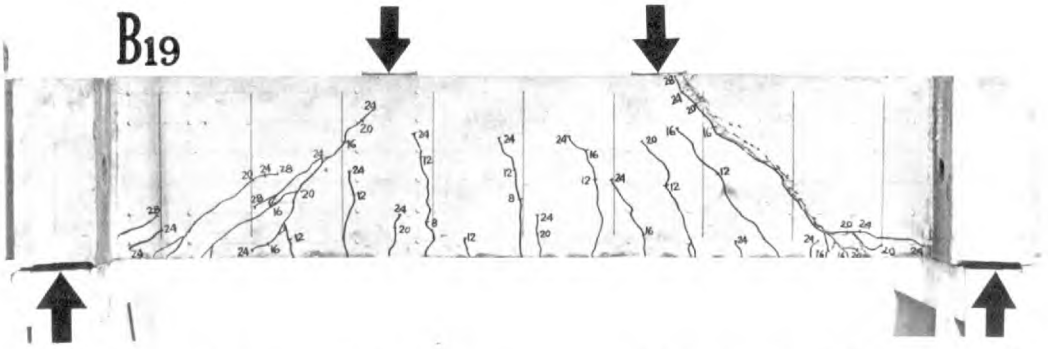
$a/d_1 = 1{\cdot}5$ rst $= 1{\cdot}46\%$ $N/bd_1 = -2{\cdot}41\ N/mm^2$



$a/d_1 = 1{\cdot}96$ rst $= 1{\cdot}46\%$ $N/bd_1 = 0\ N/mm^2$

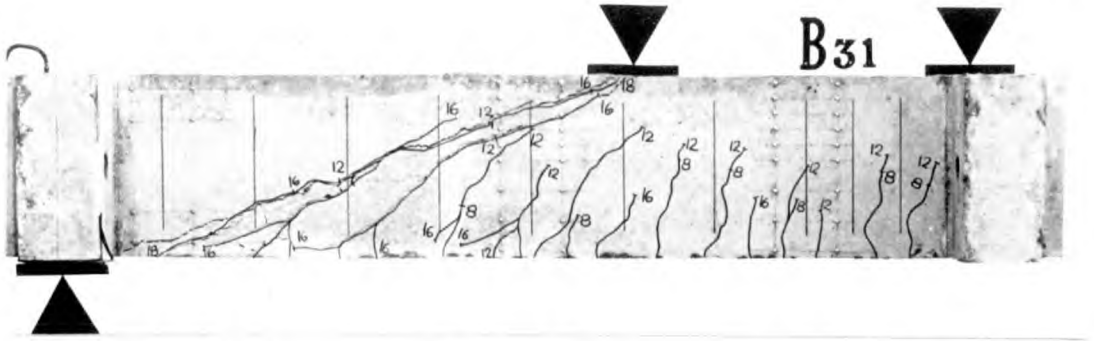


$a/d_1 = 1{\cdot}5$ rst $= 1{\cdot}46\%$ $N/bd_1 = 0\ N/mm^2$

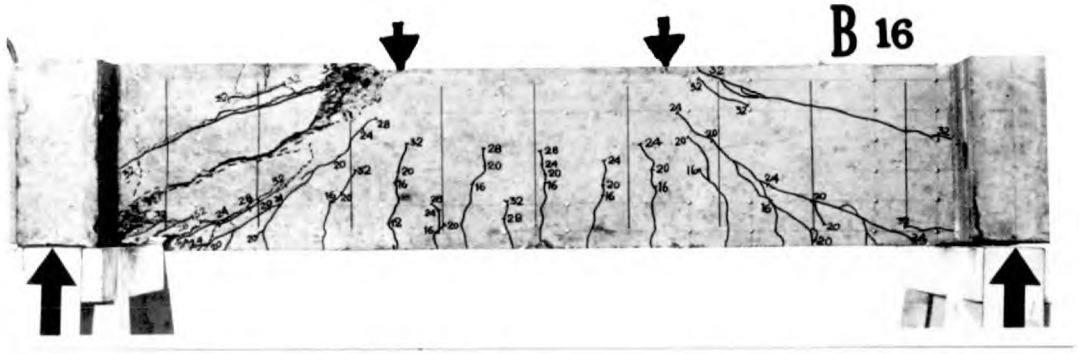


$a/d_1 = 1{\cdot}96$ rst $= 1{\cdot}46\%$ $N/bd_1 = +2{\cdot}41\ N/mm^2$

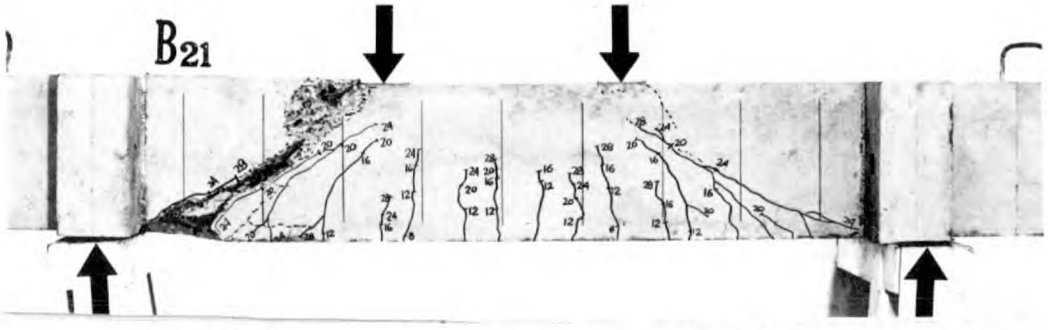
CRACK PATTERNS OF TEST BEAMS. FIG. 53.



$a/d_1 = 3{\cdot}46$ rst = 1·46 % $N/bd_1 = +2{\cdot}41\ N/mm^2$



$a/d_1 = 1{\cdot}96$ rst = 1·46 % $N/bd_1 = +3{\cdot}61\ N/mm^2$



$a/d_1 = 1{\cdot}96$ rst = 1·46 % $N/bd_1 = +3{\cdot}61\ N/mm^2$



$a/d_1 = 2{\cdot}8$ rst = 1·46 % $N/bd_1 = +4{\cdot}82\ N/mm^2$

CRACK PATTERNS OF TEST BEAMS. FIG. 54.

INVESTIGATION AND STUDY OF PAST WORK ON AGGREGATE INTERLOCK, DOWEL ACTION AND BOND FAILURE

5.1 Aggregate Interlock:

In the past, the subject of shear transfer by aggregate interlocking received little attention. Only recent research (Fenwick[43], Taylor[55], Hofbeck, Ibrahim and Mattock[19]) work in this field has made it possible to understand how important this shear carrying mechanism can be. All of them deserve credit for devising methods and techniques to measure the portion of shear carried by this mechanism. In the present investigation an attempt was made to add to their work by measuring quantitatively the shear that can be transferred across a cracked section with the help of few specimens and by explaining how shear is being transferred.

5.1.1 Mechanism of shear transfer by Aggregate Interlock:

Before going into details of shear transfer by aggregate interlocking, it would be wise to examine what are the ideal conditions for this action to develop. The aggregate interlock force comes into play across a vertical crack only when the two blocks of concrete have a vertical displacement. When this condition is satisfied, the bigger aggregate particles act as dowel and are capable of transferring shear across the crack.

The vertical movement is accompanied by a horizontal displacement at the crack and if this is sufficient the ability of the aggregate particles to contact one another can be impaired, thus in order to create ideal conditions for interlocking this horizontal displacement should be small.

5.1.2 Factors influencing aggregate interlocking:

It is believed that the shear force that is carried by aggregate interlocking is dependent on a number of factors[43] and those known to date are given below:

a) Area of contact between the two rough surfaces with projecting aggregate particles.

b) Quality of concrete and aggregate particles in the vicinity of the area of contact.

c) Inclination of the crack to the direction of loading.

Again, the area of contact between the two surfaces depends on the following parameters.

1. the grade of aggregates.

2. the shape of particles, round or angular.

3. width of the crack.

4. reinforcement (if any) crossed by the crack.

In presence of reinforcement, the following parameters affect considerably the magnitude of shear transfer[19].

a. Bond properties.

b. Yield stress of bars.

5.1.3 Past work on aggregate interlock:

Recently, a number of investigators was attracted to the field of shear transfer due to aggregate interlock. A paper by Hofbeck, Ibrahim and Mattock[19] describes tests carried out in this regard using push off specimens as shown in fig. 55, which were forced to fail along the plane indicated. Tests were done on specimens with and without preformed cracks. The preformed cracks were obtained by applying line loads along the plane in a hydraulic testing machine.

Their aim was to investigate -

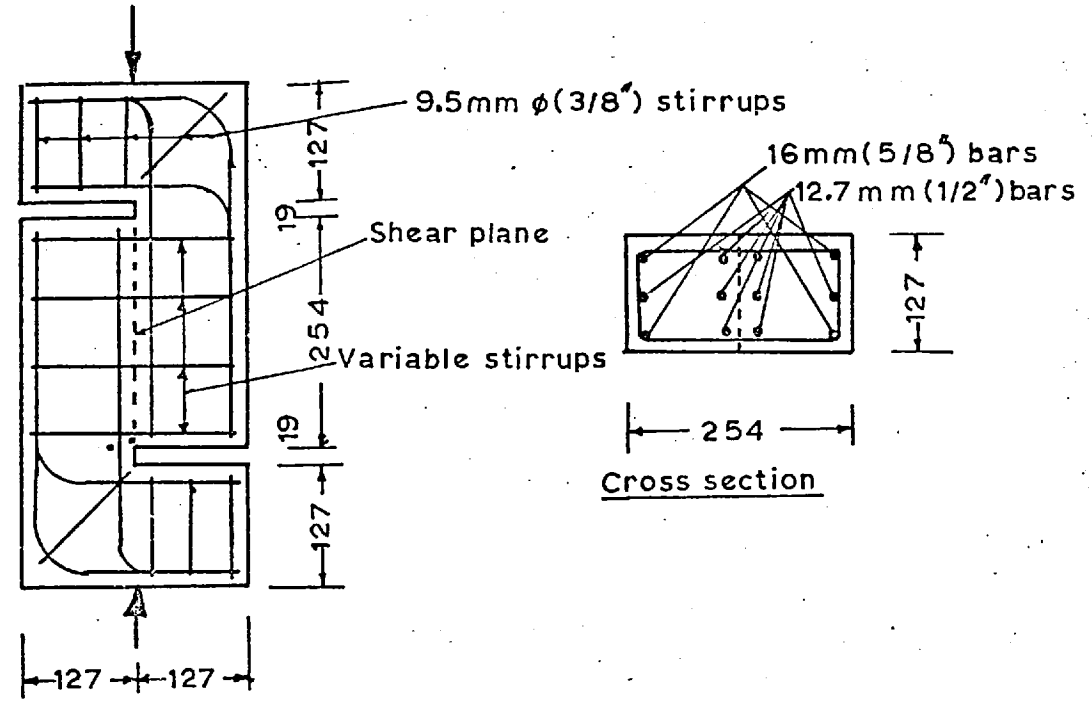
1. the influence of preformed cracks on the shear transfer along the shear plane.

2. the effect of reinforcement - detailing and strength.

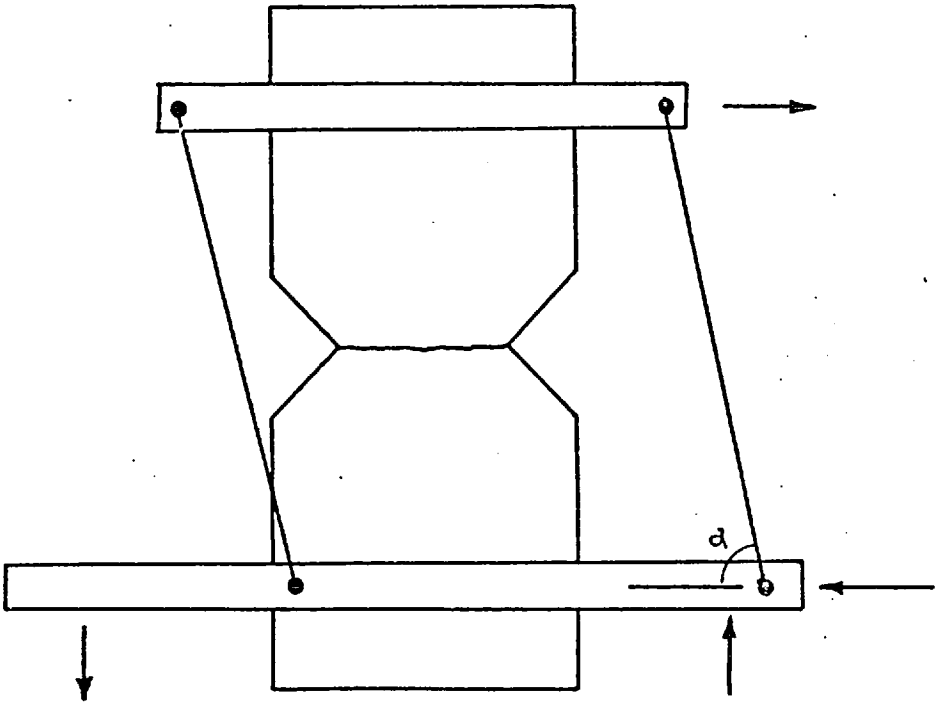
3. the effect of concrete strength.

4. the contribution of reinforcement to shear transfer by dowel action.

5. the applicability of "shear friction theory" to shear transfer in presence of a preformed crack along the shear plane.



DETAILS OF PUSH-OFF SPECIMEN FOR INTERLOCK TESTS. (MATTOCK). FIG. 55.



DETAILS OF SPECIMEN WITH TEST RIG FOR INTERLOCK TESTS (TAYLOR). FIG. 56.

Their conclusions, based on test evidence are -

1. the presence of a preformed crack along the shear plane reduces the ultimate shear transfer and increases slip at all stages of loading.

2. Shear transfer strength is dependent on $r_s fsy$, where $r_s = {}^{As}/_{bd}$,

As = total area of stirrups crossing the plane.

fsy = yield stress value of steel.

Changes in strength, size and bar spacing do not affect the shear transfer strength as long as $r_s fsy$ is not altered.

3. The upper limit of $r_s fsy$ is governed by concrete strength but below the limit, the relationship between q_u and $r_s fsy$ is not influenced by concrete strength. Beyond the limit any increase in q_u with $r_s fsy$ is very small.

4. Dowel action of reinforceing bars is significant only when they are crossed by a continuous crack.

5. Shear friction theory is found to give a conservative estimate of shear transfer in normal weight concrete in the case of specimens with preformed cracks. The strength calculation is based on the equation

$$q_u = r_s fsy \tan\phi \leq 0.15 \text{ Ucyl}$$

$$\text{or} < 600 \text{ psi}$$

$$\text{and } \tan\phi = 1.4 \text{ (as proposed by Mast).}$$

6. Zia's[61] envelope may be used to estimate the shear transfer strength in case of uncracked specimens.

Taylor[54,55]

In his papers he describes the techniques adopted to measure separately the contributions of the three main actions towards shear strength of a concrete member prior to shear cracking, namely - the concrete compressive zone, interlocking of aggregates and the dowel action of tensile reinforcement. His work on aggregate interlock is confined to flexural cracks only. His conclusion is that the contribution of each of these factors is significant. In this section, only his findings regarding aggregate interlocking across a flexural crack are discussed in detail.

Taylor carried out two types of tests. The first was a displacement controlled test on an unreinforced concrete block, (fig. 56) and the second was a beam test with initiated cracks. His idea was to simulate the beam displacements in the displacement controlled blocks and measure the interlock force for a particular value of beam displacement.

With each load increment, the cracks in the specimens open up not only vertically but also horizontally. Taylor found out that the ratio of vertical displacement to horizontal displacement at any position under consideration $(\Delta V/\Delta H)$ was a constant for a particular crack and could be related to the shape of a crack.

So he devised the test rig shown to facilitate the conduct of tests so that the ratio $\Delta V/\Delta H$ could be maintained during testing of a particular specimen and at the same time it could be varied between tests.

He investigated the effect of the following parameters on interlock:-

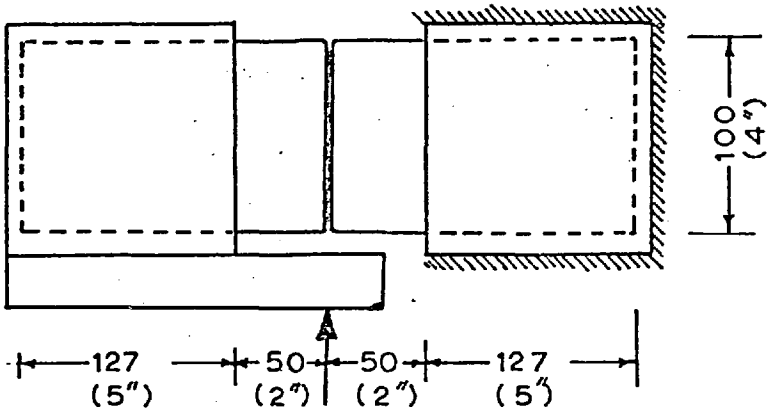
1. Displacement ratio $\Delta N/\Delta S$ i.e. the ratio of Normal displacement to shear displacement across a crack.
2. Concrete Strength.
3. Aggregate size.
4. Aggregate type.

He presented a number of curves, showing the effect of the above parameters.

Taylor's final conclusion was that about 33% to 50% of the total shear force is carried by interlock. His conclusion is entirely based on test results and relates to flexural cracks only.

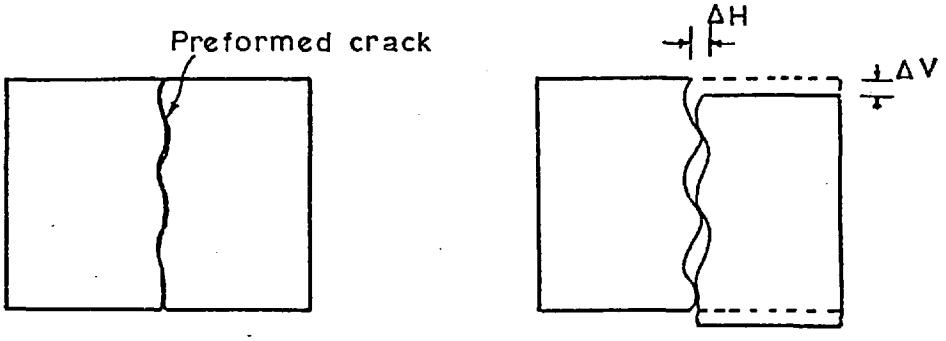
Fenwick and Paulay[14,43]

Fenwick carried out direct tests on interlocking of aggregates and studied mainly the effect of crack width. In a few specimens he studied the effect of concrete strength as well. His specimen for study of aggregate interlock forces is shown in fig. 57 and had a saw-cut (6 mm) at the centre so as to help in forming a crack along the desired plane. During his investigation, he kept the width of the crack constant throughout each test.



DETAILS OF SPECIMEN WITH TEST RIG FOR INTERLOCK TESTS (FENWICK)

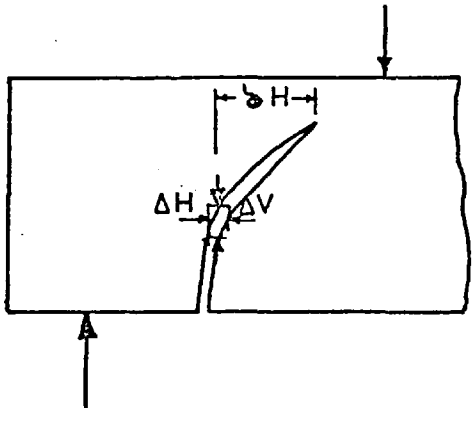
FIG. 57.



Specimen after cracking along shearing plane

Specimen after vertically loaded showing horizontal and vertical displacements

AGGREGATE INTERLOCK ACTION FIG. 58.



DISPLACEMENTS ACROSS FLEXURAL CRACK IN BEAMS (TAYLOR) FIG. 59.

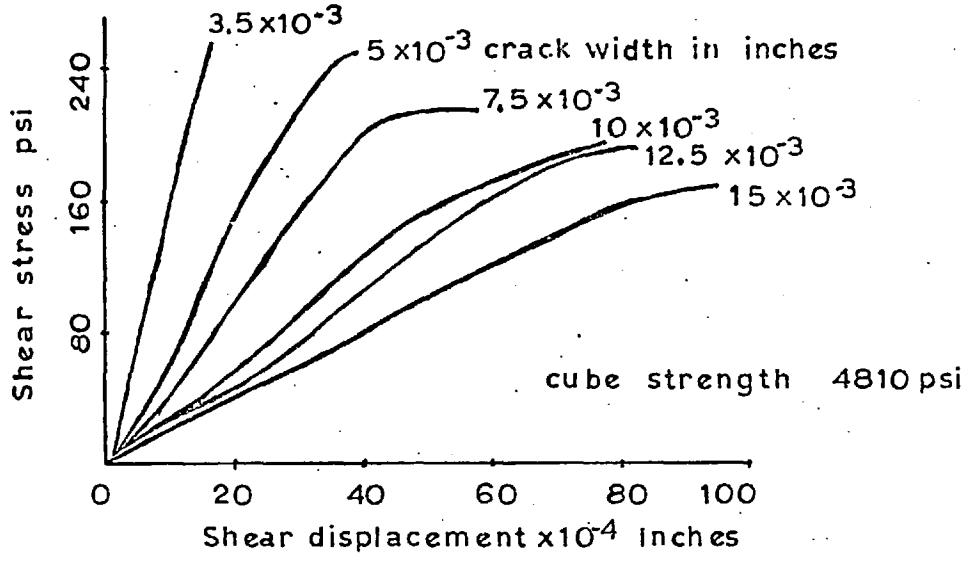
In series 1, the specimens had varying crack widths while the concrete strength was kept constant. His findings are represented in fig. 60, and the graphs suggest that the aggregate interlock force is drastically reduced as the crack width is increased. His specimens had maximum crack of 0.381 mm (0.015"). In series 2, he studied the effect of concrete strength on shear transfer with a constant crack width. A number of graphs representing his results were plotted and are shown in fig. 61. Unlike Mattock, he plots curves of shear stress against shear displacement and from the graphs it is clear that shear transfer is increased with increasing strength of concrete.

Fenwick observed that his test blocks did not fail as a result of breakdown of the aggregate interlock action. He found that the specimens failed either in diagonal tension or flexural tension (according to Fenwick).

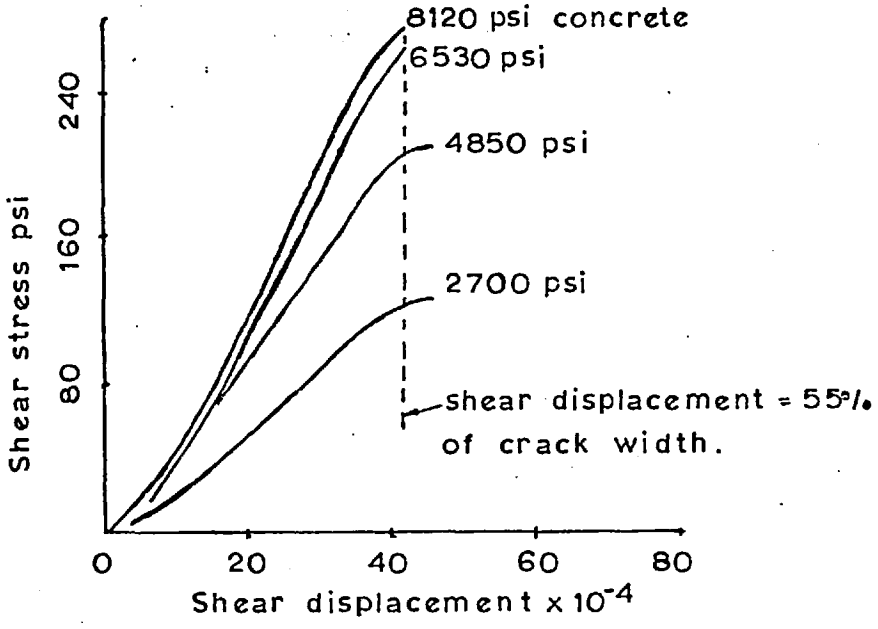
His idea was to establish a stress-displacement relationship for shear transfer across a crack due to interlock and then this relationship could be used in his beam specimens to evaluate the shear carried by aggregate interlock action.

With this idea in mind, he cast a beam FA4 (see fig. 62), on one side of which were crack initiators, spaced at 150 mm (6") . The crack initiators were inside the tensile zone of the beam and cracks could form freely in the remaining 100 mm (4") depth of compression zone.

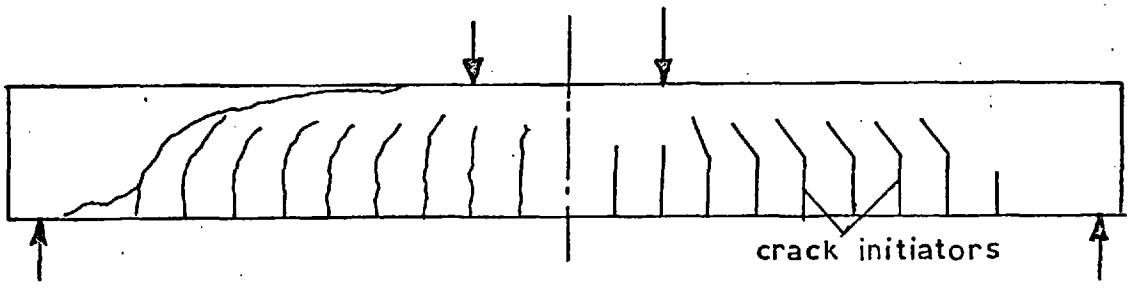
The other side of the beam had no crack initiators and hence cracks could form even in the tension zone freely. This beam had the same concrete, reinforcement and overall dimensions as other beams without crack initiators. From the measurement of tensile stress in steel, he concluded that nearly perfect beam-action developed at all stages of loading. He minimised the dowel action of the tensile steel by wrapping it with foam plastic. From his beam test he believed that interlock is of major importance so far as shear transfer is concerned and at the last load stage, over 70% of the bond force needed to develop beam action was carried by interlock action, although he concluded that in normal beams, the percentage may be less because some portion of the bond force will



SHEAR STRESS VS SHEAR DISPLACEMENT CURVES (FENWICK) FIG. 60.



SHEAR STRESS VS SHEAR DISPLACEMENT CURVES (FENWICK) FIG. 61.



DETAILS OF BEAM FA4 (FENWICK) FIG. 62.

be equilibrated by dowel action of the tensile reinforcement(max^{m} 15% according to Fenwick).

Mattock's work on interlock is different from other investigators in that he provided reinforcement at right angles to the shearing plane. He did not as such study the effect of initial crack width and in his type of test, it seems that initial crack width is of least importance.

Taylor's work is confined to flexural cracks only. Thus it seems incorrect to draw conclusions from his tests as to whether similar results could be obtained with a shear crack, as our main concern is shear transfer across a shear crack and not flexural one, excepting in connection with diagonal tension failures.

As mentioned earlier, Fenwick maintained a constant width for a particular specimen from beginning to end of the test. But this seems to be contrary to the behaviour of beams where crack widths are never constant at different stages of loading. Crack widths grow bigger with each increment of load. Thus keeping the crack width constant, he is increasing the possibility of more interlock and this would result in erronous results.

5.1.4 Experimental Investigation:

The resistance of concrete surfaces in contact when loaded vertically is limited by the fact that spalling of the area in contact takes place as the resistance of the concrete is overcome. In such a case there exists an upper limit to strength. This is more important in the case of specimens with reinforcement which provides compression between the two surfaces, and Mattock's criteria should be acceptable.

In order to obtain other useful information quantitatively a test programme was designed in such a way that the shear force carried by interlocking of aggregate could be measured independently with the elimination of the compatability problems present in beam type specimens. The idea was to study interlock with preformed cracks and no reinforcement was provided across the cracks.

As mentioned earlier, interlock itself is a function of a number of variables and each should be investigated systematically. However, in the limited time available, it was not possible to investigate the effects of all of them.

Test specimens:

Two different types of specimens were used in this investigation, as shown in figs. 63 and 64.

Group 1 - concrete blocks with notches so as to initiate preformed cracks.

Group 2 - Prisms with central notches.

The specimens were cast with the same type of concrete mix used for the beams (19 mm max^{m} size of aggregate) under identical conditions of curing. Like the beams, they were tested after 3 weeks.

The specimens of Group 1 were cracked along the shear plane applying line loads in a hydraulic testing machine (Amsler) and those of Group 2 by bending in both directions, with complete failure prevented by an external longitudinal bar.

Testing Apparatus:

The specimens were tested with variable axial loads and hence could be separated into 3 series:-

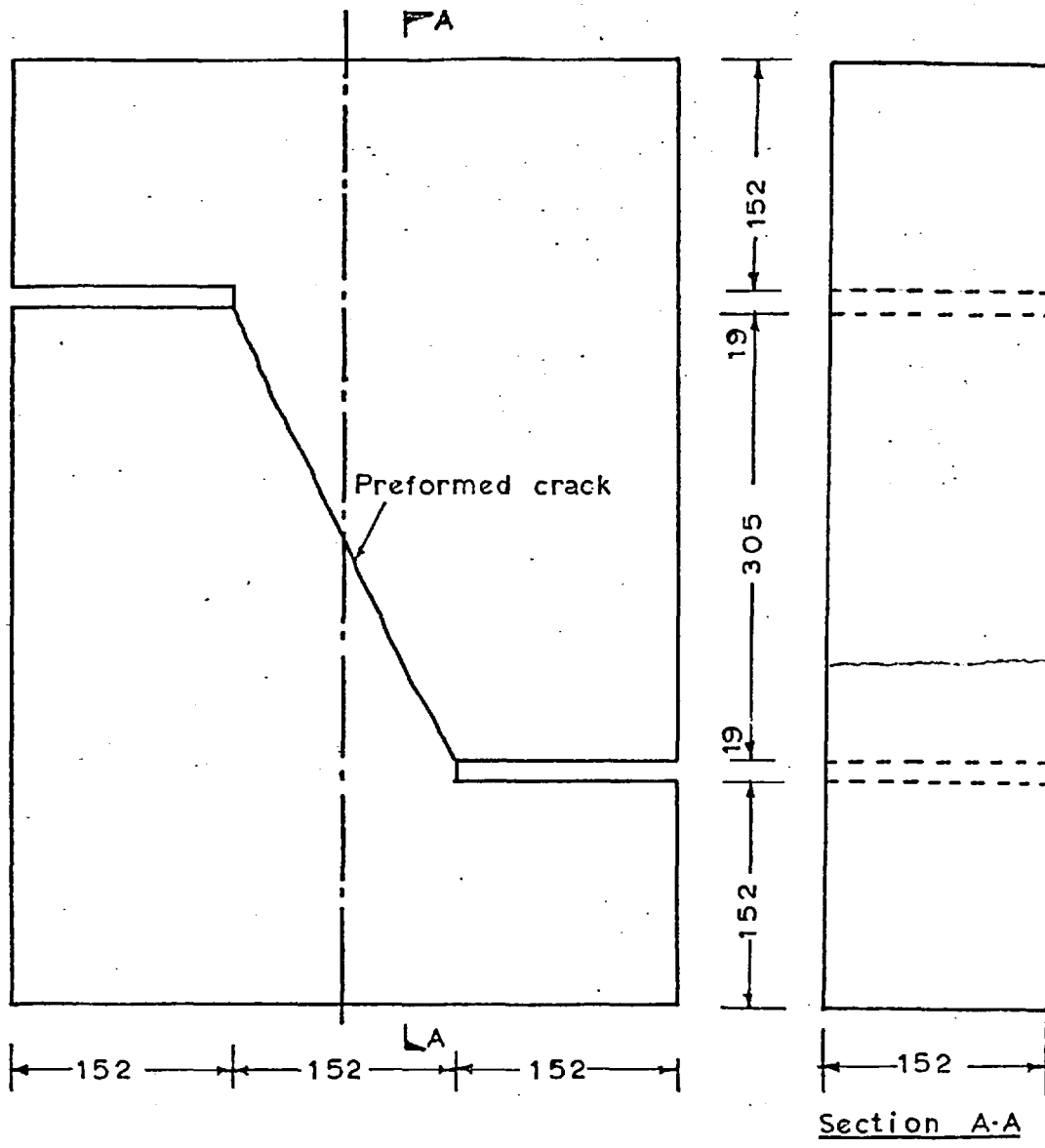
a) specimens tested with axial compression and shear.

b) specimens tested with axial tension and shear.

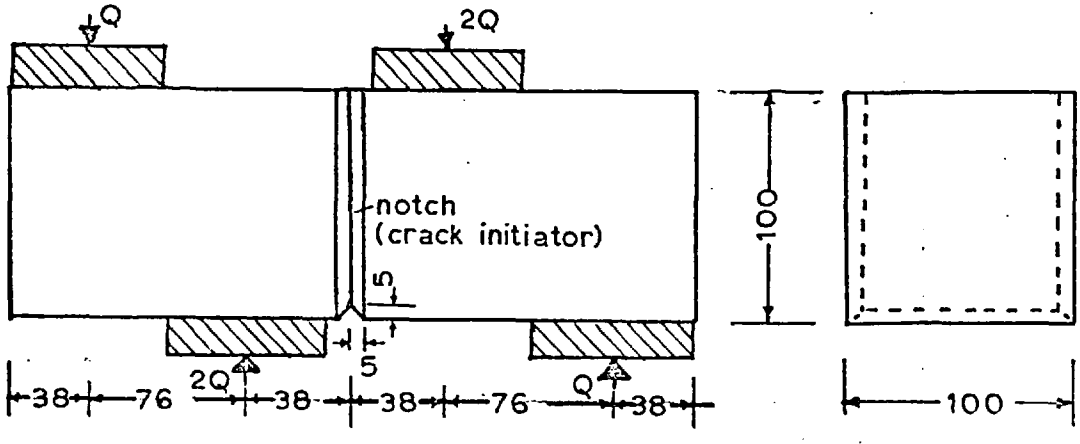
and c) specimens tested with pure shear.

Specimens in Group 1 consisted of series a) and b) only.

The testing of specimens in series a) of group 1 did not present any difficulty. All the specimens were tested in a uniaxial compression testing machine. Vertical load was applied with the help of a jack which was calibrated before testing. It is evident from fig. 63 that the shearing plane is inclined, so vertical loading caused normal (compressive) and shear stresses to develop along the shearing plane; the ratio of which was dependent on the inclination.



SPECIMEN FOR AGGREGATE INTERLOCK TEST
GROUP 1. FIG. 63.



SPECIMEN FOR AGGREGATE INTERLOCK TEST
GROUP 2. FIG. 64.

The group 1 specimens in series b) were tested in a tension machine, applying vertical pull so that shear and tensile stresses are produced along the failure plane.

A separate test rig was devised for the testing of all the specimens of group 2. In order to apply axial compression, a 22 mm ($^{7}/_{8}$") diameter hole was cast at the centre of the specimen, while axial tension was applied through a small frame manufactured for this purpose and bolted to the ends of the specimen. Loads were applied through jacks and strains recorded with the help of load cells.

Test procedure:

As described earlier, the specimens were precracked along the desired plane by applying line loads in an Amsler machine. The line load was applied with the help of two 10 mm diameter bars placed one at the top and one at the bottom of the specimens along the shearing plane. The specimens were loaded in such a way that the two halves did not fall apart, and had variable initial crack widths. Because the technique adopted for cracking did not permit the control of crack widths from specimen to specimen, loading was stopped only when the crack was visible with the naked eye.

Testing of specimens in group 1:

The specimens were placed horizontally while the cracks were formed. But to investigate the shear transfer across the cracks, they were placed vertically in the testing machine so that shear and axial stresses were produced across the shearing plane. With each increment of loading the opening of the cracks normal to it and the vertical slips were measured. The specimens were loaded monotonically until failure.

Testing of specimens in group 2:

After cracking the specimens at the plane, they were placed horizontally on the testing plane (see fig.64). In all cases in series 1 axial compression was applied first and then held constant during the testing. For each load increment, crack widths and vertical displacement

across the cracks were measured with the help of a microscope (crack measurer) and dialgauges respectively. The same procedure of recording the crackwidths and displacements was followed when vertical load was applied.

Test results:

The test results of this investigation are presented in tables 9 and 10. The plot of the crack widths against shear stress transferred across the preformed crack at different load stages are shown in figs.65,68.

Shear transfer across cracks in the presence of axial compression:

The findings of this test programme prove without doubt that a considerable amount of shear can be transferred across a preformed crack if the two surfaces are compressed. With increasing compression the magnitude of shear transfer increases. In a few specimens with higher compression (in group 2) diagonal shear cracks (independent of the preformed crack) formed, but failure was always due to breakdown of interlock.

In the specimens of group 1, the ratio of axial compression to shear was constant. During testing of these specimens, no inclined cracks were observed. Only spalling of the surfaces took place just before failure. Two specimens were subjected to eccentric loads in this group. With this little eccentricity (76 mm), a reduction in shear transfer strength was observed. This is because of the tensile stresses produced due to eccentric loading.

The effect of axial compression on interlock can be viewed from a different angle. Physically, axial compression reduces the crack width and thereby increases interlock. Internally, because of compression, frictional force is developed and is responsible for transferring shear. Unlike the forces due to reinforcement, in this case, the axial compression was an external load (group 1 and 2) and was constant throughout the test (in group 2) irrespective of vertical load. Thus the effect of external compression is two fold -

a) reduces the width of preformed crack and increases the possibility of interlock.

b) creates frictional resistance to carry shear.

Shear transfer across cracks in the presence of axial tension:

Unlike axial compression, axial tension increases the crack width and hence reduces interlock. Secondly, there can be little frictional resistance between the two surfaces when they are separated by the application of axial load. Thus the two actions responsible for shear transfer are much reduced in this case and so little shear can be transferred across a crack if normal tensile stress exists. Once the limiting value of crack width is reached there can be no shear transfer, as found in tests.

Shear transfer across preformed crack when there is no axial force:

In this case, shear transfer is possible only by the first action upto a certain value of crack width considerably less than the aggregate size. As soon as the limiting value of the crack width is attained, failure is inevitable.

Analysis of Test Results:

The test results are analysed and plotted. From fig. 65 it is evident that the possibility of shear transfer reduces with increasing crack width. This is true whether there is axial load or not. Secondly, when the crack width is small, axial tension if applied, will increase the crack width and appreciable shear transfer is unlikely. On the other hand, axial compression increases the possibility of shear transfer by holding the two blocks together. Also shear transfer increases with increasing magnitude of compression even for a constant crack width.

Test results are summarised in tables 9 and 10.

Table 9. Group 1 - Test result of interlock specimens

Specimen No.	Dimension in mm		Max^{m} size of Aggregate	Initial crack width mm	Eccentricity mm	Axial load N/bd N/mm^2	Q/bd N/mm^2
	b	d					
G. 1	152	340	19(3/4")	0.08	0	+5.06	10.12
G. 2	152	340	19(3/4")	0.06	0	+4.41	8.82
G. 3	152	340	19(3/4")	0.16	76	+3.29	6.58
G. 4	152	340	19(3/4")	0.28	76	+3.03	6.06
G. 5	152	340	19(3/4")	0.40	0	-0.08	0.16
G. 6	152	340	19(3/4")	0.60	0	-0.03	0.06

Table 10. Group 2 - Test results of interlock specimens

Specimen No.	Dimensions of Specimen			Max^{m} size of Aggregate	Initial crack width mm	N/bd N/mm^2	crack width after application of axial force mm	Q/bd N/mm^2
	b_{mm}	d_{mm}	$Area_{mm^2}$					
G. 7	90	95	8162	19(3/4")	0.4	+0.612	0.12	4.08
G. 8	90	95	8550	19(3/4")	0.12	0	0.12	0.975
G. 9	90	95	8550	19(3/4")	0.40	0	0.40	0.195
G.10	90	95	8162	19(3/4")	0.80	+1.836	0.32	4.70
G. 11	90	95	8162	19(3/4")	0.40	+1.224	0.16	3.77
G. 12	90	95	8162	19(3/4")	0.12	+1.224	0.04	6.53
G.13	90	95	8162	19(3/4")	0.40	+1.836	0.12	7.55
G. 14	90	95	8550	19(3/4")	0.36	0	0.36	0.195
G. 15	90	95	8550	19(3/4")	0.12	0	0.12	0.78
G.16	90	95	8550	19(3/4")	0.16	0	0.16	0.78
G. 17	90	95	8550	19(3/4")	0.28	0	0.28	0.39
G.18	90	95	8550	19(3/4")	0.12	0	0.12	0.585
G 19	90	95	8550	19(3/4")	0.80	0	0.80	0

concrete : cube crushing strength 41 N/mm^2 (6,000 psi)

compression +ve,

Tension -ve.

5.1.5 Estimation of shear carried by aggregate interlock:

In the previous sections various possibilities were discussed under which interlock is most effective. Generally in beams, the ideal conditions for interlock hardly exist and as a result it is difficult to estimate in a rational way the force carried by interlock, especially when a beam is approaching failure conditions. It is impossible to take account of all the parameters mentioned in this chapter while formulating an equation.

From the study of the effect of crack widths, it appears that crack width has considerable bearing on the shear transfer capacity of a preformed crack. From fig. 65, it is evident that hardly any shear can be transferred when the initial width is greater than 0.5 mm, whereas with smaller crack widths some shear can be transfered. This is attributable to the fact that increase in crack width means a reduction in surface area in contact and hence a lesser possibility of interlock.

The other parameter studied during this investigation is the effect of axial load on interlock. Interlock force increases with increasing magnitude of axial compression. But interlock force dies down with axial tension, so that practically no shear transfer is possible in the presence of tension. (see tables 9 and 10).

It was not possible to study the other parameters and hence an empirical relationship developed on the findings of this investigation may be of limited applicability.

The effects of the variables, concrete strength, size of aggregates and grades of aggregates are not treated individually but represented altogether by the tensile strength of the concrete. This is reasonable, as the mortar or aggregate whichever fails earlier, will decide the strength in interlock.

From the plot of test results of specimens in group 2 - without axial load, an empirical relationship has been developed in order to predict shear transfer as a function of crack width -

The equation is

$$\frac{Qg}{bd} = K\left(\frac{1 - Cw}{1 + Cw}\right)^3 \sqrt{Ucyl} \qquad 5.1.1$$

where Qg = shear carried by interlock

K = constant

Cw = crack width in mm.

$Ucyl$ = cylinder strength of concrete in $^{N}/_{mm^2}$

and $\sqrt{Ucyl}$ is also in $^{N}/_{mm^2}$

From the curve, the value of the constant K is found to be 0.28 for a concrete cylinder strength of 33.0 $^{N}/_{mm^2}$. This is the mix used during this investigation.

Thus after evaluation of the constant, equation 5.1.1 becomes -

$$\frac{Qg}{bd} = 0.28\sqrt{Ucyl}\ \left(\frac{1 - Cw}{1 + Cw}\right)^3 \qquad 5.1.2$$

In the presence of axial force:

Equation 5.1.2 needs modification if it is to be used when axial load is present. As explained before, axial force has an effect on the crack width and axial compression creates frictional resistance.

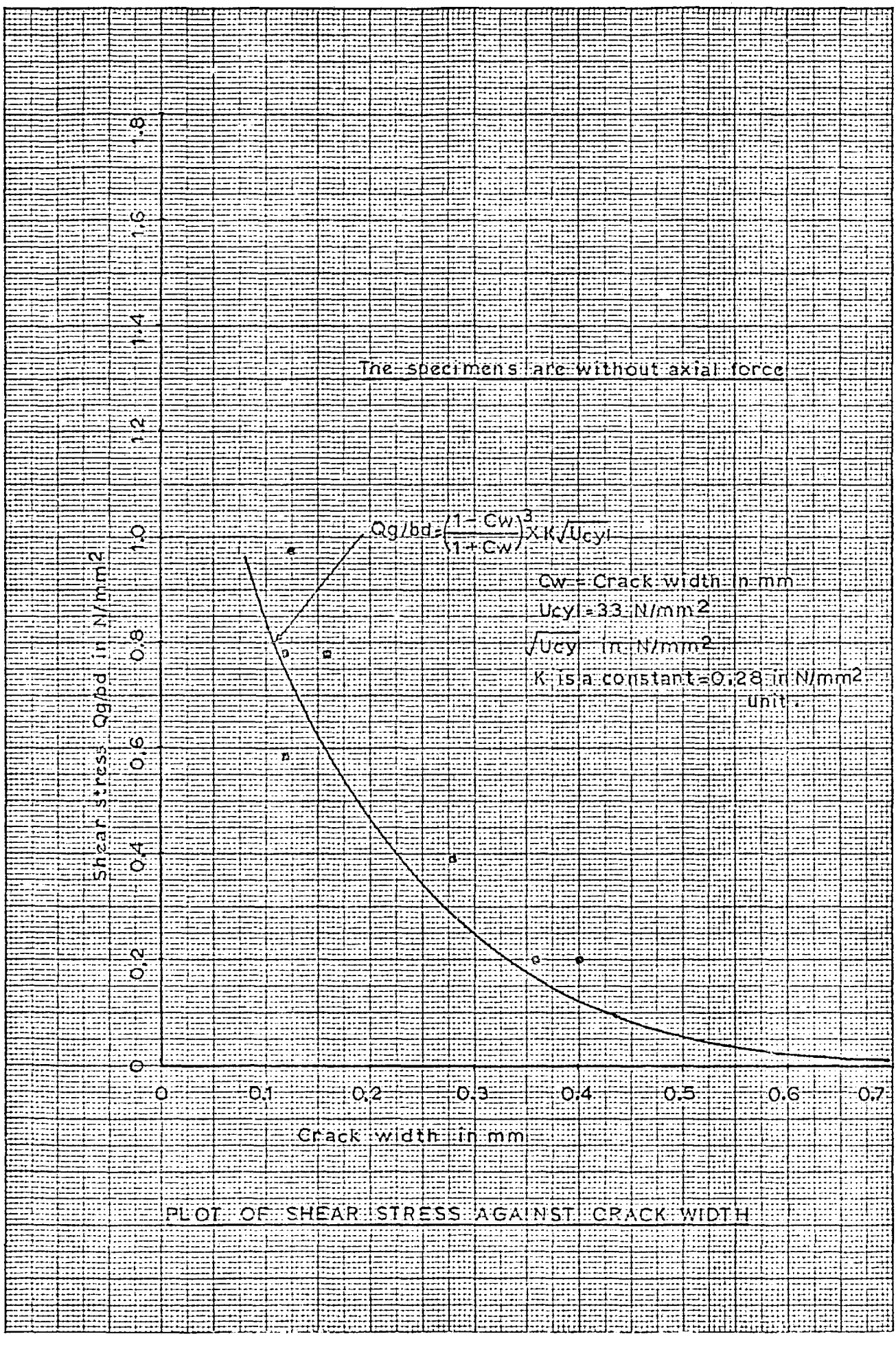
So, firstly the crack width is to be modified, which means the crack width in equation 5.1.2 be that after application of axial load. To take account of the frictional resistance, a coefficient of friction will be introduced and with the help of shear friction theory (used by Mattock mentioned earlier), the magnitude of shear that can be transfered in the presence of axial compression is

$$\frac{Qg}{bd_1} = 0.28\sqrt{Ucyl}\ \left(\frac{1 - Cw}{1 + Cw}\right)^3 + \tan\phi\ {}^{N}/_{bd} \qquad 5.1.3$$

where Cw = crack width after application of axial load in mm.

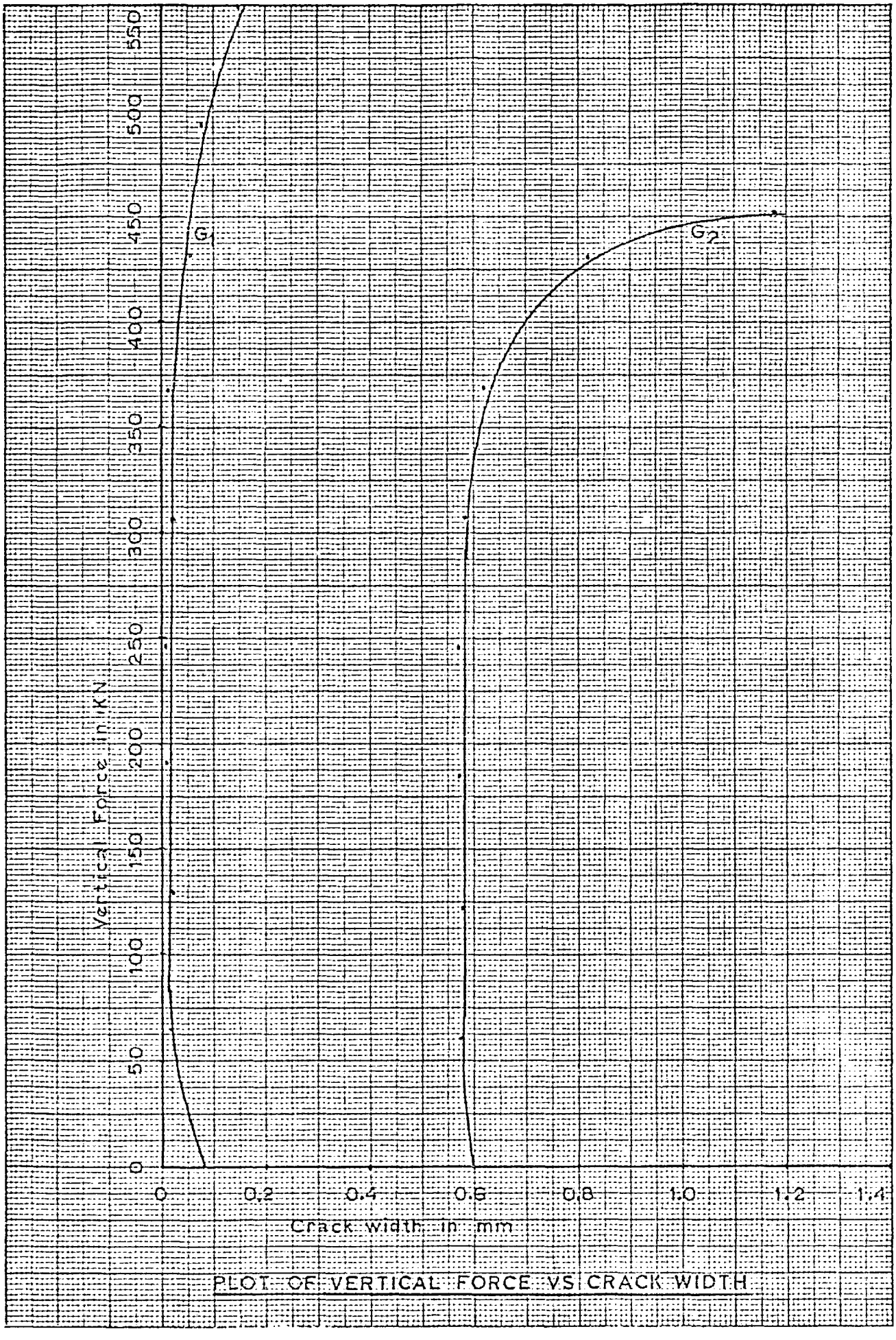
$\tan\phi$ = coefficient of friction

$^{N}/_{bd}$ = Magnitude of normal stress across the plane of failure in $^{N}/_{mm^2}$



PLOT OF SHEAR STRESS AGAINST CRACK WIDTH

FIG. 65.



PLOT OF VERTICAL FORCE VS CRACK WIDTH

FIG. 66.

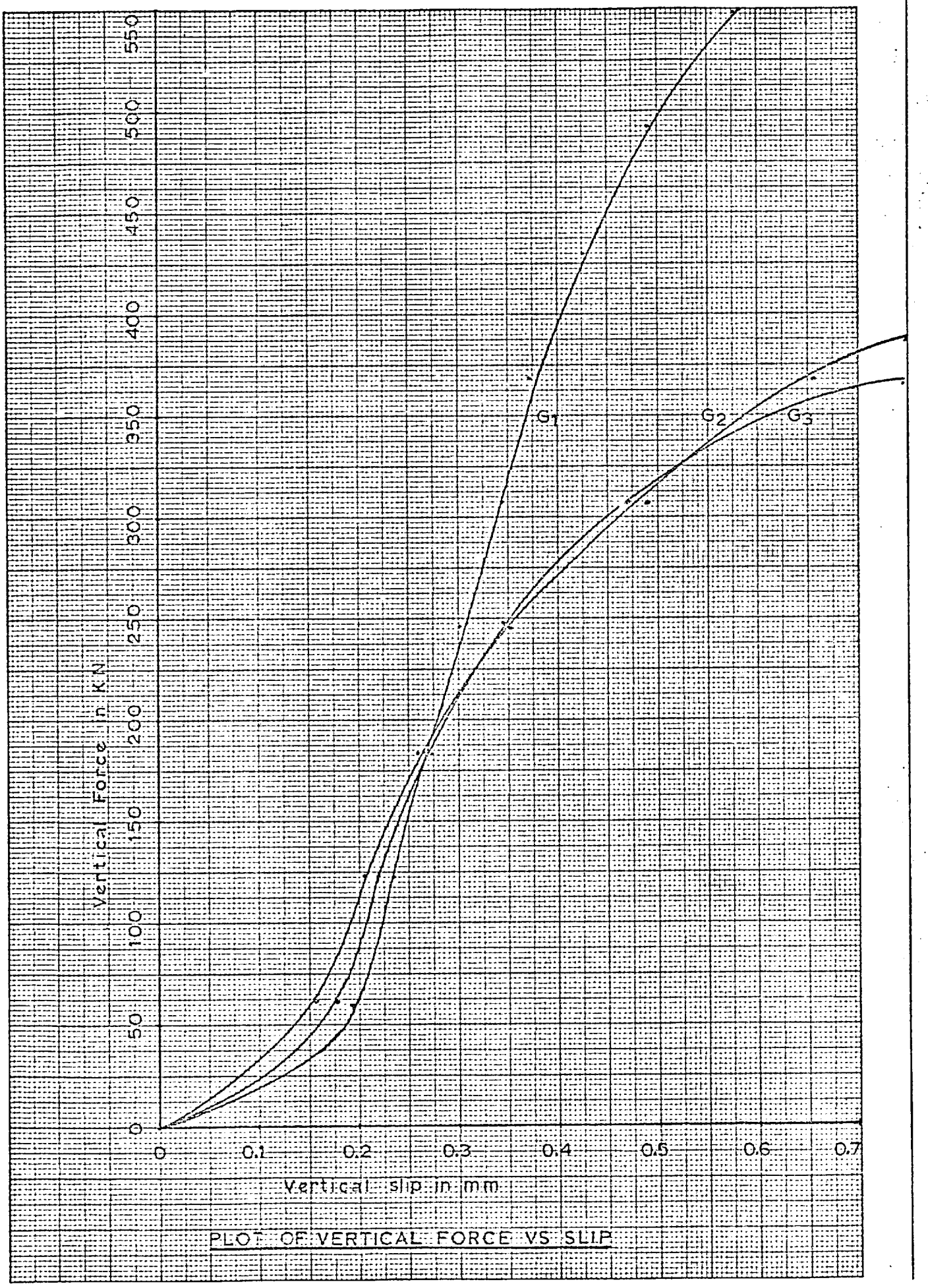
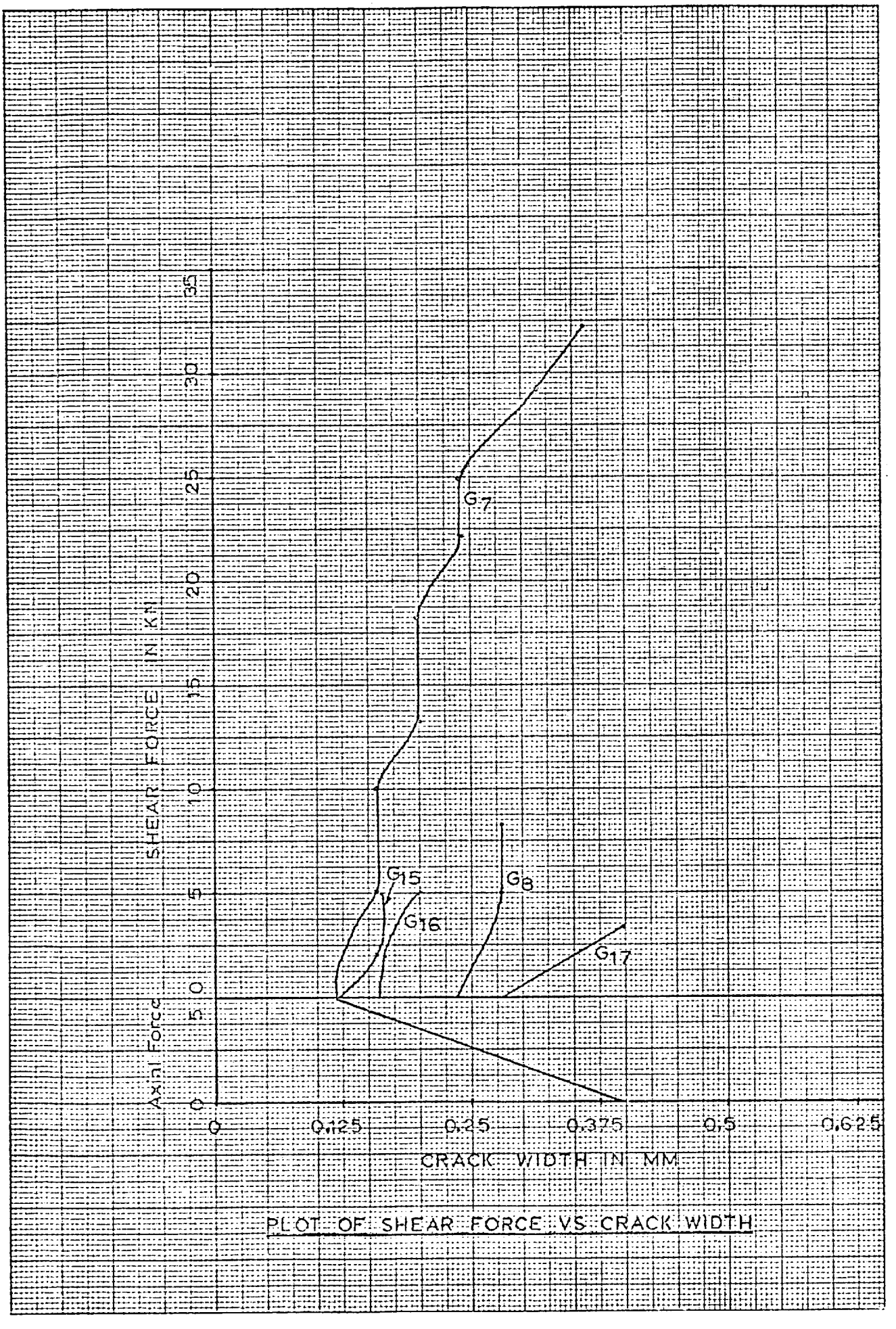
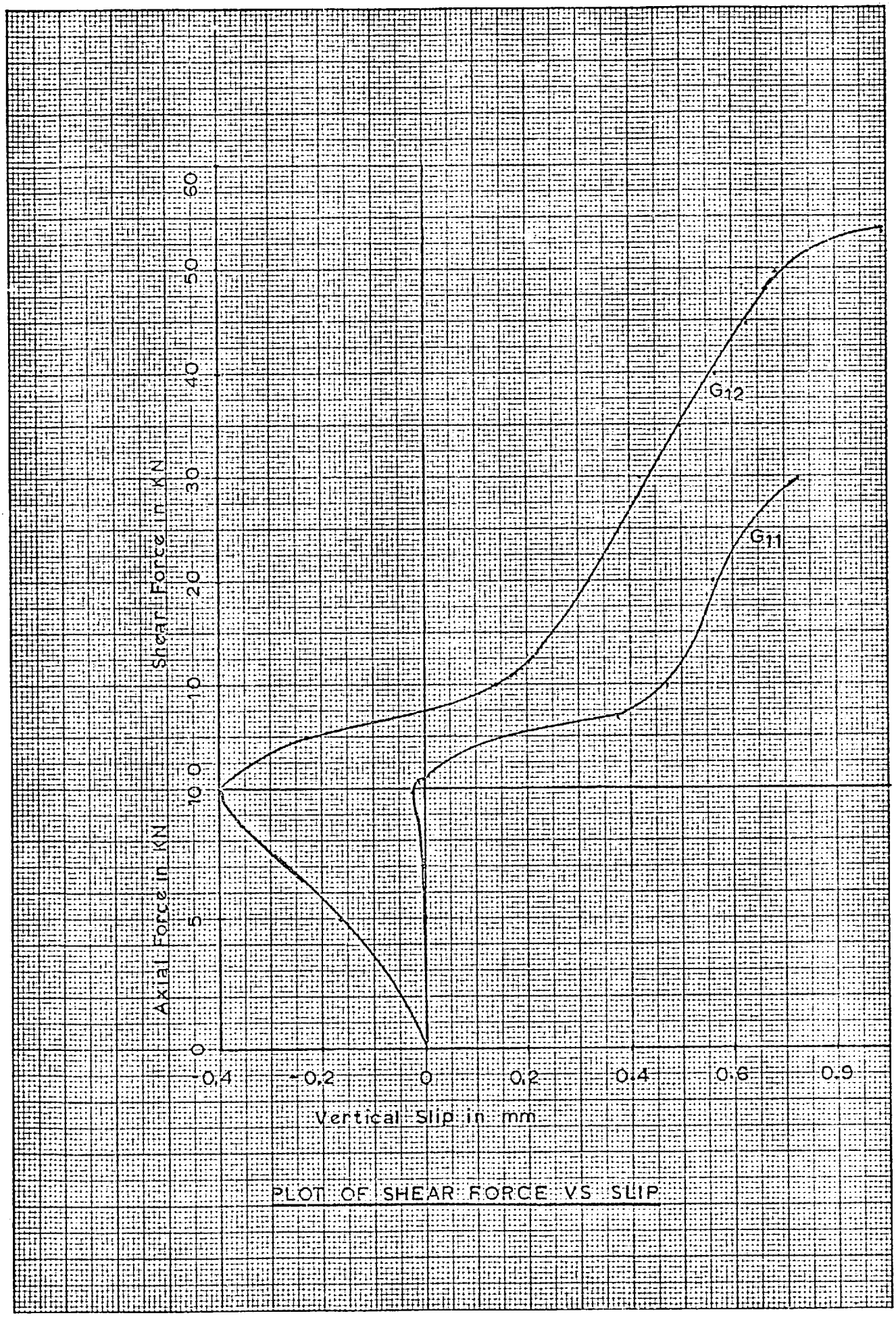

Vertical Force in KN
0
50
100
150
200
250
300
350
400
450
500
550
0
0.1
0.2
0.3
0.4
0.5
0.6
0.7
Vertical slip in mm
G1
G2
G3
PLOT OF VERTICAL FORCE VS SLIP

FIG. 67.



PLOT OF SHEAR FORCE VS CRACK WIDTH

FIG. 68.



PLOT OF SHEAR FORCE VS SLIP

FIG. 69.

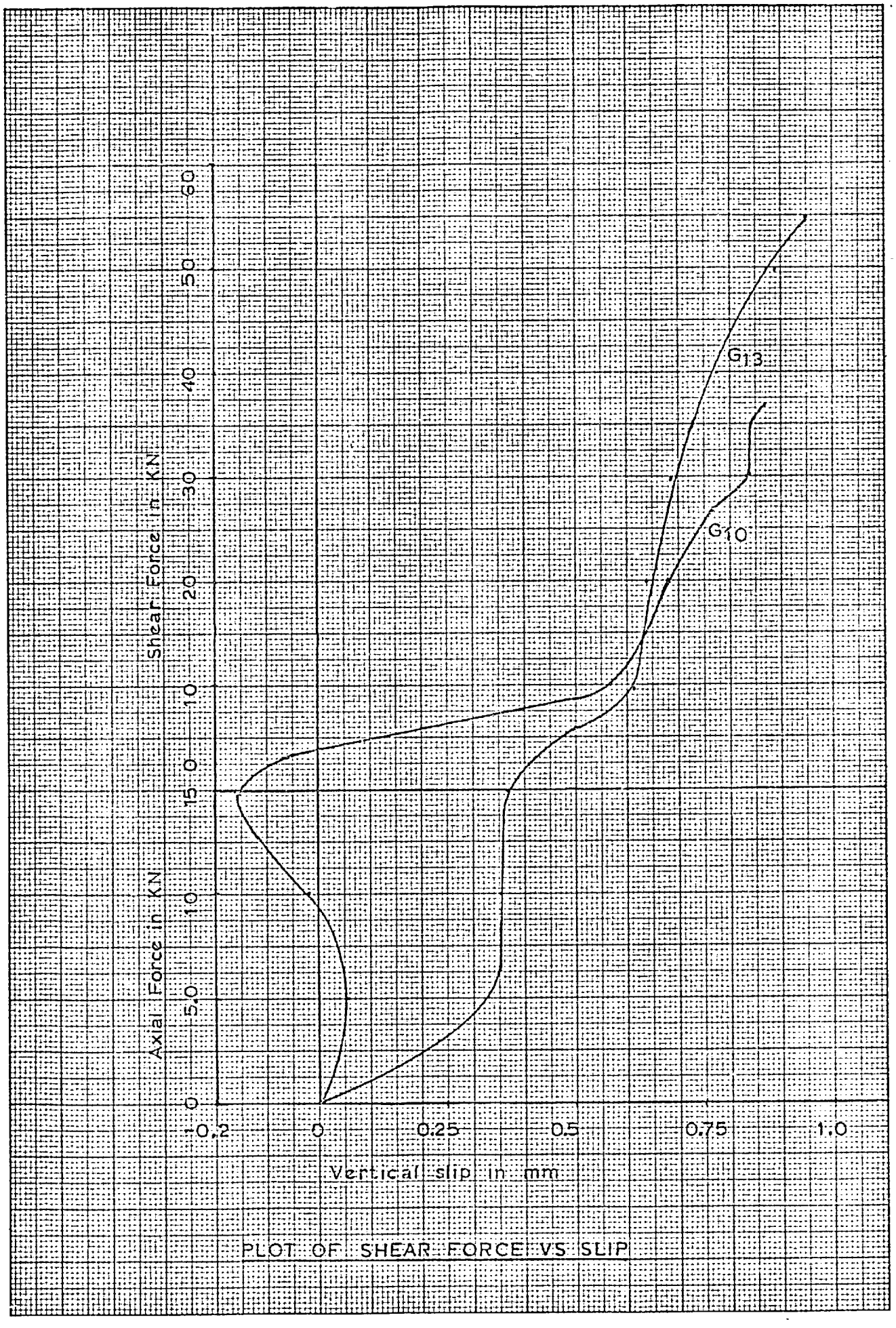

Shear Force in KN
60
50
40
30
20
10
0
15
10
5.0
0
Axial Force in KN
-0.2
0
0.25
0.5
0.75
1.0
Vertical slip in mm
G13
G10
PLOT OF SHEAR FORCE VS SLIP

FIG. 70.

Mast[25] proposed that tan ϕ could be taken to be 1.4 which is in fact, the slope of the failure envelope adopted for the development of shearing equation if Ut = 0.1 Ucyl. This seems reasonable and a value of tan ϕ = 1.4 is adopted, which from test results is found to be on the safe side.

Thus the final equation to predict shear transfer in the presence of axial load becomes -

$$\frac{Qg}{bd_1} = 0.28\sqrt{Ucyl}\left(\frac{1 - Cw}{1 + Cw}\right)^3 + 1.4\,{}^{N}/_{bd} \qquad 5.1.4$$

In case of tension, there will be no frictional resistance and if the crack width is modified, the original equation 5.1.2 will be valid.

5.2 Study of dowel Theories:

Another important action believed to carry shear in conjunction with the concrete compression zone, web reinforcement and aggregate interlock is dowel action of the tensile reinforcement. Investigations by a number of researchers (Baumann[7], Taylor[57], Krefeld and Thurston[26], Jones[20], and Paulay and Fenwick[43]) envisage that a considerable portion of the total shear is carried by this action. Their findings were based on tests of model beams or special small specimens.

Concept of "Beam on elastic foundation".

This concept was used by Jones[20], Krefeld and Thurston[26], and Regan[45] to evaluate the amount of shear that could be carried by the dowel action of the tensile steel.

R. Jones was the first to apply the concept of "beam on elastic foundation" to estimate the shear carried by the tensile steel. The same concept was used by the other investigators with minor alterations.

Jones assumes that the end of a beam is held in position and direction and the support (see fig. 71)

His second assumption is that the forces acting on the block are capable of keeping the top surface of the beam horizontal.

Now with the application of load Q_d on the tensile steel, the whole block will try to deflect but as its top is held horizontal the whole of the deflection of the tensile steel caused by Q_d will appear as tensile strain in the concrete down to the level of tensile steel. Jones thus considers that the structure is composed of a dowel element of the tensile steel and the concrete below it, supported from the top by the concrete in tension. Thus the loading conditions may be expressed as -

$$EI_2 \frac{d^4y}{dx^4} = -Ky \qquad 5.2.1$$

where EI_2 = flexural rigidity of dowel element.

K = modulus of elasticity of concrete foundations: constant

y = vertical deflection; transversal deformation of dowel element.

After the application of proper boundary conditions and simplifications, he arrives at the following equation

$$Q_d = 2\, EI_2\, z^3 y \qquad 5.2.2$$

where $$z = \sqrt[4]{\frac{K}{4\, EI_2}}$$

Equation 5.2.2 can be applied to beams to find Q_d, provided the concrete cracks, as follows.

If yd be the distance from the centre of the compression steel to the top of the tensile steel, he considers that the upward force per unit length is

$$Ky = \frac{Eyb_1}{yd}$$

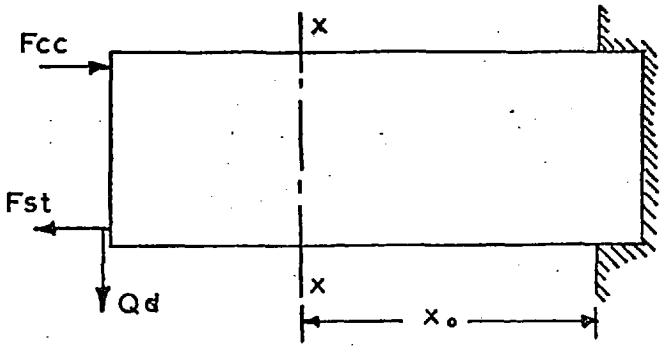
$$\therefore \quad K = \frac{Eb_1}{yd} \qquad 5.2.3$$

where b_1 = Net breadth of the section

$= b - n\phi$,

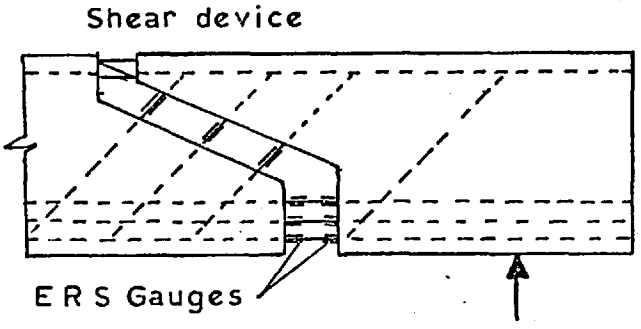
n = No. of bars

ϕ = diameter of bars



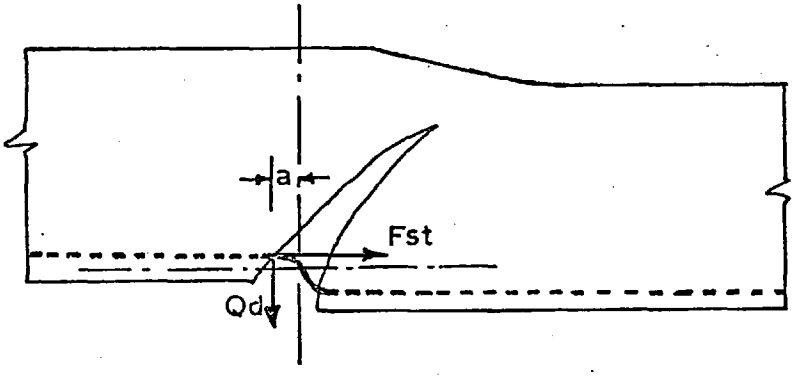
EQUILIBRIUM CONDITIONS USED BY JONES

FIG. 71.



SPECIMEN FOR DOWEL TEST (JONES)

FIG. 72.



DOWEL ACTION OF TENSILE STEEL (REGAN)

FIG. 73.

From the last assumption it appears that he considers the average tensile strain in concrete in order to estimate the upward resistance offered by concrete. But in fact, tensile strain at the level of tensile steel will be maximum the net breadth being a minimum, although in practical terms the effect of his simplification is small.

Horizontal cracking will occur when the magnitude of the principal tensile stress exceeds the limit value. The principal tension is caused by a combination of vertical stresses resulting from dowel force and longitudinal steel due to external loads.

$$\therefore \quad Ky = b_1 f_u$$

$$= \frac{Eb_1}{yd} y$$

$$\therefore \quad y = \frac{ydfu}{E} \qquad 5.2.4$$

where f_u = the limiting vertical tensile resistance as reduced by the other stresses.

After substitution of values of K and y,

Equation 5.2.2 becomes -

$$Qd_{(max)} = 2\,EI_2 \sqrt[3/4]{\frac{Eb_1}{4\,yd\,EI_2}} \times \frac{ydfu}{E}$$

or $$Qd_{(max)} = 0.7\,fu \sqrt[4]{yd\,I_2\,b_1^3} \qquad 5.2.5$$

where the value of fu will depend on the horizontal, shear and the limiting value of principal tensile stress.

Jones carried out tests on specimens as shown in fig. 72.

From test results of loads causing splitting, Jones calculated values of $q = \frac{Q}{b_1 la}$ and corresponding values of $fu = \sqrt{f_t^2 - \left(\frac{q}{f_t}\right)^2}$,

where q = shear stress

Q = shear force causing cracking

b_1 = net breadth of specimen

la = lever arm

Substituting values of fu obtained into equation 5.2.5, theoretical dowel forces were obtained.

From test results of beams with web reinforcement Jones concluded that longitudinal steel functioning as a dowel contributes a substancial part of resistance at shear failure.

Krefled and Thurston[26]

Their test specimens are shown in fig. 74.

Like Jones they applied the theory of beams on elastic foundation and derived an equation for the dowel cracking load.

$$Qd = b\sqrt{Ucyl}\left[1.3\left(1 + \frac{180rst}{\sqrt{Ucyl}}\right) c + d_1\right]\frac{1}{\sqrt{\frac{x_1}{d_1}}} \qquad 5.2.6$$

where Qd = dowel cracking load

x_1 = distance of the tail of the inclined crack from the support.

c = concrete cover

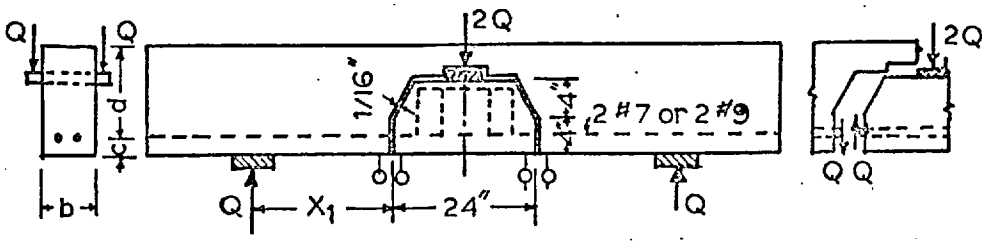
= distance from the centre of a single layer of bars to the bottom surface.

In fact, the equation derived from the theory of beams on elastic foundation did not include the effect of distance of the diagonal crack from the support.

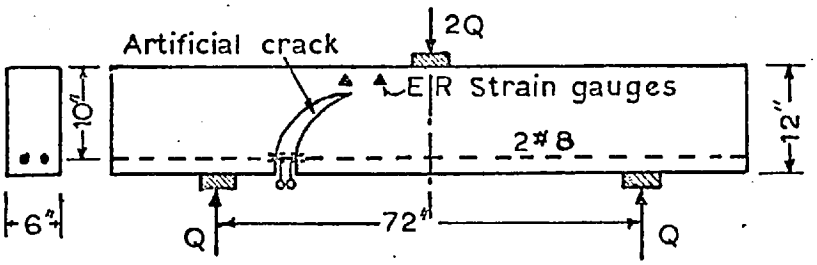
The above equation is a modified one taking account of the influence of this factor found in their tests of beams with preformed cracks.

The following are the most important points emerging from their tests on dowel specimens -

1. Dowel forces decreased with increase of the distance between the diagonal crack and the support.
2. Dowel forces increased with larger concrete cover below the bars.
3. From the tests on their specimens, they found that dowel resistance is about one-third of the total shear.

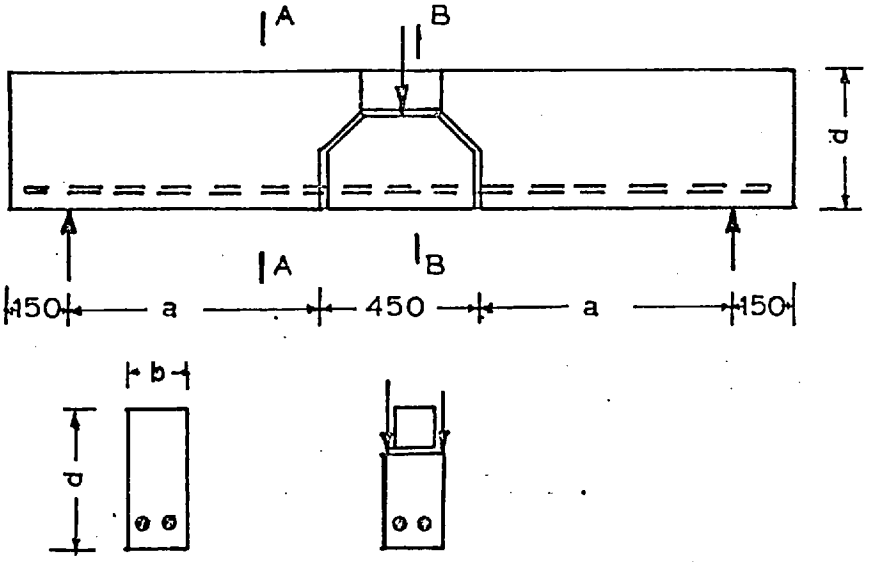


(a). DOWEL SPECIMEN



(b). BEAM SPECIMEN

DETAILS OF SPECIMENS FOR DOWEL TESTS (KREFELD & THURSTON). FIG. 74.



Section A-A Section B-B

DETAILS OF SPECIMENS FOR DOWEL TEST (BAUMANN). FIG. 75.

In order to confirm the fraction of shear carried by dowel action, Krefeld and Thurston performed a test on a beam with an artificial crack (see fig. 74b). They measured the strains in the concrete and longitudinal steel and estimated the shear carried by the concrete compressive zone and the tensile steel separately. The results of this beam test, they found, agreed with those obtained from the dowel beams.

Their main conclusions are summarised below -

1. After shear cracking, longitudinal steel carries external shear with a dowel action.

2. The shear resistance of the longitudinal bars depends on the size of the bars, depth of cover below the bars and the concrete strength.

Regan[45] assumes that the point of contraflexure of the tensile steel is at the middle of the crack, which means the bending moment are equal at the two sides of the crack. (fig. 73).

Thus the bending moment in the reinforcement at the section x', $Mx' = Qdx' - Ty'$.

Then converting the above equation into differential form and working out Heteny's solutions for the deflection profiles of members supported on elastic foundations and subject to axial and transverse loads, after simplifications, he arrives at the following equation for transverse deformation of the dowel beam -

$$y = Qd \left[\sqrt{2} \left(\frac{ko}{EI_2}\right)^{1/4} + a \left(\frac{ko}{EI_2}\right)^{1/2} \right] / ko \qquad 5.2.7$$

Then at critical stage -

$$Ut = \frac{ko\ y}{b_1}, \quad \text{and thus equation 5.2.7 becomes -}$$

$$Qd = b_1\ Ut / \left[\sqrt{2} \left(\frac{ko}{EI_2}\right)^{1/4} + a \left(\frac{ko}{EI_2}\right)^{1/2} \right] \qquad 5.2.8$$

where Qd = shear force in reinforcement

EI_2 = stiffness of "beam" (reinforcement and concrete cover).

ko = modulus of support, stress exerted by foundation per unit displacement of "beam".

y = transverse deformation of "beam" (dowel) from its unloaded position at the section considered.

a = half of the crack width at the level of tensile steel.

b_1 = net breadth of concrete (overall breadth minus the sum of the diameters of the bars in one layer).

He simplified his equation further on the assumption that 'a' is small and hence the last term of equation 5.2.8 can be neglected.

He obtained the value of modulus of elastic foundation on the assumption that stresses disperse at 45° angles in both directions inside the concrete.

Finally, considering plasticity of concrete even under tensile stresses, he reduced his equation to the following form -

$$Qd = K\, b_1 \,.\, Ut/\left(\frac{ko}{EI_2}\right)^{1/4} \qquad 5.2.9$$

The stiffness of the dowel element EI_2 is calculated on the basis of uncracked section theory. The equivalent area of steel in terms of concrete is to be considered.

Regan's theory differs from that of Jones' in that the latter assumes the foundation modulus is inversely proportional to the depth of the beam, whereas Regan believes the stresses at the level of tensile steel are dissipated towards the concrete compression zone and hence the effective depth is of little significance.

Baumann's[7] test specimen (fig. 75) was similar to those used by Krefeld and Thurston[26] and Taylor[57]. Only the tensile zone of a simply supported beam was loaded. This part of the tensile zone was separated by an artificial crack from the rest of the beam. Thus, if any load is carried by the beam, it is by dowel action, other actions being deliberately eliminated.

He studied the effects of a large number of variables, the most important of them were - width of preformed crack, thickness of bottom cover, distance from preformed crack to support, diameter of main reinforcement, number of layers of bars and concrete strength. He also studied the effect of stirrups supporting the dowel.

After analysis of his test results, he proposed two equations for dowel cracking loads, one for a single layer of bars and the other for two layers of bars in a beam.

Baumann's equation for vertical equilibrium is

$$Qd = K\,Ut\,bn\,lc \qquad 5.2.10$$

where Qd = dowel cracking force in Newton.

$K\,Ut$ = average vertical tensile stress in concrete at the level of bars along a primary bearing length.

Ut = uniaxial tensile strength of concrete

$= 0.245\,Uw^{2/3}$ in N/mm^2

Uw = cube crushing strength of concrete (N/mm^2)

bn = net breadth of beam at the level of main reinforcement.

= total breadth - sum of the diameters of bars in one layer.

lc = primary bearing length of dowel.

From his test results, he found

$$lc = 6.6\,\Phi/Uw^{1/3} \qquad 5.2.11$$

for a single layer of main reinforcement.

where Φ = diameter of reinforcement

and

$$lc = 40 + 0.032\,Ju \qquad 5.2.12$$

for two layers of main reinforcement.

where Ju = moment of Inertia of dowel bars + concrete cover directly below the bars.

Upon substitution of the values of lc into equation 5.2.10, he arrived at the following equations -

$$Qd = 1.62\ bn\ \phi\ Uw^{1/3} \qquad 5.2.13$$

for a single layer of reinforcement

and $$Qd = 0.245\ bn\ Uw^{2/3}\ (40 + 0.032\ Ju) \qquad 5.2.14$$

for two layers of reinforcement.

where Qd is the dowel force causing dowel cracking.

It seems from these equations that the dowel force is not dependent on the distance between load and supports, which the author believes is true only when the distance is large. When the distance is small the dowel force increases inversely as the distance between the support and the dowel load, (ref. 3).

Baumann gave no equations for the effects of web reinforcement, but there is evidence in his work that web reinforcement improves the dowel action of the tensile steel.

Arroyo's[3] work was completely experimental and the following information was obtained from his test results -

1. Dowel force increases with an increasing percentage of tensile steel, the increase being considerable in specimens without stirrups.
2. Dowel force increases with decreasing distance between the tail of the diagonal crack and the support when the distance is short.
3. His information regarding the type of reinforcement is inconclusive but he believes that it may have a considerable effect.
4. Dowel force increases with an increase in concrete cover below the bars, at least when the distance to the support is short.
5. Dowel shear resistance is increased with the amount of stirrup put in the specimens, but this increase is dependent, at the same time, on the distance of the stirrups from the preformed crack.

Other investigators, the names of whom are worth mentioning in this regard are Lorentsen[32], Acharya and Kemp[1], Taylor, R.[59], Ashdown[4] and Taylor, H.P.J.[57]. A full description of their work is available in reference 3.

5.3 Bond failure:

Mostly bond failure is not much of a problem in reinforced concrete structures and that is why it is often forgotten. But sometimes with poor bond properties or inadequate cover, failure can be by bond before either flexural or shear failure.

In a beam with web reinforcement, the shear carrying action is due partly to arching action with the tensile reinforcement acting as a tie and partly to truss action in the presence of web reinforcement, again using the main steel as a tie.

The reduction of stress in the main steel in the direction of decreasing moment is due to bond. After the formation of inclined cracks the ability of the web to transfer bond forces is partly destroyed, which means the rate of reduction of the force in the main steel is decreased. This implies that the force to be anchored towards the end of the span is greater and if no appreciable bond length is available, bond failure may follow. Thus shear cracking increases the possibility of bond or anchorage failure.

To avoid failure of this type, most theories[2,45,28] suggest that the main steel be extended a distance equal to the horizontal projection of the shear crack beyond its permissible cut-off point (by flexural theory).

Even then considerable differences exist between the suggestions as to what extent the cut-off position be extended.

Another type of anchorage failure (not strictly a bond failure) is caused by splitting of the concrete cover at the level of tensile reinforcement. This type of failure is observed in tests of beams

with deformed bars (KS 60 steel). Unlike the previous type of failure, splitting failure not only depends on the anchorage length but also on concrete cover.

Past work:

The parameters which are believed to influence bond or anchorage failure are -

a) concrete strength

b) diameter of main steel

c) type of bar

d) concrete cover

e) web reinforcement (if any)

f) anchorage length.

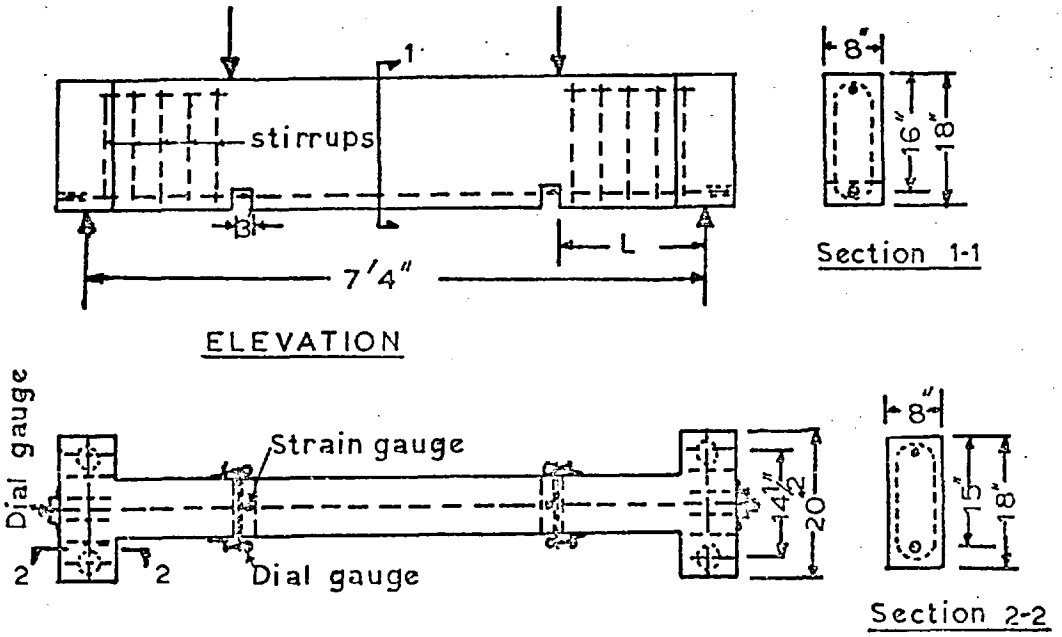
Not much work has been done on bond or anchorage failure in beams. The limited amount of work done is described below -

Mathey and Watstein[35]

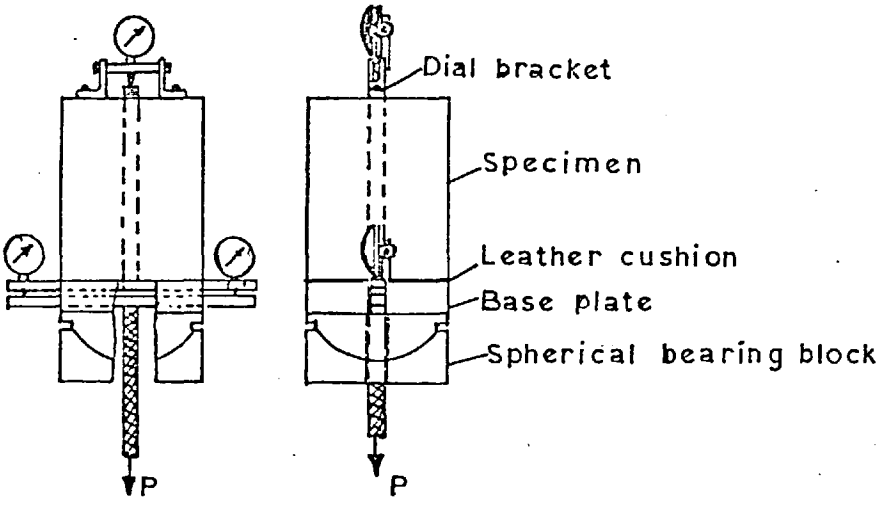
They performed tests on 18 beam specimens and 18 pull-out specimens with deformed reinforcing bars, varying the embedment lengths from 7" to 17" for $\frac{1}{2}$" bars and 7" to 34" for 1" bars. Their test-specimens are shown in fig. 76 and 77. The following are their main conclusions -

1. The bond strength per unit length decreased with the increasing length of embedment for a bar of the same size. For a given ratio of length to diameter of a bar, the bond strength decreased with increasing bar diameter.

2. Ultimate bond stresses in pull-out specimens agreed in general with those in beams with $\frac{1}{2}$" ϕ bars. But their test values on pull-out specimens with 1" ϕ bars were higher than those of beams, presumably because the 1" ϕ bars could split the cover.



DETAILS OF BEAM SPECIMENS
(MATHEY & WATSTEIN). FIG. 76.



DETAILS OF PULL-OUT SPECIMENS
(MATHEY & WATSTEIN) FIG. 77.

3. A linear relationship exists between the critical bond stress and the ratio of bar diameter to embedment length ($\frac{\Phi}{L}$) for $\frac{1}{2}$" ϕ bars; but they were not satisfied with the test results of 1" ϕ bars.

4. Increase of loaded-end-slip in the beam as well as in the pull-out specimens was observed with the stress in the bar, but it was found to be independent of the length of embedment for a particular bar. The relationships of loaded-end slip and stress in the bar were dissimilar for pull-out specimens and beams.

5. Based on their test results, they suggested two criteria of failure to define critical bond stress.

a) loaded-end slip of 0.01" and

b) free-end slip of 0.002".

Failure will occur whichever condition is reached first.

6. Another striking result emerging from their tests was that the max^m bond stress developed in all beams with $\frac{1}{2}$" ϕ bars was greater than twice the max^m allowable bond stress of ACI 318-56, 350 psi; but the load stress in beams (six out of nine) with 1" ϕ bars was less than 350 psi.

The critical bond stress in the case of pull-out specimens with 1" ϕ bars was less than twice 350 psi except the bar with only 7" of embedment. Four out of nine specimens with $\frac{1}{2}$" ϕ bars failed to develop bond stress of twice 350 psi.

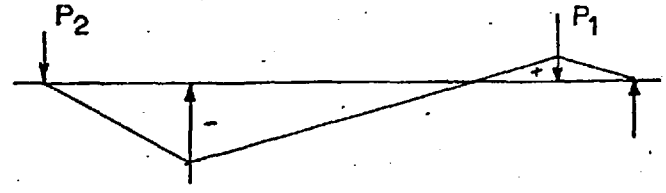
Ferguson and Thompson[17]

Ferguson and Thompson defined bond failure as a failure caused by the excessive slip at the free-end of the bars. Their investigation consisted of a study of the parameters which are given below -

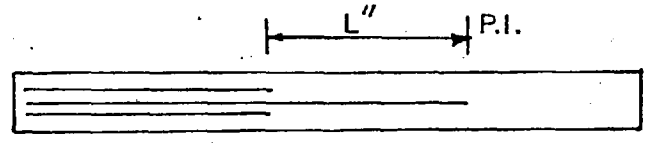
1. concrete strength

2. clear cover

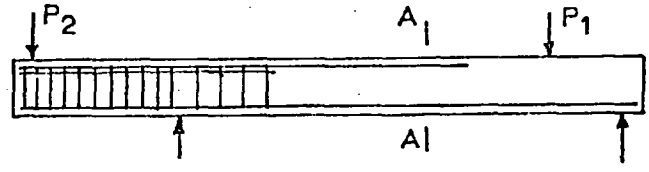
3. specimen width



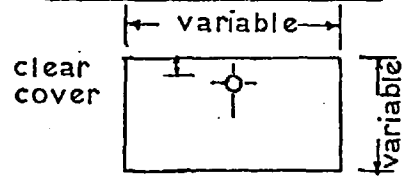
Moment diagram



Plan of top reinforcement

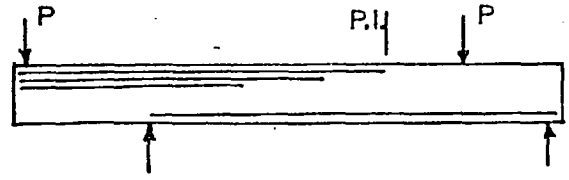


Longitudinal section

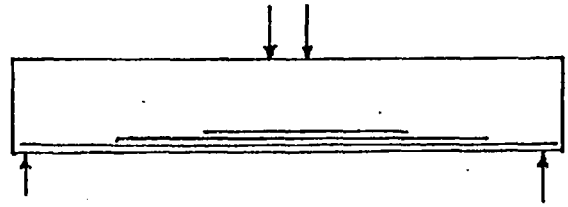


Cross section A-A

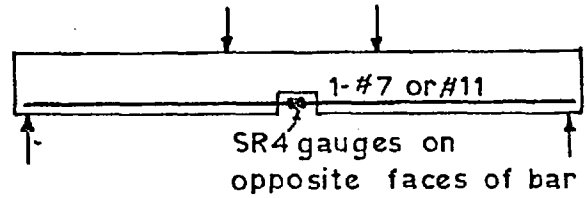
DETAILS OF BEAMS OF SERIES A, B & C.



Longitudinal section of Beams in series D.

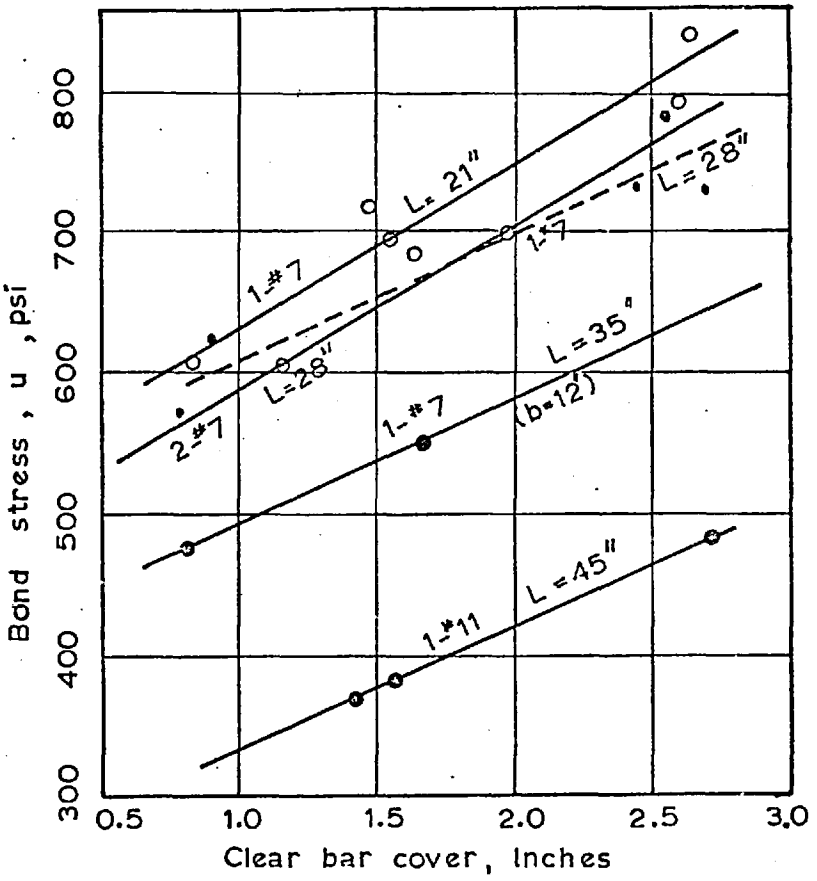


Longitudinal section of Beams in series E

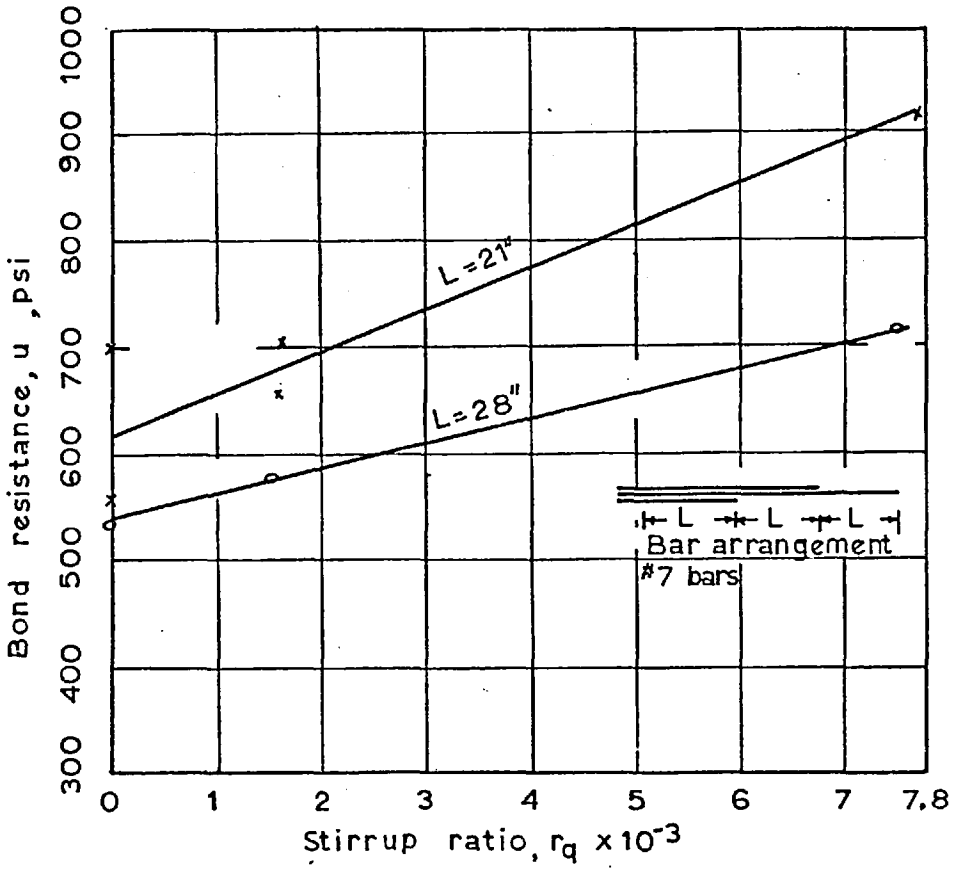


Longitudinal section of Beams in series F

DETAILS OF BEAM SPECIMENS (FERGUSON & THOMPSON). FIG. 78.



EFFECT OF BAR COVER ON BOND STRESS (FERGUSON & THOMPSON). FIG. 79.



EFFECT OF STIRRUPS ON BOND RESISTANCE

Note : u is adjusted bond stress, corresponds to concrete strength of 3300 psi and clear cover of 1.5 inch (FERGUSON & THOMPSON) FIG. 80.

4. web reinforcement and

5. bond length (development length).

Fig. 78 shows the beam specimen used during this investigation.

So far as the effects of the above-mentioned parameters are concerned, they reported that bond strength was found to vary as $\sqrt{Ucyl}$, but a non-linear relationship exists between clear cover and bond strength. Bond strength was found to increase with increasing cover (fig. 79). The increase reduced with increase in clear cover. They concluded that a large amount of data might indicate a curved line.

Bond strength was found to increase with increasing ratio of web reinforcement, which is indicated by fig. 80.

From fig. 80, it is clear that the rate of decrease of bond stress with increasing bond length is less for longer lengths.

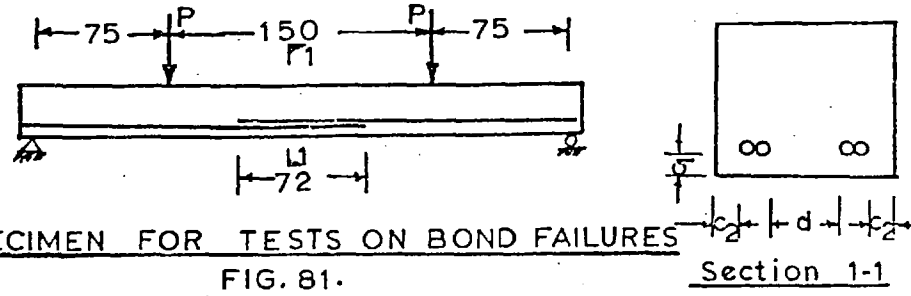
They found that narrower beams failed at bond stress of 7 to 20% lower than those of other beams. They attributed this to the development of higher diagonal tension resulting from lesser lateral resistance to splitting.

In the case of multiple cut-offs, stirrups improve bond strength. Their conclusion was that heavy stirrups can offset the loss of strength due to multiple cut-offs.

Ostlund's[42] test specimen is shown in fig. 81. His findings suggest that steel stress at failure increases with clear cover. (see table 11).

During his tests he varied not only the clear cover but also the amount of web reinforcement and the lap lengths (fig. 82).

Losberg[33] carried out a number of tests, the results of some of which are plotted and shown in figs. 83-88.

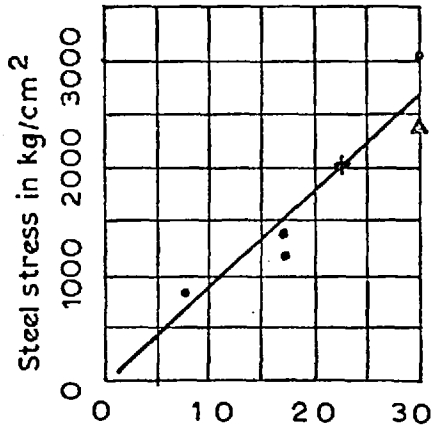


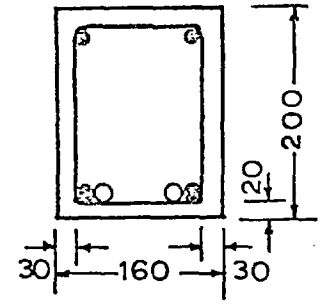
SPECIMEN FOR TESTS ON BOND FAILURES

FIG. 81.

Table 11. Effect of cover on steel stress

c_1 mm	c_2 mm	d mm	Cube strength of concrete kg / cm^2	Steel stress at failure kg / cm^2
20	30	32	243	4550
30	45	48	248	5800
40	60	64	248	6370





• lap lengths = 520 mm

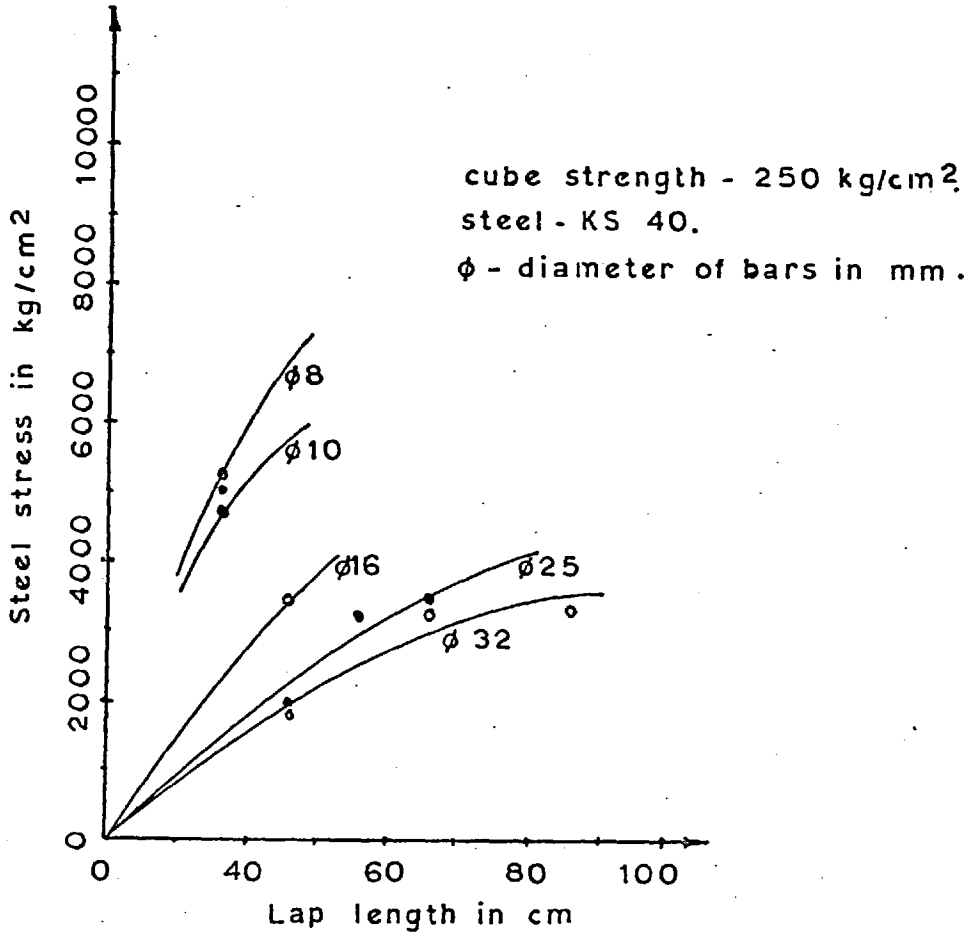
+ " = 720 mm

▲ " = 1020 mm

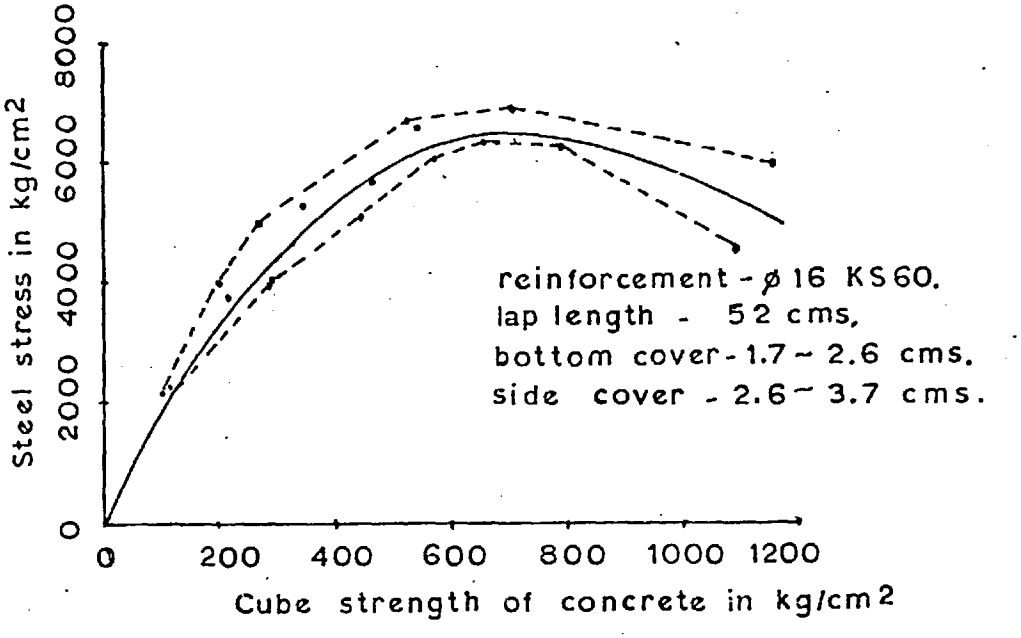
EFFECT OF WEB REINFORCEMENT ON STEEL STRESS (OSTLUND)

FIG. 82.

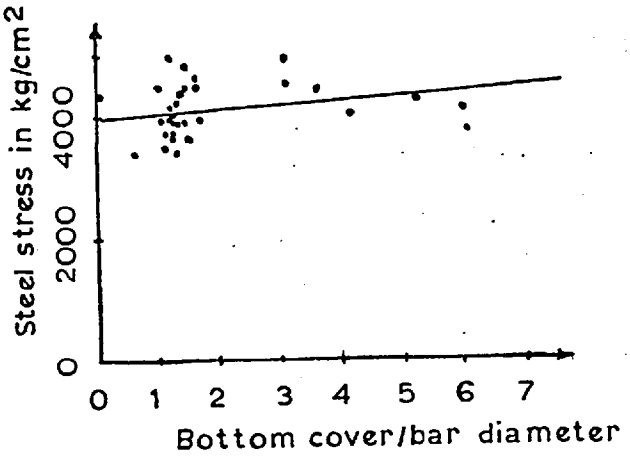
Reinforcement : 16 ø KS
(Cold worked to 9000 kg/cm^2)
Stirrup yield stress : 2600 kg/cm^2



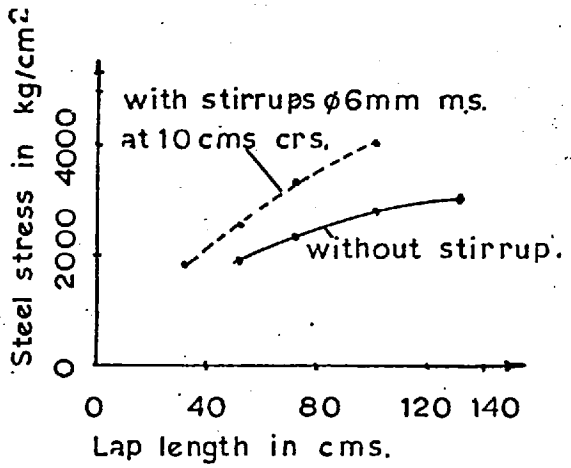
PLOT OF STEEL STRESS VS LAP LENGTH (LOSBERG) FIG. 83.



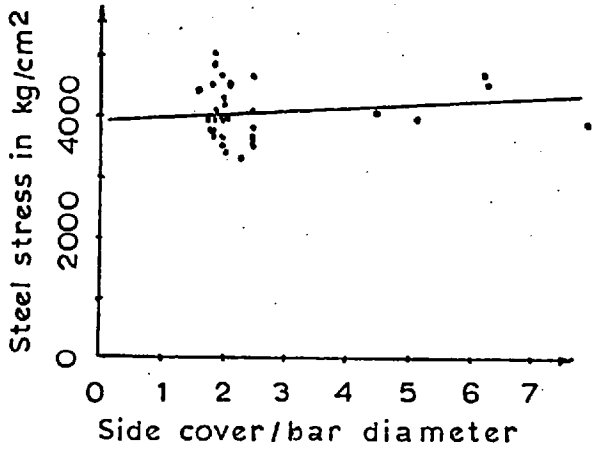
PLOT OF STEEL STRESS VS CONCRETE STRENGTH (LOSBERG) FIG. 84.



PLOT OF STEEL STRESS VS BOTTOM COVER/BAR DIAMETER (LOSBERG)
FIG. 85.

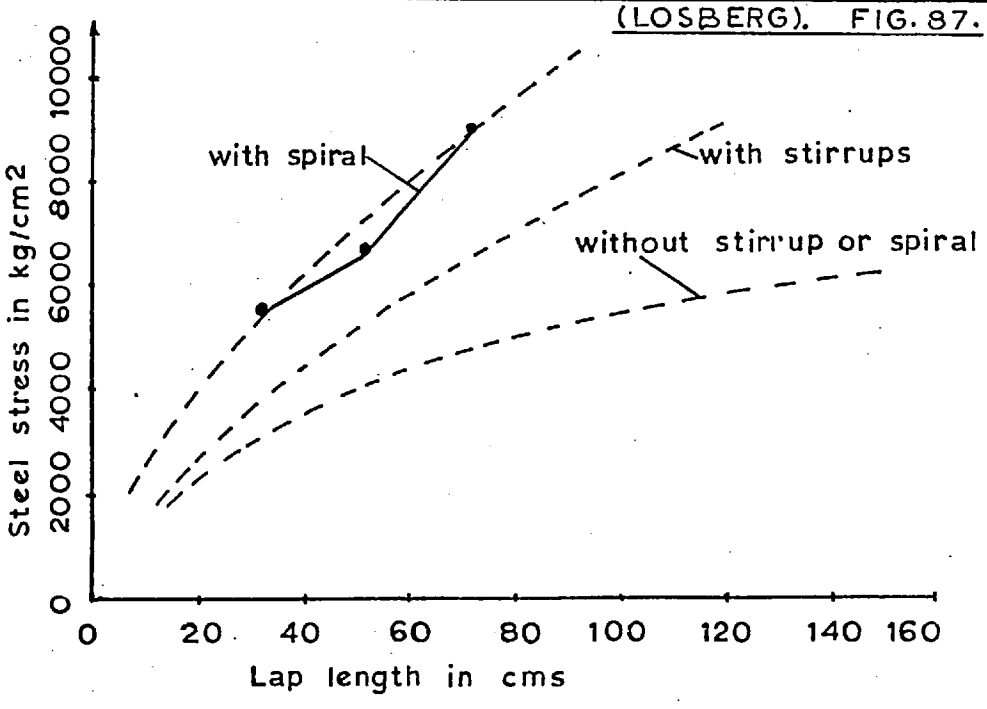


EFFECT OF STIRRUPS ON STEEL STRESS (LOSBERG)
FIG. 86.



steel- KS 60.
cube strength -250 kg/cm2.
lap length - 52 cms.

PLOT OF STEEL STRESS VS SIDE COVER/BAR DIAMETER (LOSBERG). FIG. 87.



PLOT OF STEEL STRESS VS LAP LENGTH (LOSBERG)
FIG. 88.

CHAPTER 6

THEORETICAL INVESTIGATION:

6.1 Introduction

As discussed in Chapter 2, shear failure is not a simple failure mode like flexure. Study of the behaviour of rectangular beams at the time of failure suggests three main modes which have to be dealt with separately.

6.2 Development of shear cracking theory

6.2.1 Failure criterion

Concrete at the head of a flexural crack is subject to longitudinal and transverse direct stresses as well as shear stresses.

If failure is believed to occur due to the combined action of these flexural and shear stresses, a failure criterion for biaxial stresses is necessary. It is assumed that shear cracking is the result of excessive principal tensile stress and hence the analysis to predict shear cracking load will be based on the equation representing the magnitude of principal tensile stress at a point, namely

$$f_1 = \tfrac{1}{2} ft + \sqrt{(\tfrac{1}{2} ft)^2 + q^2}$$

6.2.2 Assumptions

The following are the assumptions made in the context of the development of the shear cracking equation.

a) Shear cracking starts after the formation of flexural cracks.

b) Shear cracking is caused by the combined action of tensile and shear stresses in the tensile zone of the cross-section of the beam.

c) The shear stresses at different load stages and at different heights over the depth of the beam are proportional to the average shear stress.

d) The tensile strain in the concrete above the flexural crack is proportional to the steel strain in that section of the beam. The existance of the tensile strain can be explained with the help of fig. 95. A similar type of stress distribution is assumed by Kani[22]. The dependance on steel strain arises because crack widths are proportional to steel strains, and when the flexural cracks widen the interlock action diminishes (see Chapter 5) and an increasing proportion of the moment on a tooth caused by bond must be resisted by flexure in the tooth.

e) The stress-strain relationship of both concrete and steel is linear.

f) The tensile strength of concrete is assumed to be a function of cylinder strength.

g) Variations in the lever arm factor are neglected.

h) Since, unless it is inclined, web reinforcement does not carry any shear until the formation of shear cracks (with vertical stirrups) its contribution is neglected in the present analysis.

i) The effect of small longitudinal stresses in the vicinity of the neutral axis is negligible.

6.2.3 Derivation

The equation governing shear cracking loads of beams is

$$f_1 = \tfrac{1}{2} ft + \sqrt{(\tfrac{1}{2} ft)^2 + q^2} \qquad \ldots\ldots\ldots 6.2.1$$

where f_1 = The principal tensile stress

f_t = the tensile bending stress

q = the shear stress.

Cracking occurs when f_1 exceeds U_t, the tensile strength of concrete and so f_1 can be taken equal to U_t.

Therefore, equation 6.2.1 can be written as

$$U_t = \tfrac{1}{2} ft + \sqrt{(\tfrac{1}{2} ft)^2 + q^2}$$

or $$U_t^2 + (\tfrac{1}{2} ft)^2 - U_t\, ft = (\tfrac{1}{2} ft)^2 + q^2$$

or $$q^2 = U_t^2 \left(1 - \frac{ft}{U_t}\right)$$

or $$q = U_t \sqrt{1 - (\frac{ft}{U_t})} \qquad \ldots\ldots\ldots 6.2.2$$

Again the above equation can be simplified for small values of $(\frac{ft}{Ut})$ to the following form

$$q = Ut \left[1 - \tfrac{1}{2} (\frac{ft}{Ut})\right] \qquad \ldots\ldots\ldots 6.2.3$$

From assumption c)

$$q = K_1 \frac{Q}{bd_1} \qquad \ldots\ldots\ldots\ldots 6.2.4$$

where K_1 is a constant.

From assumptions d) and e), in the absence of axial loading,

$$ft = +K_2' \frac{M}{\text{lamrst } bd_1} \quad \text{(+ve sign is for tensile stress)}$$

where K_2' is a constant.

Neglecting the variation in lever arm factor, and considering a beam free from axial loads,

$$ft = K_2 \frac{M}{mrst\ bd_1^2} \qquad \ldots\ldots\ldots 6.2.5$$

where K_2 is a new constant.

As is evident, in the presence of an axial force, the steel stress is affected.

Fig. 89 (a) shows a section of a beam subjected to a bending moment M and an axial force N. The combination of the bending moment and axial force can be replaced by an axial force of magnitude N with an eccentricity 'e' from the centre of the tensile steel.

Then the eccentricity of N from the centre of the tensile steel :

$$e = \frac{M}{N} + (d_1 - d/_2) \text{ , where N is +ve for compression.}$$

Considering moments about the centre of the compressive force, $F_{st.la} = N\ (e - la)$

where $e > la$

Also $F_{st} = r_{st}\ bd_1\ fs$

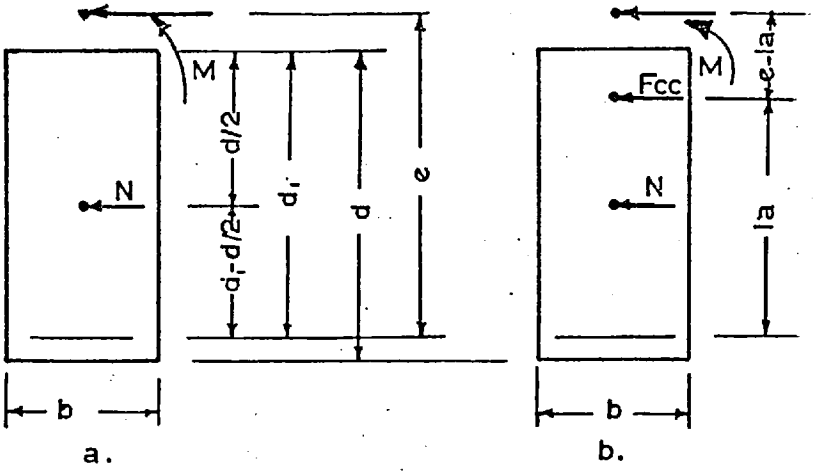
or $r_{st\ bd_1}\ fs \times la = N\ (e-la)$

$$\text{or} \quad fs = \frac{N(e - la)}{r_{st\ bd_1}\ la} \qquad \ldots\ldots 6.2.6$$

Again considering external moment equilibrium about the line of action of the compressive force F_{cd},

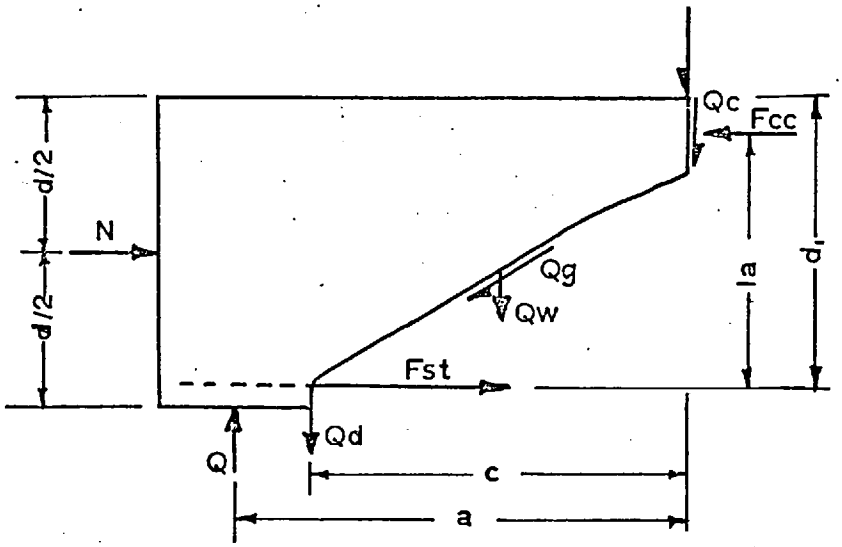
$$M\ ext. = N\ (e - la)$$

$$= M - N\left[la - (d_1 - d/_2)\right]$$



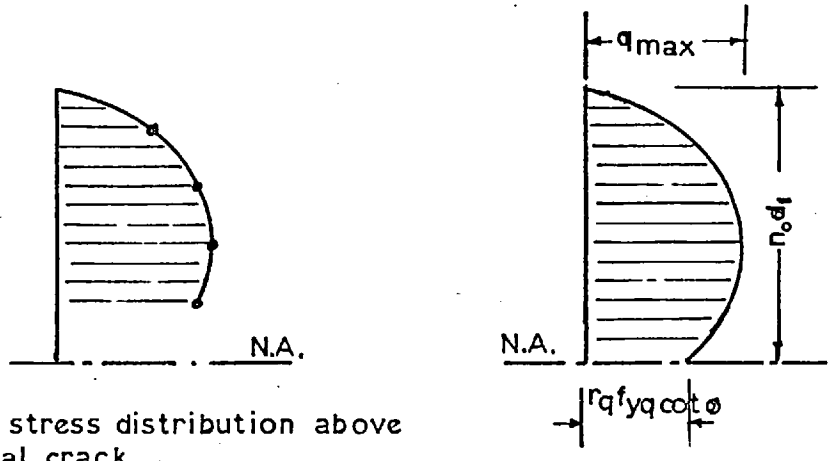
SECTION SUBJECTED TO AXIAL FORCE

FIG. 89.



EQUILIBRIUM OF SHEAR SPAN AFTER SHEAR CRACKING

FIG. 90.



a. Shear stress distribution above flexural crack (Taylor)

b. Assumed shear stress distribution above shear crack.

SHEAR STRESS DISTRIBUTION IN COMPRESSION ZONE

FIG. 91.

Replacing N(e-la) in equation 6.2.6 by

$$M - N\,(la - d_1 + {}^{d}/_{2}),$$

$$fs = \frac{M - N\,(la - d_1 + {}^{d}/_{2})}{r_{st}\, bd_1\, la}$$

$$= \frac{M - Nd_1\,(j + \frac{d}{2d_1} - 1)}{r_{st}\, bd_1\, la}$$

The two assumptions d) and e) give

$$ft = +K_2' \frac{M - Nd_1\,(j + \frac{d}{2d_1} - 1)}{m\ rst\ bd_1\ la}$$

where K_2' is a constant.

Neglecting the variation in lever arm factor and writing

$$k = (j + \frac{d}{2d_1} - 1)$$

$$ft = K_2 \frac{M - kNd_1}{r_{st}\ m\ bd_1^2}, \quad \text{where } K_2 \text{ is a new constant.}$$

$$\text{or } ft = K_2 \left[\frac{M}{Qd_1} \cdot \frac{Q}{bd_1} \cdot \frac{1}{mrst} - k\,{}^{N}/_{bd_1} \cdot \frac{1}{mrst} \right] \quad \ldots\ldots\ 6.2.7$$

Substituting the values of q and ft in 6.2.3

$$K_1 \frac{Q}{bd_1} = Ut \left[1 - \tfrac{1}{2} \frac{K_2(\frac{M}{Qd_1} \cdot \frac{Q}{bd_1} \cdot \frac{1}{mrst} - k\frac{N}{bd_1} \cdot \frac{1}{mrst})}{Ut} \right]$$

$$= Ut - \tfrac{1}{2} K_2 \left(\frac{M}{Qd_1} \frac{Q}{bd_1} \frac{1}{mrst}\right) + \frac{K_2}{2} k \frac{N}{bd_1} \frac{1}{mrst}$$

$$\frac{Q}{bd_1} \left[K_1 + \tfrac{1}{2} K_2 \frac{{}^{M}/_{Qd_1}}{mrst} \right] = Ut + \frac{K_2}{2} k \frac{{}^{N}/_{bd_1}}{mrst}$$

$$\text{or } \frac{Q}{bd_1} = \frac{Ut + \frac{K_2}{2} k \frac{N/bd_1}{mrst}}{K_1 + \frac{K_2}{2} \frac{M/Qd_1}{mrst}} \quad \ldots\ldots\ 6.2.8$$

Equation 6.2.8 predicts the shear cracking load of a section already cracked in flexure. Since beams without web reinforcement and with long shear spans ($a/d_1 > 2.5$) fail following shear cracking, this equation can be used to predict the ultimate strength of such beams failing in shear.

The above equation is useful when axial force is independent of external moment. If the magnitude of axial force is dependent on the external moment, it can be modified to the following form :

$$\frac{Q}{bd_1} = \frac{Ut}{K_1 + \frac{K_2}{2}\frac{(M/Qd_1 - k\frac{N}{Q})}{mrst}} \qquad \ldots\ldots\ldots 6.2.9$$

The use of the shear cracking equations requires the following additional limitations and data :

a) The equation is applicable to a section at a distance of d_1 either from the load point or from the support, and hence the M/Qd_1 ratio at that section is to be used. This is reasonable because the first shear crack occurs at a distance approximately equal to d_1 (effective depth) from the load point. The ACI-ASCE Committee 326[2] also based their equation on the assumption that first shear cracking will occur at a section at least a distance d_1 away from the load point. Sections closer than d_1 to the support remain uncracked in flexure.

b) When $d_1 < a < 2d_1$, the equation can be applied at the section located in the middle of the shear span.

c) When $a < d_1$, nominal elastic theory distributions of stresses can be applied based on an uncracked section.

When the shear span becomes short ($a < d_1$) the flexural stresses will not be able to cause flexural cracks in positions

which can initiate shear cracks. So the elastic theory can be applied.

d) The modular ratio ($m = \frac{Es}{Ec}$) is given by the relationship $m = 5 + \frac{70}{U\ cyl}$, when U cyl is in N/mm^2 unit.

and $m = 5 + \frac{10,000}{U\ cyl}$ when U cyl is in psi.

This relationship is suggested by Laupa[45].

e) The tensile strength of concrete (split cylinder strength) Ut is already assumed to be function of cylinder strength is equal to

$$Ut = 0.47 \sqrt{U\ cyl}$$

where both Ut and U cyl are in N/mm^2 unit. This relationship is obtained by plotting test results of Mattock[18], Moayer[37], Narasionhan[40] and author's own which is shown in fig. 92.

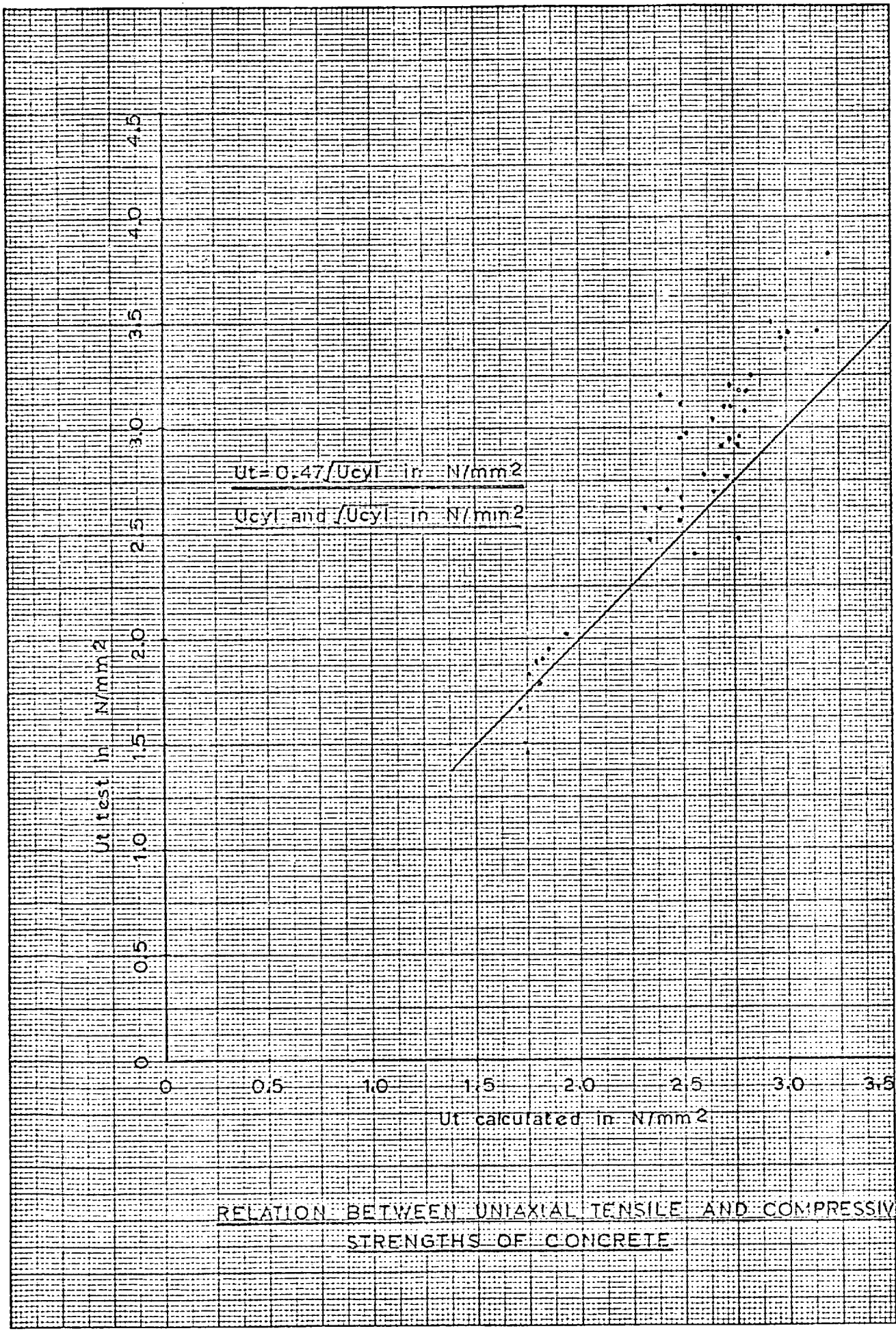
f) Evaluation of the constants by test results gives $K_1 = 1.35$ and $K_2 = 0.08$.

Upon substitution of the values of the constants, the equation becomes :

$$\frac{Q}{bd_1} = \frac{Ut + 0.04\ k \frac{N/bd_1}{mrst}}{1.35 + 0.04 \frac{M/Qd_1}{mrst}} \qquad \ldots\ldots\ldots 6.2.10$$

and $$\frac{Q}{bd_1} = \frac{Ut}{1.35 + 0.04 \frac{M/Qd_1 - k\ N/Q}{mrst}} \qquad \ldots\ldots\ldots 6.2.11$$

With the values of m and Ut as given above. The validity of these above equations has been checked with a number of test results for varying percentages of main steel, concrete strengths and moment shear ratios. A full account of the comparison is given in Chapter 7.



RELATION BETWEEN UNIAXIAL TENSILE AND COMPRESSIVE STRENGTHS OF CONCRETE

FIG. 92.

6.3 Equilibrium conditions of the shear span after shear cracking

Fig. 90 shows the forces acting in a shear span after formation of an inclined crack. The equations of equilibrium for the shear span can be written as

considering vertical equilibrium -

$$Q = Qc + Qd + Qw + Q_G \sin\theta \qquad \ldots\ldots 6.3.1$$

considering horizontal equilibrium -

$$Fcc = F_{st} + N - Q_G \cos\theta \qquad \ldots\ldots 6.3.2$$

and considering moment equilibrium about the centre of the tensile steel at the section of vertical loading

$$Qa = F_{cc}la - N\,(d_1 - d/2) + Qw\,\frac{c}{2} + Q_d c + Q_G z \qquad \ldots\ldots 6.3.3$$

Now, in the tests of beams reported in Chapter 4 it was observed that the width of the critical inclined crack grows sufficiently wide that the possibility of the aggregate interlock force carrying any appreciable shear can be ignored. Tests on small blocks (see Chapter 5) show that a little amount of shear can be transferred across a narrow preformed crack even in the absence of compression, but this dies down rapidly with increased crack widths.

Baumann's[7] tests have shown that for dowel action of the tensile steel to develop beyond one stirrup near the tail of the crack, a large vertical displacement is needed, which is

much larger than those occurring in normal beams. Thus if c/s is taken as the effective number of stirrups carrying shear, then the dowel action of the tensile steel is of negligible consequence in beams failing in diagonal tension and shearing. Dowel action of the tensile steel in the case of shear-compression failure will be discussed later.

Thus the three equations of equilibrium of the shear span become :

$$Q = Q_c + Q_w \quad \ldots\ldots\ldots 6.3.4$$

$$F_{cc} = F_{st} + N \quad \ldots\ldots\ldots 6.3.5$$

and $$Qa = F_{cc}la - N(d_1 - d/2) + Q_{w2}\frac{c}{} \quad \ldots\ldots\ldots 6.3.6$$

so far as diagonal tension and shearing failures are concerned.

In general these are the principal equations governing the shear failure of beams.

Equation 6.3.4 governs the failure mode if it is vertical failure e.g. shearing failure.

6.4 Development of shearing equation

Shear distress in a beam starts after the formation of shear cracks in the web. In absence of any additional component to replace the web, the failure of a beam is imminent after shear cracking with long shear span/effective depth ratios [$a/d_1 > 2.5$ for normal tensile steel ratios and concrete strengths]. At this stage if web-reinforcement is present it can cooperate to carry loads and ultimate failure is caused by shearing of the compressive zone.

Unlike shear-compression, this type of failure is governed by the conditions of vertical equilibrium. Moreover, failure of the compression zone is not preceded by crushing of the

concrete as is the case in shear compression failure.

The shear stress plays a dominant part in failure of beams by this mode. Referring to equation 6.3.4, the critical condition is given by

$$Q_{ult} = Q_c + Q_w \qquad \ldots\ldots\ldots 6.4.1$$

where Q_{ult} is the maximum load that can be carried by a beam with stirrups of long shear spans ($a/d_1 > 2.5$). To evaluate Q_{ult}, the individual magnitudes of Q_c (concrete contribution) and Q_w (stirrup contribution) must be known.

6.4.1 Evaluation of concrete's contribution in carrying shear

In order to estimate the amount of shear carried by the compressive zone of concrete, the depth of the compressive zone must be known. Then a distribution of shear stress across the compressive zone can be assumed.

The propagation of the shear crack is partly dependent on the web reinforcement ratio. As the crack propagates further, more stirrups become operative and thus the contribution of concrete is partially replaced by that of stirrups.

Shear cracks are formed from the existing flexural cracks due in a sense to the action of interlock. After this some shear is transferred across early shear cracks by interlock. Then presumably when only negligible shear is transferred by interlock, the formation of new inclined cracks is halted and the crack widths increase considerably until failure.

If failure is assumed to take place due to lack of vertical equilibrium, and the components of resistance are the concrete compression zone and web reinforcement, either of them may fail first. Generally, it is assumed that web reinforcement

attains yield stress at failure and that failure takes place when web reinforcement is unable to carry more shear, as is the concrete which has been in a critical condition from the cracking stage onward. Yielding of web reinforcement is supported by strain readings on it during this investigation (see Chapter 4).

After shear cracking, with each increment of load, the inclined crack propagates both ways. As a result, the depth of compressive zone is reduced, and the depth of concrete at the section at the head of the inclined crack is smaller than the depth of flexural neutral axis. If web reinforcement is present, the growth of the inclined crack into the compressive zone is restricted. Until today no theory has been developed to estimate analytically the actual depth of compressive zone above the crack but since there is no dominant arch action it must be close to the flexural value (see fig. 99). As already mentioned, a small reduction of the depth of compressive zone will result in a reduction of concrete contribution to shear capacity but on the other hand, with the increase in crack length, more stirrups will become operative and increase the stirrup contribution. Thus in absence of any rational approach to find out the depth of compressive zone at the head of an inclined crack it is reasonable to assume that the depth is proportional to the flexural neutral axis depth. This will mean overestimation of the concrete contribution and underestimation of the contribution of web reinforcement, but will have very little effect on overall accuracy in what are in any case partially empirical equations.

If a distribution of shear stress in the compressive zone at the time of failure is assumed, then the total shear force carried by the concrete can be evaluated.

Taylor[54] computed the shear stress distributions in the compressive zones of 6 beams above flexural cracks from strain readings on the surface of the concrete. His beams were not reinforced in shear. Fig. 91(a) shows his shear stress block. The shear stress distribution above an inclined crack may not be exactly the same as that above a flexural crack. Moreover, web reinforcement if present, will affect the distribution, but the shape of the upper part of the stress block should not be very different from that computed by Taylor.

In the presence of web reinforcement, a shear stress distribution is assumed, which is shown in fig. 91(b).

The magnitude of shear stress at the level of neutral axis follows from the following analysis of the free body diagrams of a shear span.

From the free body diagram (fig. 96) it is evident that the magnitude of shear force at the depth of neutral axis is $r_q f_{yq} b_s \cot\theta$.

$\therefore$ shear stress at the position of neutral axis,

$$= \frac{r_q f_{yq} \cot\theta\, b_s}{b_s}$$

$$= r_q f_{yq} \cot\theta$$ when b_s is the area of the shear plane.

The parabolic shear stress distribution inside the compressive zone is theoretically correct provided the distribution

of longitudinal stress is linear and not much in error for other distribution of longitudinal stresses.

Taylor's stress block though it is above a flexural crack, suggests that the maximum value of shear stress is not at the level of neutral axis but above and well inside the compressive zone. So far as the estimation of shear force carried by the compressive zone is concerned, only important point is the magnitude of maximum shear stress.

From the failure envelopes suggested by Guralnick and Walther[45,60] (fig. 93), when plotted in terms of the stresses on a vertical plane, (fig. 94) it appears that a maximum shear stress is a valid criterion for a wide range. This magnitude of maximum shear stress is little influenced by longitudinal stress within the practical range of ratios of stresses.

The magnitude of maximum shear stress for Ut/U cyl = 0.1 is approximately 0.16 U cyl or in terms of Ut,

$$q_{max} = 1.6 \text{ Ut (Guralnick's envelope)}$$

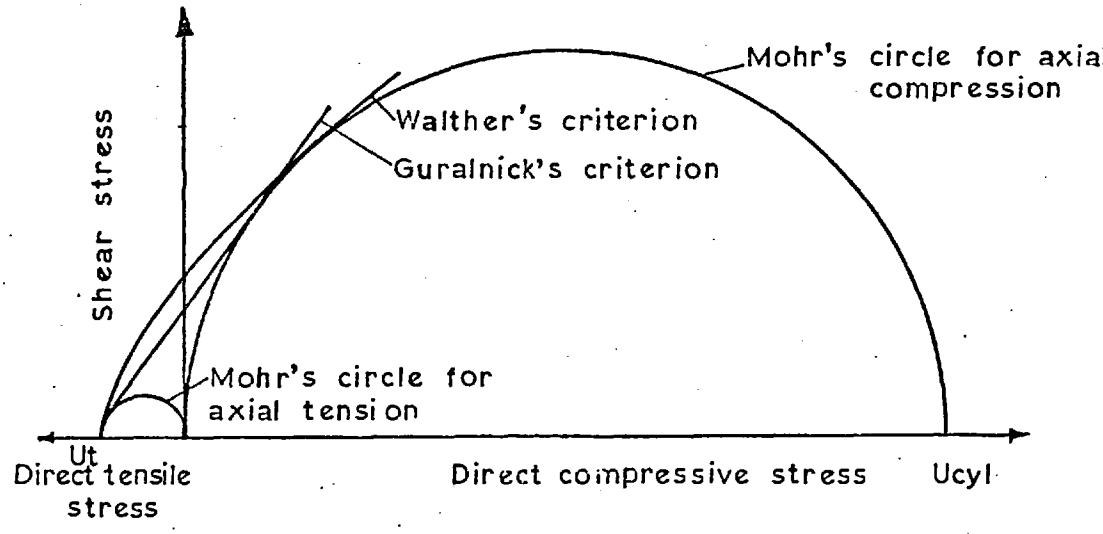
In the present theory, $Ut = 0.47 \sqrt{U \text{ cyl}}$, which means the relationship between Ut and U cyl is not linear and is varying for different concrete strengths. If calculated, the concrete of practical use, the relationship gives Ut = ($\frac{1}{8}$ to $\frac{1}{12}$) U cyl. As the ratio changes, the magnitude of q_{max} will change in terms of Ut. For simplicity, q_{max} in the present analysis is assumed to be equal to 1.6 Ut.

Thus total shear force carried by the compression zone becomes :

$$Q_c = K q_{max} b n_o d_1 ,$$

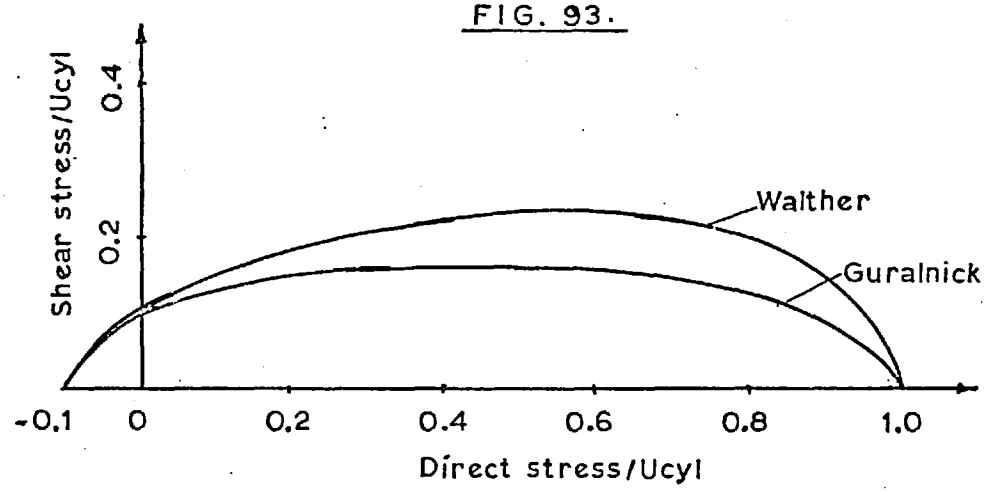
where K is a constant

$$= K_1 Ut\ b\ n_o\ d_1, \text{ where } K_1 = 1.6K.$$



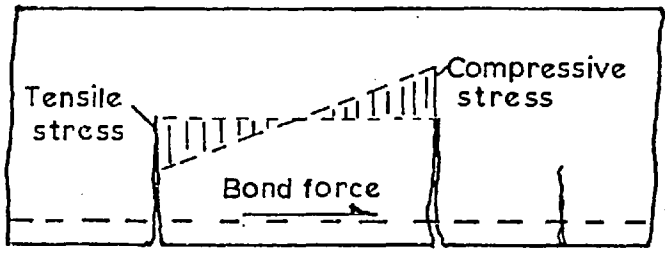
FAILURE CRITERIA EXPRESSED AS FAILURE ENVELOPES

FIG. 93.



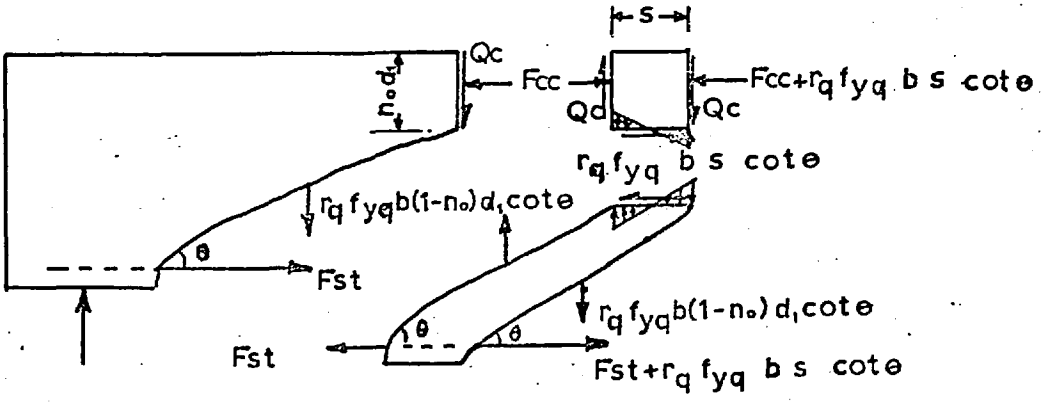
FAILURE CRITERIA EXPRESSED AS LIMITING SHEAR STRESSES (Ut/Ucyl = 0.1)

FIG. 94.

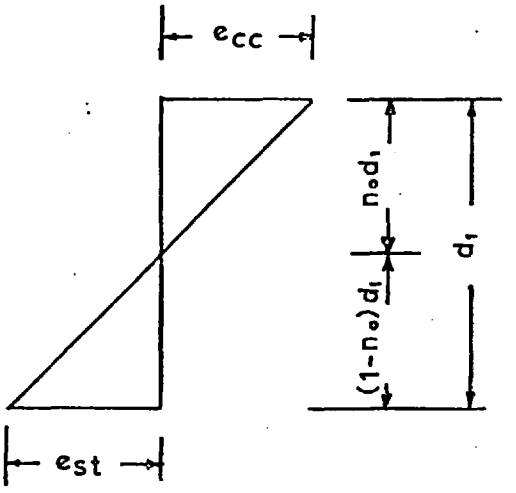


Stresses above flexural cracks due to bond force.

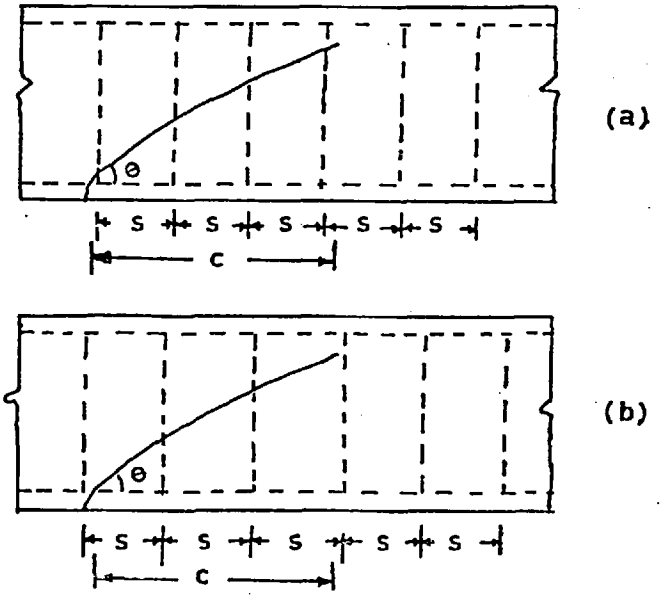
FIG. 95.



FREE-BODY DIAGRAM OF INTERNAL FORCES AFTER SHEAR CRACKING. FIG. 96



STRAIN DIAGRAM FOR FLEXURAL NEUTRAL AXIS DEPTH. FIG. 97.



STIRRUPS CROSSED BY SHEAR CRACK. FIG. 98.

The value of K_1 is evaluated for a parabolic shear stress distribution where $K = \frac{2}{3}$, and is equal to 1.067.

Upon substitution of the value of Ut, and the constant K_1, $Q_c = 1.067 \times 0.47 \sqrt{U\ cyl}\ b\ n_o\ d_1$

$$= 0.5 \sqrt{U\ cyl}\ b\ n_o\ d_1 \quad \ldots\ldots\ldots 6.4.2$$

Evaluation of the depth of flexural neutral axis (n_o) :

From fig. 97, assuming linear strain distribution

$$\frac{e_{cc}}{n_o d_1} = \frac{e_{st}}{(1-n_o)d_1}$$

$$\text{or} \quad \frac{n_o}{1-n_o} = \frac{e_{cc}}{e_{st}} \quad \ldots\ldots\ldots 6.4.3$$

Again, equating the compressive force to the tensile force at a section subject to axial compression of magnitude N,

$$rstbd_1 e_{st} E_s = n_o bd_1 \times 2.2\ U\ cyl^{\frac{2}{3}} - N \quad \ldots\ldots 6.4.4$$

in N and mm units.

The above equation is based on the assumed compressive stress block in the following section.

Eliminating e_{st} from 6.4.3 and 6.4.4 and solving for n_o,

$$n_o = \sqrt{\left(\frac{e_{cc} rst E_s}{2.2\ U\ cyl^{\frac{2}{3}}} - \frac{N/bd_1}{2.2\ U\ cyl^{\frac{2}{3}}}\right)^2 + 4 \times \frac{e_{cc} rst E_s}{2.2\ U\ cyl^{\frac{2}{3}}}} - \frac{\left(\frac{e_{cc} rst E_s}{2.2\ U\ cyl^{\frac{2}{3}}} - \frac{N/bd_1}{2.2\ U\ cyl^{\frac{2}{3}}}\right)}{2} \quad \ldots\ldots\ldots 6.4.5$$

where $e_{cc} = 0.0035$

6.4.2 Evaluation of contribution of web reinforcement

To evaluate the amount of shear carried by stirrups, the number of effective stirrups must be known. As mentioned earlier stirrups become operative only when they are crossed by a crack and so only the stirrups which are crossed by the critical inclined crack will be effective. Thus, the number of effective stirrups is calculated on this hypothesis.

If s be the spacing of stirrups along the axis of the longitudinal steel and c the horizontal projection of the inclined crack, the number of effective stirrups crossed by an inclined crack could be as high as

$$ne = \frac{c}{s} + 1$$

This is true so long as detailing and formation of the inclined crack are as shown in fig. 98(a).

Another type of crack formation and detailing as shown in fig. 98(b) suggest that the number of effective stirrups could be as low as

$$ne = \frac{c}{s} - 1$$

Thus, though $c \simeq 2s$, the actual number of stirrup crossed by the incurred crack can vary.

In general, number of effective stirrups crossed by an inclined crack is taken equal to $\frac{c}{s}$. This is considered to take account of the dowel action of the tensile steel in cases where $ne = (\frac{c}{s} - 1)$. When the tail of an inclined crack approaches a stirrup not crossed by it, dowel action of the tensile steel will stress that stirrup. As a result, if $\frac{c}{s}$ is taken as the number of effective stirrups, the dowel action of the tensile steel is also taken care of.

The length of the horizontal projection of the crack is dependent on its inclination. So far as beams with short shear spans are concerned ($a/d_1 < 2.5$), the whole shear span is crossed by the inclined crack. But the same is not true in cases of shearing failure in beams with $a/d_1 > 2.5$. From test results (see Chapter 4) the critical slope is found to be 1:2 approximately.

Thus the force carried by web reinforcement is

$$Q_w = rqfyqbc \quad \text{and} \quad c = 2(1 - n_o)d_1$$

$$= 2rqfyqb\ d_1(1-n_o) \qquad \ldots\ldots\ 6.4.6$$

Upon substitution of values of Q_c and Q_w in equation 6.4.1.

$$Q_{ult} = 0.5\ n_o\sqrt{U\ cyl}\ bd_1 + 2rqfyq\ bd_1\ (1-n_o) \qquad \ldots 6.4.7$$

in N and mm units.

$$\text{or} \quad \frac{Q_{ult}}{bd_1} = 0.5\ n_o\sqrt{U\ cyl} + 2\ rq\ fyq\ (1-n_o) \qquad \ldots\ldots\ 6.4.8$$

in N and mm units

6.5 Development of shear-compression equation

6.5.1. Introduction

When beams without shear reinforcement are tested with varying shear spans, a critical value of shear span to effective depth ratio is observed. Beams with a/d_1 ratios smaller than the critical one shows a marked difference not only in behaviour but also in strength when they fail in shear. This critical ratio of a/d_1 is about 2.5 for beams with normal percentages of tensile reinforcement. But it can be somewhat higher with increasing percentages of tensile steel[23].

Below the critical value it is generally acknowledged that shear strength increases with decreasing a/d_1 ratio, but the

degree of increase of shear strength with decreasing a/d_1 ratios is still a debatable point. If this type of failure is assumed to be governed by the rotational equilibrium condition, then this implies that the ultimate moment remains constant so long as a/d_1 is below the critical value. Another theory[23] is that the ultimate moment does not remain constant but increases to reach the flexural value when $a/d_1 = 1$.

Based on the above findings, differing design proposals have been extended to predict shear strengths of short beams with web reinforcement. Even in the estimation of stirrup forces differences of opinion exist. In fact, there are three schools of thought :

1. The ultimate moments are varying but stirrup force is remaining constant; that is, independent of the shear span[2,50,51].
2. The ultimate moment provided by the concrete above the crack, at the time of failure remains constant but the stirrup force decreases with decreasing a/d_1 ratios, on the ground that number of effective stirrups crossing the critical crack will depend on the length of the shear span (or crack length)[47].
3. The last proposal[30] allows both the concrete and stirrup forces to increase with decreasing a/d_1 ratios so that the total ultimate moment remains constant.

So far as the present analysis is concerned, the equation of rotational equilibrium will be used to predict failure loads, in this mode.

Because of the rotation taking place prior to failure, aggregate interlock forces will not be of much importance in this type of failure. On the other hand, the tensile steel can develop a considerable amount of dowel force. This is due

to the extention of the inclined crack to the edge of the support plate causing the dowel force to be resisted by compression in the concrete cover between the reinforcement and the plate rather than tension in the concrete above the steel. This action can transfer a relatively large portion of shear but a first analysis can be carried out ignoring the contribution of dowel action which can be superimposed subsequently. This will not affect the analysis at all, because the line of action of the dowel force is almost the same as that of the reaction (shear force). So the load calculated from the equation of rotational equilibrium ignoring the dowel action is (Q ult - Qd), when Qd is the shear carried by the dowel action of the tensile steel.

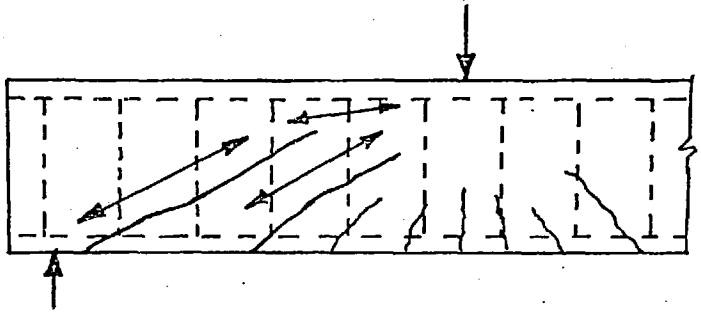
6.5.2 Assumptions for the development of shear-compression equation

1. Shear-compression failure is believed to take place due to excessive compressive stress in the concrete. The effect of shear stress can be neglected since the transverse load is carried almost entirely by inclined compression (fig. 100).

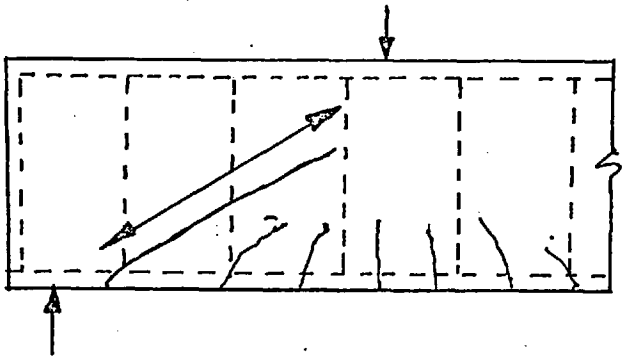
2. The possibility of any shear transfer due to aggregate interlocking is neglected.

3. The dowel action of the tensile steel is recognised and so its effect will be superimposed subject to the condition that the crack extends to the edge of the support plate and the beam is loaded and supported directly on the top and bottom respectively.

4. So far as the contribution of the web reinforcement is concerned, the problem is simple so long as c = a. If c is smaller than a, the value of c must be ascertained. An expression is developed to find the value of c/d_1.

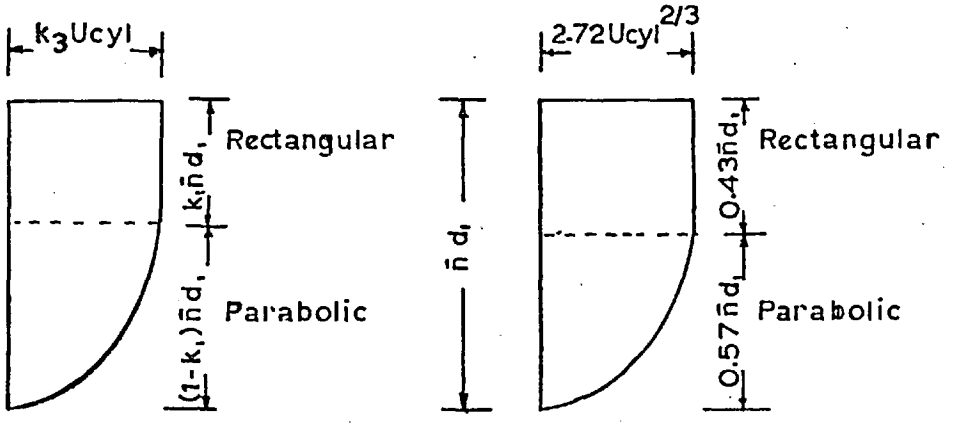


NO ARCHING IN BEAMS WITH LONG SHEAR SPANS.
($a/d_1 > 2.5$) FIG. 99.



TRANSVERSE FORCE CARRIED BY INCLINED COMPRESSION AFTER SHEAR CRACKING. ($a/d_1 < 2.5$)

FIG. 100.



CEB STRESS BLOCK (a)

ASSUMED STRESS BLOCK (b)

CONCRETE STRESS BLOCKS. FIG. 101.

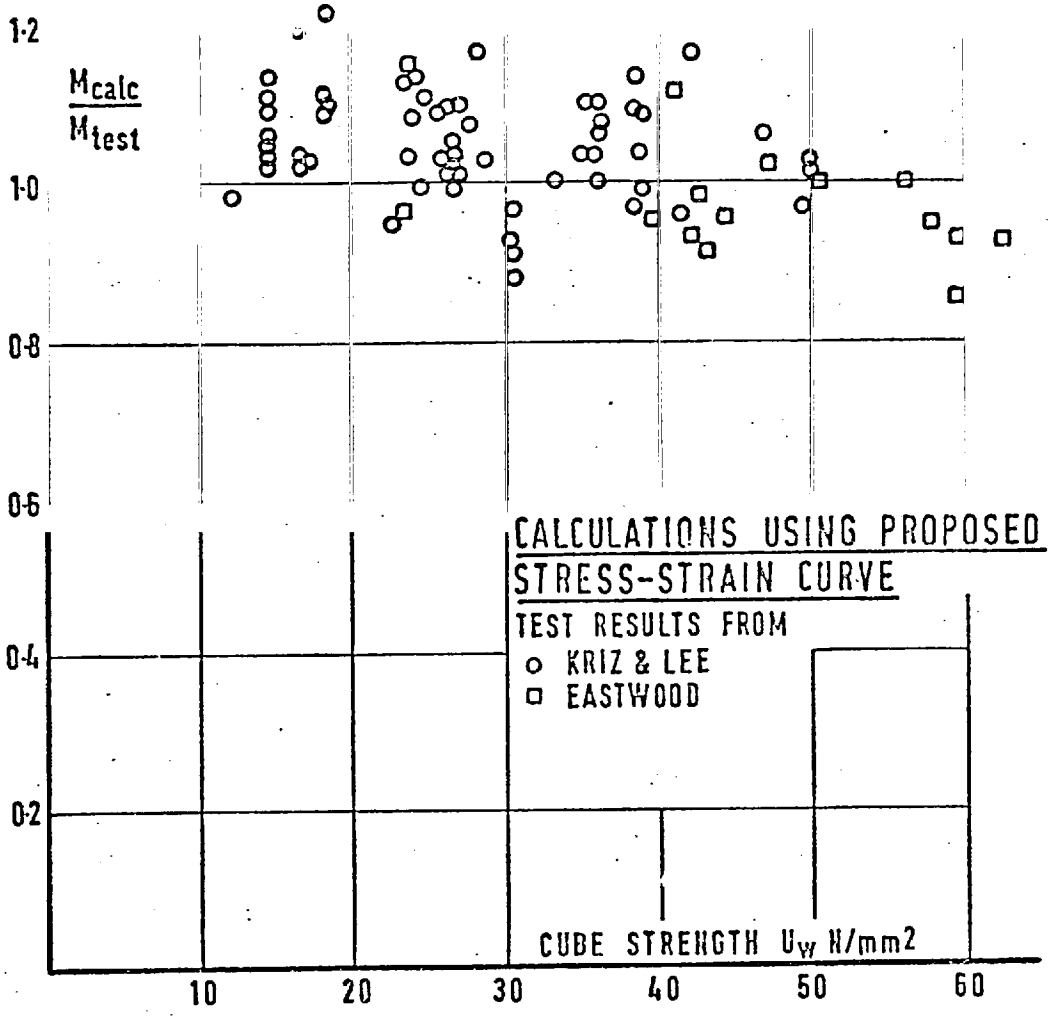
5. The compression reinforcement in a beam contributes to its moment of resistance. But the effect of compression reinforcement on the ultimate neutral axis depth cannot be estimated with any theory once shear cracking has occurred and thus its effect is not known. It is likely that due to the presence of compression steel, the neutral axis depth is reduced. On the other hand, the equivalent steel area may offset the loss and thus only be self-balancing. However, because of the complexity involved in any analysis considering the effect of compression steel, the effect is totally neglected in the following and a beam is assumed to be singly reinforced.

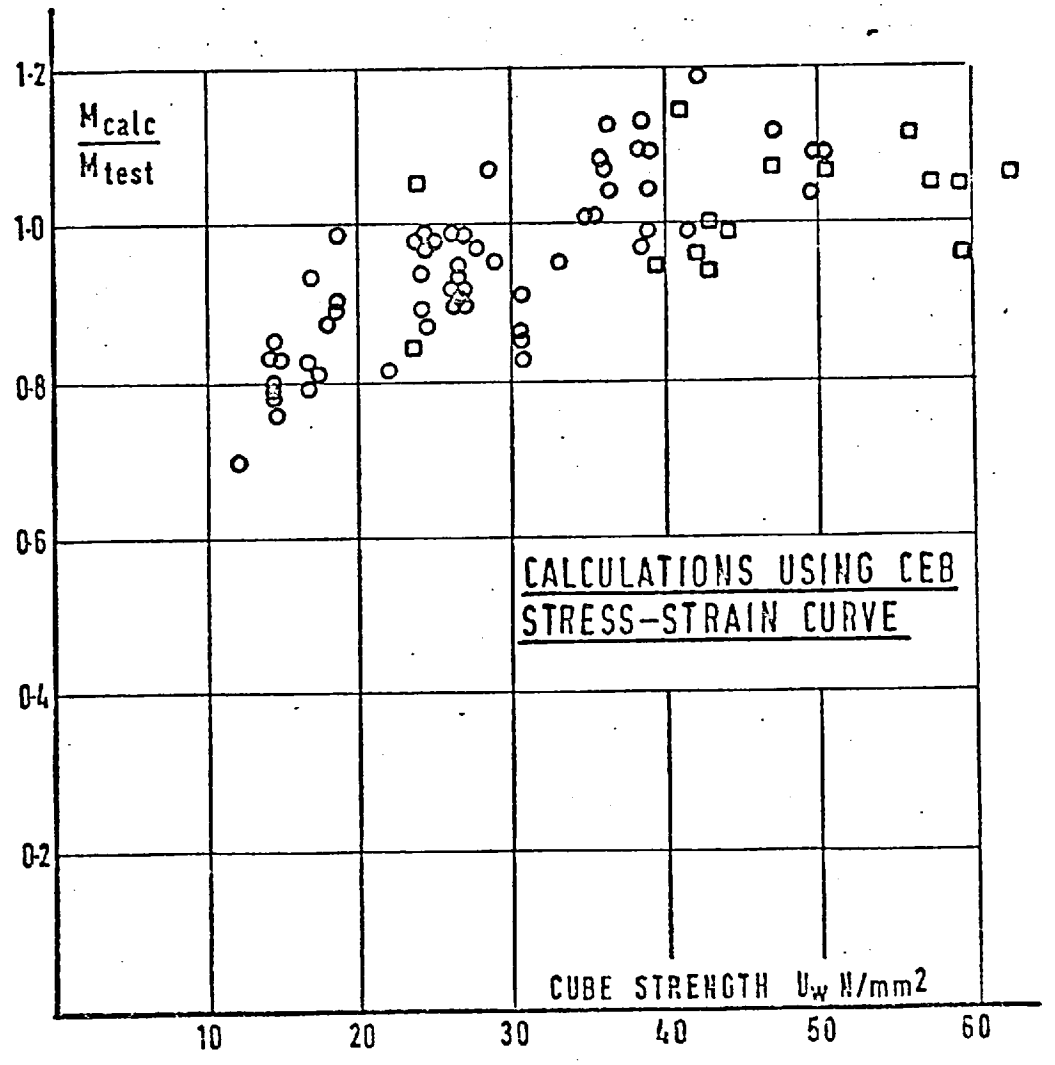
6. Failure is caused by crushing of the compression zone. Thus to calculate the horizontal force, a stress distribution is to be assumed. The assumed stress block is shown in fig. 101(b).

Where U cyl and U cyl$^{\frac{2}{3}}$ are in N/mm^2 unit and U cyl = 0.8 U_w, where U_w is cube crushing strength of 100 x 100 mm cube; also in N/mm^2.

Again most theories assume that the horizontal compressive force F_{cc} is proportional to the cylinder strength of concrete, which means shear-compression failure strength is much more dependent on cylinder strength and assume stress blocks as shown in Fig. 101 (a)

The stress block adopted is based on the consideration that stronger concretes are less ductile than weaker ones with the result that the stress block factor $F_{cc}/ b \bar{n} d_1$ U cyl is lower when U cyl is higher. This observation is supported not only by tests of simple concrete specimens but also by the values of ultimate moments recorded in tests of overreinforced beams failing in flexure. Figure 102 shows the correlations obtained with the test results of such tests by using on the one hand the proposed





ULTIMATE MOMENTS OF OVER-REINFORCED BEAMS FAILING IN FLEXURE (Ref. 62).

FIGURE 102

stress block and on the other the CEB version.

6.5.3 Solution for ultimate neutral axis depth

From the observed behaviour of the beams tested (see Chapter 4), it is evident that the depth of neutral axis prior to failure is very much less than the flexural neutral axis depth. This reduction of the neutral axis depth is more important in the case of beams failing in shear-compression already described in Chapter 2. Another important factor in the behaviour of short beams is that arch action predominates in carrying the load after the formation of the inclined crack. In other words, when the beam action is destroyed, the arch action continues to carry further load.

Considering these factors a model of a rectangular beam is adopted for analysis. In it the influence of web reinforcement on the depth of the neutral axis is taken into account considering the force carried by the reinforcement to be known and assuming it to act in the middle of the shear span when $a = c$. In the cases when $a > c$, the stirrup force is assumed to act at the middle of the crack length.

If a beam with two point loads is considered the flexural cracks in between the two point loads do not rise beyond the flexural neutral axis (see beams B8, B9, B10 etc.) and as a result the stiffness of the part of beam between the two loads is much greater than that of the section at the head of the inclined crack, and thus only conditions in the shear spans need be considered. Thus the loading system becomes a beam with a single point load as in fig. 103.

Although the slope of the inclined crack in fact, is not truly uniform for simplicity of analysis it is assumed to be

uniform and it can be seen later that it hardly affects the analysis.

In cases when the inclined crack does not extend over the whole of the shear span, then l is not equal to 2a, but is equal to 2c.

The above model is one time statically indeterminate, and the steel force, Fst can be treated as the unknown redundant action.

If the crack does not extend over the whole of the shear span, the beam model will be as shown in fig. 103.

Properties of the sections

E_{ca} = Modulus of elasticity of concrete at section a-a (at support section)

Ia = Second moment of area of the section a-a

E_{cb} = Modulus of elasticity of concrete at section b-b (at a distance of a/2 from the support).

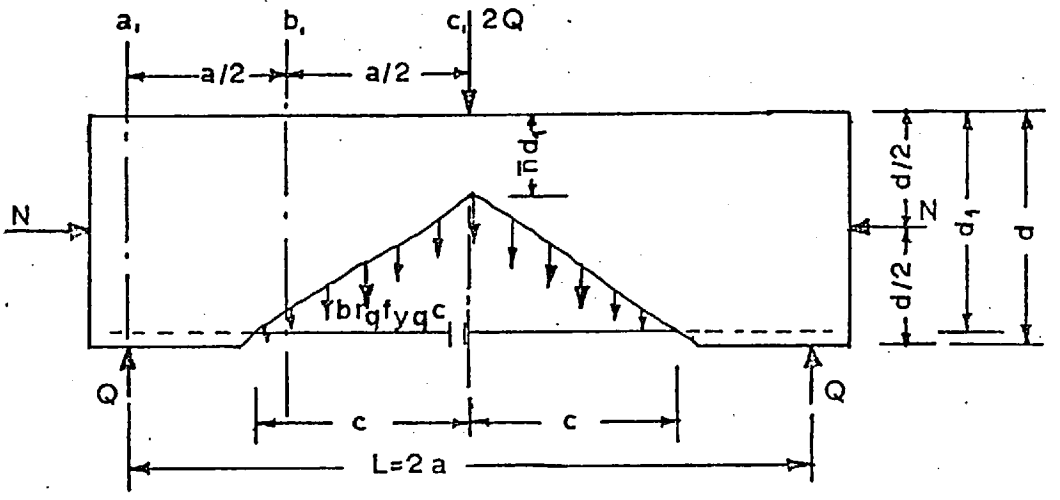
I_b = Second moment of area of the section b-b.

E_{cx} = Modulus of elasticity of concrete at the loaded section - $c_1 - c_1$

I_x = Second moment of area of the section $c_1 - c_1$

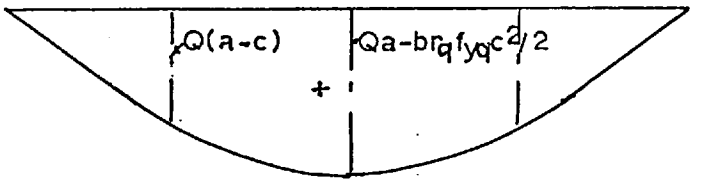
The particular solution diagrams and the flexibility coefficient diagrams are given in figs. 104 and 105 respectively.

Using Simpson's rule and neglecting the axial force energy of the concrete,

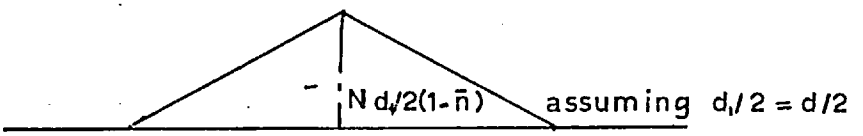


STATICALLY DETERMINATE MODEL BEAM.

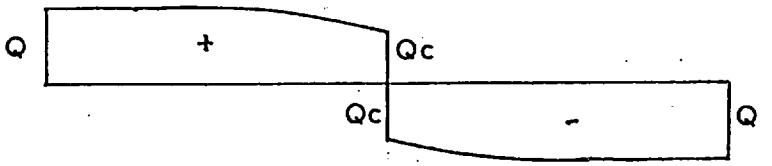
FIG. 103.



m_{oQ} DIAGRAM



m_{oN} DIAGRAM



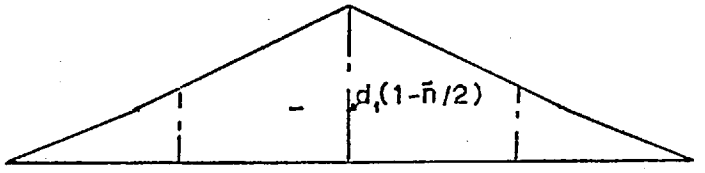
s_{oQ} DIAGRAM



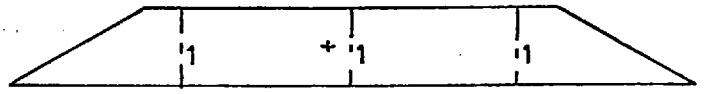
n_{oN} DIAGRAM (IN CONCRETE)

PARTICULAR SOLUTION DIAGRAMS

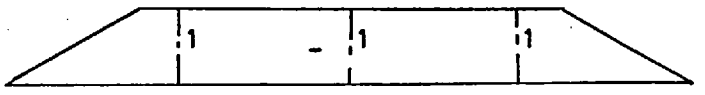
FIG. 104.



m_1 DIAGRAM

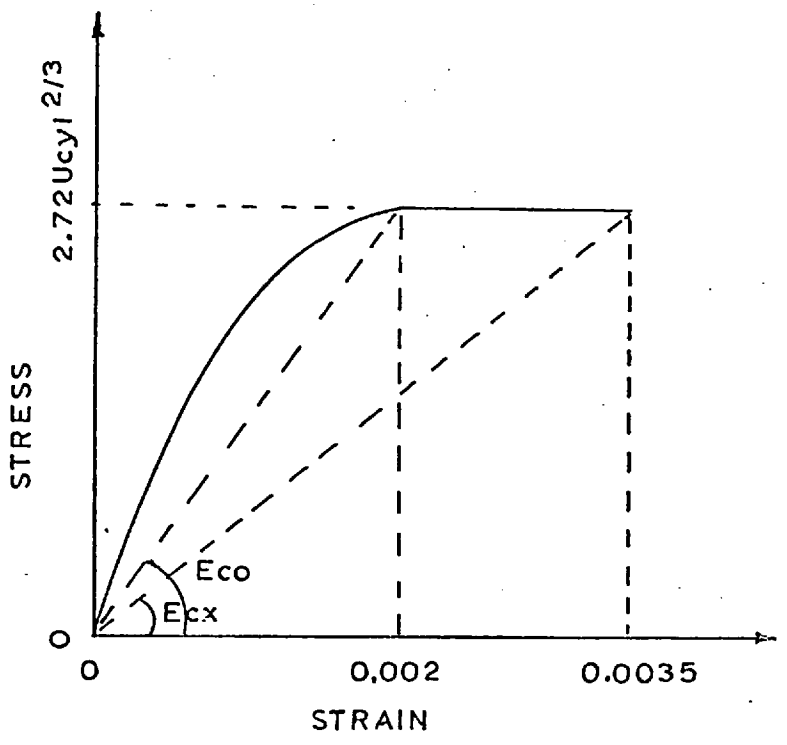


n_1 DIAGRAM (IN TENSILE STEEL)



n_1 DIAGRAM (IN CONCRETE)

FLEXIBILITY COEFFICIENT DIAGRAMS
FIG. 105.



STRESS STRAIN CURVE USED FOR ESTIMATION OF Ec VALUE AT ULTIMATE STAGE. FIG. 106.

the flexibility coefficient :

$$f_{11} = \frac{1}{3} \times \frac{a}{2} \left[2 \left\{ \frac{d_1}{2} \times \frac{d_1}{2} \times \frac{1}{I_a E_{ca}} + 4 \frac{d_1^2}{4^2} (3-\bar{n})^2 \times \frac{1}{E_{cb} I_b} + \frac{d_1^2 (1-\frac{\bar{n}}{2})^2}{E_{cx} I_x} \right\} \right] + E_s \frac{2c}{A_{st}}$$

$$\text{or} \quad f_{11} = \frac{a}{12} \left[\frac{d_1^2}{I_a E_{ca}} + \frac{d_1^2 (3-\bar{n})^2}{E_{cb} I_b} + \frac{4 d_1^2 (1-\frac{\bar{n}}{2})^2}{E_{cx} I_x} \right] + \frac{2c}{E_s A_{st}}$$

Now, in the right hand side of the above equation the first two terms are negligible compared to the third and fourth terms, because I_a and I_b are much greater than I_x, and hence, for all practical purposes, those two terms can be neglected.

Thus

$$f_{11} = \frac{a}{3} \times \frac{d_1^2 (1 - \frac{\bar{n}}{2})^2}{E_{cx} I_x} + \frac{2c}{E s r_{st} b d_1}$$

$$= \frac{a}{3} \times \frac{d_1^2 (1 - \frac{\bar{n}}{2})^2}{E_{cx} \times \frac{1}{12} b d_1^3 \bar{n}^3} + \frac{2c}{E_s r_{st} b d_1}$$

where $I_x = \frac{1}{12} b d_1^3 \bar{n}^3$

$$= \frac{4a (1 - \frac{\bar{n}}{2})^2}{E_{cx} b d_1 \bar{n}^3} + \frac{2c}{E_s r_{st} b d_1} \qquad \ldots\ldots 6.5.1$$

Similarly,

$$u_{10} = -\frac{1}{3} \times \frac{a}{2} \left[2 \left\{ 4 \frac{d_1}{4} \times (3-\bar{n}) (Q \frac{a}{2} - b r_q f_{yq} \frac{c^2}{2}) \times \frac{1}{I_b E_{cb}} + d_1 (1 - \frac{\bar{n}}{2}) \frac{Q c - b r_q f_{yq} \frac{c^2}{2}}{E_{cx} I_x} \right\} \right]$$

$$+\tfrac{1}{3} \times \frac{a}{2}\left[2\left\{\frac{4 \times \frac{d_1(3-\bar{n})}{4} \quad \frac{Nd_1}{4}(1-\bar{n})}{E_{cb}\, I_b} + \frac{d_1(1-\frac{\bar{n}}{2}) \quad \frac{Nd_1}{2}(1-\bar{n})}{E_{cx}\, I_x}\right\}\right]$$

Again neglecting the first two terms inside the brackets,

$$u_{10} = \tfrac{1}{3} \times a \times \frac{1}{E_{cx} I_x} \times d_1(1-\tfrac{\bar{n}}{2})(Qa - br_q f_{yq} \tfrac{c^2}{2}) + \frac{a \times \frac{Nd_1^2}{2}(1-\tfrac{\bar{n}}{2})(1-\bar{n})}{3\, E_{cx}\, I_x}$$

$$\text{or } u_{10} = -\frac{a(1-\frac{\bar{n}}{2})}{3\, E_{cx}\, I_x}\left[d_1\,(Qa - br_q f_{yq}\tfrac{c^2}{2}) - \frac{Nd_1^2}{2}(1-\bar{n})\right]$$

substituting value of $I_x = \frac{1}{12}\, bd_1^3 \bar{n}^3$,

$$u_{10} = -\frac{a(1-\frac{\bar{n}}{2}) \times 12}{3\, Ec \times bd_1^3 \bar{n}^3}\left[d_1(Qa - br_q f_{yq}\tfrac{c^2}{2}) - \frac{Nd_1^2}{2}(1-\bar{n})\right]$$

$$u_{10} = -\frac{4a\,(1-\frac{\bar{n}}{2})}{Ec \times bd_1\bar{n}^3}\left[Q\frac{a}{d_1} - \frac{Q_w}{2}\frac{c}{d_1} - \frac{N}{2}(1-\bar{n})\right] \qquad \ldots.6.5.2$$

where $Q_w = br_q f_{yq} c$

$$\text{Thus } F_{st} = -\frac{u_{10}}{f_{11}}$$

$$\therefore\ F_{st} = \frac{\frac{4a\,(1-\frac{\bar{n}}{2})}{E_{cx} bd_1\bar{n}^2}\left[Q\frac{a}{d_1} - \frac{Q_w}{2}\frac{c}{d_1} - \frac{N}{2}(1-\bar{n})\right]}{\frac{4a(1-\frac{\bar{n}}{2})^2}{E_{cx} bd_1\bar{n}^3} + \frac{2c}{E_s r_{st} bd_1}}$$

$$\text{or } F_{st} = \frac{\frac{(1-\frac{\bar{n}}{2})}{\bar{n}^3}\left[Q\frac{a}{d_1} - \frac{Q_w}{2}\frac{c}{d_1} - \frac{N}{2}(1-\bar{n})\right]}{\frac{(1-\frac{\bar{n}}{2})^2}{\bar{n}^3} + \frac{c/a}{2rst\,\frac{E_s}{E_{cx}}}} \qquad \ldots..6.5.3$$

Equating for horizontal equilibrium -

$F_{st} + N = F_{cc}$ - and $F_{cc} = 2.2\ U\ cyl^{\frac{2}{3}}\ \bar{n}\ bd_1$ from the assumed stress block

$$\frac{\frac{1-\frac{\bar{n}}{2}}{\bar{n}^3}\left[Q\frac{a}{d_1} - \frac{Q_w}{2}\frac{c}{d_1} - \frac{N}{2}(1-\bar{n})\right]}{\frac{(1-\frac{n}{2})^2}{\bar{n}^3} + \frac{c/a}{2r_{st}\frac{E_s}{E_{cx}}}} + N = F_{cc} = 2.2\ U\ cyl^{\frac{2}{3}}\bar{n}\ bd_1$$

$$\text{or } \frac{\frac{1-\frac{\bar{n}}{2}}{\bar{n}^3}\left[Q\frac{a}{d_1} - \frac{Q_w}{2}x\frac{c}{d_1} - \frac{N}{2}(1-\bar{n})\right]}{\frac{(1-\frac{\bar{n}}{2})^2}{\bar{n}^3} + \frac{c/a}{2\,r_{st}\frac{E_s}{E_{cx}}}} = 2.2\ U\ cyl^{\frac{2}{3}}\bar{n}\ bd_1 - N$$

$$\text{or } \frac{Q\frac{a}{d_1} - \frac{Q_w}{2}\frac{c}{d_1} - \frac{N}{2}(1-\bar{n})}{2.2\ U\ cyl^{\frac{2}{3}}\bar{n}\ bd_1 - N} = (1-\frac{\bar{n}}{2}) + \frac{c/a\,\bar{n}^3}{2\,r_{st}\frac{E_s}{E_{cx}}(1-\frac{\bar{n}}{2})}$$

$$\text{or } \frac{\frac{1}{d_1}\left[Qa - \frac{Q_w}{2}c - \frac{N}{2}(1-\bar{n})d_1\right] - 2.2\ U\ cyl^{\frac{2}{3}}\bar{n}bd_1 + N}{2.2\ U\ cyl^{\frac{2}{3}}\bar{n}\ bd_1 - N} +$$

$$\frac{2.2\ U\ cyl^{\frac{2}{3}}\bar{n}\ bd_1\frac{\bar{n}}{2} - N\frac{\bar{n}}{2}}{2.2\ U\ cyl^{\frac{2}{3}}\bar{n}\ bd_1 - N} = \frac{c/a\,\bar{n}^3}{2r_{st}\frac{E_s}{E_{cx}}(1-\frac{\bar{n}}{2})}$$

$$\text{or } \frac{1}{d_1} x \left(\frac{Qa - \frac{Q_w}{2}c - \frac{N}{2}d_1 - 2.2\ U\ cyl^{\frac{2}{3}}\bar{n}\ bd_1 x\ d_1 + Nd_1}{2.2\ U\ cyl^{\frac{2}{3}}\bar{n}\ bd_1 - N}\right.$$

$$\left. + \frac{2.2\ U\ cyl^{\frac{2}{3}}\bar{n}\ bd_1 x\frac{\bar{n}}{2}d_1}{2.2\ U\ cyl^{\frac{2}{3}}\bar{n}\ bd_1 - N}\right) = \frac{c/a\,\bar{n}^3}{2r_{st}\frac{E_s}{E_{cx}}(1-\frac{\bar{n}}{2})}$$

$$\text{or } \frac{1}{d_1} \times \frac{Qa - Qw\,\frac{c}{2} + \frac{N}{2}d_1 - 2.2\ U\ cyl^{\frac{2}{3}}\ \bar{n}\ bd_1 \times d_1\left(1 - \frac{\bar{n}}{2}\right)}{2.2\ U\ cyl^{\frac{2}{3}}\ \bar{n}\ bd_1 - N}$$

$$= \frac{c/a\ \bar{n}^3}{2\ r_{st}\frac{E_s}{E_{cx}}\left(1 - \frac{\bar{n}}{2}\right)}$$

From the equation of rotational equilibrium

$$Qa - Q_w\frac{c}{2} + \frac{N}{2}\ d_1 \simeq 2.2\ U\ cyl^{\frac{2}{3}}\ \bar{n}\ bd_1\ la \quad \text{if } \frac{d_1}{2} = d_1 - \frac{d}{2}$$

$$\therefore \frac{1}{d_1} \times \frac{2.2\ U\ cyl^{\frac{2}{3}}\ \bar{n}\ bd_1\left[la - d_1\left(1-\frac{\bar{n}}{2}\right)\right]}{2.2\ U\ cyl^{\frac{2}{3}}\ \bar{n}\ bd_1 - N} = \frac{c/a\ \bar{n}^3}{2r_{st}\frac{E_s}{E_{cx}}\left(1-\frac{\bar{n}}{2}\right)}$$

$$\text{or } \frac{2.2\ U\ cyl^{\frac{2}{3}}\ \bar{n}\ bd_1\left[\frac{la}{d_1} - 1 + \frac{\bar{n}}{2}\right]}{2.2\ U\ cyl^{\frac{2}{3}}\ \bar{n}\ bd_1 - N} = \frac{\bar{n}^3 \times c/a}{2r_{st}\frac{E_s}{E_{cx}}\left(1-\frac{\bar{n}}{2}\right)}$$

From the assumed stress block, $\frac{la}{d_1} = 1 - 0.4\ \bar{n}$

$$\therefore \frac{la}{d_1} - 1 + \frac{\bar{n}}{2} = 1 - 0.4\ \bar{n} - 1 + 0.5\ \bar{n} = 0.1\ \bar{n}$$

$$\therefore \frac{2.2\ U\ cyl^{\frac{2}{3}}\ bd_1 \times \bar{n}/10}{2.2\ U\ cyl^{\frac{2}{3}}\ \bar{n}\ bd_1 - N} = \frac{\bar{n}^2\ c/a}{2\ r_{st}\frac{E_s}{E_{cx}}\left(1-\frac{\bar{n}}{2}\right)}$$

$$\text{or } \frac{2.2\ U\ cyl^{\frac{2}{3}}\ \bar{n}\ bd_1 - N}{2.2\ U\ cyl^{\frac{2}{3}}\ \bar{n}\ bd_1 \times \frac{1}{10}} = \frac{2r_{st}\frac{E_s}{E_{cx}}\left(1 - \frac{\bar{n}}{2}\right)}{\bar{n}^2\ c/a}$$

$$\text{or} \quad 10 \left[1 - \frac{N}{2.2\ U\ cyl^{\frac{2}{3}}\ \bar{n}\ bd_1} \right] = \frac{2 r_{st} \frac{E_s}{E_{cx}} \left(1 - \frac{\bar{n}}{2}\right)}{\bar{n}^2\ c/a}$$

$$\text{or} \quad \bar{n}^2 = \frac{0.2\ r_{st} \frac{E_s}{E_{cx}} \left(1 - \frac{\bar{n}}{2}\right)}{c/a \left[1 - \frac{N}{2.2\ U\ cyl^{\frac{2}{3}}\ \bar{n}\ bd_1} \right]}$$

assuming $\left(1 - \frac{\bar{n}}{2}\right) \simeq 0.9$ since $\bar{n}$ is very small

$$\bar{n} = \sqrt{0.18\ r_{st} \frac{E_s}{E_{cx}} \frac{a}{c} \times \frac{1}{1 - \frac{N/bd_1}{2.2\ U\ cyl^{\frac{2}{3}} \bar{n}}}}$$

$$= \bar{n}_o \sqrt{\frac{1}{1 - \frac{N/bd_1}{2.2\ U\ cyl^{\frac{2}{3}} \bar{n}}}}, \quad \text{where } \bar{n}_o = \sqrt{0.18\ r_{st} \frac{E_s}{E_{cx}}\ a/c}$$

$$\text{or} \quad \bar{n} \sqrt{1 - \frac{N/bd_1}{2.2\ U\ cyl^{\frac{2}{3}} \bar{n}}} = \bar{n}_o$$

For small values of $\left(\frac{N/bd_1}{2.2\ U\ cyl^{\frac{2}{3}} \bar{n}}\right)$

$$\sqrt{1 - \frac{N/bd_1}{2.2\ U\ cyl^{\frac{2}{3}} \bar{n}}} = 1 - \tfrac{1}{2} \times \frac{N/bd_1}{2.2\ U\ cyl^{\frac{2}{3}}\ \bar{n}}$$

$$\text{Therefore,} \quad \bar{n}_c = \bar{n} - \tfrac{1}{2} \times \frac{N/bd_1}{2.2\ U\ cyl^{\frac{2}{3}}}$$

$$\text{giving} \quad \bar{n} = \bar{n}_o + \tfrac{1}{2} \times \frac{N/bd_1}{2.2\ U\ cyl^{\frac{2}{3}}} \qquad \ldots\ldots\ldots 6.5.4$$

Since the modulus of elasticity of concrete is varying, and at the ultimate stage is much smaller than at earlier stages, and considering the secant modulus at a strain of 0.002 (an "elastic" one) and at strain of 0.0035. (fig. 105)

E_{cx} at ultimate stage

$$= \frac{2.72\ U\ cyl^{\frac{2}{3}}}{0.0035} = \frac{2.72\ U\ cyl^{\frac{2}{3}}}{0.002} \times \frac{0.002}{0.0035} = E_{co} \times 0.571$$

Substituting value of E_{cx}

$$\bar{n} = \sqrt{\frac{0.18}{0.571}\ r_{st}\ \frac{E_s}{E_{co}} \times \frac{a}{c}} + \frac{1}{2} \times \frac{N/bd_1}{2.2\ U\ cyl^{\frac{2}{3}}}$$

or $$\bar{n} = \sqrt{0.315\ r_{st} m \times \frac{a}{c}} + \frac{1}{2} \times \frac{N/bd_1}{2.2\ U\ cyl^{\frac{2}{3}}} \qquad \ldots\ldots\ldots 6.5.5$$

where $m = \frac{E_s}{E_{co}} = 5 + \frac{70}{U\ cyl}$, U cyl in N and mm units

In the above expression, unless the value of c is known $\bar{n}$ cannot be estimated. So in order to find an expression for c, the equation of moment equilibrium will be differentiated with respect to 'c' so that the plane of weakest resistance is ascertained.

The equation of moment equilibrium gives -

$M = 2.2\ U\ cyl^{\frac{2}{3}}\ \bar{n}\ bd_1 la + brq\ f_{yq}\ \frac{c^2}{2} - N(d_1 - \frac{d}{2})$, considering moments about the centre of tensile steel below the point load.

Substituting the value of $\bar{n}$.

$$M = 2.2\ U\ cyl^{\frac{2}{3}} \left[\sqrt{.315\ rst\ \frac{E_s}{E_{co}} \times \frac{a}{c}} + \frac{1}{2} \times \frac{N/bd_1}{2.2\ U\ cyl^{\frac{2}{3}}} \right]$$

$$bd_1 la + brqfyq\ \frac{c^2}{2} - N(d_1 - \frac{d}{2})$$

Assuming the lever arm to be independent of 'e' and differentiating the moment with respect to 'c' and equating the derivative to zero for minimum strength -

$$\frac{dM}{dc} = 2.2\ U\ cyl^{\frac{2}{3}}\left[\sqrt{.315\ rst\ \frac{E_s}{E_{co}}}\ ax\ (-\tfrac{1}{2}c^{-\frac{3}{2}})\right] bd_1 la + brqfyqc = 0$$

$$\text{or}\quad 2.2\ U\ cyl^{\frac{2}{3}}\ bd_1 la\ \sqrt{.315\ rst\ \frac{E_s}{E_{co}}}\ a\ x\ \tfrac{1}{2}\ x\ c^{-\frac{3}{2}} = brqfyq\ c.$$

Multiplying both orders by $c^{3/2}$ and cancelling b from both sides

$$2.2\ U\ cyl^{\frac{2}{3}}\ d_1 la\ \sqrt{.315\ rst\ \frac{E_s}{E_{co}}}\ a\ x\ \tfrac{1}{2} = rqfyq\ c^{5/2}$$

$$\therefore\ c^{5/2} = \frac{2.2\ U\ cyl^{\frac{2}{3}}\ d_1 la\ \sqrt{.315\ rst\ \frac{E_s}{E_{co}}}\ a}{2\ rqfyq}$$

$$\text{or}\ \left(\frac{c}{d_1}\right)^{5/2} = \frac{2.2\ U\ cyl^{\frac{2}{3}}\ \frac{la}{d_1}\ x\ \sqrt{.315\ rst\ \frac{E_s}{E_{co}}}\ x\ \frac{a}{d_1}}{2\ rq\ fyq}$$

diving both sides of the equation by $d_1^{5/2}$.

$$\therefore\ \frac{c}{d_1} = \frac{1}{0.4}\sqrt{\frac{2.2\ U\ cyl^{\frac{2}{3}}\ \frac{la}{d_1}\ \sqrt{.315\ rst\ \frac{E_s}{E_{co}}}\ x\ \frac{a}{d_1}}{2\ rqfyq}} \qquad \ldots 6.5.6$$

The increase of neutral axis depth due to axial load predicted by equation 6.5.5 is inadequate in comparison with the results of beams tested during this investigation. As a result it is found that the ultimate loads predicted by the above equation of neutral axis depth are conservative with axial

compression while beams with axial tension are found to be unsafe.

In fact, with the application of the axial tension - vertical cracks form along the beam at certain intervals. These cracks definitely reduce the stiffness of the beam. In a section, when a vertical crack due to tension is fully formed, the only means of shear transfer across the crack are due to interlock and dowel action of tensile steel.

On the other hand, beams with axial compression are stiffer and without any vertical cracks.

So equation 6.5.5 is modified empirically so as to fit the test results.

Thus the equation of neutral axis depth taking the effect of axial load into account becomes :

$$\bar{n} = \sqrt{0.315\ rst\ \frac{E_s}{E_{co}}\ \frac{a}{c}} + \frac{N/bd_1}{2.2\ U\ cyl^{\frac{2}{3}}} \qquad \ldots\ 6.5.7$$

If the crack extends over the whole shear span, then c = a, in that case

$$\bar{n} = \sqrt{0.315\ rst\ \frac{E_s}{E_{co}}} + \frac{N/bd_1}{2.2\ U\ cyl^{\frac{2}{3}}} \qquad \ldots\ 6.5.8$$

when N is +ve for compression

6.6 Shear carried by dowel action of tensile steel

There is sufficient evidence that dowel action of the tensile steel can be significant if the distance between the

tail of the diagonal crack and the support is very small.

Baumann[7] carried out a large number of tests which are described in Chapter 5. His dowel cracking equation

$$Qd_{cr} = K\ Ut\ bnlc$$

based on test results cannot be accepted for the prediction of maximum dowel forces when the inclined crack extends to the support plate, which is the case in beams with short shear spans. However, his values of the bearing length lc can be taken to be applicable.

When shear compression failure takes place, the tail of the inclined crack extends to the face of the support plate. Thus the reaction from the support and the downward force due to the dowel action cause the concrete inbetween to crush and not to fail in tension. (see fig. 108). The bearing area = nØlc,

where lc = is the bearing length
n = number of bars in one layer
Ø = diameter of bars.

After evaluation of Q neglecting the dowel force, the ultimate load can be found out by adding the dowel force

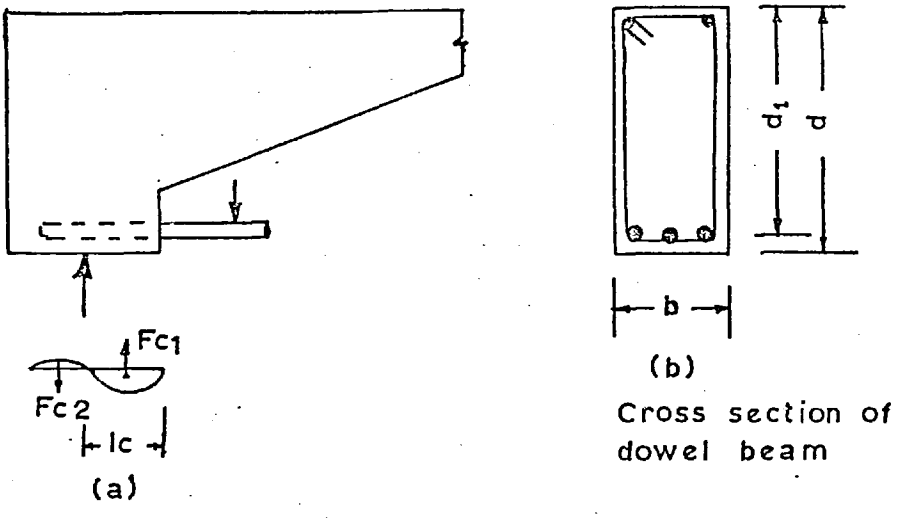
i.e. $Q\ ult = Q_{sc} + Qd.$

The compressive stress due to dowel force on the concrete

$$= \frac{Qd}{n\emptyset lc} \qquad \text{.....6.6.1}$$

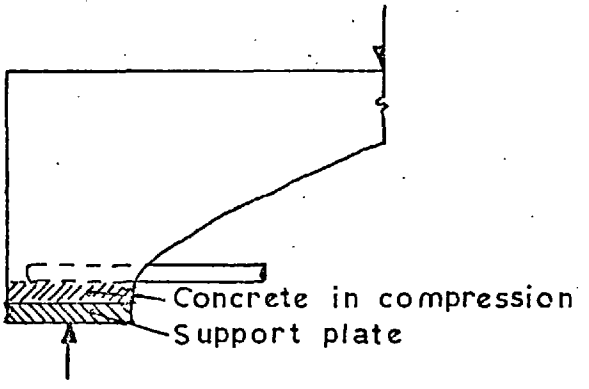
Assuming at the time of failure, the compressive stress in the concrete is equal to K Uw,

where K is constant,

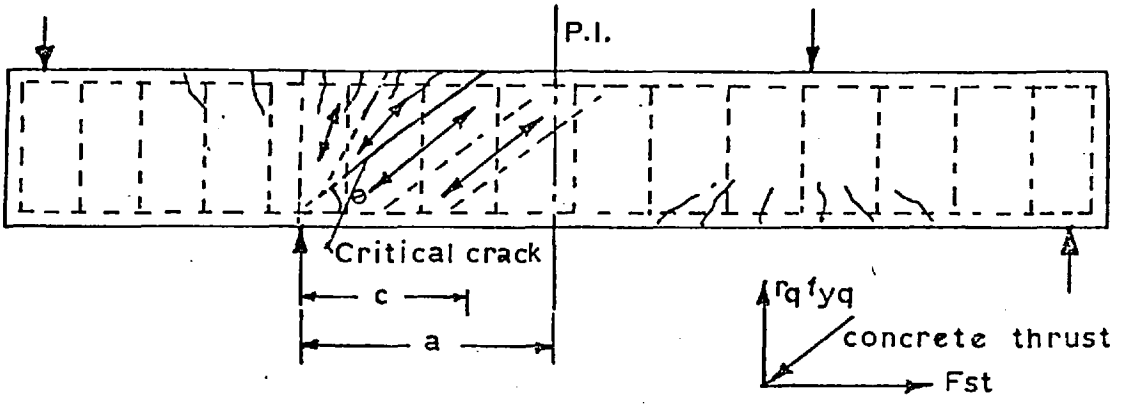


STRESS IN CONCRETE DUE TO DOWEL SHEAR AT THE LEVEL OF TENSILE STEEL (BAUMANN)

FIG. 107.



DOWEL ACTION IN SHORT BEAMS. FIG. 108.



INTERNAL FORCES OF A BEAM WITH STIRRUPS AFTER CRACKED IN FLEXURE AND SHEAR. FIG. 109.

then $\frac{Qd}{n\emptyset lc} = K\ Uw$

or $Qd = K\ Uw\ n\ \emptyset\ lc$ 6.6.2

Substituting the value of $lc = 6.6\ \emptyset/Uw^{\frac{1}{3}}$, (after Baumann)

$Qd = K\ Uw\ n\ \emptyset\ x\ 6.6\ \emptyset/Uw^{\frac{1}{3}}$

$\frac{Qd}{bd_1} = K_1\ U_w^{\frac{2}{3}}\ n\ \emptyset^2/bd_1$, where K_1 is a constant

$= K_2\ U\ cyl^{\frac{2}{3}}\ n\ \emptyset^2/bd_1$ where K_2 is a new constant,

and $U\ cyl = 0.8\ Uw$.

or $\frac{Qd}{bd_1} = K_2\ U\ cyl^{\frac{2}{3}}\ x\ \frac{A_{st}}{bd_1}\ x\ \frac{4}{\pi}$

$= K_3\ U\ cyl^{\frac{2}{3}}\ rst$

where K_3 is a constant and is found to be 5.0 in N and mm units (from beam tests by considering differences between Q ult and Q sc) giving

$Qd/bd_1 = 5.0\ rst\ U\ cyl^{\frac{2}{3}}$ 6.6.3

Equation 6.6.3 is applicable for a single layer of reinforcement and only in case of shear compression failure where the inclined crack extends to the edge of the support plate. The members must be supported on the bottom faces.

An estimate of Qd with reinforcement arranged in more than one layer can be made provided the bearing length lc is modified according to Baumann's equation.

After evaluation of Qd/bd_1, the strength of a beam failing in shear compression with the inclined crack extending over the whole shear span, can be obtained from the following equation

$$Q_{ult} = Q_{sc} + Qd$$

or $$Q_{ult}/bd_1 = 2.2\, U_{cyl}^{\frac{2}{3}} \bar{n} \frac{la}{a} + r_q f_{yq} \frac{e^2}{2d_1 a} - N/bd_1 \frac{(d_1 - \frac{d}{2})}{a} + \frac{Qd}{bd_1} \quad \ldots\ldots\ldots\ldots 6.6.4$$

Equation 6.6.4 is applicable to beams failing in shear compression subject to axial load and with or without web reinforcement.

If the inclined crack does not extend to the support even though the failure is by shear compression the above analysis for dowel force will not be valid. As mentioned earlier, in that case, the over estimation of the effect of web reinforcement will account for the dowel force.

6.7 Transition from diagonal tension or shearing failure to shear compression failure

a) Diagonal tension failure to shear compression

Equation 6.6.4 is based on the assumption that arching must take place in beams; and arching becomes important after the breakdown of beam action i.e. after shear cracking. In order to predict shear strength of a beam, the first step is to calculate its shear cracking load applying equations 6.2.10

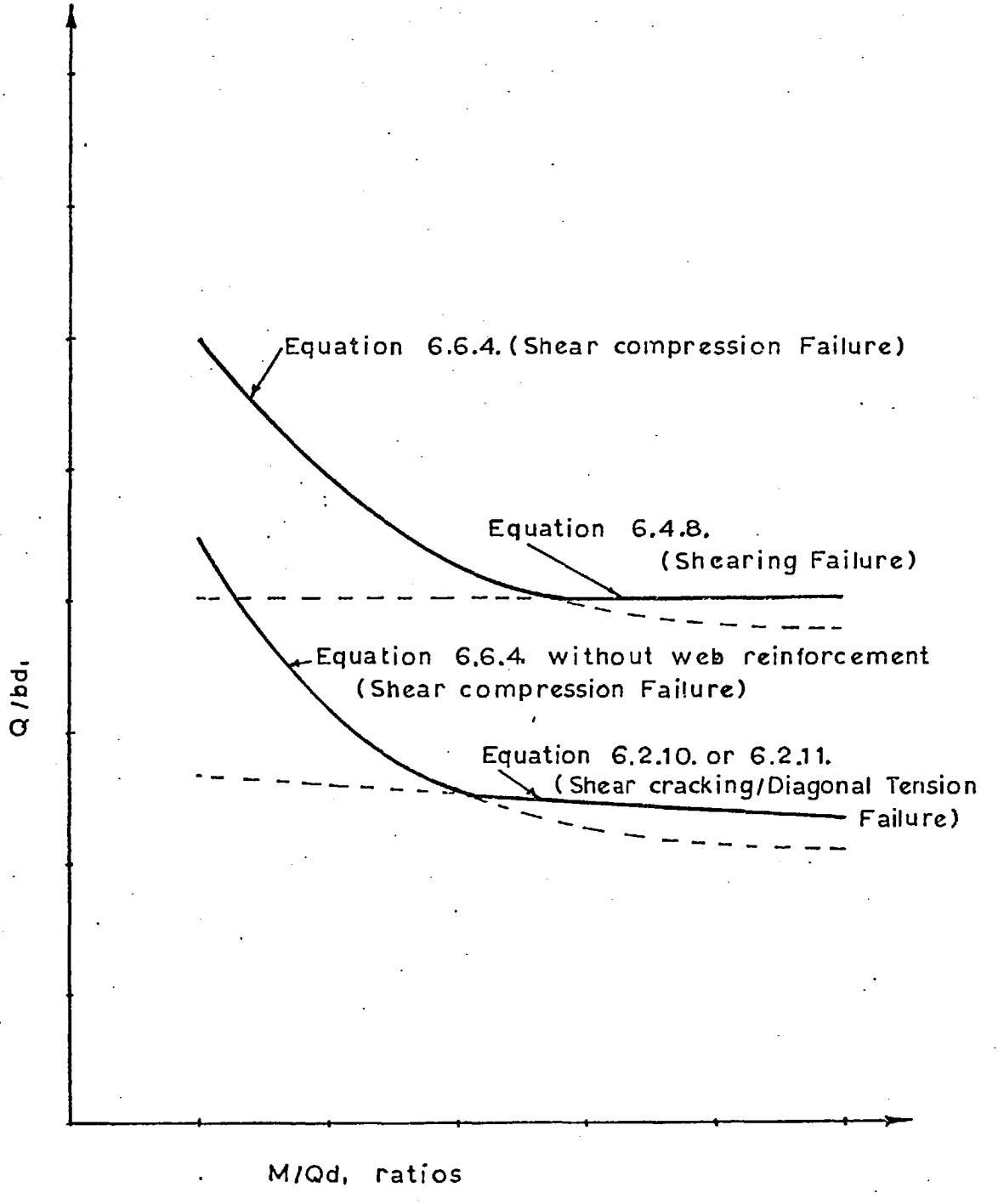
and 6.2.11. Then applying equation 6.6.4. ultimate strength of the beam can be found out. If the strength predicted by equation 6.6.4 (based on arch action) is less than the shear cracking strength, the beam would fail at shear cracking load. This implies that arching is not possible in this particular beam. Similarly, if the ultimate strength predicted by equation 6.6.4 is higher than the shear cracking strength, the beam would sustain additional load after shear cracking implying that arching is possible in this case.

So in order to predict shear strengths of beams without web reinforcement, the strengths by both these equations should be calculated and the higher predicted strength be considered as the true strength.

b) Shearing failure to shear compression

In beams with web reinforcement, it is believed loads at different stages are carried by a number of mechanisms, firstly, by the beam action until shear cracking, following shear cracking by the truss action comprising of the web reinforcement and concrete compressive thrusts. In the short beams, the load is transferred to the support, primarily by the arch action. Beams with long shear spans fail after the breakdown of the indeterminate truss action following yielding of the web reinforcement. Since there is little scope for the arch action to develop, the beam fails by shearing of the concrete compressive zone. On the other hand, in the beams with short shear spans, arching can take place and additional loads can be sustained.

In order to predict ultimate shear strengths equations



TRANSITION OF THE FAILURE MODES FOR VARYING M/Qd, RATIOS. FIG. 110.

6.4.8 and 6.6.4 can be applied within the limitations laid down. As already explained, the true shear strength of a beam will be the maximum value of the two predicted by the equations. This again does not imply that shear compression strength in long beams is less than shearing strength but it implies that arching cannot occur in such beams as the load which can be carried by this action is smaller than the applied load and this is the reason why failure is sudden.

6.8 Proposed Theory on Bond Failure

When a beam is loaded the longitudinal steel is stressed and the resulting forces must be transferred to the surrounding concrete by bond or mechanical anchorage.

According to flexural theory, bond force per unit length

$$f_b = \frac{Q}{la} \qquad \text{..... 6.8.1}$$

Equation 6.8.1 does not consider the effect of shear cracking and thus suggests a rectangular bond stress distribution when Q is constant, which is not true once shear cracking occurs. Because of the formation of the shear crack, the ability of the web to transmit bond to the compressive zone is lost.

A separate analysis is presented below considering the effect of shear cracking on bond.

Considering only a part of a beam, already cracked in shear, and from the observations during the investigation presented in this thesis, it is assumed that near the load the flexural and shear cracks tend to radiate from a point close to the load point as shown in fig. 109.

In a beam with web reinforcement the variation in steel stress is due to the inclined compressed struts of concrete

in the web.

Thus the bond force per unit length

$$= br_q f_{yq} \cot \theta \qquad \text{.....6.8.2}$$

where θ is the inclination of the shear cracks.

In the calculation of stirrup forces, the yield stress is used on the assumption that stirrups will attain yield stress prior to bond failure (B_{25} - fig. 42).

Now the steel stress at a distance of 'c' from the support (c = distance between the tail of the inclined crack and the end of the radial zone)

$$F_{st}^{c} = \frac{Qa}{la} - br_q fyq \frac{c^2}{2la} \qquad \text{..... 6.8.3}$$

The above equation is obtained considering moments about the C.G. of the compressive force.

So the net tensile force left over at the section of zero moment

$$F_{st}^{anch} = F_{st}^{c} - \sum_{c}^{a} brqfyq \text{ Cot } \theta$$

$$\text{or } F_{st}^{anch} = \frac{Qa}{la} - brqfyq \frac{c^2}{2la} - \sum_{c}^{a} brqfyq \text{ Cot } \theta \qquad \text{.....6.8.4}$$

The value of Cot θ is determined on basis of test evidence and it seems reasonable to assume Cot θ = 2 for the present analysis, ie. $c = 2d_1$

Hence equation 6.8.4 gives

$$F_{st}^{anch} = \frac{Qa}{la} - 2brqfyq \frac{d_1^2}{la} - 2brqfyq (a-2d_1) \qquad \text{..... 6.8.5}$$

The above equation predicts the tensile force to be anchored beyond the section of zero moment. The bond strength of a beam depends on a number of variables, such as anchorage length, concrete strength, concrete cover, web reinforcement and diameter of the bars if well-deformed bars are used. Plain round bars might develop only smaller anchorage forces and fail by pull-out in which case the parameters would not include cover and web reinforcement.

From equation 6.8.5 the anchorage force can be equated to the resistance (in case of well-deformed bars only).

$$F_{anch} = F\left[n\,\phi,\ U_{cyl},\ \text{cover},\ L,\ \text{stirrups}\right] \qquad \ldots\ldots 6.8.6$$

From the tests reported in Chapter 5, the following information can be used.

1. Bond strength increases with increasing concrete strength; and is found to be proportional to the square root of cylinder strength of concrete ($U_{cyl} \leq 50\ N/mm^2$).

2. Bond strength also increases with increase in concrete cover, the increase in strength is marked until about $\frac{c}{\phi} = 2$. The plot of $\frac{c}{\phi}$ suggests that bond strength is proportional to the square root of $\frac{c}{\phi}$.

3. Bond strength is improved with increase in anchorage length. But it does not go on increasing for a very long length, which means there is a limit to the anchorage length. Test results show that if an anchorage length is increased beyond about $30\ \phi$, the gain in strength is negligible. Thus, the limit to useful anchorage length may be assumed to be $30\ \phi$.

4. Stirrups have a beneficial effect on the bond strength.

5. With increasing bar diameter, the magnitude of the anchorage force is increased.

Using this information and assumptions equation 6.8.6 can be written as

$$F_{anch} = K \left[n \pi \phi \, U_{cyl}^{\frac{1}{2}} L \left(\frac{c}{\phi}\right)^{\frac{1}{2}} + \sum_{l=0}^{l=L} brqfyq \right] \quad ....6.8.7$$

where ϕ = Diameter of bars

n = Number of bars

U_{cyl} = Cylinder strength of concrete $\leqslant 50$ N/mm^2

L = Anchorage length $\leqslant 30\,\phi$

c = Concrete clear cover $\leqslant 2\,\phi$

rq = Ratio of area of stirrups (Aq/bs)

fyq = Yield or proof stress of stirrup steel.

K = Constant

Equating Fst to be anchored and the resistance offered by equation 6.8.7 the ultimate load corresponding to bond failure can be obtained.

Evaluating the constant K from test results of beams failing in bond, K is found to be 0.55 in N and mm units (see Chapter 7).

Thus resistance against bond failure offered by concrete and web reinforcement

$$F^{anch} = 0.55 \left[n \pi \phi \, U_{cyl}^{\frac{1}{2}} L \left(\frac{c}{\phi}\right)^{\frac{1}{2}} + \sum_{l=0}^{l=L} brqfyq \right] \quad .....6.8.8.$$

Equating equations 6.8.5 and 6.8.8

$$\frac{Qa}{la} - 2\,brqfyq\,\frac{d_1^2}{la} - 2\,brqfyq\,(a-2d_1) = 0.55\left[n\pi\phi\ U\ cyl^{\frac{1}{2}}L\left(\frac{c}{\phi}\right)^{\frac{1}{2}} + \sum_{l=0}^{l=L} brqfyq\right].$$

$$\text{or } \frac{Qa}{la} = 0.55\left[n\pi\,\phi\ U\ cyl^{\frac{1}{2}}L\ \left(\frac{c}{\phi}\right)^{\frac{1}{2}}\right] + rqfyq\left[2\,bd_1\,\frac{d_1}{la} + 2ba\,\left(1-\frac{2d_1}{a}\right) + 0.55\,bL\right]$$

Therefore, average bond stress

$$\frac{Q}{\Sigma Ola} = 0.55\ U\ cyl^{\frac{1}{2}}\left(\frac{L}{a}\right)\ x\ \left(\frac{c}{\phi}\right)^{\frac{1}{2}} + \frac{brqfyq}{n\pi\phi}\left[2\,\frac{d_1}{a}\,x\,\frac{d_1}{la} + 2\,\left(1-\frac{2d_1}{a}\right) + 0.55\,\frac{L}{a}\right] \quad \ldots\ldots\ldots\ 6.8.9$$

and when c = a,

$$\frac{Q}{\Sigma Ola} = 0.55\ U\ cyl^{\frac{1}{2}}\left(\frac{L}{a}\right)x\left(\frac{c}{\phi}\right)^{\frac{1}{2}} + \frac{brqfyq}{n\pi\phi}\left[\frac{a}{2la} + 0.55\,\frac{L}{a}\right] \quad \ldots 6.8.10$$

where ΣO = perimeter of the bars

$= n\pi\phi$

and la = internal (flexural) lever arm.

6.9 Treatment of a section at the point of contraflexure when subject to axial force

A section at the point of contraflexure appears to be most vulnerable in shear with axial tension, if the transference of shear across the vertical crack by interlock and dowel action of the tensile steel are not recognised. In fact in such a case aggregate interlock becomes most effective depending on the width of the crack. Due to the presence of the longitudinal steel at top and bottom, compressive force is induced between the two cracked surfaces as soon as any slip occurs. This is due to the tensile stress produced in steel when loaded. This fact is recognised by Mattock[19] and he suggested that under similar circumstances the shear-friction theory can be used to predict shear transfer across preformed cracks by interlock.

The maximum amount of shear that can be transferred is governed by three criteria

1) magnitude of Asfy;

where As = area of longitudinal steel crossing the crack at right angles.

fy = yield stress of longitudinal steel.

2) concrete strength, and

3) the external axial load.

Since after the formation of the vertical crack, the cohesive strength of concrete is zero, Q can be written as

$$Q = (Asfy + N) \tan \phi \qquad \ldots\ldots 6.9.1$$

where Q = External shear force

As = Area of longitudinal steel perpendicular to crack.

and Tan ϕ = Coefficient of friction.

Mast[19] proposed that tan ϕ be taken equal to 1.4, and Mattock also used this value of tan ϕ for predicting shear transfer across cracks. Test results (see Chapter 5) suggest an even higher value of tan ϕ than 1.4, but this value is retained to be on the safe side.

Failure may occur before the longitudinal steel attains yield stress if the ratio of reinforcement is high. For this reason, Mast put a limit to the value of $\frac{As}{bd}$ fy tan ϕ = 0.15 U cyl, for members without axial forces.

Mattock believes shear-friction theory gives a conservative estimate of the shear that can be transferred across a preformed crack if tan ϕ is assumed to be equal to 1.4. His limit to the value of $\frac{Asfy}{bd}$ tan ϕ is 0.15 U cyl or 4.2 N/mm^2 (600 psi) whichever is less.

So long as there is no web reinforcement, shear transfer due to dowel action is of little significance, But if web reinforcement is present, dowel action is considerably improved provided there are shear and dowel cracks. The shear and dowel cracks will stress the stirrups and thus enable the dowel action to pick up more load.

Besides, in the early stages, most of the shear force is transferred by interlock. When the external load is high, an inclined crack may form independent of the preformed crack and thus brings the stirrups into action. In fact, in none of the beams tested with axial tension were any inclined cracks formed.

Even neglecting the dowel action of the longitudinal steel, a much higher strength of a section at the point of contraflexure can be attained if one recognises the shear transfer by interlock.

Mattock's limit of strength of a section at point of contraflexure of 4.2 N/mm^2 (600 psi) or 0.15 U cyl is found to be much higher than that of any other section predicted by other theories. Hence, the possibility of failure at the section at point of contraflexure is remote.

Thus, the strength of a section at point of contraflexure of a beam when subject to axial tension can be obtained from the following equation based on shear friction theory

$$\frac{Q}{bd_1} = \left(\frac{As}{bd} fy + N\right) \tan \phi \text{ , } \leqslant 0.15 \text{ U cyl or } 4.2 \text{ N/mm}^2 \text{ (600 psi)}$$

$$= \left(\frac{As}{bd} fy + N\right) \times 1.4, \leqslant 0.15 \text{ U cyl or } 4.2 \text{ N/mm}^2 \text{ (600 psi)}$$

whichever is smaller.

where N is +ve for tension

So far as axial compression is concerned, the section at the point of contraflexure can be said to be the strongest section without reservation since the whole of the section is effective in resisting shear. This is supported by test evidence as not a single sign of distress was observed at such sections during the testing of beams with axial compression. So an analysis at the section so far as shear is concerned is believed to be unwanted.

CHAPTER 7

COMPARISON OF TEST RESULTS WITH DIFFERENT THEORIES:

7.1 Shear scracking/diagonal tension failure of simply supported point-loaded rectangular beams with $a/d_1 > 2.5$.

In this chapter, only those theories taking account of axial load in addition to bending and shear are considered.

Four equations including the author's are compared with the test results of a number of investigators and the results are given in tables - 12-18.

All four equations have been mentioned earlier.. The author's equation to predict shear cracking/diagonal tension failure loads is given in Chapter 6, whereas the ACI-ASCE Committee (326) equation, Mattock's modified ACI-318-63 equation and the CEB method are reviewed in Chapter 3. All these four equations predict shear cracking loads and failure loads in the case of beams failing in diagonal tension.

Author's equations:

The proposed approach gives the shear cracking load

$$\frac{Qcr}{bd_1} = \frac{Ut + 0.04\, k \frac{N/bd}{mrst}}{1.35 + 0.04 \frac{M/Qd}{mrst}} \quad , \quad \text{where the } N/Q \text{ ratio is}$$

not constant.

In cases when N/Q is constant,

$$\frac{Qcr}{bd_1} = \frac{Ut}{1.35 + 0.04 \left(\frac{M/Qd_1 - k\,N/Q}{mrst}\right)} \quad ,$$

where

Ut = tensile strength of concrete = $0.47\sqrt{Ucyl}$ in $^{N}/mm^{2}$

and N is +ve for compression.

All other parameters are as explained in Chapter 6.

$$m = 5 + \frac{70}{Ucyl} \qquad \text{in } ^{N}/mm^{2} \text{ units}$$

$$k = \left(\frac{d}{2d_1} + j - 1\right) \quad \text{and} \quad j = {}^{7}/_{8} \text{ (internal lever arm factor).}$$

The $^{M}/Qd_1$ ratio is to be considered at a section of distance d_1 from the loaded section if $a \geq 2d_1$.

ACI-ASCE Committee (326) equation:

The equation proposed by ACI-ASCE Committee to predict shear cracking loads is

$$\frac{Qcr}{bd_1} = 1.9\sqrt{Ucyl} + 2500\ rst.\ \frac{Qd_1}{M + \beta Nd_1} \leq 3.5\sqrt{Ucyl\left(1 + 0.002\,{}^{N}/bd_1\right)}$$

in lbs and inch units.

The value of $^{M}/Qd_1$ at a section distance d_1 from the loaded section is to be used in the equation so long as $a > 2d_1$.

Mattock's (modified ACI-318-63) equation:

The original ACI equation for prestressed beams is modified by Mattock and is given as

$$\frac{Qcr}{bd_1} = \left(1.75 - \frac{0.036}{mrst} + 4.0\ mrst\right)\sqrt{Ucyl} + \left(\frac{I}{y}\right).\frac{\left(6\sqrt{Ucyl} + {}^{N}/bd - \frac{Qd}{bd}\right)}{\left(\frac{M}{Q} - \frac{d_1}{2}\right) bd_1}$$

$$\leq \left(3.5\sqrt{Ucyl} + 0.3\ {}^{N}/bd\right)$$

in lbs and inch units.

where $m = 29{,}000{,}000/(w^{1.5}33\sqrt{Ucyl})$

w = unit weight of concrete

I = Second moment of area of the section.

y = distance from the C.G. of the section to the outer most fibre.

N = axial force, +ve for compression

Qd = Dead load shear.

$\frac{M}{Q}$ ratio is at the loaded section.

Although Mattock considered the M/Q ratio at the edge of the loading plate, because of the complications arising from the unknown loading plate dimensions, the M/Q ratio is here considered at the loaded section.

The contribution of dead load shear is ignored in all cases.

Mattock's other equation is not compared because of the condition imposed on it regarding ratio of tensile steel.

CEB equation :

The last equation is that of the CEB. In fact, the CEB does not recommend the design of any beams without web reinforcement.

For comparison, the ordinary ultimate equation of the CEB is modified by ignoring the contribution of web reinforcement, on the assumption that after shear cracking, the additional shear is carried by web reinforcement. Thus neglecting the web reinforcement term, the CEB equation becomes -

$$\frac{Qcr}{bd_1} = 0.1875\sqrt{Ucyl}\ (1 + 2\frac{N/bd_1}{Ucyl})(0.5 + 33\frac{Ast}{bd_1})$$

for beams with axial compression, in N and mm units.

and $$\frac{Qcr}{bd_1} = 0.1875\sqrt{Ucyl}\ (1 - 6\frac{N/bd_1}{Ucyl})\ (0.5 + 33\frac{Ast}{bd_1})$$

for beams with axial tension, in N and mm units.

In both cases $(0.5 + 33 \frac{Ast}{\sigma_{cyl}}) \leq 1$ and in both the constants have been increased from "design" to ultimate values.

Tables 13-18 summarise the test results of a number of investigators (Mattock, Mukhopadhyay, De Cossio and Siess) of 61 simply supported beams giving the ratio Q_{clac}/Q_{test} for each of the four equations considered for comparison. Only results of series of beams without web reinforcement and subjected to axial loads (tension and compression) are considered. Because of the uncertainty of assessing the shear cracking load of a beam with web reinforcement accurately, no such test results are included in the comparison. None of the beams had compression reinforcement.

All beams excepting those of Mukhopadhyay had widths greater than or equal to 152 mm (6"). Mikhopadhyay's beams had a width equal to 127 mm (5").

The beams were loaded directly on the top and supported at the bottom. In no case was any tensile reinforcement curtailed.

The statistical analysis of the comparisons obtained for test results of each investigator and then for all beams together are given in the following table 12.

Table 12. Statistical comparison of $^{Qcalc}/_{Qtest}$ values of simply supported beams without web reinforcement.

Name of Investigator	Values of	No. of test results	Proposed theory	ACI-ASCE equation	Mattock's equation	CEB equation
Mattock	Mean of $\frac{Qcalc}{Qtest}$	31	0.89	0.76	0.90	0.72
	Standard deviation	-	0.101	0.153	0.124	0.144
	Coefficient of Variation	-	0.113	0.201	0.137	0.200
Mukhopadhyay	Mean of $\frac{Qcalc}{Qtest}$	23	0.99	0.77	0.99	0.80
	Standard deviation	-	0.11	0.086	0.126	0.125
	Coefficient of Variation	-	0.111	0.112	0.127	0.156
De Cossio and Siess	Mean of $\frac{Qcalc}{Qtest}$	7	0.87	0.71	0.90	0.76
	Standard deviation	-	0.105	0.087	0.142	0.137
	Coefficient of variation	-	0.120	0.122	0.157	0.180
All together	Mean of $\frac{Qcalc}{Qtest}$	61	0.92	0.76	0.93	0.75
	Standard deviation	-	0.114	0.126	0.133	0.140
	Coefficient of Variation	-	0.124	0.165	0.143	0.187

Table 13: Shear cracking/Diagonal tension failure of simple supported single-point loaded rectangular beams with $a/d_1 > 2.5$.
(A.H. Mattock).[36]

b = 152 mm (6"), d = 305 mm (12") d_1 = 254 mm (10")

Beam No.	Ucyl N/mm^2	A_a/d_1	rst%	N/bd_1 N/mm^2	$Qtest/bd_1$ N/mm^2
1	17.1	3	1.03	0	0.94
2	15.5	3	1.03	+1.57	1.06
3	46.9	3	1.03	0	1.41
4	46.2	3	1.03	-0.74	1.15
5	16.1	3	2.07	-0.74	0.86
6	18.4	3	2.07	+1.57	1.39
7	17.5	3	2.07	+3.31	1.55
8	43.7	3	2.07	+1.57	2.39
9	48.0	3	2.07	+3.31	2.72
10	18.6	3	3.10	0	1.45
11	15.3	3	3.10	-1.57	1.09
12	16.2	3	3.10	+1.57	1.60
13	49.80	3	3.10	+1.57	2.30
14	49.0	3	3.10	+3.31	2.87
15	25.9	5.4	1.03	0	0.80
16	30.40	5.4	1.03	-1.24	0.72
17	27.80	5.4	1.03	+3.31	0.98
18	18.10	5.4	2.07	0	0.92
19	18.50	5.4	2.07	-0.74	1.03
20	48.30	5.4	2.07	-0.74	1.49
21	50.60	5.4	2.07	-1.57	1.47
22	16.10	5.4	3.10	0	1.03
23	18.50	5.4	3.10	-0.74	1.09
24	29.2	5.4	3.10	0	1.36
25	27.6	5.4	3.10	-1.24	1.32
26	28.9	5.4	3.10	-2.06	1.09
27	30.6	5.4	3.10	+1.66	1.38
28	24.3	5.4	3.10	+3.31	1.36
29	53.20	5.4	3.10	-0.74	1.72
30	55.20	5.4	3.10	+1.57	1.72
31	52.7	5.4	3.10	+3.31	1.72

Table 14: Comparison of Q_{calc}/Q_{test} values of simply supported single point loaded rectangular beams with $a/d_1 > 2.5$.

(A.H. Mattock)[36]

Beam No.	Q_{calc}/Q_{test}			
	Proposed theory	ACI-ASCE equation	Mattock's equation	CEB equation
1	0.93	0.79	0.88	0.69
2	0.94	0.72	0.87	0.70
3	0.88	0.83	0.81	0.77
4	1.02	1.00	0.94	0.84
5	1.20	0.91	1.10	0.63
6	0.88	0.66	0.85	0.68
7	0.84	0.66	0.84	0.70
8	0.72	0.52	0.64	0.56
9	0.70	0.49	0.64	0.54
10	0.85	0.66	0.84	0.56
11	0.99	0.75	0.68*	0.63
12	0.77	0.61	0.81	0.56
13	0.86	0.63	0.79	0.61
14	0.70	0.51	0.70	0.52
15	0.84	1.05	1.03	1.00
16	0.86	1.25	1.14	0.91
17	0.93	0.91	1.00	1.05
18	0.94	0.82	1.04	0.87
19	0.81	0.73	0.90	0.60
20	0.80	0.79	0.85	0.80
21	0.79	0.81	0.86	0.74
22	0.94	0.74	1.04	0.73
23	0.91	0.77	1.00	0.56
24	0.88	0.72	0.94	0.75
25	0.85	0.71	0.92	0.55
26	1.02	0.87	0.95*	0.53
27	0.93	0.73	0.99	0.83
28	0.92	0.69	0.99	0.87
29	0.87	0.74	0.88	0.73
30	0.94	0.76	0.95	0.86
31	0.97	0.76	0.98	0.89

* upper limit of Q_{cr}/bd_1

Table 15. Shear cracking/Diagonal tension failure of simply supported two-point loaded rectangular beams with $a/d_1 > 2.5$ (M. Mukhopadhyay)[39]

b = 127 mm (5"), d = 254 mm (10")

Beam No.	Ucyl N/mm^2	d_1 mm	a/d_1	rst%	N/bd_1 N/mm^2	$Qtest/bd_1$ N/mm^2
A_{11}	22.6	218	3.27	2.8	0	1.32
A_{12}	25.2	218	3.27	2.8	1.08	1.64
A_{13}	21.4	218	3.27	2.8	1.80	1.37
A_{14}	22.5	218	3.27	2.8	2.53	1.52
B_{11}	21.6	218	3.74	2.8	0	1.05
B_{12}	18.0	218	3.74	2.8	1.08	0.97
B_{13}	22.80	218	3.74	2.8	1.80	1.36
B_{14}	16.70	218	3.74	2.8	2.53	1.01
C_{11}	21.40	218	4.90	2.8	0	1.28
C_{13}	17.30	218	4.90	2.8	1.80	0.93
C_{14}	24.30	218	4.90	2.8	2.53	1.29
B_1	18.30	220.7	3.46	2.09	0	1.06
B_2	16.10	220.7	3.46	2.09	1.07	0.99
B_3	17.00	220.7	3.46	2.09	1.78	1.11
B_4	16.40	220.7	3.46	2.09	2.49	1.11
C_1	17.90	220.7	4.61	2.09	0	1.27
C_2	19.70	220.7	4.61	2.09	1.07	1.10
C_3	18.60	220.7	4.61	2.09	1.78	1.03
C_4	19.40	220.7	4.61	2.09	2.49	0.99
A_1	17.30	220.7	2.76	2.09	0	1.15
A_2	17.30	220.7	2.76	2.09	1.07	1.34
A_3	14.30	220.7	2.76	2.09	1.78	1.19
A_4	14.80	220.7	2.76	2.09	2.49	1.37

Table 16. Comparison of Q_{calc}/Q_{test} values of simply supported two point loaded rectangular beams with $a/d_1 > 2.5$.

(M. Mukhopadhyay)[39]

Beam No.	Q_{calc}/Q_{test}			
	Proposed theory	ACI-ASCE equation	Mattock's equation	CEB equation
A_{11}	0.97	0.73	0.92	0.68
A_{12}	0.85	0.63	0.82	0.62
A_{13}	0.97	0.74	0.97	0.74
A_{14}	0.92	0.70	0.92	0.72
B_{11}	1.14	0.87	1.12	0.83
B_{12}	1.19	0.92	1.21	0.92
B_{13}	0.96	0.72	0.96	0.76
B_{14}	1.17	0.94	1.23	0.99
C_{11}	0.84	0.67	0.89	0.68
C_{13}	1.14	0.88	1.23	1.01
C_{14}	0.96	0.73	0.98	0.87
B_1	1.01	0.78	0.96	0.76
B_2	1.08	0.83	1.05	0.86
B_3	1.02	0.77	0.99	0.84
B_4	1.03	0.80	1.02	0.89
C_1	0.74	0.60	0.75	0.62
C_2	0.92	0.74	0.94	0.84
C_3	1.00	0.78	1.02	0.94
C_4	1.09	0.86	1.13	1.05
A_1	0.99	0.75	0.91	0.68
A_2	0.89	0.68	0.84	0.65
A_3	0.96	0.78	0.95	0.75
A_4	0.88	0.72	0.88	0.70

Table 17. Shear cracking/Diagonal tension failure of simply supported single point loaded rectangular (stub) beams with $a/d_1 > 2.5$.
(De Cossio and Siess)[11].

b = 152 mm (6"), d = 305 mm (12") and d_1 = 254 mm (10")

Beam No.	Ucyl N/mm^2	rst%	a/d_1	N/bd_1 N/mm^2	Qcr/bd_1 N/mm^2
B-2	28.5	1.0	3	+2.3	1.70
B-3	26.3	1.0	4	+2.3	1.25
B-4	28.3	1.0	5	+2.3	1.09
B-12	27.1	3.33	3	+2.3	1.94
B-13	27.9	3.33	4	+2.3	1.60
B-14	29.3	3.33	5	+2.3	1.37
B-15	28.4	3.33	6	+2.3	1.21

Table 18. Comparison of $Qcalc/Qtest$ values for simply supported (stub) beams subject to single point load.
(De Cossio and Siess).[11]

Beam No.	$Qcalc/Qtest$			
	Proposed theory	ACI-ASCE equation	Mattock's equation	CEB equation
B-2	0.71	0.57	0.68	0.57
B-3	0.82	0.71	0.81	0.75
B-4	0.81	0.83	0.87	0.88
B-12	0.81	0.64	0.82	0.59
B-13	0.91	0.68	0.93	0.72
B-14	0.99	0.76	1.05	0.86
B-15	1.03	0.81	1.13	0.96

7.2 Shear cracking/Diagonal tension failure of restrained and knee frame point-loaded rectangular beams with $M/Qd_1 > 2.5$.

The four equations used to predict shear cracking/Diagonal tension failure loads in the preceeding section can be applied to the members of this section without modification except that the cross-section to be considered is at a distance d_1 (or $d_1/2$) from the support instead of the load.

Table 19 gives a comparison of a number of test results with the different equations.

Table 19. Statistical comparison of $Qcalc/Qtest$ values of knee frame and restrained beams.

Investigator	Values of	No. of test results	Proposed theory	ACI-ASCE equation	Mattock's equation	CEB equation
Morrow and Viest (knee frames)	Mean of $\frac{Qcalc}{Qtest}$	18	0.99	0.79	0.93	0.82
	Standard deviation	-	0.090	0.070	0.098	0.127
	Coeff. of variation	-	0.091	0.090	0.106	0.154
Sayani (Restrained Beams)	Mean of $\frac{Qcalc}{Qtest}$	15	1.07	0.88	0.91	0.64
	Standard deviation	-	0.101	0.16	0.085	0.157
	Coeff. of variation	-	0.094	0.182	0.093	0.245
Morrow and Viest and Sayani	Mean of $\frac{Qcalc}{Qtest}$	33	1.02	0.83	0.92	0.74
	Standard deviation	-	0.103	0.127	0.093	0.167
	Coeff. of variation	-	0.101	0.153	0.101	0.226

Table 20. Shear cracking/Diagonal tension failure of restrained (knee frame) point loaded rectangular beams with $M/Qd_1 > 2.5$ (Morrow and Viest)[38].

Beam No.	b mm	d_1 mm	d mm	Ucyl N/mm^2	rst%	M/Qd_1	N/Q	$Qult/bd_1$ N/mm^2
$F38B_2$	305	362	419	12.4	1.91	2.71	1.0	1.01
$38E_2$	305	368	419	14.1	0.50	2.66	1.0	0.88
$F38B_4$	305	375	416	31.4	1.84	2.62	1.0	1.52
$38D_4$	305	381	416	26.9	1.32	2.57	1.0	1.44
$38E_4$	305	378	419	32.2	0.91	2.60	1.0	1.28
$F38A_6$	305	356	419	45.6	2.91	2.76	1.0	2.19
$38B_6$	305	381	419	41.6	1.81	2.57	1.0	1.71
$F55B_2$	305	368	419	11.9	1.88	3.83	1.0	0.84
$F55A_4$	305	372	419	26.4	1.98	3.80	1.0	1.32
$55B_4$	305	381	419	29.5	1.81	3.71	1.0	1.08
$55D_4$	305	381	410	25.6	1.45	3.71	1.0	1.08
$55E_4$	305	387	429	28.4	0.94	3.64	1.0	1.10
$F55A_6$	305	350	419	42.0	3.32	4.04	1.0	1.77
$55B_6$	305	368	419	43.7	1.88	3.83	1.0	1.26
$F70B_2$	305	362	419	14.4	1.91	4.91	1.0	0.81
$70A_4$	305	362	410	29.0	2.16	4.91	1.0	1.25
$70A_6$	305	368	419	38.7	3.34	4.83	1.0	1.54
$F84B_4$	305	375	416	29.7	1.84	5.70	1.0	1.14

Table 21. Comparison of Q_{calc}/Q_{test} values for knee frame rectangular members. $M/Qd_1 > 2.5$ (Morrow and Viest)[38].

Beam No.	Q_{calc}/Q_{test}			
	Proposed theory	ACI-ASCE equation	Mattock's equation	CEB equation
$38B_2$	1.02	0.79	0.99	0.76
$38E_2$	0.86	0.75	0.77	0.60
$38B_4$	1.02	0.76	0.89	0.76
$38D_4$	0.95	0.71	0.81	0.70
$38E_4$	1.02	0.81	0.84	0.70
$F38A_6$	0.89	0.66	0.82	0.63
$38B_6$	1.03	0.76	0.86	0.77
$F55B_2$	1.06	0.81	1.03	0.88
$F55A_4$	0.93	0.73	0.85	0.80
$55B_4$	1.16	0.92	1.07	1.01
$55D_4$	1.02	0.85	0.91	0.93
$55E_4$	0.87	0.83	0.83	0.79
$F55A_6$	0.95	0.70	0.94	0.75
$55B_6$	1.17	0.93	1.09	1.04
$F70B_2$	1.05	0.86	1.10	1.00
$70A_4$	0.92	0.76	0.94	0.88
$70A_6$	0.98	0.75	0.98	0.82
$F84B_4$	0.86	0.82	0.95	0.97

Table 22. Shear cracking/Diagonal tension failure of rectangular Restrained beams with $M/Qd_1 > 2.5$.

(Sayani)[48]

b = 152 mm, d_1 = 272 mm, d = 305 mm.

Beam No.	Ucyl N/mm^2	M/Qd_1	rst%	rsc%	N/bd_1 N/mm^2	$Qult/bd_1$ N/mm^2
N_1	31.4	2.8	1.46	1.46	0	1.21
N_3	32.9	2.8	1.46	1.46	-2.90	1.02
N_4	34.4	2.8	1.46	1.46	-2.17	1.02
N_5	32.0	2.8	1.46	1.46	-1.44	1.15
N_6	32.8	2.8	1.46	1.46	-1.68	1.21
N_7	35.8	2.8	1.46	1.46	-3.13	1.08
N_9	31.1	2.8	1.46	1.46	-2.05	1.02
N_{11}	33.4	2.8	0.97	0.97	-1.81	0.91
N_{14}	31.6	2.8	1.46	-	-0.97	1.26
N_{15}	32.5	2.8	1.46	-	-0.49	1.21
N_{18}	31.0	2.8	1.46	1.46	-1.44	1.08
N_{19}	29.2	2.8	1.46	1.46	-1.92	0.97
N_{20}	46.2	2.8	1.46	1.46	-1.44	1.02
N_{21}	14.7	2.8	1.46	1.46	-1.44	0.97
N_{24}	22.5	2.8	1.46	1.46	-1.44	0.91

Table 23. Comparison of $^{Qclac}/_{Qtest}$ values of rectangular restrained beams. $^{M}/_{Qd_1} > 2.5$.

(Sayani)[48]

Beam No.	$^{Qcalc}/_{Qtest}$			
	Proposed theory	ACI-ASCE equation	Mattock's equation	CEB equation
N_1	1.07	0.85	0.93	0.85
N_3	1.06	0.66	0.88	0.49
N_4	1.15	1.00	0.96	0.66
N_5	1.03	0.89	0.88	0.66
N_6	0.98	0.84	0.83	0.60
N_7	1.03	0.49	0.84	0.48
N_9	1.10	0.96	0.93	0.61
N_{11}	1.04	1.08	0.94	0.66
N_{14}	0.97	0.80	0.83	0.66
N_{15}	1.05	0.85	0.91	0.79
N_{18}	1.09	0.91	0.92	0.68
N_{19}	1.13	0.98	0.97	0.62
N_{20}	1.35	1.15	1.14	1.00
N_{21}	0.88	0.73	0.76	0.30
N_{24}	1.13	0.94	0.98	0.59

7.3 Shear cracking of knee frames with $M/Qd_1 < 2.5$

So far as shear cracking is concerned, all four equations mentioned in the earlier two sections are applicable in this case also. The proposed theory is not applicable to predict ultimate loads of members failing in modes other than diagonal tension. The remaining three equations are presumably intended to be so.

Tables 27 and 28 give a comparison of the test results of Morrow and Viest and Baldwin and Viest with all the equations.

Table 24. Statistical comparison of Q_{calc}/Q_{test} (cracking) values of knee frame members.

Investigator	Value of	No. of test results	Proposed theory	ACI-ASCE equation	Mattock's equation	CEB equation
Morrow and Viest	Mean of $\frac{Q_{calc}}{Q_{test}}$	11	0.86	0.82	0.91	0.83
	Standard deviation	-	0.044	0.085	0.058	0.069
	Coeff. of variation	-	0.051	0.104	0.064	0.083
Baldwin and Viest	Mean of $\frac{Q_{calc}}{Q_{test}}$	7	0.92	0.91	0.88	0.73
	Standard deviation	-	0.120	0.168	0.086	0.071
	Coeff. of variation	-	0.131	0.184	0.098	0.097
Morrow and Viest and Baldwin and Viest	Mean of $\frac{Q_{calc}}{Q_{test}}$	18	0.89	0.86	0.90	0.79
	Standard deviation	-	0.087	0.142	0.072	0.084
	Coeff. of variation	-	0.098	0.165	0.080	0.106

Table 25. Shear failure of knee frame members with no web reinforcement. $M/Qd_1 < 2.5$.

(Morrow and Viest). d = 419 mm (16.5")

Beam No.	b mm	d_1 mm	Ucyl N/mm^2	rst%	M/Qd_1	N/Q	Qcr/bd_1 N/mm^2	$Qult/bd_1$ N/mm^2
$F21B_2$	305	368	10.14	1.88	1.49	1.0	1.18	1.83
$21B_{2R}$	305	368	14.10	1.88	1.49	1.0	1.54	2.52
$21B_4$	305	368	29.70	1.88	1.49	1.0	2.22	3.30
$21B_{4R}$	305	368	29.20	1.88	1.49	1.0	2.10	3.64
$21C_4$	305	368	26.60	1.59	1.49	1.0	1.96	2.50
$21C_{4R}$	305	375	30.90	1.56	1.49	1.0	2.20	3.88
$21D_4$	305	368	31.50	1.22	1.49	1.0	1.96	3.96
$21E_4$	305	381	30.70	0.80	1.49	1.0	1.86	3.42
$21F_4$	305	368	30.00	0.75	1.49	1.0	1.95	3.06
$21A_6$	305	368	48.50	2.36	1.49	1.0	2.52	5.61
$21B_6$	305	368	45.00	1.88	1.49	1.0	2.52	5.55

Table 26. Shear failure of knee frame members with no web reinforcement. $M/Qd_1 < 2.5$.

(Baldwin Jr., Viest). d = 406 mm (16")

Beam No.	b mm	d_1 mm	Ucyl N/mm^2	rst%	M/Qd_1	N/Q	Qcr/bd_1 N/mm^2	$Qult/bd_1$ N/mm^2
2F28	305	368	28.45	1.86	1.93	0.33	1.53	2.78
3F28	305	368	25.80	1.86	1.93	0.50	1.63	3.29
4F28	305	368	27.50	1.86	1.93	0.67	1.90	2.60
6F28	305	368	21.20	1.86	1.93	1.00	1.60	2.52
9F28	305	368	23.70	1.86	1.93	1.50	1.40	2.82
12F28	305	368	23.90	1.86	1.93	2.00	2.08	3.36
18F28	305	368	26.00	1.86	1.93	3.00	2.44	2.94
12F21	305	368	30.80	1.83	1.45	2.00	3.39	4.25

Table 27. Comparison of $^{Qcalc}/_{Qtest}$ (cracking) values of knee frame members with no web reinforcement. $^{M}/_{Qd_1} < 2.5$.
(Morrow and Viest)[38]

Beam No.	$^{Qcalc}/_{Qtest}$(cracking)			
	Proposed theory	ACI-ASCE equation	Mattock's equation	CEB equation
$F21B_2$	0.94	0.90	1.04	0.95
$21B_{2R}$	0.81	0.84	0.95	0.85
$21B_4$	0.80	0.85	0.88	0.81
$21B_{4R}$	0.84	0.90	0.92	0.84
$21C_4$	0.86	0.86	0.90	0.86
$21C_{4R}$	0.82	0.77	0.87	0.81
$21D_4$	0.91	0.79	0.91	0.82
$21E_4$	0.90	0.69	0.86	0.73
$21F_4$	0.85	0.65	0.81	0.68
$21A_6$	0.91	0.94	0.97	0.88
$21B_6$	0.86	0.82	0.90	0.85

Table 28. Comparison of $^{Qcalc}/_{Qtest}$ (cracking) values of knee frame members with no web reinfacement. $^{M}/_{Qd_1} < 2.5$
(Baldwin Jr. and Viest)[5].

Beam No.	$^{Qcalc}/_{Qtest}$(cracking)			
	Proposed theory	ACI-ASCE equation	Mattock's equation	CEB equation
2F28	1.03	0.80	0.88	0.77
3F28	0.94	0.75	0.84	0.71
4F28	0.84	0.68	0.76	0.65
6F28	0.91	0.83	0.87	0.71
9F28	1.14	1.25	1.06	0.88
12F28	0.80	1.02	0.85	0.68
18F28	0.78	1.07	0.93	0.70
12F21*	0.59	0.79	0.79	0.48

* Not included for statistical analysis.

7.4 Shear failure of knee frame members without web reinforcement. $M/Qd_1 < 2.5$. Shear compression failure.

Since the ACI-ASCE and Mattock's equations are primarily intended for the prediction of shear cracking loads, their deliberate neglect of strength after shear cracking makes them conservative if failure is by shear compression. Their application to the present class of members is justified by their authors' view that post cracking resistance is unreliable.

The proposed equation for this type of failure is given in chapter 6. For beams without web reinforcement the equation becomes -

$$Qult/bd_1 = \bar{n} \times 2.2\, Ucyl^{2/3} \frac{la}{a} - \frac{N/bd_1(d_1 - d/2)}{a} + Qd/bd_1$$

The value of the dowel cracking shear Qd/bd_1 as already emphasised, will be of any significance provided the beams is supported directly on the bottom surface.

For comparison 19 test results of knee frame members are used and the contribution of dowel action (Qd/bd_1) is neglected as the members were not supported on their bottom faces.

Table 29 gives the test results and $Qcalc/Qtest$ values of 19 knee frame members by the four equations.

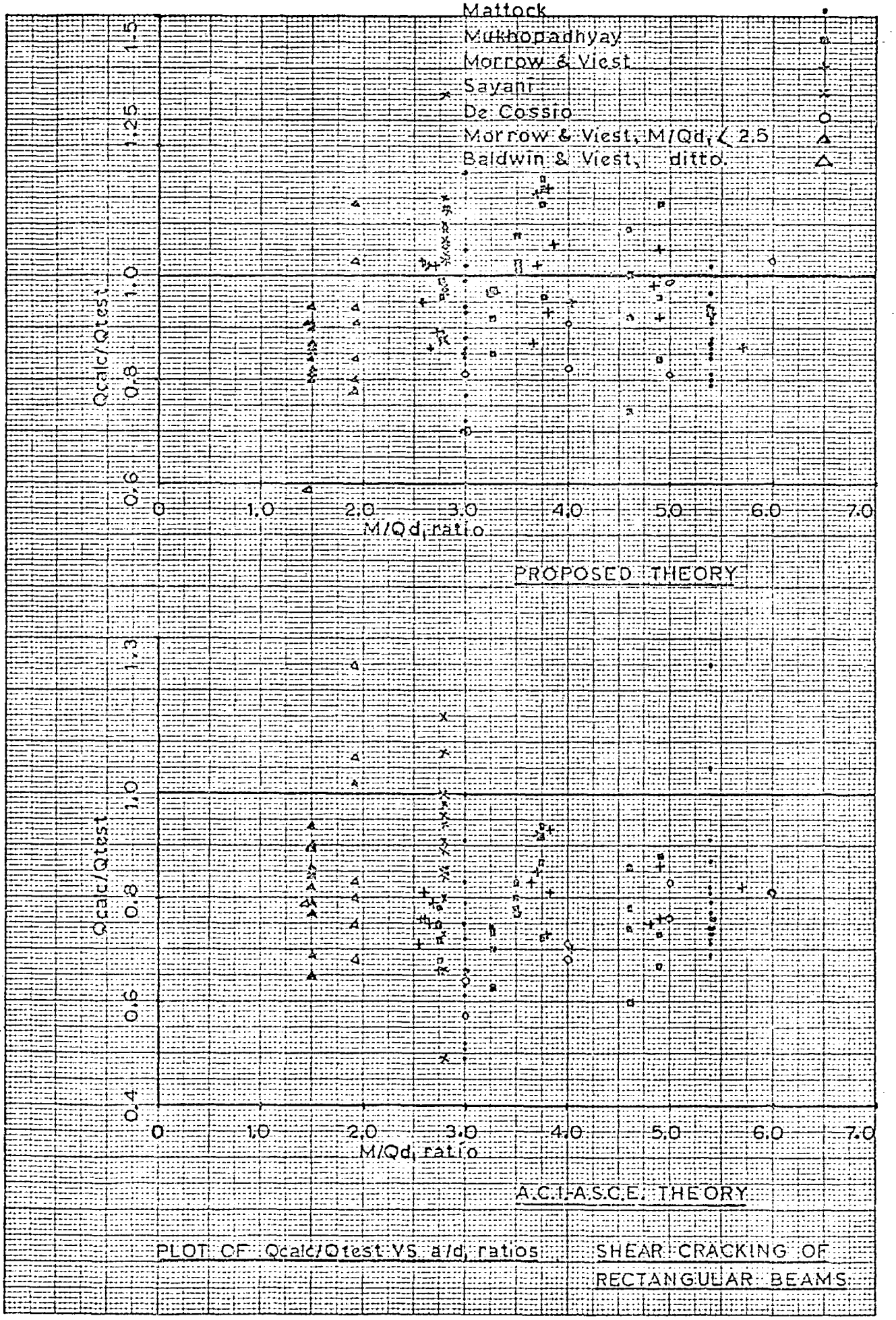
Table 29. Statistical comparison of $^{Qcalc}/_{Qtest}$ values of knee frame members without web reinforcement.

$^{M}/_{Qd_1} < 2.5$. Shear compression failure.

Investigator	Value of	No. of test results	Proposed theory	ACI-ASCE equation	Mattock's equation	CEB equatio
Morrow and Viest	Mean of $\frac{Qcalc}{Qtest}$	11	0.93	0.49	0.61	0.53
	Standard deviation	-	0.119	0.098	0.075	0.091
	Coeff. of variation	-	0.128	0.200	0.122	0.172
Baldwin and Viest	Mean of $\frac{Qcalc}{Qtest}$	8	0.85	0.61	0.62	0.49
	Standard deviation	-	0.091	0.175	0.11	0.057
	Coeff. of variation	-	0.107	0.287	0.177	0.116
Morrow and Viest and Baldwin and Viest	Mean of $\frac{Qcalc}{Qtest}$	19	0.90	0.54	0.62	0.51
	Standard deviation	-	0.115	0.148	0.091	0.082
	Coeff. of variation	-	0.128	0.274	0.147	0.160

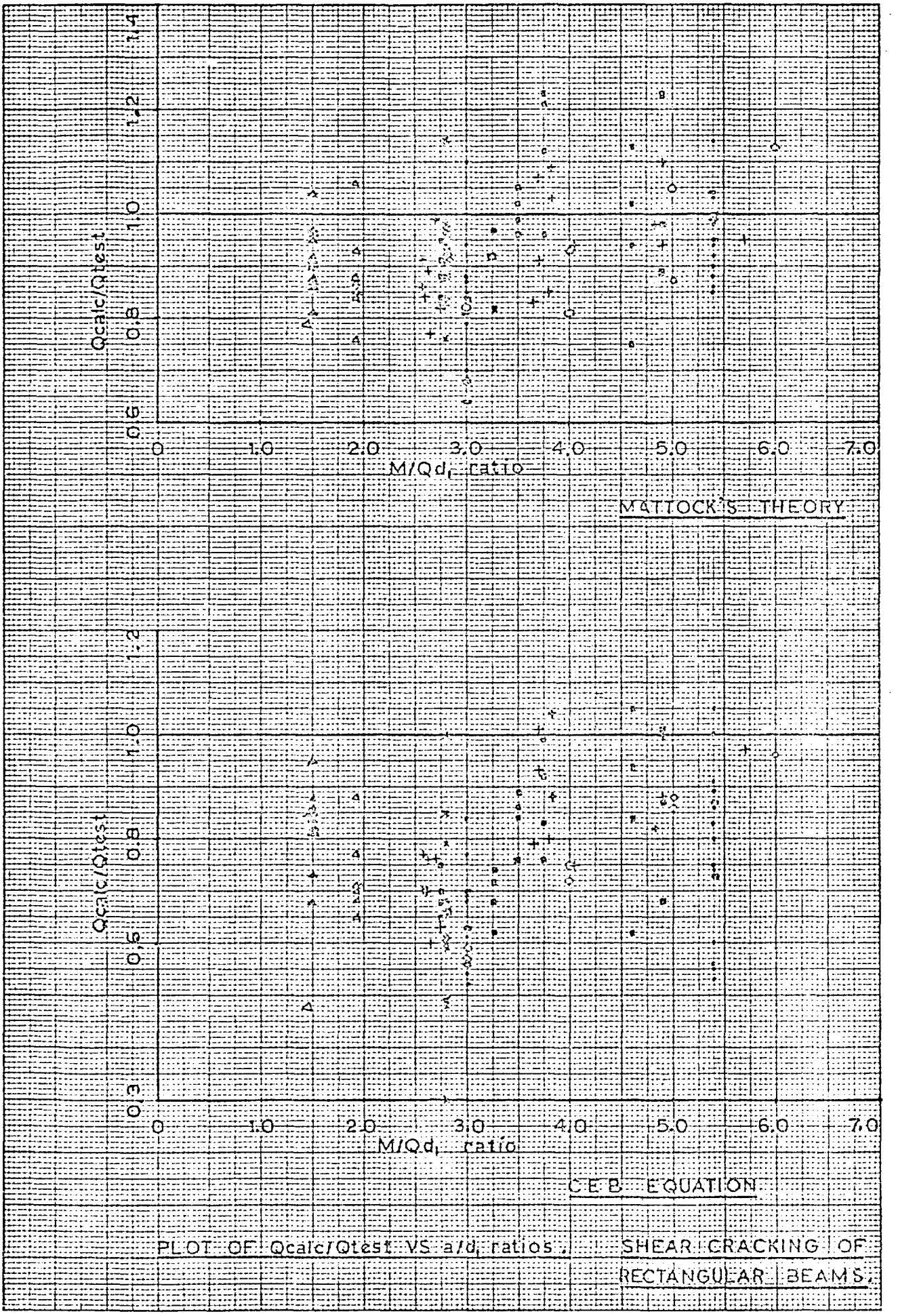
Table 30. Comparison of $^{Qcalc}/_{Qtest}$ (Ult) values of Knee frame members without web reinforcement. $^{M}/_{Qd_1} < 2.5$. Shear compression failure.

Beam No.	$^{Qcalc}/_{Qtest}$ (ultimate)			
	Proposed theory	ACI-ASCE equation	Mattock's equation	CEB equation
Morrow and Viest[38]				
$F_{21}\ B_2$	1.07	0.61	0.74	0.68
$21\ B_{2R}$	0.94	0.56	0.65	0.58
$21\ B_4$	1.03	0.57	0.66	0.58
$21\ B_{4R}$	0.95	0.52	0.61	0.53
$21\ C_4$	1.18	0.67	0.75	0.69
$21\ C_{4R}$	0.87	0.44	0.58	0.51
$21\ D_4$	0.81	0.39	0.55	0.46
$21\ E_4$	0.78	0.38	0.56	0.43
$21\ F_4$	0.84	0.42	0.59	0.46
$21\ A_6$	0.98	0.42	0.54	0.44
$21\ B_6$	0.82	0.38	0.52	0.43
Baldwin Jr., J.M. and Viest I.M.[5]				
$2F_{28}$	0.8	0.44	0.51	0.44
$3F_{28}$	0.68	0.37	0.45	0.42
$4F_{28}$	0.85	0.50	0.58	0.49
$6F_{28}$	0.86	0.53	0.60	0.49
$9F_{28}$	0.88	0.62	0.63	0.50
$12F_{28}$	0.80	0.73	0.62	0.49
$18F_{28}$	0.97	0.95	0.81	0.62
$12F_{21}$	0.98	0.71	0.75	0.43



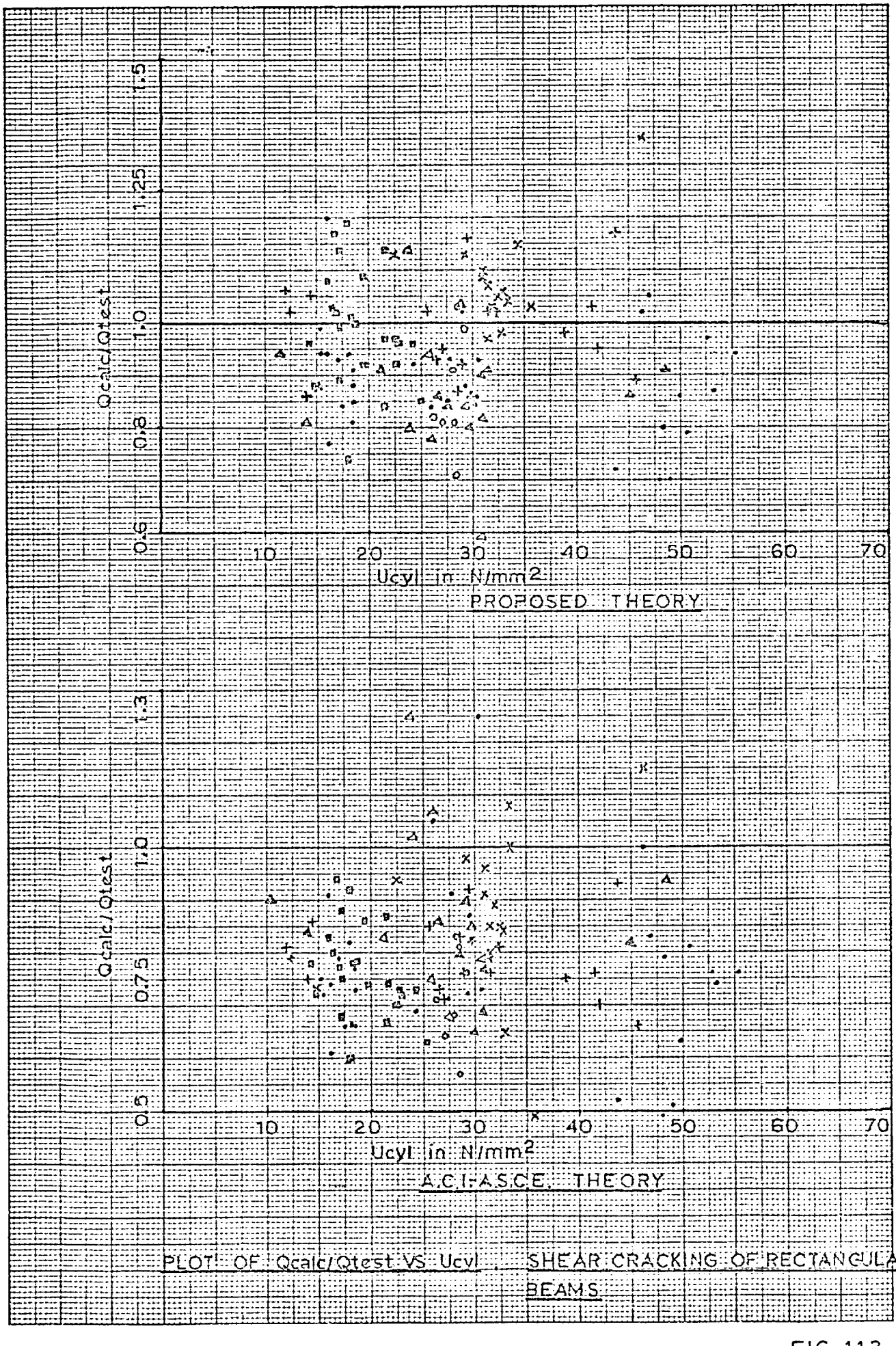
PLOT OF Qcalc/Qtest VS a/d, ratios SHEAR CRACKING OF RECTANGULAR BEAMS

FIG. 111.



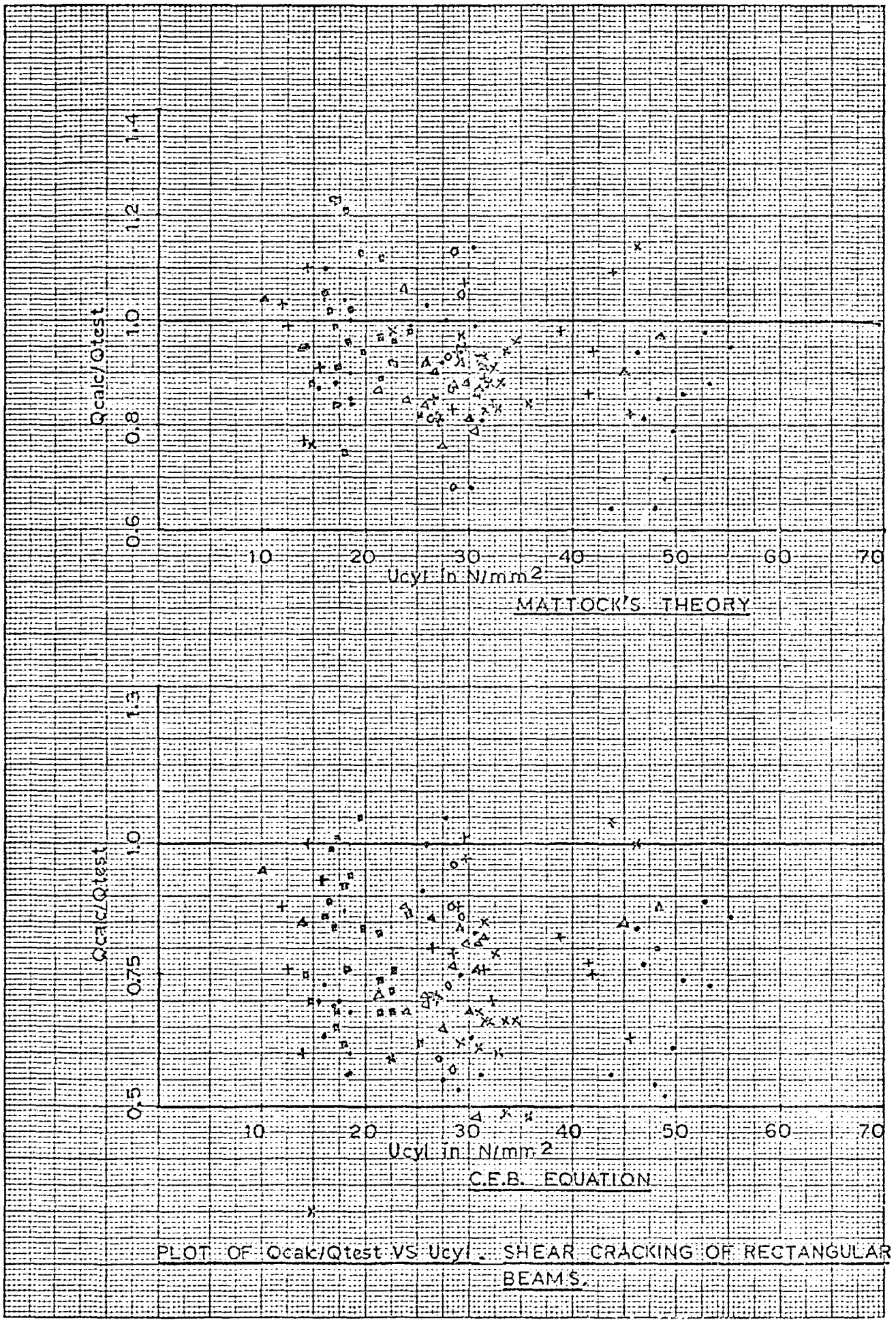
PLOT OF Qcalc/Qtest VS a/d, ratios. SHEAR CRACKING OF RECTANGULAR BEAMS.

FIG. 112.



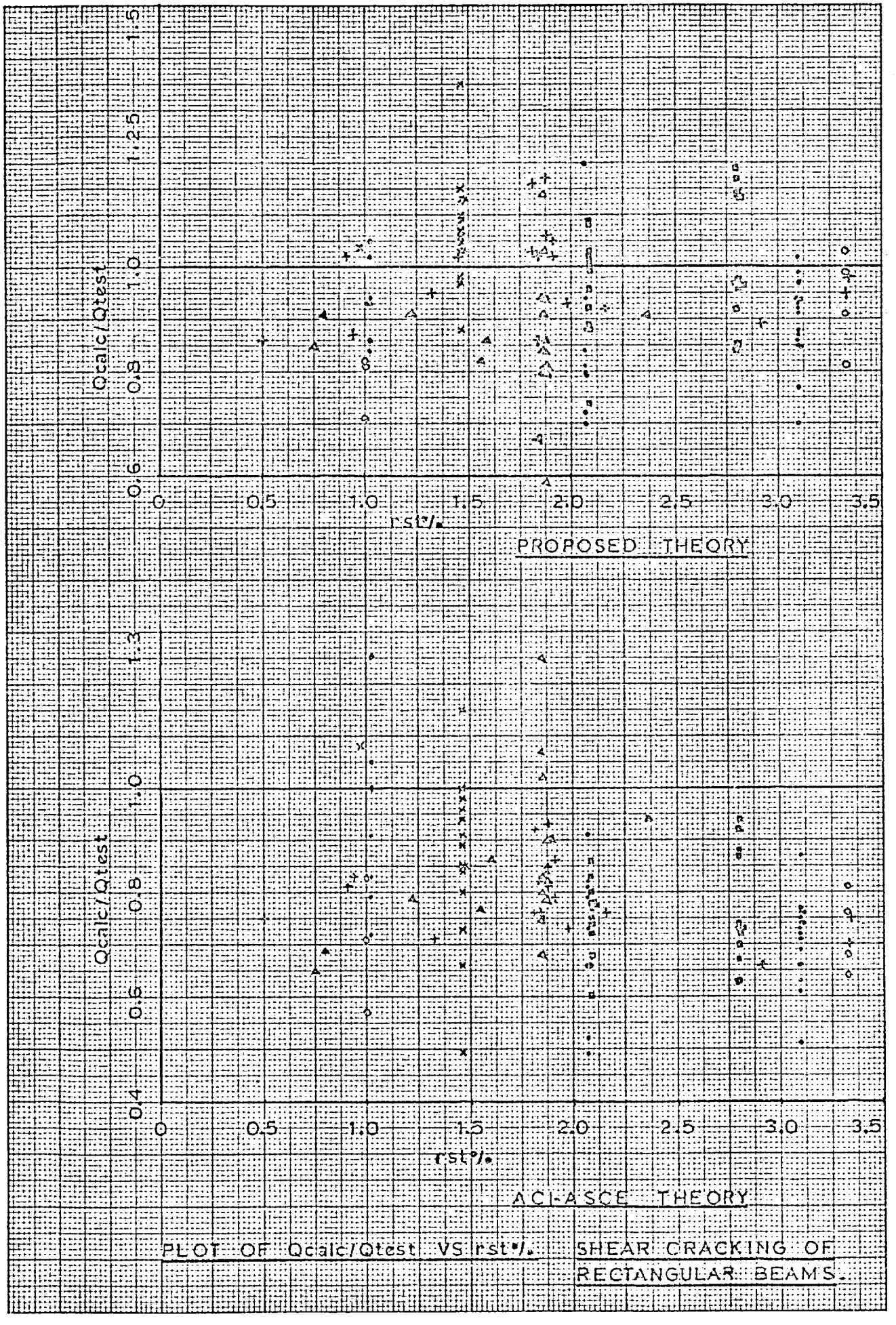
PLOT OF Qcalc/Qtest VS Ucyl. SHEAR CRACKING OF RECTANGULAR BEAMS

FIG. 113.



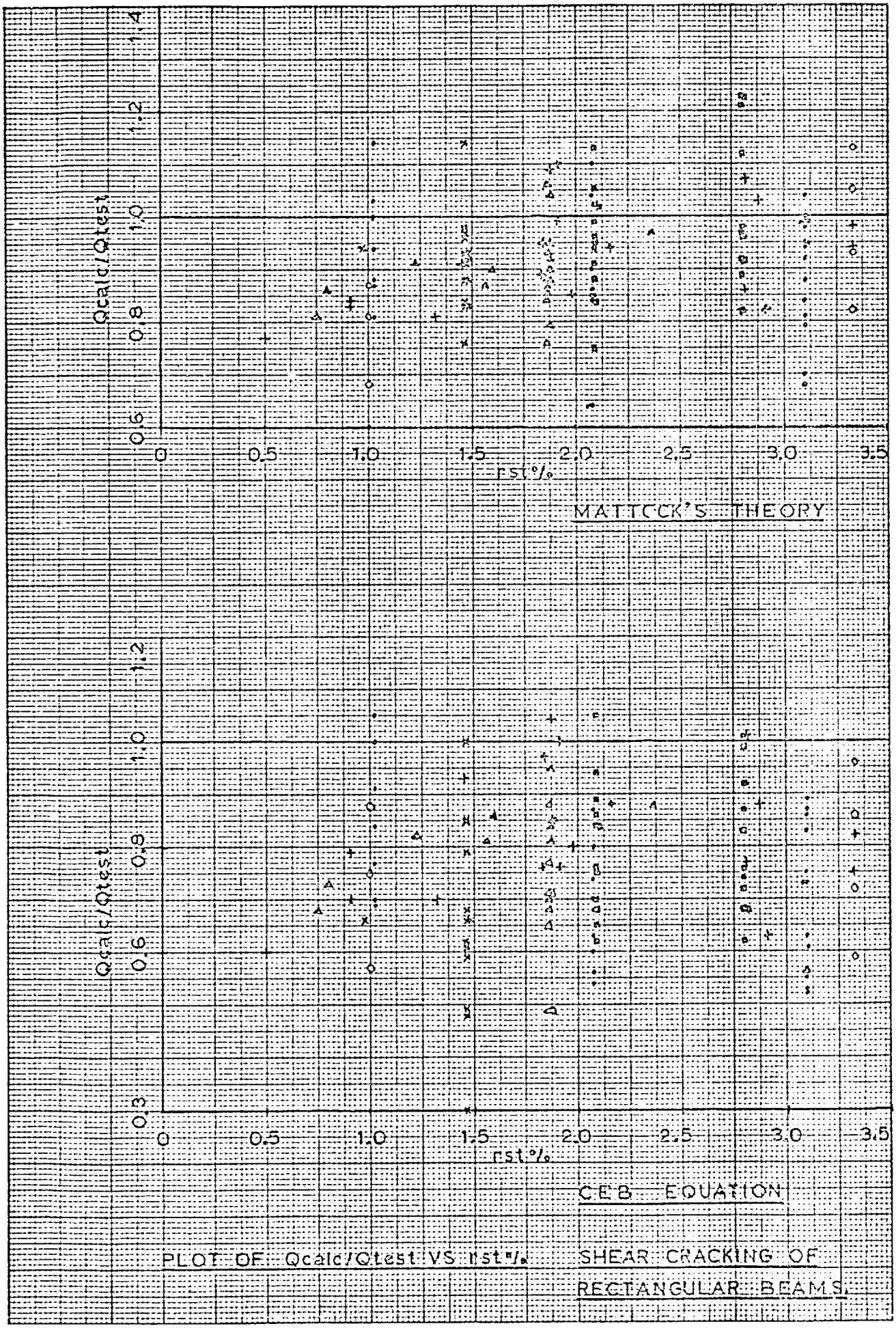
PLOT OF Qcalc/Qtest VS Ucyl. SHEAR CRACKING OF RECTANGULAR BEAMS.

FIG. 114.



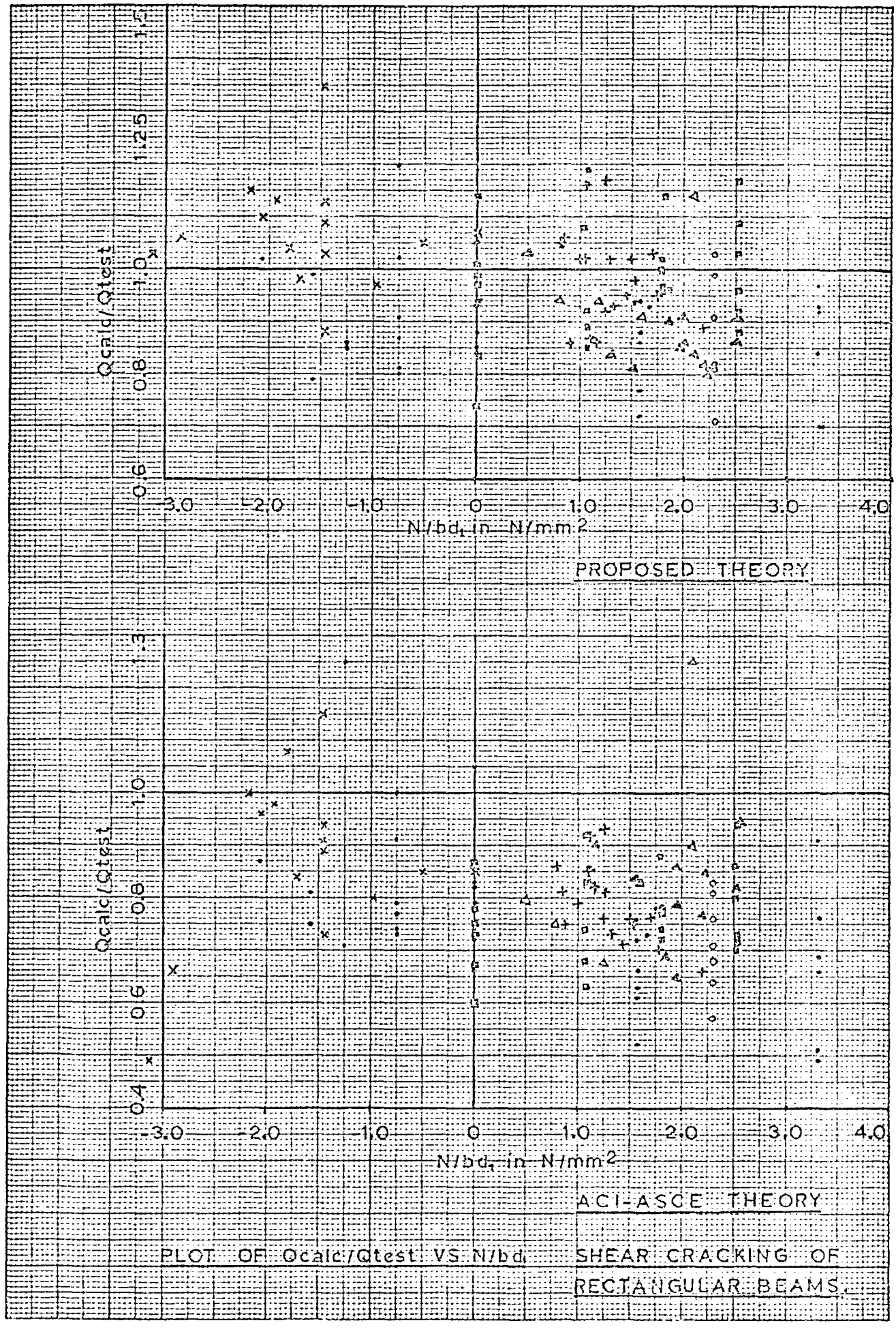
PLOT OF Qcalc/Qtest VS rst°/. SHEAR CRACKING OF RECTANGULAR BEAMS.

FIG. 115.



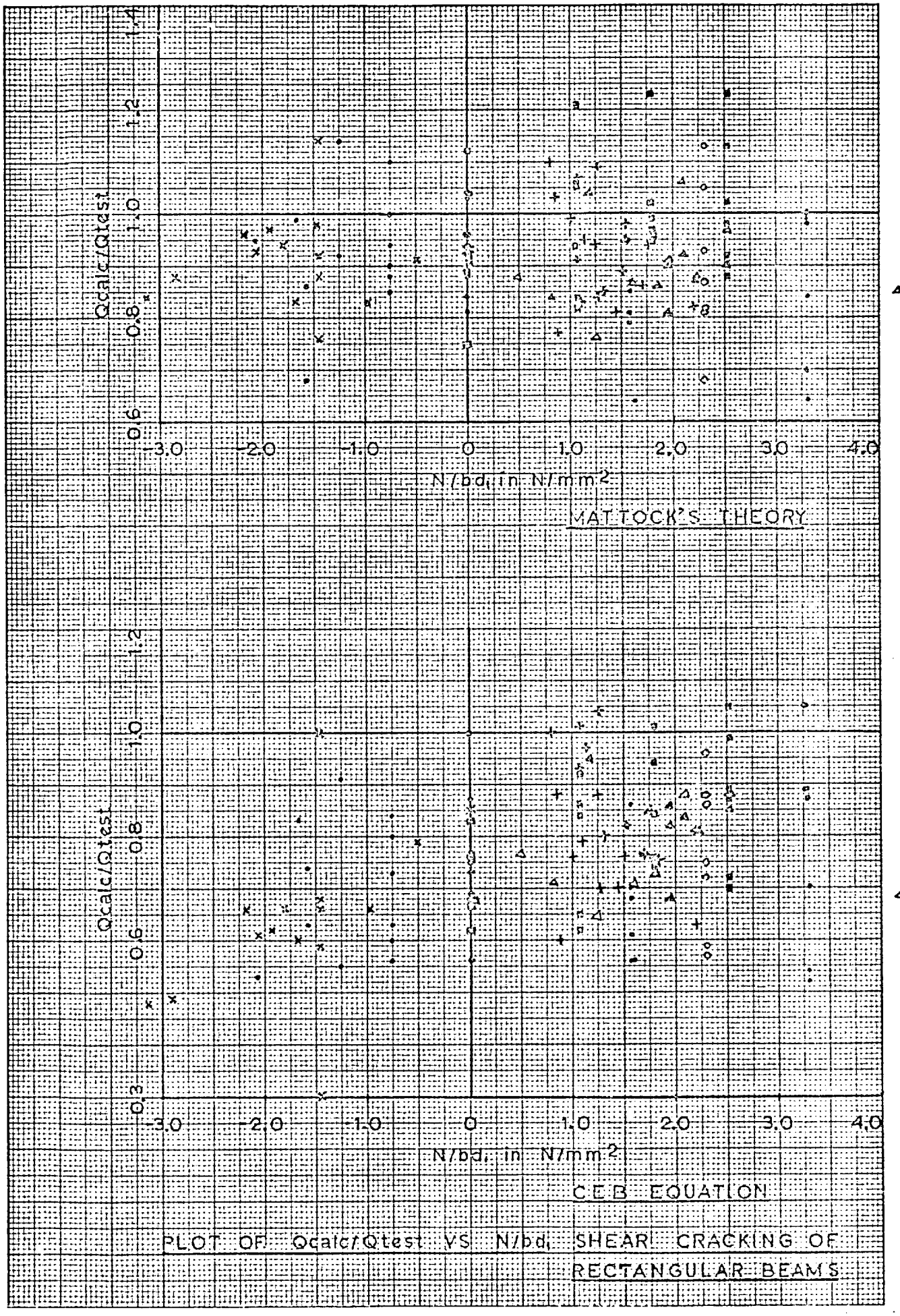
PLOT OF Qcalc/Qtest VS rst% SHEAR CRACKING OF RECTANGULAR BEAMS.

FIG. 116.



PLOT OF Qcalc/Qtest VS N/bd SHEAR CRACKING OF RECTANGULAR BEAMS.

FIG. 117.



PLOT OF Qcalc/Qtest VS N/bd, SHEAR CRACKING OF RECTANGULAR BEAMS

FIG. 118.

7.5 Shear failure of restrained and simply supported rectangular beams with vertical stirrups: (shearing failure)

In this section, the results used are the author's own as no other test results of beams with web reinforcement and axial forces are available.

Five equations including the author's are used to predict failure loads.

With the addition of the contribution of web reinforcement, the ACI-ASCE Committee and Mattock's equations are applicable in this case also.

Thus the ACI-ASCE equation becomes

$$\frac{Qult}{bd_1} = 1.9\sqrt{Ucyl} + 2500\,\frac{rst}{\frac{M + \beta N d_1}{Qd_1}} + K\,rq\,fyq \quad \text{in lbs and inch units}$$

and for vertical stirrups and 45° cracks

$$K = 1$$

Mattock's equation for ultimate load becomes -

$$\frac{Qult}{bd_1} = (1.75 - \frac{0.036}{m\,rst} + 4.0\,m\,rst)\sqrt{Ucyl} + \frac{I}{y}\left[\frac{6\sqrt{Ucyl} + N/bd}{bd_1(\frac{M}{Qd_1} - \frac{1}{2})d_1}\right]$$

$$+ 1.75\,rq\,fyq \text{ in lbs and inch units}$$

Mattock suggested upper limits to the contribution of web reinforcement and based on those limits, 1.75 is applicable so far as the beams used for comparison in this section are concerned. The limits are explained in chapter 3.

The CEB proposed two different equations, one with axial tension and the other with axial compression. The following are two equations used in comparison.

a) $\frac{Qult}{bd_1} = 0.87\ rq\ fyq + 0.1875\sqrt{Ucyl}\ (1 + 2\frac{N/bd}{Ucyl})(0.5 + 33\frac{Ast}{bd_1})$

when axial compression is applied, in N/mm^2 units.

and b) $\frac{Qult}{bd_1} = 0.87\ rq\ fyq + 0.1875\sqrt{Ucyl}\ (1 - 6\frac{N/bd}{Ucyl})(0.5 + 33\frac{Ast}{bd_1})$

when axial tension is applied, in N/mm^2 units.

and in both cases $(0.5 + 33\frac{Ast}{bd_1}) \leqslant 1.$

If $\frac{a}{d_1} < 2$, $\frac{Qult}{bd_1}$ is to be multiplied by $\frac{a}{2d}$.

The Russian code equation is

$$Qult = K.\frac{0.15\ bd_1^2\ pcb}{c} + c\ qw$$

where $K = \frac{eo}{d_1} - 0.5 \leqslant 1.$ and is a reduction factor to take account of the effect of axial force. K is equal to 1 in cases when axial force is zero or compressive.

and eo = eccentricity of the resultant tensile force in the section at the head of the inclined crack.

When c found by differentiating the above equation for minimum strength is less than a, the equation becomes -

$Qult = \sqrt{0.6\ K\ pcb\ bd_1^2\ qw}$ and with a conservative estimate of web reinforcement,

$$Qult = \sqrt{0.6\ K\ pcb\ bd_1^2\ qw} - qws$$

and if c is greater than a, c is put equal to a.

so $Qult = K.\frac{0.15\ bd_1^2\ pcb}{a} + aqw - qws = K\frac{0.15\ bd_1^2\ pcb}{a} + qw(a-s)$

In the comparison these equations have been applied to the section at which failure occurred although in many cases the Russian Code would predict failure at the section of contraflexure and give extremely conservative results.

The proposed equation is given in chapter 6 and is

$$\frac{Qult}{bd_1} = 0.5n_o\sqrt{Ucyl} + 2(1 - n_o)\, rq\, fyq \quad \text{in N/mm}^2 \text{ units.}$$

The follwoing table gives the statistical comparative values of the test results by each theory.

Table 31. Statistical comparison of $\frac{Qcalc}{Qtest}$ values of rectangular beams with web reinforcement.

Values of	No. of test results	Proposed Theory	ACI-ASCE equation	CEB equ.	Russian code equation	Mattock's equ.
Mean of $\frac{Qcalc}{Qtest}$	8+2	0.94	0.62	0.59	1.34	0.94
Standard deviation	-	.060	.206	0.169	0.110	.142
Coefficient of variation	-	.064	.332	.287	0.082	.151

Table 32. Shear failure of Restrained and Simply Supported rectangular beams with vertical web reinforcement. (Shearing failure)

Beam No.	Uw N/mm^2	Ucyl N/mm^2	M/Qd_1	rst%	rq fyq N/mm^2	N/bd_1 N/mm^2	$Qult/bd_1$ N/mm^2
a) Restrained beams							
B_1	41.8	33.5	2.8	1.46	0.66	-2.41	2.28
B_2	41.1	32.9	2.8	1.46	0.66	-4.09	2.08
B_3	45.7	36.6	2.8	1.46	0.66	0	2.05
B_4	43.9	35.1	2.8	1.46	0.66	-2.41	2.28
B_5	40.9	32.7	2.8	1.46	0.66	-1.68	1.92
B_7	40.2	32.2	2.8	1.46	0.66	-4.09	2.28
B_{12}	38.7	31.0	2.8	1.46	0.66	-4.09	2.23
B_{17}	36.9	29.5	2.8	1.46	0.66	+3.61	2.29
b) Simply supported beams							
B_6	41.4	33.1	3.9	1.46	0.66	-2.88	2.10
B_{31}	39.3	31.5	3.36	1.46	0.66	+2.41	2.34

Table 33. Comparison of Q_{calc}/Q_{test} values of shear failure of restrained and simply supported rectangular beams with vertical web reinforcement. (Shearing failure).

Beam No.	Q_{calc}/Q_{test}				
	Proposed theory	ACI-ASCE equation	CEB equation	Russian Code equation	Mattock's equation
a) Restrained beams:					
B_1	0.89	0.69	0.52	1.30	0.91
B_2	0.96	0.32	0.41	1.35	0.76
B_3	1.04	0.85	0.82	1.53	1.13
B_4	0.90	0.71	0.54	1.34	0.92
B_5	1.05	0.87	0.68	1.53	1.11
B_7	0.87	0.29	0.36	1.27	0.75
B_{12}	0.87	0.30	0.35	1.27	0.75
B_{17}	0.91	0.76	0.80	1.20	1.10
b) Simply supported beams:					
B_6	0.96	0.63	0.63	1.40	0.96
B_{31}	0.90	0.74	0.76	1.22	1.00

7.6 Shear failure of simply supported and restrained rectangular beams with web reinforcement and axial force. (Shear compression failure).

Excepting the author's equation mentioned in section 7.5 all other equations will be applicable for prediction of ultimate loads in this section as well.

The proposed equation is derived in chapter 6 and is

$$\frac{Qult}{bd_1} = 2.2\,\bar{n}\,Ucyl^{2/3} \times \frac{la}{a} - \frac{N/bd_1 \times (d_1 - d/2)}{a} + \frac{c^2}{2d_1 a} rq\,fyq + \frac{Qd}{bd_1}$$

in N/mm^2 units

and if $c = a$,

$$\frac{Qult}{bd_1} = 2.2\,Ucyl^{2/3}\,\bar{n}\,\frac{la}{a} + \frac{a}{2d_1} rq\,fyq - N/bd_1\left(\frac{d_1 - d/2}{a}\right) + \frac{Qd}{bd_1}$$

in N/mm^2 units

where the contribution of dowel is

$$\frac{Qd}{bd_1} = 5\,Ucyl^{2/3}\,rst \quad ; \quad \text{in } N/mm^2 \text{ units}$$

$$\bar{n} = \bar{n}_o + \frac{N/bd_1}{2.2\,Ucyl^{2/3}}$$

$$\bar{n}_o = \sqrt{.315\,m\,rst\,\frac{a}{c}}$$

and

$$\frac{c}{d_1} = \frac{1}{0.4}\sqrt{\frac{2.2\,Ucyl^{2/3}\,\frac{la}{d_1}}{2\,rq\,fyq}\sqrt{.315\,\frac{Es}{Eco} \times \frac{a}{d_1}}}$$

In the expression for $\frac{c}{d_1}$, the value of the lever arm factor can be assumed to be 0.9 i.e. $\frac{la}{d_1} = 0.9$, errors here are of little importance so far as the value of $\frac{c}{d_1}$ is concerned.

The following table gives the statistical comparative values of the test results by each theory.

Table 34. Statistical comparison of Q_{calc}/Q_{test} values of simply supported and restrained beams with vertical web reinforcement. (Shear compression failure).

Loading condition	Values of	No. of test results	Proposed theory	ACI-ASCE equation	CEB equation	Russian equation	Mattock's equation
Simply supported beams	Mean of Q_{calc}/Q_{test}	10	0.92	0.52	0.53	0.96	0.73
	Standard deviation	-	0.074	0.060	0.067	0.132	0.105
	Coeff. of Variation	-	0.080	0.115	0.126	0.138	0.144
Restrained beams	Mean of Q_{calc}/Q_{test}	11	0.84	0.64	0.67	1.01	0.96
	Standard deviation	-	0.069	0.070	0.066	0.114	0.103
	Coeff. of variation	-	0.082	0.110	0.099	0.113	0.107

Table 35. Shear failure of rectangular simply supported and Restrained beams with web reinforcement.

(Shear compression failure).

Beam No.	Uw N/mm^2	Ucyl N/mm^2	rst%	M/Qd_1	rq fyq N/mm^2	N/bd_1 N/mm^2	$Qult/bd_1$ N/mm^2
a) Simply supported beams:							
B_8	39.0	31.2	1.46	1.96	0.66	-2.41	2.76
B_9	39.2	31.4	1.46	1.96	0.66	0	3.34
B_{10}	42.8	34.3	1.46	1.96	0.66	-2.41	2.97
B_{11}	39.7	31.7	1.46	1.5	0.66	0	3.95
B_{13}	37.7	30.2	1.46	1.5	0.66	-2.41	3.71
B_{14}	36.2	29.0	1.46	1.5	0.66	-2.41	3.26
B_{16}	36.9	29.5	1.46	1.96	0.66	+3.61	4.10
B_{19}	37.5	30.0	1.46	1.96	0.66	+2.41	3.72
B_{21}	37.1	29.7	1.46	1.96	0.66	+3.61	3.72
B_{26}	38.0	31.5	1.46	2.8	1.05	+4.82	3.37
b) Restrained beams:							
B_{15}	40.5	32.4	1.46	2.8	0.66	+4.82	3.13
B_{18}	36.6	29.3	1.46	2.8	0.66	+3.61	3.01
B_{20}	35.6	28.5	1.46	2.8	0.66	+2.41	2.41
B_{22}	34.4	27.5	1.46	2.8	0.66	+4.82	3.13
B_{23}	37.9	30.3	1.46	2.8	0.66	+3.61	2.89
B_{24}	38.5	30.8	1.46	2.8	0.66	+4.82	2.89
B_{25}	37.8	30.2	1.46	2.8	1.05	+4.82	3.37
B_{27}	35.8	28.6	1.46	2.8	1.05	+4.82	3.37
B_{28}	17.4	13.9	1.46	2.8	0.66	+3.61	1.93
B_{29}	44.2	35.4	0.97	2.8	0.66	+4.82	2.41
B_{30}	39.1	31.3	2.0	2.9	0.66	+2.41	2.73

Table 36. Comparison of Q_{calc}/Q_{test} values of rectangular simply supported and restrained beams with web reinforcement. (Shear compression failure).

a) Simply supported beams.	Q_{calc}/Q_{test}				
Beam No.	Proposed theory	ACI-ASCE equation	CEB equation	Russian Code equation	Mattock's equation
B_8	0.96	0.60	0.47	1.13	0.77
B_9	0.96	0.54	0.55	0.94	0.73
B_{10}	0.95	0.54	0.46	1.13	0.73
B_{11}	0.94	0.48	0.61	0.93	0.66
B_{13}	0.78	0.42	0.45	0.95	0.57
B_{14}	0.87	0.47	0.49	1.04	0.64
B_{16}	0.920	0.47	0.51	0.73	0.70
B_{19}	0.97	0.51	0.54	0.82	0.73
B_{21}	1.01	0.53	0.56	0.81	0.77
B_{26}	0.79	0.63	0.67	1.08	0.99
b) Restrained beams:					
B_{15}	0.82	0.57	0.62	0.93	0.86
B_{18}	0.78	0.57	0.60	0.91	0.85
B_{20}	0.91	0.70	0.72	1.12	1.01
B_{22}	0.76	0.55	0.60	0.85	0.84
B_{23}	0.82	0.60	0.63	0.97	0.89
B_{24}	0.85	0.61	0.66	0.98	0.92
B_{25}	0.77	0.63	0.67	1.08	0.99
B_{27}	0.75	0.62	0.66	1.05	0.98
B_{28}	0.90	0.78	0.84	0.93	1.20
B_{29}	0.97	0.74	0.72	1.28	1.07
B_{30}	0.89	0.65	0.66	1.04	0.98

7.7 Shear failure of point-loaded Simply supported and Restrained T-beams with web reinforcement.

Although the author has not developed any equation to predict shear strengths of T-beams with or without shear reinforcement, nevertheless, the equation below developed for rectangular beams is compared with available results of tests of T-beams.

$$\frac{Qult}{bd_1} = 2.2\sqrt{n}\,Ucyl^{2/3}\frac{la}{a} - \frac{N/bd_1(d_1-d/2)}{a} + \frac{c^2}{2d_1 a}\,rq\,fyq \quad \text{in } N/mm^2$$

neglecting the contribution of dowel shear as in all cases c/d_1 is smaller than a/d_1. The comparison of the $Qcalc/Qtest$ values is given in table 37. This, of course, is based on the total neglect of the effect of the flange and the tensile reinforcement ratio is calculated assuming the beam to be a rectangular one and so $rst = \frac{Ast}{brd_1}$ where br = breadth of rib of a T-beam.

The equation gives a conservative estimate of the shear strengths of T-beams within a range of 30%; and average value of $Qcalc/Qtest$ is 0.71 for simply supported beams.

The behaviour of restrained beams at the support is similar to rectangular beams, as such the equation can be made use of without reservation and is found to be satisfactory. The average value of $Qcalc/Qtest$ for six beams is 0.82.

Under the circumstances, no attempt has been made to compare the $Qcalc/Qtest$ values given by the author's theory with those given by other theories. The author's intention is to show that the same equation developed to predict shear strengths of rectangular beams is safe under all circumstances when applied to T-beams.

The following table 37 gives the comparison of $Qcalc/Qtest$ values of 59 T-beams tested by Mattock.

Table 37. Shear failure of Simply Supported and point-loaded T-beams with web reinforcement. (Shear compression failure). (Mattock).

Beam No.	Ucyl N/mm^2	M/Qd_1	rst%	rsc%	rq fyq N/mm^2	N/bd_1 N/mm^2	$Qult/bd_1$ N/mm^2	$\frac{Qcalc}{bd_1}$ N/mm^2	$\frac{Qcalc}{Qtest}$
Series I. Simply supported beams.									
A_2	29.2	2.5	3.80	0.42	0.66	0	2.87	2.95	1.03
A_{3c}	34.0	2.5	3.80	0.42	1.45	+3.4	4.86	3.98	0.82
A_3	30.1	2.5	3.80	0.42	1.45	0	4.30	3.42	0.80
A_{3T}	29.2	2.5	3.80	0.42	1.45	-2.12	3.61	3.10	0.86
A_{4c}	28.4	2.5	3.80	0.42	2.71	+3.4	5.75	4.00	0.70
A_4	28.6	2.5	3.80	0.42	2.71	0	5.05	3.69	0.73
A_{4T}	29.6	2.5	3.80	0.42	2.71	-2.12	5.10	3.51	0.69
A_{5c}	27.10	2.5	3.80	0.42	4.35	+3.4	6.90	4.22	0.61
A_5	26.3	2.5	3.80	0.42	4.35	0	5.71	3.88	0.68
A_{5T}	27.5	2.5	3.80	0.42	4.35	-2.12	5.98	3.73	0.62
A_6	25.6	2.5	3.80	0.42	6.20	0	5.75	4.06	0.71
B_{3c}	27.7	3.375	3.80	0.42	1.45	+3.4	4.34	2.88	0.66
B_3	27.7	3.375	3.80	0.42	1.45	0	4.01	2.67	0.67
B_{3T}	24.1	3.375	3.80	0.42	1.45	-2.12	3.59	2.36	0.66
C_{2c}	28.0	4.25	3.80	0.42	0.66	+3.4	2.99	2.23	0.75
C_2	27.8	4.25	3.80	0.42	0.66	0	2.56	2.04	0.80
C_{2T}	30.3	4.25	3.80	0.42	0.66	-2.12	2.71	1.99	0.73
C_{3c}	26.7	4.25	3.80	0.42	1.45	+3.4	4.05	2.41	0.60
$C_{3c'}$	27.3	4.25	3.80	0.42	1.45	+1.7	3.87	2.40	0.62
C_3	24.10	4.25	3.80	0.42	1.45	0	3.84	2.19	0.57
C_{3T}	29.30	4.25	3.80	0.42	1.45	-2.12	3.54	2.24	0.63
$C_{3T'}$	27.60	4.25	3.80	0.42	1.45	-2.55	2.81	2.15	0.77
C_{4c}	26.30	4.25	3.80	0.42	2.71	+3.4	4.47	2.57	0.58
C_4	25.70	4.25	3.80	0.42	2.71	0	4.59	2.48	0.54
C_{4T}	27.80	4.25	3.80	0.42	2.71	-2.12	4.29	2.45	0.57
C_5	30.40	4.25	3.80	0.42	4.35	0	5.29	2.88	0.55
D_{3c}	29.90	6.0	3.80	0.42	1.45	+3.4	3.34	1.96	0.59
D_3	29.20	6.0	3.80	0.42	1.45	0	3.56	1.88	0.53
D_{3T}	26.20	6.0	3.80	0.42	1.45	-2.12	3.20	1.71	0.53

Table 37 (cont.) Shear failure of point loaded simply supported and restrained T-beams with web reinforcement. (Mattock). Shear compression failure.

Series II Simply supported beams:

Beam No.	Ucyl N/mm^2	M/Qd_1	rst%	rsc%	rq fyq N/mm^2	N/bd_1 N/mm^2	$Qult/bd_1$ N/mm^2	$\frac{Qcalc}{bd_1}$ N/mm^2	$\frac{Qcalc}{Qtest}$
E_2	15.2	2.5	3.8	0.42	0.66	0	2.5	2.25	0.90
E_{3c}	15.45	2.5	3.8	0.42	1.45	+3.4	3.45	2.79	0.81
E_3	13.65	2.5	3.8	0.42	1.45	0	2.80	2.47	0.88
E_{3T}	14.70	2.5	3.8	0.42	1.45	-2.12	2.93	2.27	0.78
E_4	13.4	2.5	3.8	0.42	2.71	0	3.71	2.75	0.74
E_5	17.10	2.5	3.8	0.42	4.35	0	4.54	3.22	0.71
F_{3c}	40.55	2.5	3.8	0.42	1.45	+3.4	5.19	4.27	0.82
F_3	45.0	2.5	3.8	0.42	1.45	0	4.87	4.11	0.85
F_{3T}	40.0	2.5	3.8	0.42	1.45	-2.12	3.89	3.57	0.92
G_{3c}	31.8	2.5	3.8	0.42	1.91	+3.4	6.07	4.00	0.66
G_3	26.2	2.5	3.8	0.42	1.91	0	4.92	3.38	0.69
G_{3T}	29.4	2.5	3.8	0.42	1.91	-2.12	4.68	3.27	0.70
G_{4c}	25.2	2.5	3.8	0.42	2.87	+3.4	5.60	3.81	0.68
G_4	26.8	2.5	3.8	0.42	2.87	0	5.66	3.65	0.65
G_{4T}	28.1	2.5	3.8	0.42	2.87	-2.12	5.55	3.47	0.63
G_{5c}	27.85	2.5	3.8	0.42	4.78	+3.4	6.84	4.25	0.62
G_5	26.15	2.5	3.8	0.42	4.78	0	6.32	3.93	0.62
G_{5T}	26.65	2.5	3.8	0.42	4.78	-2.12	5.83	3.73	0.64
H_{1c}	30.5	2.5	1.90	0.42	1.45	+3.4	4.8	3.14	0.65
H_1	29.2	2.5	1.90	0.42	1.45	0	4.19	2.65	0.63
H_{1T}	32.3	2.5	1.90	0.42	1.45	-2.12	3.46	2.40	0.69
H_{2c}	30.1	2.5	5.7	0.42	1.45	+3.4	4.8	4.21	0.88
H_2	28.2	2.5	5.7	0.42	1.45	0	4.7	3.82	0.81
H_{2T}	31.5	2.5	5.7	0.42	1.45	-2.12	3.78	3.75	0.99
								Mean	= 0.71
								standard deviation	= 0.117
								coeff. of variation	= 0.164

Series III Restrained beams:

J_{3c}	30.9	2.5	3.80	3.80	1.45	+3.4	4.40	3.82	0.87
J_3	30.4	2.5	3.80	3.80	1.45	0	3.88	3.44	0.89
J_{3T}	28.5	2.5	3.80	3.80	1.45	-2.12	2.77	3.05	1.10
J_{4T}	27.3	2.5	3.80	3.80	2.71	-2.12	4.74	3.40	0.72
J_5	32.5	2.5	3.80	3.80	4.35	0	6.40	4.26	0.67
J_{5T}	31.7	2.5	3.80	3.80	4.35	-2.12	6.10	3.98	0.65
								Mean	= 0.82
								standard deviation	= 0.175
								coeff. of variation	= 0.213

7.8 Discussion of Comparisons:

7.8.1 Scale and shape effects:

Because of the limited laboratory facilities, test specimens are generally smaller in size than real structural members. Thus a scale effect is introduced which influences the test results. Tests reported on small specimens show that smaller specimens are found to be relatively stronger for the following reasons -

1. The possibility of a weaker section coinciding with the critical section is less in smaller specimens, and

2. The strain gradient across the compressive zone is steeper in smaller specimens and as a result a smaller specimen can sustain larger strains.

Regan gives an elaborate discussion of scale and shape effects in reference 45 and concludes that the scale effect is important if d_1 is less than 380 mm (15").

In fact, no test results are available with d_1 greater than 380 mm (15"), the largest balue of d_1 being 368 mm (Morrow and Viest[38] and Baldwin and Viest[5]) and the smallest 254 mm. The range of scale is thus small and although there may be a general scale effect, it will not influence the comparison much.

7.8.2 Comparison of test results with shear cracking equations:

All the available test results with axial forces are compiled and verified with the theories mentioned earlier. The test results are of rectangular beams subject to point loads.

The following table summarises the statistical data obtained in the previous sections from comparison of theories of rectangular beams.

Table 38. Statistical data from comparisons of shear cracking theories of rectangular beams.

Type of Test	Values of	Proposed theory	ACI-ASCE equation	Mattock's equation	CEB equation
Simply supported beams, $a/d_1 > 2.5$ 61 beams	Mean of $\frac{Qcalc}{Qtest}$	0.92	0.76	0.93	0.75
	Standard deviation	0.114	0.126	0.133	0.140
	Coeff. of variation	0.124	0.165	0.143	0.187
Restrained and Continuous beams $M/Qd_1 > 2.5$ 33 beams	Mean of $\frac{Qcalc}{Qtest}$	1.02	0.83	0.92	0.74
	Standard deviation	0.103	0.127	0.093	0.167
	Coeff. of variation	0.101	0.153	0.101	0.226
Restrained and Continuous beams $M/Qd < 2.5$ 18 beams	Mean of $\frac{Qcalc}{Qtest}$	0.89	0.86	0.90	0.79
	Standard deviation	0.087	0.142	0.072	0.084
	Coeff. of variation	0.098	0.165	0.080	0.106

From the above table, it is seen that the coefficient of variation by the proposed theory is about the same in all cases and the mean value is near to unity. The theory gives unsafe results so far as knee frame members and restrained beams are concerned, mainly for the test results of Sayani which are of beams supported by cross beams. If the influence of the manner of loading on shear strength and the porosity of concrete at the top of a beam are recognised, then the unsafe prediction by the theory is explained.

The ACI-ASCE and CEB equations are conservative in general, though on a few occasions the ACI-ASCE equation predicts unsafe results.

Mattock's modified ACI-318-63 equation is found to be satisfactory although its coefficient of variation is higher than the author's in the case of simply supported beams.

The values of $\frac{Qcalc}{Qtest}$ by the theories are plotted (see figs. 111-118) against the variables $\frac{M}{Qd_1}$, rst% Ucyl and N/bd_1.

Figs. 111 and 112 show the plot of $\frac{Qcalc}{Qtest}$ against $\frac{M}{Qd_1}$ ratio, from the trend of the plot, it is evident that the proposed theory is the best in correctly estimating the effect of M/Qd_1 ratio on the shear cracking strength of beams. The ACI-ASCE Committee equation is also found to be satisfactory in this regard, whereas the other two theories are more conservative for smaller $\frac{M}{Qd_1}$ ratios.

So far as concrete strength is concerned, figs. 113 and 114 show that within the practicable limits of concrete strength, its effect is adequately taken into account by all four methods.

The effect of the next important variable, the ratio of tensile steel is taken care of by all the theories, the ACI-ASCE Committee equation predicts more conservative results with higher percentages of tensile steel. Judging from the scatter in the plot, (figs. 115 and 116) the proposed theory is again found to be the most satisfactory.

Figs. 117 and 118 show the plots of $\frac{Qcalc}{Qtest}$ against N/bd_1. The ACI-ASCE Committee equation predicts conservative results with higher magnitudes of axial compression. Generally it is not far out so far as axial tension is concerned, but because of its upper limit of shear strength with high magnitudes of axial tension, it becomes oversafe for N/bd_1 greater than about 2.0 N/mm^2. The proposed theory on the other hand, does not limit the strength in this way and so is found to be in good agreement either with axial tension or axial compression. Mattock's and CEB equations have a trend to be conservative with axial tension, the trend being more pronounced in the latter case.

7.8.3 Comparison of test results of beams without web reinforcement and $\frac{a}{d_1} < 2.5$. Shear compression failure.

Table 38 gives the statistical data obtained from the comparison by different theories. Except the proposed theory, all are found to be conservative. This is attributable to the total rejection of strength after shear cracking by the theories. Although Mattock's theory gives a satisfactory magnitude of coefficient of variation, the mean value is very low. The same is true for CEB equation as well. The ACE-ASCE equation is not only conservative, but also gives the highest coefficient of variation.

7.8.4 Comparison of test results of beams with web reinforcement and $\frac{a}{d_1} > 2.5$. Shearing failure:

As no other test results are available, only the test results of the author are compared with the various theories. From the statistical comparison of the $\frac{Qcalc}{Qtest}$ values in table 31, the proposed theory is found to give the best mean value with the lowest standard deviation and coefficient of variation. The second best is undoubtedly Mattock's although the coefficient of variation is higher than that of the Russian method. Both the ACI and CEB equations are found to be conservative while the Russian method is found to predict very unsafe results.

7.8.5 Comparison of test results of rectangular beams with web reinforcement: Shear compression failure:

The statistical data for the different theories are presented in section 7.6 and from all considerations, the proposed theory is found to be preferable. Although Mattock's equation is satisfactory in the case of restrained beams, but it predicts conservative results for simply supported beams. The Russian code equation is also found to be satisfactory, but gives higher coefficients of variation.

The other two theories are found to be conservative in both cases, of them the CEB equation is to be preferred as it gives a lower coefficient of variation than the ACI's.

7.9 Comparison of test results of beams failing in bond (Secondary failure mode)

The proposed theory on bond after shear cracking gives the bond stress at failure as:

$$\frac{Q}{\Sigma o\ la} = 0.55\sqrt{Ucyl}\ \left(\frac{L}{a}\right)\left(\frac{c}{\phi}\right)^{\frac{1}{2}} + \frac{b\ rq\ fyq}{n\ \pi\phi}\left[2\frac{d_1^2}{a.la} + 2\left(1-\frac{2d_1}{a}\right) + 0.55\ \frac{L}{a}\right]$$

where la = internal (flexural) lever arm.

Although the results of all the restrained beams subject to compression are compared in the previous section with the shear compression equation and found to be in good agreement, in fact, a few of them showed signs of bond failure. (see figs49, 50 and 51) and so it is reasonable to compare the strengths of those beams with the proposed equation to predict failure in bond. The following table gives a comparison of the $\frac{Qcalc}{Qtest}$ values of the beams failing in bond.

Table 39. Comparison of $\frac{Qcalc}{Qtest}$ values of beams failing in bond calculated by the proposed equation.

Beam No.	Ucyl N/mm^2	rst%	M/Qd_1	rq fyq N/mm^2	N/bd_1 N/mm^2	$\frac{Qtest}{ola}$ N/mm^2	$\frac{Qcalc}{Qtest}$
B_{15}	32.4	1.46	2.8	0.66	+4.82	3.97	0.93
B_{18}	29.3	1.46	2.8	0.66	+3.61	3.90	0.92
B_{22}	27.5	1.46	2.8	0.66	+4.82	4.13	0.85
B_{23}	30.3	1.46	2.8	0.66	+3.61	3.72	0.97
B_{25}	30.2	1.46	2.8	1.05	+4.82	4.41	0.99
B_{26}	30.4	1.46	2.8	1.05	+4.82	4.41	0.99
B_{28}	13.9	1.46	2.8	0.66	+3.61	2.66	1.09

$\bar{x}$ = 0.95
s = 0.070
coeff. of variation ==0.074

From table 39 it is evident that the proposed theory on bond is in good agreement with the test results, coefficient of variation being as low as 0.074.

CHAPTER 8

CONCLUSIONS AND PROPOSALS FOR FUTURE RESEARCH

8.1 General conclusions:

Shear failure is influenced by a number of variables, such as, concrete strength, ratio of tensile steel, shear span to effective depth ratio, web reinforcement and axial force. The influence of compression reinforcement is not precisely known.

The behaviour of a beam changes after shear cracking and the shear carrying mechanism following shear cracking is composed of the following actions -

a) Shear carried by the concrete compressive zone.

b) dowel action of the tensile steel.

c) Aggregate interlocking if possible.

and d) Web reinforcement if any.

It is observed that in short beams a modified arch action is developed after shear cracking. In long beams there is less or no scope to develop arch action. From a study of physical behaviour three different major modes of shear failure are observed.

a) Shear cracking/Diagonal tension failure.

b) Shearing failure.

and c) Shear compression failure.

The initiation of a shear crack(cracks) is a precondition for a beam to fail in shear by any one of these modes, and thus shear cracking is the first step towards shear distress of a beam. After shear cracking a beam may fail in either of the last two modes, depending primarily on $\frac{M}{Qd_1}$ ratio if it does not fail in diagonal tension.

The contribution of dowel action of the tensile steel and aggregate interlock towards shear strength of a beam is recognised to be significant.

The dowel action of the tensile steel when the diagonal cracks extend up to the edge of the support plate is considered in the analysis. Although interlock forces are significant in the presence of compression, little shear can be transferred across a crack in the presence of tension.

An important secondary mode of failure considerably influenced by the action of shear is bond failure. From the available data on bond failures of concrete beams, bond or anchorage resistance is believed to be influenced by the following variables -

a) Concrete strength.

b) Diameter of bars.

c) Concrete cover.

d) Anchorage length.

e) Web reinforcement if present.

Two different types of bond failures are common.

1) Pull-out failure

and

2) Splitting failure (of concrete cover).

In the present investigation, the latter type of failure was observed. Such failure is determined by the physical behaviour of the beam and not by any criterion of bond failure.

The main experimental work of this investigation was comprised of tests of 31 beams with axial loads. During testing of these beams, surface strains on the beam measured by demec gauges showed linear elastic behaviour at the initial stages although after flexural cracking and then after shear cracking, the readings showed increasing non-linearity of strain distributions.

Strains both on tensile and compression steel were measured with electrical resistance gauges and were found to be useful. In none of these beams tensile steel yielded prior to shear failure.

Stirrup strains recorded showed that the stirrups were appreciably not stressed until shear cracking. Thereafter the shear carried by web reinforcement was found to be unaffected by axial loading. Similar results were observed by Mattock in T-beams.

Although axial forces influenced the inclination of the critical crack to the axis of the tensile steel, its horizontal projection remained more or less unaffected. The inclination was found to be the same for beams with axial tension and for beams without any axial force, but it decreased with the application of axial compression. This is explainable, as in the case of axial compression the thrust line is flatter.

None of the beams subjected to axial tension showed any sign of distressat the section at contraflexure. The section in question is believed in general, to be the most vunerable in shear when subjected to axial tension. The presence of tension cracks as wide as 0.8 mm did no harm and thus indicates the strength of shear transfer by interlocking of aggregates and dowel action of the tensile steel.

The magnitude of the external moment $\left[Qulta - N(1a - d_1 + {}^{d}/_{2})\right]$ about the point of action of the compressive force Fcc is observed to be approximately constant for varying axial loads when failure is due to shear compression. The same is not true when failure is due to shearing.

8.2 Influence of the parameters affecting the shear strength of a beam.

8.2.1 Influence of axial force:

Shear strength is found to be affected by axial forces, decreased by tension and increased by compression. This increase or decrease is not very pronounced when the failure mode is shearing, but is significant for shear compression failures. A contrary finding is reported by Morrow and Viest whose conclusion was based on a single test in which one beam failed without showing any substancial increase

in ultimate shear strength (3.2% increase). In other cases, the increase is more or less similar to that reported by the author. Mattock's findings confirm the conclusion of the author for beams with both axial tension and compression. Sayani's test results also show a similar trend.

The effect of axial forces on the shear strength is attributable to the following -

a) axial compression increases the neutral axis depth thereby increasing the shear carried by the concrete compressive zone.

b) axial compression reduces the effective M/Qd_1 ratio at a particular section and hence increases the shear cracking load.

c) In both cases, axial tension does the reverse.

The effect of axial tension may be more significant if the ratio of compression steel is small or the compression steel is cut beyond the point of contraflexure. A beam is weakened due to the curtailment of compression steel. Since, after the formation of vertical cracks, almost whole of the axial tension is carried by longitudinal steel and thus in absence of any longitudinal steel, failure would be immediate after vertical cracking. A slight excess of 'compression' steel is required to ensure the safety of points of contraflexure as discussed in chapter 6.

8.2.2 Influence of shear span to effective depth ratio (M/Qd_1 or a/d_1)

The effect of shear span to effective depth ratio on the shear strength and behaviour of a beam is considerable. With normal percentages of tensile steel and normal concrete strengths, different failure modes can be caused by varying only M/Qd_1 ratios. Diagonal tension or shearing failures of such beams can occur with M/Qd_1 (or a/d_1) ratios > 2.5 depending on whether web reinforcement is present or absent. In shorter beams, failure is generally by shear compression.

The effect of the M/Qd_1 (or a/d_1) ratio on strength is more prominent in short beams whereas its influence is of little consequence when the M/Qd_1 (or a/d_1) ratio becomes large enough.

8.2.3 Concrete strength:

The effect of concrete strength on shear resistance was not studied in the present investigation. However, from a study of the test results of previous investigators, it can be concluded contrary to Kani that concrete strength does have some bearing on the shear strength of a beam. Shear strength is found to increase with increasing concrete strength, and this increase is more pronounced in weaker concretes.

8.2.4 Influence of ratio of tensile steel: ($rst = Ast/bd_1$):

The ratio of tensile steel was varied in only two tests but its effect was found to be significant. The beam with 2% tensile steel ratio showed an increase while the beam with 0.97% showed a reduction in shear capacity as compared with the remaining beams with 1.46% of tensile steel. The influence of tensile steel on shear strength is widely recognised and a large amount of experimental evidence by other investigators is available to support this.

8.2.5 Effect of aggregate interlock:

A considerable amount of shear can be transferred across a crack by the action of interlock due to the compression induced by the longitudinal steel and the effect is most pronounced if the other actions (e.g. shear in the concrete compressive zone) are absent, as is the case at the section of contraflexure of a restrained or continuous beam, when axial tension is applied to it. Although its effect is recognised qualitatively, for the simplicity of analysis, it is not taken into direct quantitative account owing to the number of variables involved influencing its magnitude.

8.2.6 Web reinforcement ratio: ($^{Aq}/_{bs}$)

The shear strength of beams is found to increase with increasing web reinforcement. In the present tests the value of $^{Aq\ fyq}/_{bs}$ was varied from 0.66 N/mm^2 to 1.05 N/mm^2 and the increase of strength exhibited by the beams was independent of the axial forces applied to them.

8.3 Proposals for future research:

The research work reported in this thesis is limited. The experimental work comprised tests only of rectangular beams subjected to point loads. Because of the limited laboratory facilities and time the effect of variable cross-sections, higher ratios of $^{M}/_{Qd_1}$ etc. could not be systematically studied. Owing to the limitations of test data the author believes that the following subjects should be thoroughly investigated before drawing final conclusions.

a) The effect of the axial loads should be further studied in T-beams with both point and uniformly distributed loads.

b) The test results of rectangular beams with uniformly distributed loads and subjected to axial loads are rather limited, and so more tests are needed to support any theoretical or semi-empirical equations using $^{M}/_{Qd_1}$ ratios to define conditions at any section.

c) The contribution of interlock in carrying shear is recognised by a number of investigators across flexural and shear cracks. The problem however still remains to measure quantitatively the magnitude of interlock forces. Without the knowledge of the various parameters and their influences it seems impossible to draw any definitive conclusions, so the author would like to emphasise on more experimental evidence regarding the influence of all the parameters listed in chapter 5.

Lightweight aggregate concretes are of special interest here since if cracks go through rather than around the aggregate the capacity for interlocking could be seriously reduced. This could lower shear cracking/diagonal tension resistance very considerably and could affect the contribution of shear reinforcement if failures occurred at steeper cracks.

d) Bond failure of reinforced concrete beams should be thoroughly re-investigated in the light of current practice using deformed bars and the new methods of design for shear. During the experimental part of the author's work, bond failure occurred in a few beams. Although a theory to predict the bond strength of a beam after shear cracking is put forward in this thesis, the authenticity of it could not be checked with a large number of test results, except the author's own, because of the lack of available data.

REFERENCES

1. ACHARYA D.N. and KEMP K.O. Significance of dowel forces on the shear failure of rectangular reinforced concrete beams without web reinforcement. A.C.I. Journal, Oct., 1965.

2. ACI-ASCE COMMITTEE (326). Report on shear and diagonal tension.

3. ARROYO J. Study of dowel action by the main reinforcement of reinforced concrete beams. D.I.C. Thesis, Imperial College, 1969.

4. ASHDOWN A.J. Private Communication to shear study Group.

5. BALDWIN J.W. and VIEST I.M. Effect of axial compression on shear strength of reinforced concrete frame members. ACI Journal, nov. 1958.

6. BAKER A.L.L. and AHMAD S. A statically Indeterminate Truss model for Reinforced concrete beams failing by shear. Bulletin d'Information No. 37, Comite European du Beton, Oct. 1962.

7. BAUMANN T. An experimental study of dowel action by the main reinforcement of reinforced concrete beams - a synopsis of "versuche zum Studium der Verdübelungswirkung der Biegezugbewehrung eines Stahlbetonbalken". Bericht Nr. 77, Materialprüfungsamt für das Bauwesen der Technischen Hochschule München.

8. BORISHANSKI M.S. Calculations for Reinforced Concrete members subjected to Transverse forces.
A synopsis of a paper in Russian.

9. CLARK A.P. Diagonal tension in Reinforced concrete beams. ACI Journal, Proceedings, V. 48, Oct. 1951.

10. CEB Federation Internationale de la Preconstrainte. (International recommendation for the design and construction of concrete members), June 1970, FIP Sixth Congress, Prague.

11. DE COSSIO R.D. and SEISS C.P. Behaviour and strength in shear of beams and frames without web reinforcement. ACI Journal, Feb. 1960.

12. DIB E.M. Reinforced Concrete Deep Beams. Ph.D. Thesis, University of London, (To be published).

13. ELSTNER R.C. and HOGNESTAD E. Laboratory investigation of rigid frame failure. ACI Journal, Jan. 1957.

14. FENWICK R.C. Shear strength of reinforced concrete beams. Ph.D. Thesis, University of Canterbury, Christchurch, New Zealand.

15. FENWICK R.C. and PAULAY J. Mechanism of shear resistance of concrete beams. Journal of the structural division, Proceedings of the American Society of Civil Engineers, Oct. 1968.

16. FERGUSON P.M. and MATUOB F.N. Effect of bar cut-off on bond and shear strength of reinforced concrete beams. ACI Journal, July, 1959.

17. FERGUSON P.M. and THOMPSON J.N. Development length of high strength reinforcing bars in bond. ACI Journal, Proceedings, July, 1962. Vol. 59.

18. HADDADIN M.J., HONG S. and MATTOCK A.H. A study of the effectiveness of web reinforcement in reinforced concrete beams subject to axial forces. Structures and Mechanics Report SM 69-2. University of Washington, College of Engineering, Dept. of Civil Engineering, Sept. 1969.

19. HOFBECK J.H., IBRAHIM I.O. and MATTOCK A.H. Shear transfer in Reinforced concrete. ACI Journal, Feb. 1969.

20. JONES R. The ultimate strength of reinforced concrete beams in shear. Magazine of Concrete Research. Vol. 8, No. 22.

21. KANI G.N.J. A rational Theory for the Function of web reinforcement. ACI Journal, March 1969.

22. KANI G.N.J. The riddle of Shear failure.
ACI Journal, Proceedings, V. 61, No. 4, April 1964.

23. KANI G.N.J. Basic facts concerning shear failure.
ACI Journal, Proceedings V. 63 No. 6, June 1966.

24. KAR J.N. Shear strength of prestressed concrete beams without web reinforcement.
Magazine of concrete Research, Vol. 21, No. 68, Sept. 1969.

25. KREFELD W.J. and THURSTON C.W. Studies of the shear and Diagonal Tension Strength of Simply Supported Reinforced concrete beams.
ACI Journal, April 1966.

26. KREFELD W.J. and THRUSTON C.W. Contribution of Longitudinal steel to shear resistance of reinforced concrete beams.
ACI Journal, March 1966.

27. KRIZ L.B. and LEE S.L. Ultimate strength of Over-Reinforced Beams. Journal of the Engineering Mechanics Division. Proceedings of the ASCE, June 1960, Vol. 86.

28. LEONHARDT F. Reducing the shear reinforcement in reinforced concrete beams and slabs.
Magazine of Concrete Research. Dec. 1965.

29. LEONHARDT F. and PANDIT G.S. Discussion of the paper "Diagonal tension cracking in concrete beams with axial forces", by MATTOCK A.H. reference 36.

30. LEONHARDT F. Private communication of proposals for shear recommendations - discussed at CEB XII session Pleniere, Lausanne, April, 1968.

31. LITCHTENBERG S. Statistisk brudhypotese for beton. Nordisk Betong, 1959 : 4.

32. LORENTSEN M. Shear and bond in prestressed concrete beams without shear reinforcement. Statens Rad för Byggnads forskning, Handlingar, No. 47 Stockholm, 1967.

33. LOSBERG A. Några undersökningar av förankringsfrågor som bakgrund till nya svenska betongbestämmelser. Chalmers Tekniska Högskola. Institutianen För Konstruktionstenknik. Betongbyggnad Publikation 169 : 7.

34. MACGREGOR J.G. and HANSON J.M. Proposed changes in shear provisions for reinforced and prestressed concrete beams. ACI Journal, April 1969.

35. MATHEY R.G. and WATSTEIN D. Investigation of Bond in beams and pull out specimens with High-yield-strength deformed bars. ACI Journal, proceedings, July, 1962, Vol. 59.

36. MATTOCK A.H. Diagonal tension cracking in concrete beams with axial forces. Journal of the structural division, Proceedings of the American Society of Civil Engineers. Vol. 95, No. ST9, Sept. 1969.

37. MOAYER M. Shear and Torsion in Prestressed concrete beams. Ph.D. Thesis, University of London. (To be published).

38. MORROW J. and VIEST I.M. Shear strength of reinforced conc concrete frame members without web reinforcement. ACI Journal, March 1957.

39. MUKHAPADHYAY M. Ultimate strength of reinforced concrete members without web reinforcement subjected to combined bending moment, shear and axial forces. Ph.D. Thesis submitted to the Indian Institute of Technology, Kharagpur, 1970.

40. NARASIMHAN N. Shear reinforcement in Reinforced concrete column heads. Ph.D. Thesis, University of London, March, 1971.

41. OJHA S.K. The shear strength of rectangular reinforced and prestressed concrete beams. Magazine of Concrete Research, Vol. 19, No. 60 Sept. 1967.

42. OSTLUND L. Armeringsutformning och funktionskrav. (Design of reinforcement in accordance with functional requirements). Nordisk Betongkongress, 1967, Nummer 3.

43. PAULAY T. and FENWICK R.C. The nature of shear resistance in reinforced concrete beams. The Institution of Engineers, Australia. Civil Engineering Transactions, Oct. 1967.

44. PLACAS A. Shear failure of Reinforced concrete beams. Ph.D. Thesis, University of London, Nov. 1969.

45. REGAN P.E. Combined shear and Bending of Concrete members. Ph.D. Thesis, University of London, 1967.

46. REGAN P.E. and PLACAS A. Collapse and servicibility criterion in shear. Departmental report. Department of Civil Engineering, Imperial College, July, 1969.

47. REGAN P.E. Shear strengths of reinforced concrete beams. Departmental report, Department of Civil Engineering. 1968. Imperial College of Science and Technology.

48. SAYANI F.H.N. Influence of axial tension on the shear strength of reinforced concrete beams. M. Phil. Thesis, University of London, July 1968.

49. SOWEN M.A., ZWOYER E.M. and SIESS, C.P. Investigation of prestressed concrete for highway bridges, Part I. Strength in shear of prestressed beams without reinforcement. University of Illinois, Engineering Experiment Station, Bulletin No. 452.

50. Shear Study Group Report (Detailed Report). Institution of Structural Engineers, London, 1969.

51. Shear Study Group Report of the Institution of Structural Engineers, London 1969. "The shear strength of Reinforced concrete Beams".

52. SWAMY R.N., ANDRIOPOULOS A., ADEPEGBA D., Arch action and bond in concrete shear failures. Journal of the Structural Division. Proceedings of the ASCE. Vol. 96, No. ST6, June 1970.

53. TAUB J. and NEVILLE A.M. Resistance to shear reinforced concrete beams, Part 2. Beams with stirrups. ACI Journal, Sept. 1960, No. 3 V 32.

54. TAYLOR H.P.J. Distribution of shear forces in Reinforced Concrete beams carrying shear.

55. TAYLOR H.P.J. Investigation of the forces carried across cracks in Reinforced Concrete beams in shear by Interlock of aggregates. C. and C.A. report.

56. TAYLOR H.P.J. Shear stresses in Reinforced concrete beams without shear reinforcement. TRA/407. Cement and concrete Association, London, 1968.

57. TAYLOR H.P.J. Investigation of the Dowel shear forces carried by the tensile steel in Reinforced concrete beams. TRA/431. Cement and concrete Association, London; Nov. 1969.

58. TAYLOR H.P.J. Further tests to determine shear stresses in Reinforced concrete beams. TRA/438. Cement and concrete Association, London, Feb. 1970.

59. TAYLOR R. A new method of proportioning stirrups in Reinforced Concrete Beams. Magazine of Concrete Research, 1963. Vol. 5.

60. WALTHER R. Calculation of the shear strength of reinforced and prestressed concrete beams by the shear failure theory. A C. and C.A. translation No. 110 of the article in German "Beton- und Stahlbetonbau", vol. 57, No. 11 Nov. 1962.

61. ZIA P. Torsional strength of prestressed concrete members. ACI Journal, Proceedings, V57, No. 10, April 1961.

62. Shear in Reinforced concrete - an analytical study. Report to the Construction Industry, Research and Information Association (CIRIA), April, 1971. (to be published).